

Department of Chemical Engineering
Technical University of Denmark

Graduate School
Yearbook
2003

Editors:
Kim Dam-Johansen
Martin Skov Skjøth-Rasmussen

Kongens Lyngby 2004

Address: Department of Chemical Engineering
Søltofts Plads, Building 229
Technical University of Denmark
DK-2800 Kgs. Lyngby
Denmark

Telephone: (+45) 45 25 28 00
Fax: (+45) 45 88 22 58
e-mail: kt@kt.dtu.dk
Internet: <http://www.kt.dtu.dk>

Printed by: BookPartner, Nørhaven Digital
Copenhagen, Denmark

ISSN: 1604-5521

Contents

PREFACE TO GRADUATE SCHOOL YEARBOOK by Professor Kim Dam-Johansen	1
---	---

Contributions

Andersen, Michael <i>PM-IRRAS AS AN IN SITU METHOD FOR INVESTIGATIONS OF REACTIONS OF RELEVANCE FOR FUEL CELLS</i>	3
Andreasen, Anders <i>PREPARATION AND CHARACTERIZATION OF NEW METALS AND ALLOYS FOR HYDROGEN STORAGE</i>	5
Bagnoli, Mariana Gonzalez <i>TRANSPORT COEFFICIENTS IN HYDROCARBON MIXTURES UNDER MICROGRAVITY CONDITIONS</i>	7
Berenblyum, Roman <i>INTRODUCTION OF COMPLEX PHYSICS INTO STREAMLINE SIMULATION</i>	13
Biran, Suzan <i>STABILITY OF ENZYMES IN GRANULAR ENZYME PRODUCTS FOR LAUNDRY DETERGENTS</i>	17
Boisen, Astrid <i>STUDY OF ALLOY CATALYSTS FOR USE IN PRODUCTION OF HYDROGEN</i>	19
Bonné, Dennis <i>DATA DRIVEN MODELING OF BATCH PROCESSES FOR STATE ESTIMATION, CONTROL AND OPTIMIZATION</i>	23
Chakraborty, Debasish <i>ONE STEP FLAME SYNTHESIS OF DIRECT METHANOL FUEL CELL CATALYST</i>	27
Christensen, Mikkel Stochkendahl <i>COMPUTATIONAL FLUID DYNAMICS IN CHEMICAL ENGINEERING</i>	31
Christensen, Søren Gregers <i>MODELING OF ION EXCHANGE PROCESSES IN BOTH DILUTE AND CONCENTRATED SOLUTIONS</i>	35
d'Anterrodres, Loïc <i>GROUP CONTRIBUTION BASED PROCESS FLOWSHEET SYNTHESIS, DESIGN AND MODELLING</i>	39
Eden, Mario Richard <i>PROPERTY BASED PROCESS AND PRODUCT SYNTHESIS AND DESIGN</i>	43
Frederiksen, Søren Søndergaard <i>MODELLING OF THE ADSORPTIVE PROPERTIES OF WHEY PROTEINS ON ANION EXCHANGERS</i>	49
Hindiyarti, Lusi <i>GAS PHASE SULFUR, CHLORINE, AND ALKALI METAL CHEMISTRY IN BIOMASS COMBUSTION</i>	53
Jiménez, Edgar Ramírez <i>MODELING, DESIGN, OPERABILITY AND ANALYSIS OF REACTION-SEPARATION SYSTEMS WITH RECYCLE</i>	55
Johansen, Johnny <i>ACTIVATION OF METHANE BY PARTIAL OXIDATION IN MEMBRANE REACTORS</i>	59
Jørgensen, Kåre <i>THE EFFECT OF FORMULATION INGREDIENTS ON THE DRYING KINETICS AND MORPHOLOGY OF SPRAY DRIED ENZYME SUSPENSION PARTICLES</i>	61

Knudsen, Jacob Nygaard <i>TRANSFORMATION OF ASH-FORMING ELEMENTS DURING THERMAL CONVERSION OF ANNUAL BIOMASS</i>	67
Kouskoumvekaki, Irene A <i>PREDICTIVE EQUATION OF STATE FOR PAINTS</i>	71
Krogh, Anne <i>FROM STEP-SITES ON SINGLE CRYSTALS TO TECHNICAL CATALYSTS</i>	77
Larsen, Morten Boberg <i>COMBUSTION MECHANISMS USING WASTE AS A FUEL IN CEMENT PRODUCTION</i>	79
Li, Hong Wen <i>MODELING FOR DESIGN AND PREDICTIVE CONTROL OF INTEGRATED PROCESS PLANT</i>	81
van Lith, Simone C. <i>RELEASE OF INORGANIC METAL SPECIES, SULFUR AND CHLORINE DURING COMBUSTION OF WOODY BIOMASS ON A GRATE</i>	85
Medvedev, Oleg <i>TRANSPORT PROPERTIES IN FREE SPACE AND IN POROUS MEDIA</i>	89
Merino-García, Daniel <i>CALORIMETRIC INVESTIGATIONS OF ASPHALTENE SELF-ASSOCIATION AND INTERACTION WITH RESINS</i>	95
Monsalvo, Matías A. <i>PHASE BEHAVIOUR AND VISCOSITY MODELLING OF REFRIGERANT-LUBRICANT MIXTURES</i>	101
Rasmussen, Jan Kamyno <i>DATADRIVEN AND MECHANISTIC MODEL BASED CONTROL AND OPTIMIZATION OF FED-BATCH FERMENTATIONS</i>	103
Suñé, Núria Muro <i>PREDICTION OF THE SOLUBILITY AND DIFFUSION PROPERTIES OF PESTICIDES IN POLYMERS</i>	105
Sales-Cruz, Alfonso Mauricio <i>DEVELOPMENT OF A COMPUTER AIDED MODELING SYSTEM FOR BIO AND CHEMICAL PROCESS AND PRODUCT DESIGN</i>	109
Verdier, Sylvain <i>EXPERIMENTAL STUDY AND MODELLING OF ASPHALTENE PRECIPITATION CAUSED BY GAS INJECTION</i>	115
Villafáfila García, Ada <i>MODELING OF MINERAL SCALE DEPOSITION IN GEOTHERMAL AND OILFIELD OPERATIONS</i>	117
Winther-Jensen, Bjørn <i>MICRO-PATTERNING OF CONDUCTING POLYMERS</i>	119
Yebra, Diego Meseguer <i>EFFICIENT AND ENVIRONMENTALLY FRIENDLY ANTIFOULING PAINTS</i>	121
Zeuthen, Jacob <i>LABORATORY INVESTIGATION OF FORMATION OF AEROSOLS AND CHEMICAL REACTIONS IN FLUE GAS FROM BIOMASS- AND WASTE-COMBUSTION</i>	127

Preface to the Chemical Engineering Graduate School Yearbook

The 2003 Chemical Engineering Graduate School Yearbook is the first yearbook in a series of yearbooks to come, which will be published by the Department of Chemical Engineering, at the Technical University of Denmark on behalf of the graduate students associated to the department, and on behalf of the associated graduate schools: *MP₂T* in chemical engineering, and the graduate school of Polymer Science, which are both co-funded by the Danish Research Training Council - **FUR** under the Ministry of Science, Technology and Development.

In the graduate school yearbooks, graduate students in progress will present an annual status of their research project, while newly immatriculated graduate students will present the background and aims that motivate their studies. Readers of the yearbooks may thereby follow the progress of individual graduate students and studies from one year to another over the entire immatriculation period and read about the numerous research activities at the department.

This first edition of a graduate school yearbook sincerely illustrates the broad spectrum of research activities performed by graduate students associated to the department. Our graduate students demonstrate first class and innovative research by mastering the use of classical chemistry, chemical and biochemical engineering disciplines within major research fields such as: chemical kinetics and catalysis, process simulation and control, integration and development, reaction engineering, thermodynamics and separation processes, oil and gas technology, combustion, polymers, aerosols, mathematical modeling, and our new field of chemical and biochemical product design. The graduate students' individual works contribute significantly to the department's research activities, and is a factor that allows the department to continue to be among the leaders in its focused research areas.

It is with great pleasure that I present you **The Chemical Engineering Graduate School Yearbook 2003**.

Kim Dam-Johansen

Professor, Head of Department



Michael Andersen
Address: ICAT, Dept. of Chemical Engineering
Building 312
Technical University of Denmark
Phone: (+45) 45 25 31 36
Fax: (+45) 45 93 23 99
e-mail: manders@fysik.dtu.dk
www: www.icat.dtu.dk
Supervisor(s): Ib Chorkendorff
Søren Dahl, Haldor Topsøe A/S
Ph.D. Study
Started: 1 September 2002
To be completed: September 2005

PM-IRRAS as an *in situ* Method for Investigations of Reactions of Relevance for Fuel Cells

Abstract

The fundamental mechanisms behind the poisoning of fuel cells such as the PEMFC and the DMFC will be investigated, the goal is to gain knowledge about the fundamentals and thereby enhance the development of better catalysts for anode material by for example alloying. This work includes the identification of surface species under catalytic reactions such as methanol reforming and CO exchange on platinum. In order to perform *in situ* experiments an existing UHV chamber has been rebuilt and a PM-IRRAS system capable of detection of surface species under reaction conditions is being installed.

Introduction

The study of adsorption of molecules on surfaces under well-defined conditions gives much needed insight into the kinetics and thermodynamics governing heterogeneous reactions. For many years experiments have been carried out under UHV (Ultra High Vacuum) conditions with pressures in the order of 10^{-8} Pa. Even though much knowledge has been gained during such experiments, attention has been given to the fact, that pressure conditions in industrial production are many orders of magnitude larger. This is the so-called pressure gap, and it is well known, that this difference in conditions can have great influence on the state of a surface, especially concerning alloys, where surface segregation is an important issue. When developing catalysts for heterogeneous reactions, insight into the coverage of the catalyst surface and the nature of adsorbents is vital. Often improving a catalysts means lowering the chemisorption energy of the most abundant species on the catalyst surface as this species may lead to self-poisoning of the catalyst. The chemisorption energy of smaller molecules on late transition metals can be manipulated by inducing stress or strain on atom by alloying. The trend is, that induced strain increases chemisorption energy, while compression leads to a decrease in chemisorption energy[1]. This knowledge is a helpful guideline in designing new catalysts, but experiments identifying the most abundant species and its coverage under reaction conditions are needed. Such insight can only be gained under operating conditions.

Thus new methods for analysis of well-defined systems under ambient pressures have been developed. Among these is PM-IRRAS (polarization modulated infrared reflection absorption spectroscopy). This method is based upon the fact, that if a plane metal surface is illuminated by p- or s-polarized infrared light at near grazing incidence, around 80° , only p-polarized can be absorbed by vibrational and rotational excitation of adsorbents, as the electrical component of s-polarized light will vanish due to destructive interference. In PM-IRRAS a fast modulation between s- and p-polarized light combined with electrical filtering and demodulation makes it possible to extract the reflectivities ($R_p - R_s$) and ($R_p + R_s$) of the sample. By taking the ratios between these, the sample absorption can be distinguished from gas phase absorption [2].

Specific Objectives

The idea behind this Ph.D. project is to investigate the poisoning mechanism in fuel cells such as the PEMFC (polymer electrolyte membrane fuel cell) and the DMFC (Direct methanol fuel cell). The key parameters are the nature of the poisoning adsorbents and the dynamics of the system. In this field results from *in situ* methods such as PM-IRRAS are needed, both from the viewpoint of understanding the fundamental mechanisms and for developing better and more resistant catalysts. To meet this lack of results an existing UHV chamber will be completely rebuilt and fitted with a new high-pressure cell and a PM-IRRAS

setup. Initial experiments will be done on platinum single crystals. In time focus will be turned upon alloys, made by metal evaporation on single crystals.

Experimental

Figure 1 shows a representation of the rebuild UHV system. A metal single crystal is mounted in such a way, that it can be annealed to above 1000°C or cooled if needed. The chamber is fitted with ion guns, allowing cleaning of the sample by sputtering with Ar ions. Also the sample can be sputtered with He ions with the purpose of achieving LEIS (low energy ion scattering) spectra. Other methods of analysis available on the chamber are XPS (X-ray photoemission spectroscopy), LEED (low energy electron diffraction), TPD (temperature programmed desorption) and HREELS (high resolution electron energy loss spectroscopy). The chamber is equipped with a range of gas dosers, and 2 metal evaporators wherefrom different metal can be dosed.

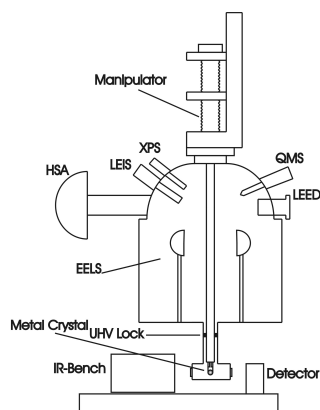


Figure 1: Schematic overview of the UHV chamber

Dynamics in the Platinum-CO system

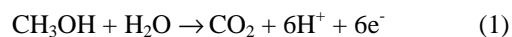
It is now well established, that CO present in hydrogen fuel is one of the major causes of poisoning of the anode in low temperature fuel cells such as the PEMFC. This poisoning reduces the cell voltage significantly, thereby of course lowering the efficiency [3]. As CO is inherently present in syngas, the major source of hydrogen fuel today, this presents an important problem. A clean up of the gas is expensive, and research has been focused towards improving anode catalysts. The best catalysts currently known are all platinum alloys, with platinum-ruthenium catalysts being the most promising. Two different theories have been developed to explain this enhancement relative to pure platinum. The first is the so-called ligand effect, which states that alloying with ruthenium causes surface platinum atoms to weaken interaction with CO. The other theory, the bifunctional theory, states that surface ruthenium atoms dissociate water and removes CO from platinum by oxidation.

We plan to use PM-IRRAS to examine the dynamic properties of the platinum-CO system. Experiments measuring the exchange of C¹⁸O with C¹⁶O from the

surface will be carried out. By evaporation of different metals onto the platinum crystal, the effect of alloying can also be measured. Finding a catalytic alloy, which allows the water-gas reaction to proceed at the working temperature of the fuel cell, would of course be a major breakthrough for the hydrogen fuel cell.

Methanol Reforming

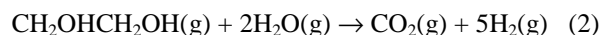
Equation 1 shows the anode reaction in the DMFC is the following:



In methanol reforming the same overall reaction proceeds, however in this case hydrogen atoms recombine to produce hydrogen gas. The DMFC suffers from even worse loss of cell voltage due to poisoning as the PEMFC. In this case the poisoning species is not necessarily CO. Studies done on methanol synthesis on copper have shown that formate is the predominant surface species. PM-IRRAS studies could be very useful to identify the surface species and the reaction-limiting step in methanol reforming.

Glycol as a Possible Hydrogen Source

A possible renewable hydrogen source as an alternative to fossil fuels is the catalytic reforming of biomass. Even though this field has been given attention, the mechanisms in the reforming process are not well understood [4]. Again identification of surface species is information, which is needed to understand the fundamentals of reaction. In this project catalytic reforming of ethylene glycol is to be studied as a model reaction. Equation 2 shows the reaction:



Results

The UHV chamber has been rebuild and the PM-IRRAS equipment is currently being optimized and tested. The first project to be undertaken is the examination of dynamical behavior of the platinum-CO system.

Acknowledgements

We thank STVF for financing the rebuilding and purchasing of new equipment through the "Towards the Hydrogen Society" research programme.

References

1. I. Chorkendorff, J. W. Niemantsverdriet, Concepts of Modern Catalysis and Kinetics, Wiley-VCH GmbH & Co, Weinheim, Germany, 2003, p. 252.
2. T. Buffeteau, B. Desbat, J. M. Turlet, App. Spectrosc. 45 (3) (1991) 380-389.
3. V.M. Schmidt, U. Stimming, F. Trila, J. Electrochem. Soc., 143 (1996) 3838.
4. R. D. Cortright, R. R. Davda, J. A. Dumesic, Nature, 418 (2002) 964-967.



Anders Andreassen
Address: Materials Research Department
Risø National Laboratory
Frederiksborgvej 399
DK-4000 Roskilde, Denmark.
Phone: (+45) 46 77 57 76
Fax: (+45) 46 77 57 58
e-mail: anders.andreassen@risoe.dk
www: www.risoe.dk/afm/personal/andr/andr.htm
Supervisor(s): Ib Chorkendorff
Allan Schrøder Pedersen, Risø
Flemming Besenbacher, Aarhus University
Søren Dahl, Haldor Topsøe A/s

Ph.D. Study
Started: 1 October 2002
To be completed: October 2005

Toward a hydrogen based society:
**Preparation and Characterization of New Metals and Alloys
for Hydrogen Storage¹**

Abstract

The main objective for this Ph.D. project is to explore new metals and alloys for hydrogen storage by forming metal hydrides. In order to be realizable as hydrogen storage medium for mobile applications there are specific demands to the properties of a metal hydride candidate to be met. Besides that it should contain enough hydrogen to be of practical interest it should also take up hydrogen and subsequently release it at an appropriate speed (kinetics) and at least, it should also be able to supply hydrogen to the engine at a sufficiently low temperature (thermodynamics). Different ways of tailoring the kinetic and thermodynamic properties are investigated in this project.

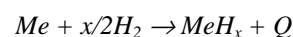
Introduction

The hydrocarbon based society may eventually face problems due to limited reserves of fossil fuel. Hydrogen has been proposed as a promising alternative energy carrier to hydrocarbons (coal, oil, natural gas): *i*) it can be utilized from renewable energy sources through electrolysis of water using electricity produced by wind mills, solar cell or water power *ii*) Ideally, the only combustion product is water *iii*) The heat of combustion pr. mass is very high approx. 3 times higher than liquid hydrocarbons.

For the hydrogen society to be fully implemented there are however some challenges to be met e.g. The fuel cell technology must be matured and a proper way of storing hydrogen must be found (more could be mentioned). These challenges are dealt with in the Danish research project "*Toward a hydrogen based society*" with the following participants: Technical University of Denmark, Risø National Laboratory, Aarhus University, IRD fuels cells, Haldor Topsøe A/S and Danfoss. The main topic of the Ph.D. Project described here is to explore metals and alloys for reversible hydrogen storage.

Metal hydrides

Many metals and alloys are known to react with hydrogen under formation of metal hydride and release of heat:



In order to be of practical interest the US Department of Energy has determined that a potential metal hydride storage material must be able to absorb at least 6.5 wt. % hydrogen and that thermodynamics enable desorption of hydrogen at around $T_{des} = 100$ °C. The specified gravimetric capacity allows a fuel cell powered car to have a working radius of approx. 400 km [1]. For instance magnesium reacts with hydrogen and forms MgH_2 . Thus, magnesium is capable of storing 7.6 wt. % of hydrogen. However, magnesium suffers from poor thermodynamics (approx. 300 °C is required to desorb hydrogen at 1 bar corresponding to a heat of reaction of approx. 75 kJ/mol) and according to some, poor kinetics.

¹ The Danish Technical Research Council through research grant #2025-01-0054 finances the project.

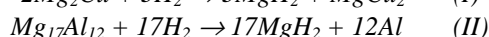
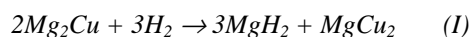
Improving kinetics and thermodynamic properties

The equilibrium desorption pressure is given by the van't Hoff equation:

$$\ln(p_{eq}/p_{ref}) = -\Delta H/(RT) + \Delta S/R$$

From the above equation it can easily be calculated that for a material to desorb hydrogen at 1 bar and 100°C the enthalpy of formation of the hydride must equal approx. 48 kJ/mol.

It is possible to alter the thermodynamic properties by alloying e.g. Mg₂Ni forms Mg₂NiH₄ from which hydrogen desorbs at 280°C which is a slight improvement. However, the hydrogen density is reduced to 3.6 wt. %. Below are other examples:



For both of the above reactions desorption of hydrogen at 1 bar takes place at approx. 280°C. The hydrogen capacity is 2.6 wt. % and 4.4 wt. %, respectively.

Improved kinetics may be achieved in a variety of different ways e.g. reduction of particle size by ball milling [2] thereby reducing the diffusion path and increasing the active surface area for hydrogen dissociation, adding small amounts of transition metal that catalyzes the dissociation of H₂.

From time resolved in-situ powder x-ray diffraction (TRIPXD) of Mg and Mg with 2 wt. % Ni at different temperatures by constructing transformation curves from the integration of selected diffraction peaks and performing an Arrhenius analysis we have found that Ni reduces the effective activation barrier of dehydrogenation of MgH₂ with approx. 50 kJ/mol. With the use of TRIPXD we have also studied the dehydrogenation of MgH₂ + MgCu₂, MgH₂ + Mg₂Cu, MgH₂ + Al (see figure 1 below) and LiNH₂ + LiH [3].

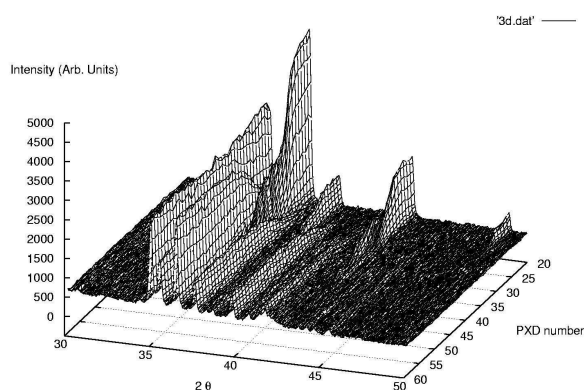


Figure 1 Time-resolved in-situ powder x-ray diffraction of the dehydrogenation of MgH₂ + Al to Mg,Al

It is well known that most materials that readily react with hydrogen also are very sensible to impurities of oxygen and water. Formation of a surface oxide layer of e.g. magnesium powder slows down the kinetics remarkably. To study the hydrogenation and dehydroge-

nation of powders at conditions essentially free of impurities a new apparatus have been designed at ICAT² (cf. figure 2 for a simplified layout), which is currently being tested. It allows evacuation of the system down to approx. 10⁻⁸ mbar. The hydrogen uptake can be determined from a pressure change in a container with a known volume and the process may also be monitored by the measured mass flow. The hydrogen desorption can be monitored in a similar fashion. The quadropole mass spectrometer (QMS) allows monitoring of leaks and impurities and allows for desorption experiments where the hydrogen signal is measured. The reactor is a custom build ball-milling container that can be dismounted and transported to a ball mill without exposing the sample to air. Ball milling optimally reduces the particle size to approx. 100 nm and allows mechanical alloying e.g. by introducing a small amount of a catalytically active material to the sample this may be deposited on the surface of the powder and during the ball milling process. A similar but simpler apparatus is also being made at Risø.

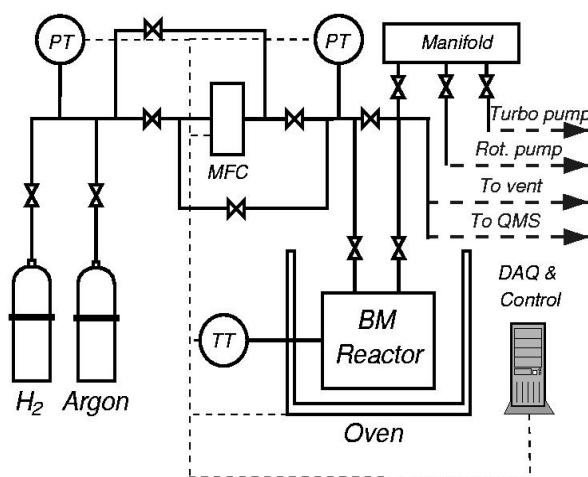


Figure 2 Apparatus for studying hydrogenation/dehydrogenation of ball milled (BM) powder samples

Conclusions

The effect on the activation barrier of dehydrogenation of MgH₂ by doping with Ni has been investigated with TRIPXD. Scientific apparatus to test hydrogenation properties at clean conditions have been constructed. The work is continuing with focus on alloying, ball milling and catalysis in order to improve the properties of hydrogen storage candidates.

References

1. L. Schlapbach and A. Züttel, *Nature* 414 (2001) 353-358
2. A. Zaluska, L. Zaluski and J.O. Ström-Olsen, *Appl. Phys. A* 72 (2001) 157-165
3. P. Chen, Z. Xiong, J. Luo, J. Lin and K. L. Tan, *Nature* 420 (2002) 302-304

² The work has been coordinated by Post. Doc. Jon Davies, Department of Physics, DTU and many (both students and technicians) have contributed so far.



Mariana Gonzalez Bagnoli
Address: IVC-SEP, Dept. of Chemical Engineering
Building 229, Office 250
Technical University of Denmark
Phone: (+45) 45 25 28 87
Fax: (+45) 45 88 22 58
e-mail: mgb@kt.dtu.dk
www: www.ivc-sep.kt.dtu.dk
Supervisor(s): Alexander Shapiro
Erling Stengby
Ph.D. Study
Started: 1 August 2001
To be completed: July 2004

Transport Coefficients in Hydrocarbon Mixtures under Microgravity Conditions

Abstract

It is of great importance in petroleum engineering to determine the transport coefficients associated with the fluxes occurring inside a reservoir. There is vast literature on this subject and different approaches for determining the coefficients involved can be obtained, like gravity effect, pressure gradient and even temperature gradient. For the last case, also known as Soret effect, the literature is mainly referring for binary mixtures and the extension for multicomponent systems is not be easily or can not be done. Furthermore, the combination of gravity and thermal gradient almost always leads to convection, being difficult to analyze the Soret effect independently. The involvement of space technology is required to obtain reliable measured data. It is the goal of this project to put some light into the inconsistencies, propose good correlations for the prediction of the Soret coefficient in a general way so in can be applied both for binary and multicomponents.

Introduction

Within petroleum engineering it is important to estimate the composition of the fluids that impregnate the reservoir and the fluxes between the different reservoir units in order to get an optimal development of the field [8]. Several forces may contribute to the distribution of the components in a reservoir, among them, gravity, thermal gradient, pressure gradient, etc. Gravity has the most striking effect and has been widely studied. However of its importance, it was not enough to correctly estimate the distribution of the components inside a reservoir and other forces had to be taken into account. The pressure gradient has been satisfactorily incorporated by the use of Darcy's law. Further detail analysis had been done for diffusion, where the link between the measured Fick diffusion coefficients and the Maxwell-Stephan diffusion coefficients had been obtained and studied [18]. However when considering the thermal force big uncertainties are found, especially for multicomponent mixtures. The correct estimation of the transport coefficients involved in the description of the fluxes occurring inside the reservoir is crucial for an optimal evaluation of the composition.

Our motivation for the study is to understand the irreversible processes occurring inside the reservoir in order to find correlations for the prediction of the transport coefficients. We focus our work mainly on the

thermal diffusion effect. There is a vast literature on this area, also know as Soret effect, which is mainly limited to binary mixtures. For multicomponent systems several uncertainties appeared due to the fact that the definitions are given for a two component system [13] and the extension to multicomponent is not direct.

Furthermore, the combination of gravity and heating almost always leads to convection, being difficult to analyze each effect separately. There is no reliable method to determine the thermal diffusion coefficients on the Earth. Therefore the involvement of the space technologies is necessary, in order to interpret the results of the measurements correctly [19]. The value of the Soret coefficient obtained in the space may serve as a basis for selection of the right experimental method for routine determination of the transport coefficients and calibration of the experimental data obtained on the Earth. Presently IVC-SEP is participating in the **SCCO project (Soret Coefficient in the Crude Oil)?** related to the measurements of the transport properties performed under microgravity conditions. Several institutions and industries are involved in the same project as MIRC (Microgravity Research center – Université Libre de Bruxelles), Total (Industrial partner), Department of Aerospace, Mechanical and Industrial Engineering of Ryerson, Polytechnic University, Master-ENSCP (laboratory of ENSCPB is

associated to Bordeaux I University) and C-CORE (a non-profit research corporation located on the campus of Memorial University of Newfoundland in St-John's). The aim of the project is to measure the thermal diffusion coefficient in hydrocarbon mixtures. Unfortunately the previous launch failed and experiments were obtained. A new laboratory box is being created at the present time. The new launch is expected for 2005 where diffusion and thermal diffusion coefficients are going to be measured for the different types of systems.

The goal of the thesis is within the frame work of the **SCCO project**, to study the transport coefficients, analyzing the experimental values (which unfortunately will not be ready before the end of the thesis) and find correct estimations for their determination. It is the purpose of the present paper to show the results obtained so far. Firstly, calculations for binary mixtures will be presented, presenting the existent models and their dependency with the equations of state used for their estimation. The results had been compared with experimental data. Furthermore, an analysis for ternary systems, as a first approach to multicomponent mixtures, will be presented. The results will be compared with some molecular dynamics data found in the literature. Further work has been performed on the theory. Finally an insight to the theory will be presented.

Calculations in Binary Systems

Along the years several thermodynamic models for the thermal diffusion factors for binary mixtures have been proposed. Seven of these models had been tested in combination with different equations of state. These are: Rutherford and Drickamer [10], Dougherty and Drickamer [1,2], Haase [4], Kempers [6], Kempers [7], and Shucla and Firoozabadi [12]. In its beginning the modeling for the thermal diffusion factor was largely based on the work of Denbigh [14], who described in detail the thermodynamic approach to thermal diffusion based on the concept of the thermal heat of transport. Most of the proposed models have been based on this concept, with different expressions for the heats of transport, like, Rutherford and Drickamer, Dougherty and Drickamer and even Shucla and Firoozabadi.

Denbigh determines individual heats of transport Q_i of the components in the mixture in the following way: Let us assume that a mixture is divided into the two layers or regions, each at a different thermodynamic state. The heat of transport of a component i is defined as the heat that must be provided in layer I and removed from layer II in order that a mole of this component may pass from state I to state II, with temperature and pressure constant.

An expression for the thermal diffusion factor of a binary mixture in terms of the heats of transport depends on the "system of coordinates" with regard to which the relative motion of the species of the mixture is considered: whether it is associated with the centre of

masses, of volumes, or of molar amounts. The general expression is as follows:

$$\alpha = \frac{a_1 Q_2 - a_2 Q_1}{a z_1 \left(\frac{\partial \mu_1}{\partial z_1} \right)} \quad \text{Equation (1)}$$

Here a_i ($i=1,2$) are the partial molar properties corresponding to the system of coordinates selected: partial molar volumes V_i for the system associated with the center of volumes, molar masses M_i for the center of masses, and unities for the center of molar amounts. The value of a is an average determine as $z_1 a_1 + z_2 a_2$. Some authors do not compute the absolute values of the heats of transport, but the relative values with regard to a fixed (normally, ideal) state. If the superscript 0 refers to this state, Equation (1) is modified to

$$\alpha = \frac{\alpha_r^0 RT}{z_1 \frac{\partial \mu_1}{\partial z_1}} + \frac{a_1(Q_2 - Q_2^0) - a_2(Q_1 - Q_1^0)}{a z_1 \frac{\partial \mu_1}{\partial z_1}} \quad \text{Equation (2)}$$

The ideal state is normally considered as a state at a small pressure, where the mixture becomes an ideal gas. In this case the value of α_r^0 is computed on the basis of the Boltzmann gas kinetic theory. The formula for the thermal diffusion ratios for binary mixtures, in the first approximation of the Chapman-Enskog expansion, may be found in Hirshfelder, 1954 [15].

The different models will not be explained in detail, just a small introduction to the equations will be made. Detailed explanation can be found in the correspondent references. To begin, we have Rutherford and Drickamer [10] who presented an approach for evaluation of the heats of transport based on a molecular model for such transport, obtaining an expression like

$$\alpha = \frac{(z_1 H_1^{1/2} + z_2 H_2^{1/2})(H_2^{1/2} - H_1^{1/2})}{2(RT - z_1 z_2 (H_1^{1/2} - H_2^{1/2})^2)} \quad \text{Equation (3)}$$

Dougherty and Drickamer [1] presented an approach based on the previous work of Rutherford and Drickamer, but the energies involved were expressed in the final expression as functions of the internal energies of the mixtures and of the solution, finding an equation of the type

$$\alpha = \frac{1}{\tau} \frac{U_1 - U_2 - U_e}{z_1 \frac{\partial \mu_1}{\partial z_1}} \quad \text{Equation (4)}$$

In the same year, Dougherty and Drickamer [2] presented a second approach where the heats of transport were calculated from viscosity measurements and the solution thermodynamic data. They expressed the thermal diffusion factor in terms of the activation energies $U_{a,i}$:

$$\alpha = \frac{M_1 V_2 + M_2 V_1}{2M} \left(\frac{U_{a,2}}{V_2} - \frac{U_{a,1}}{V_1} \right) \frac{1}{z_1 \frac{\partial \mu_1}{\partial z_1}} \quad \text{Equation (5)}$$

Haase [4] obtained the formula for the thermal diffusion factor by exploiting analogy with barodiffusion. The thermal diffusion factor was expressed in a way similar to Equation (2), with the values of a_i equal to the molecular weights, and Q_i equal to the partial molar enthalpies:

$$\alpha = \frac{\alpha_r^0 RT}{z_1 \frac{\partial \mu_1}{\partial z_1}} + \frac{M_1(H_2 - H_2^0) - M_2(H_1 - H_1^0)}{M z_1 \frac{\partial \mu_1}{\partial z_1}} \quad \text{Equation (6)}$$

Shucla and Firoozabadi [12] based their theory on the approach by Dougherty and Drickamer. Their modified expression for the thermal diffusion factor had the form of:

$$\alpha = \frac{\frac{U_1}{\tau_1} - \frac{U_2}{\tau_2}}{z_1 \left(\frac{\partial \mu_1}{\partial z_1} \right)_{T,P}} + \frac{(V_1 - V_2) \left(z_1 \frac{U_1}{\tau_1} + z_2 \frac{U_2}{\tau_2} \right)}{V z_1 \left(\frac{\partial \mu_1}{\partial z_1} \right)_{T,P}} \quad \text{Equation (7)}$$

For practical calculations the authors used the values of $\tau_1 = \tau_2 = 4$. Let us note that for this case Equation (8) is reduced to Equation (1) with a_i equal to partial molar volumes and Q_i equal to $U_i/4$.

Kempers [6,7] introduced a new way of calculating the thermal diffusion factor, by statistical mechanics and assuming that a non-equilibrium steady state is the macroscopic state accomplished by the maximum number of microstates. The canonical partition function for the whole system was expressed as the product of the canonical partition functions of each bulb, and maximized under two constraints: the material conservation and pressure equality in the whole system. In the first work of Kempers [6] the final expression for binary thermal diffusion factor was similar to Equation (1):

$$\alpha = \frac{V_1 H_2 - V_2 H_1}{V z_1 \frac{\partial \mu_1}{\partial z_1}} \quad \text{Equation (8)}$$

Such an expression for the thermal diffusion factor assumes some problems since the values of partial molar enthalpies are determined within a constant. In the second work (2002) Kempers [7] eliminated this constant and obtained the expression similar to Equation (2):

$$\alpha = \frac{\alpha_r^0 RT}{z_1 \frac{\partial \mu_1}{\partial z_1}} + \frac{V_1(H_2 - H_2^0) - V_2(H_1 - H_1^0)}{V z_1 \frac{\partial \mu_1}{\partial z_1}} \quad \text{Equation (9)}$$

The author assumed the centre of mass or the centre of volume to be fixed. In the first case he obtained Haase expression (7), and in the second case expression (10). The extension of the theory for multicomponent mixtures will be explain in the following section.

For simulation of partial molar properties involved in the models simple equations of state (EoS), such as Soave-Redlich-Kwong (SRK) and Peng-Robinson (PR) EoS were used. It was noticed that the thermal diffusion factors are extremely sensitive to the values of the

partial molar properties and, thus, to an EoS selected. Furthermore, two different corrections for the determination of the partial molar volumes were implemented; the Peneloux correction and the correction based on the principle of corresponding states.

A systematic comparison of all the existing models on the same sets of experimental data implementing different EoS has been carried out and two corrections for the partial molar volume, one based on the Peneloux [17] correction and a second one base on the corresponding states approach [16]. The models were tested against four sets of experimental data for binary systems, for which the thermodynamic properties may be calculated with common equations of state: n-Pentane + n-Decane [9], Benzene + Cyclohexane [1], Methane + Propane [5], Methane + n-Butane [11].

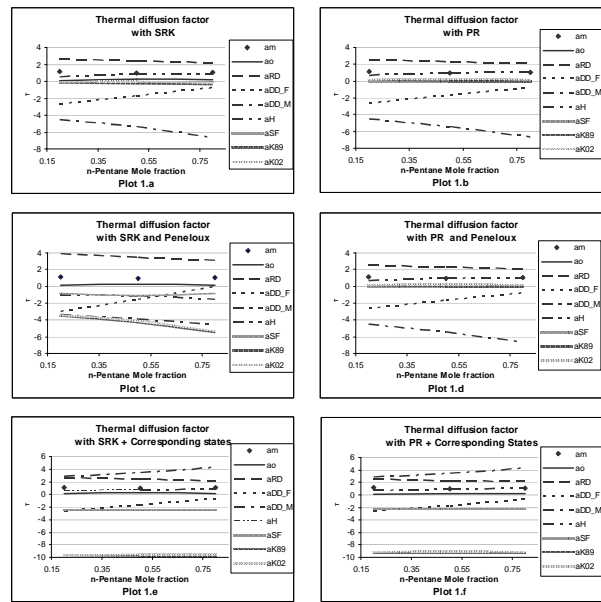


Figure 1: Comparison between experiments and calculations for the thermal diffusion factor for n-Pentane - n-Decane mixture at 300.15K and atmospheric pressure using different equations of state. The measured values are denoted by am. The calculated values are represented by seven curves, which represent the different models tested. Rutherford and Drickamer model is represented by aRD; Dougherty and Drickamer model by aDD_F; Dougherty and Drickamer by aDD_M; Haase by aH; Shucla and Firoozabadi by aSF; Kempers from 1989 by aK89; and finally Kempers from 2002 by aK02

The figures presented are organized in the same way for all the cases and general conclusions for all the calculations are presented after the figures. The thermodynamic properties are calculated by the SRK EoS (plots #.a, #.c and #.e), and the PR EoS (#.b, #.d and #.f). The Peneloux correction was used in plots #.c and #.d. The plots #.e and #.f are produced with application of the principle of corresponding states. # represents the correspondent figure number.

Figure 1 shows the results obtained for three different compositions of a mixture of n-Pentane + n-Decane at 300.15 K and atmospheric pressure.

The measurements of the thermal diffusion factor for the mixture of Benzene Cyclohexane were carried out by Dougherty and Drickamer [1] at 313K and atmospheric pressure, at three different concentrations. The results of comparison of the measured points with our simulation are shown in Figure 2.

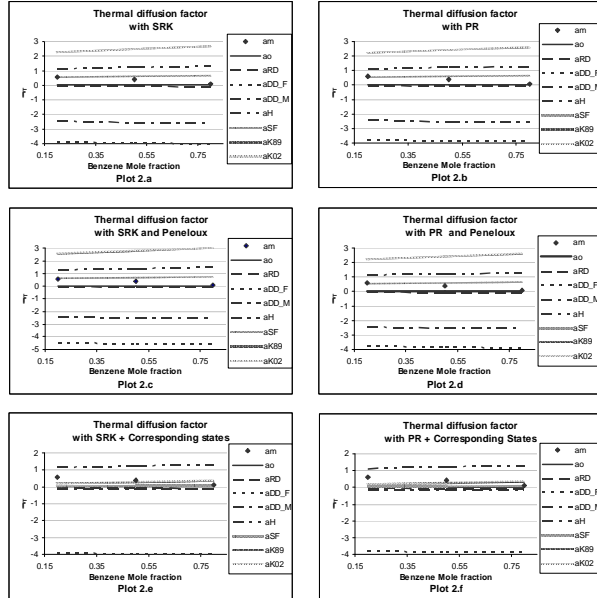


Figure 2: Comparison between experiments and calculations for the thermal diffusion factor for Benzene - Cyclohexane mixture at 313K and atmospheric pressure using different equations of state. The measured values are denoted by *am*. The calculated values are represented by seven curves, which represent the different models tested. Rutherford and Drickamer model is represented by *aRD*; Dougherty and Drickamer model by *aDD_F*; Dougherty and Drickamer by *aDD_M*; Haase by *aH*; Shucla and Firoozabadi by *aSF*; Kempers from 1989 by *aK89*; and finally Kempers from 2002 by *aK02*.

The measurements for the system of Methane Propane were carried out under near-critical conditions, at 346.08K and 5.6 MPa at seven different mole fractions. The experimental data were obtained by Haase, Borgmann, Dücker and Lee [5]. Comparison of the measured points with our simulations is shown in Figure 3

Finally we have Methane n-Butane mixture which measurements were carried out by Rutherford and Roots [11] for a single composition (40 molar percent of methane), but different pressures and temperatures.

One can see the Haase model (7) is the best for the systems of n-Pentane + n-Decane and Methane + n-Butane. For the systems of Benzene + Cyclohexane and Methane + n-Propane the best approach is that of Shucla and Firoozabadi (8). However for the last system the Haase model gives a good approximation as well. The Kempers model is capable of correctly predict the sign

of the thermal diffusion factor; however, it overestimates its value with respect to the experimental data.

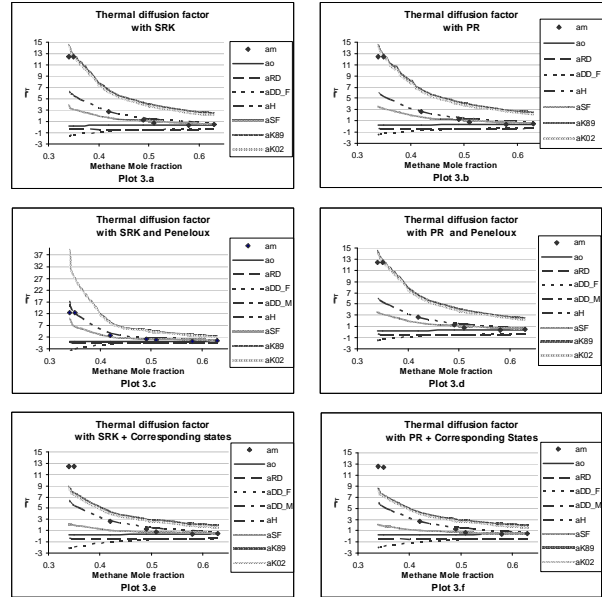


Figure 3: Comparison between experiments and calculations for the thermal diffusion factor for Methane - Propane mixture at 346.08 K and 5.6 MPa using different equations of state. The measured values are denoted by *am*. The calculated values are represented by seven curves, which represent the different models tested. Rutherford and Drickamer model is represented by *aRD*; Dougherty and Drickamer model by *aDD_F*; Dougherty and Drickamer by *aDD_M*; Haase by *aH*; Shucla and Firoozabadi by *aSF*; Kempers from 1989 by *aK89*; and finally Kempers from 2002 by *aK02*.

One may conclude that the Haase model provides generally the reasonable and stable results. The Shucla and Firoozabadi and the Kempers models may be better for some systems or experimental values, however they may give large errors for other systems. The models of Dougherty and Drickamer and of Rutherford and Drickamer do not provide good results with all the investigated mixtures, even for the mixtures of similar molecules, for which they were originally designed. We can confirm an observation by Kempers [7] that the thermal diffusion factors are very sensitive to the values of partial molar properties and, therefore, to an EoS chosen as well as to a method applied for calculation of the partial molar volume. As mentioned in the work of Kempers, there is a need for improving the existing equations of state in such a way that they are not only able to predict the phase equilibria, but also the partial molar properties with a high degree of accuracy. This is the well-known limitation for the presently available equations of state for hydrocarbon mixtures. It should be pointed out that the fact that the Peneloux corrections do not improve the results in the most cases (while they improve prediction of the partial molar properties) may

be interpreted as insufficiency and roughness of the existing models for the thermal diffusion factors.

Analyses for Multicomponent Systems

When studying the thermal diffusion effect in multicomponent mixtures we found the correlation of Kempres [6,7]. The expression for thermal diffusion factor was obtained in the same way as done for the binary mixtures, a general formulation can be

$$\sum_{j=1}^{N-1} \left(\frac{1}{a_i} \frac{\partial \mu_i}{\partial x_j} - \frac{1}{a_N} \frac{\partial \mu_N}{\partial x_j} \right) x_j (1-x_j) \alpha_{Tj} \quad \text{Equation (10)}$$

$$= \frac{h_N - h_N^0}{a_N} - \frac{h_i - h_i^0}{a_i} \quad (i = 1, \dots, N-1)$$

Here a_i ($i = 1, \dots, N$) are the partial molar properties corresponding to the system of coordinates selected: partial molar volumes V_i for the system associated with the center of volumes, molar masses M_i for the center of masses, and unities for the center of molar amounts. Some authors do not compute the absolute values of the heats of transport, but the relative values with regard to a fixed (normally, ideal) state. If the superscript 0 refers to this state, Equation (1) is modified to

$$\sum_{j=1}^{N-1} \left(\frac{1}{a_i} \frac{\partial \mu_i}{\partial x_j} - \frac{1}{a_N} \frac{\partial \mu_N}{\partial x_j} \right) x_j (1-x_j) \alpha_{Tj} \quad \text{Equation (11)}$$

$$= \frac{h_N - h_N^0}{a_N} - \frac{h_i - h_i^0}{a_i} + RT \left(\frac{\alpha_{Ti}^0 (1-x_N)}{a_i} - \frac{\alpha_{Tn}^0 (1-x_N)}{a_N} \right) \quad (i = 1, \dots, N-1)$$

The ideal state is normally considered as a state at a small pressure, where the mixture becomes an ideal gas. In this case the value of α_{Ti}^0 is computed on the basis of the Kinetic gas theory [15]. Analyzing the expressions given a general approach for the computation of the thermal diffusion factor can be given as

$$\sum_{j=1}^{N-1} \left(\frac{1}{a_i} \frac{\partial \mu_i}{\partial x_j} - \frac{1}{a_N} \frac{\partial \mu_N}{\partial x_j} \right) x_j (1-x_j) \alpha_{Tj} \quad \text{Equation (10)}$$

$$= \frac{e_N - e_N^0}{a_N} - \frac{e_i - e_i^0}{a_i} + RT \left(\frac{\alpha_{Ti}^0 (1-x_N)}{a_i} - \frac{\alpha_{Tn}^0 (1-x_N)}{a_N} \right) \quad (i = 1, \dots, N-1)$$

Here a_i ($i = 1, \dots, N$) are the partial molar properties as mention before and e_i, e_i^0 ($i = 1, \dots, N$) is the measure of the energetic state of each component in the mixture and in the ideal gas state.

Since there are no experimental data on the thermal diffusion coefficient in multicomponent mixtures the models were compared with some molecular dynamic results [3]. The simulations were performed neat the critical point at constant reduce conditions, in order to assure we are at the same distance from the critical

point. The real temperature and pressure are calculated from the relations

$$T = T^* \varepsilon_x / k_B \quad \text{Equation (12)}$$

$$P = P^* \varepsilon_x / \sigma_x^3 \quad \text{Equation (13)}$$

Where T, T^*, P, P^* are the temperature, reduce temperature, pressure and reduce pressure correspondingly. k_B is the Boltzmann constant. The mainly difficulty is to find appropriate relations for σ_x (typical atomic diameter) and ε_x (interaction strength coefficient characteristic of the mixture). In agreement with the reference paper we have used the van der Waals one-fluid (vdW1) approximation that for an N-component mixture will be

$$\sigma_x^3 = \sum_{i=1}^N \sum_{j=1}^N x_i x_j \sigma_{ij}^3 \quad \text{Equation (14)}$$

$$\varepsilon_x \sigma_x^3 = \sum_{i=1}^N \sum_{j=1}^N x_i x_j \varepsilon_{ij} \sigma_{ij}^3 \quad \text{Equation (15)}$$

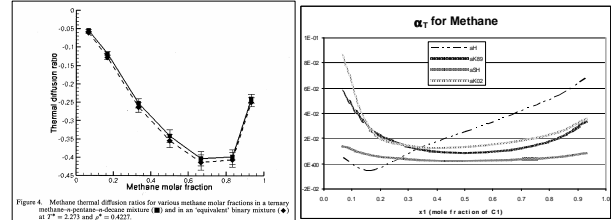


Figure 4: Comparison between molecular dynamic simulations and calculations for the thermal diffusion factor of Methane in a ternary mixture of Methane - n-Pentane - n-Decane mixture at constant reduce temperature 2.273 and reduce pressure 1.017 using SRK equations of state. The simulations are shown in the first graph. The calculated values are represented by four curves, which represent the different models tested. Haase by aH; Shucla and Firoozabadi by aSF; Kempers from 1989 by aK89; and finally Kempers from 2002 by aK02.

The calculation for the thermal diffusion factor was done on a ternary mixture of Methane, n-pentane and n-decane at constant reduce temperature ($T^* = 2.273$) and constant reduce pressure ($P^* = 1.017$). The original expression of Kempers both for volume frame of reference and mass frame of reference (Haase approximation) were used. Furthermore, an extension of Shucla and Firoozabadi model for multicomponent mixture has been calculated as well. The results obtained are shown in Figure 4.

Big discrepancy with the literature data is observed. To begin with both results differed in the sign. The values of the thermal diffusion factor differed with those in the literature by an order of 10. Comparing the curves no similarity in the trends can be seen for any of the models.

Most of the actual models are based on the theory of de Groot [13]. In his book most of the definitions for the different coefficients describing the thermal diffusion

effect, (Soret coefficient, thermal diffusion factor, thermal diffusion ratio) are given for binary systems. However, some authors [5,6,7] extended this theory to multicomponent systems. Two different expression for the variation of composition with temperature were found

$$\Delta c_1 = -c_1(1-c_1)\alpha_T\Delta T/T \quad \text{Equation (16)}$$

$$\Delta x_i = -x_i(1-x_i)\alpha_{Ti}\Delta T/T \quad \text{Equation (17)}$$

Equation (16) is defined by de Groot for binary systems, while equation (17) is given by Kempers, based on de Groot, form multicomponent mixtures. We performed the transcription from one equation to the other one, finding for binary mixtures that both equations are equivalent. However in multicomponent mixtures both equations are related by

$$\alpha_{Ti}^{mass} / \alpha_{Ti}^{molar} = (1-x_i) \left(\sum_{j=1}^{n-1} x_j(Mr_j - Mr_n) - x_i(Mr_i - Mr_n) \right) / \left(\sum_{j=1}^{n-1} x_j(Mr_j - Mr_n) - x_i Mr_i \right) \quad \text{Equation (18)}$$

It is evident that both definitions are not equivalent in the case of three or more component. Molar and mass diffusion coefficient should be defined according to the reference used. However of its importance this has not previously been specified.

Conclusions

We have shown the performance of the existing models against experimental data, finding some good correlations for some of the mixtures. However, our work was complicated by the fact that the experimental data on thermal diffusion coefficients are relatively difficult to find. It may be hoped that the existing models for thermal diffusion coefficients will be checked better as the new reliable methods for measuring the thermal diffusion coefficients and the new values of these coefficients will appear.

Furthermore, there is thus a need for a comprehensive theory that can explain and predict the thermal diffusion effect in mixtures of three or more components. It is the goal of the thesis to be able to find such a theory that can correctly describe the thermal diffusion effect in this type of mixtures, clarifying the discrepancies. And finally apply the theory for the determination of the fluxes appearing in the reservoir of so much interest for the petroleum companies.

Acknowledgements

I will like to thank Francois Montel and Guillaume Galliero for very fruitful discussion during my stay in Total, (Pau, France).

References

1. DOUGHERTY, E.L. JR., and DRICKAMER, H.G., 1955, *J. Chem. Phys.*, **23**, 295-309

2. DOUGHERTY, E.L. JR., and DRICKAMER, H.G., 1955, *J. Chem. Phys.*, **59**, 443-449
3. GALLIERO, G., 2003, *Philosophical Magazine*, **83**, 2097
4. HAASE, R., 1949, *Z. Phys.* **127**, 1
5. HAASE, R., BORGMANN, H.W., DÜCKER, K.H., LEE, W.P., 1971, *Z Naturforsch .Teil A*, **26**, 1224
6. KEMPERS, L.J.T.M., 1989, *J. Chem. Phys.*, Vol. 90, Nr. 11, 6541-6548
7. KEMPERS, L.J.T.M., 2002, IN: *Thermal non-equilibrium phenomena in Fluid Mixtures*,
8. MONTEL, F., BICKERT, J., HY-BILLIOT, J., ROYER, M., 2003, *SPE*, 1
9. PERRONACE A., LEPPLA C., LEROY F., ROUSSEAU B., WIEGAND S., 2002, *J. Chem. Phys.*, Vol. 116, Nr. 9, 3718-3729
10. RUTHERFORD, W.M., DRICKAMER, H.G., 1954, *J. Chem. Phys.*, Vol. 22, Nr. 7, 1157-1165
11. RUTHERFORD, W.M., ROOF, J.G., 1959, *AIChE Journal*, **63**, 1506-1511
12. SHUCLA, K., FIROOZABADI, A., 1998, *Ind.Eng.Chem. Res.*, **37**, 3331-3342
13. DE GROOT, S.R., 1952, *The Thermodynamic of Irreversible Processes*, Chapter 4
14. DENBIGH, K.G., 1951, *The Thermodynamic of Steady State*, Chapter 2
15. HIRSCHFELDER J.O., CURTIS C.H., BIRD R.B., 1954, *Molecular Theory of Gases and Liquids*, Chapter 8
16. MOLLERUP J.M., MICHELSEN M.L., 1992, *Fluid Phase Equilibria*, **74**, 1-15
17. PRAUNITS, J.M., LICHTENTHALER R.N., GOMES DE AZEVEDO E., 1999, *Molecular thermodynamics of fluid-phase equilibria, Third Edition*.
18. GANI R., KONTOGEORGIS G., 2002, *Computer Aided Property Estimation, Edition5*. Elsevier 2002

List of Publications

1. GONZALEZ-BAGNOLI, M.G., SHAPIRO A.A., STENGBY E.H., 2003, *Phys. Magazine*, **83**, 2171-2183



Roman Berenblyum
Address: IVC-SEP, Dept. of Chemical Engineering
Building 229, Office 262
Technical University of Denmark
Phone: (+45) 45 25 28 89
Fax: (+45) 45 25 28 00
e-mail: rb@kt.dtu.dk
www: www.ivc-sep.kt.dtu.dk
Supervisor(s): Erling H. Stenby
Michael L. Michelsen
Alexander A. Shapiro

Ph.D. Study
Started: 1 September 2001
To be completed: September 2004

Introduction of Complex Physics into Streamline Simulation

Abstract

The focus of a research is an introduction of capillary effects into streamline simulation. The black oil streamline simulator [3DSL 0.25 by R.P. Batycky, SUPRI-C group, Department of Petroleum Engineering, Stanford University, 1997] is modified to incorporate capillary effects.

The new simulator (CapSL) is applied to a number of simulation cases. The influence of different factors that may impact performance prediction of water floods is investigated. The capillary forces are demonstrated to stabilize the displacement front and increase oil production even in rather viscous-dominated cases.

The new approach can provide a fast and a reliable tool for the simulation of water flooding in low permeable and heterogeneous oil reservoirs as well as for reservoir screening and upscaling studies.

Introduction

Reservoir simulators based on the streamline principle have been developed as an alternative to conventional finite difference simulators. The main advantages of the streamline simulators are the high speed and the smaller impact of the numerical dispersion, making them useful tools for fast evaluation of multiple methods of reservoir development prior to computationally expensive full-scale simulations. A limitation of the currently available black-oil streamline simulators is the absence of a representation of the effect of capillary forces.

Streamline methods work well for flows that are dominated by convection. They are less well suited to describe physical phenomena that transport fluid across the streamlines. In the streamline method the flow along each streamline is treated as independent, and the effects of flow transverse to the streamlines are not represented. Capillary pressure difference between phases, for example, can lead to flow transverse to streamlines. In some flow settings, capillary forces can alter significantly the character of the flow, as crossflow drives imbibition of wetting phase into low permeability zones adjacent to high permeability flow paths.

Here I present the streamline simulator, modified to incorporate capillary effects. Modification of the pressure equation changes the locations of the streamlines. Modification of the saturation equation

allows description of crossflow effects by means of an operator splitting technique [1]. I briefly discuss the modification of governing equations to account for the gravity and the capillary forces. The focus is made on the prediction of water flooding performance in cases when capillary and gravity effects cannot be neglected. The potential, advantages and possible further improvements of the existing streamline simulator is discussed.

Solution Procedure

Streamline simulators are based on the IMplicit Pressure Explicit Saturation (IMPES) approach to solve the governing conservation equation. The general conservation equation is represented by the pressure and the saturation equations. The numerical solution incorporates the following routine for each time step:

- The pressure equation is solved implicitly on the finite difference grid
- The Darcy velocity is computed based on a cell centered pressure values
- Streamlines are traced from injection wells
- The saturation equation is solved explicitly along the streamlines
- Saturation values are mapped back from the irregular grid (streamlined nodes) to the regular (finite difference) grid

Streamline methods are not restricted by the global CFL (Courant-Freidrichs-Lewy [2]) stability condition, but rather local CFL along each streamline. As a result they have an advantage over conventional finite difference IMPES simulators, allowing less frequent pressure updates. They also suffer less numerical dispersion. Details of the streamline methods can be found in [3-6].

Another important principle of streamline simulation is Time-of-flight concept, allowing to solve 3D saturation equation as a set of 1D problems. The time-of-flight is defined as a travel time of a particle to a certain point on a streamline. It was introduced by Pollock in [8] and is also discussed by King [9] and Thiele [4].

Introduction of Capillary Effects in Streamline Simulation

The introduction of capillary forces requires the modification of the pressure and the saturation equations.

Modifications of the pressure equation. The continuity equation for the incompressible fluids considered here is written as:

$$\nabla u_t = \nabla (u_w + u_o) = 0. \quad (1)$$

The velocity of phase j is obtained as:

$$u_j = -k\lambda_j \nabla P_j. \quad (2)$$

The capillary pressure is defined as the difference between the pressure of the non-wetting and the wetting phases. In what follows, water is assumed to be the wetting phase, hence:

$$P_c = P_o - P_w. \quad (3)$$

Introducing phase velocities from equation (2) into the total velocity equation (1) and then substituting the oil pressure with water and capillary pressures from equation (3) leads to:

$$\nabla u_t = \nabla (k\lambda_t \nabla P_w + k\lambda_o \nabla P_c) = 0. \quad (4)$$

A method for inclusion of gravity into streamline simulation has been developed by Bratvdet [1]. Gravity effects were introduced into 3DSL0.25 by Batycky [6]. The pressure equation with both gravity and capillary forces is:

$$\nabla (k\lambda_t \nabla P_w + k\lambda_o \nabla P_c + k\lambda_g \nabla D) = 0. \quad (5)$$

The no-flow boundary condition is automatically specified by setting the overall and capillary pressure gradients over the no-flow boundary to zero.

Modification of the saturation equation. The total flow velocity is found as the sum of phase velocities. Substitution of the oil pressure with the capillary and water pressures makes it possible to obtain the water pressure gradient as a function of total velocity and the capillary pressure:

$$-\nabla P_w = \frac{1}{k\lambda_t} u_t + \frac{\lambda_o}{\lambda_t} \nabla P_c. \quad (6)$$

The mass balance for the water phase is formulated as:

$$\phi \frac{\partial s_w}{\partial t} + \nabla u_w = 0. \quad (7)$$

Introducing the water velocity from the equation (2) and substituting the water pressure gradient from the equation (6) gives the Rapaport – Leas equation [12]:

$$\phi \frac{\partial s_w}{\partial t} + \nabla \left[\frac{\lambda_w}{\lambda_t} u_t + (1-f) k\lambda_w \nabla P_o \right] = 0. \quad (8)$$

The saturation equation is then solved using the operator splitting technique:

$$\phi \frac{\partial s}{\partial t_1} + u_t \nabla f = q_i; \quad (9)$$

$$\phi \frac{\partial s}{\partial t_2} + \nabla G = 0. \quad (10)$$

Here q_i stands for the sources or sinks and G stands for the gradient of gravity and / or capillary forces.

Solution of equation (9) is described by Batycky in [6]. Equation (10) is solved explicitly on the finite difference grid. A first-order time approximation is used. The capillary and gravity gradients are discretized using a 7-point stencil.

The amount of water transferred by gravity is calculated for every block as a function of difference of depth of neighboring blocks and the densities of the fluids. The amount of the water transferred by the capillary forces is calculated differently as capillary forces do not have a uniform direction of action. First we compute the total capillary gradient directed out of the block. Then the amount of the water transferred through each face of the block is calculated as:

$$\nabla S = \frac{\Delta t_2}{\phi V_i} \Delta P_c^{total,i} \cdot \frac{T_{ij} \Delta P_c^{ij}}{\sum_{m=1}^6 T_{ij} \Delta P_c^{im}}. \quad (11)$$

Here Δt_2 stands for the time step size, V_i stands for the volume of the block, $\Delta P_c^{total,i}$ stands for the total capillary gradient directed out of the block, T stands for the transmissibility coefficient, subscripts i, j and m denotes neighboring blocks.

Equation (9) contains source and sink terms. Therefore it is responsible for the amount of water in the reservoir by propagating the displacement front along the streamlines. Saturation is then mapped back on the finite difference grid followed by the solution of equation (10). We refer to this step as a corrector step, capable of relocating the fluids inside the porous media, but not changing their total amounts.

Time step selection. The proposed approach has 3 different time steps, automatically chosen by the software. The details about time step selection and capillary effects in streamline simulation may be found in the papers presented in the publication list.

Modified solution procedure. The solution procedure for each time step is presented below with the modifications typed in bold italic:

- ***The pressure equation is modified to include gravity and capillary effects.***
- The ***modified pressure*** equation is solved implicitly on the finite difference grid
- The Darcy velocity is computed based on cell centered values ***of the modified pressure***
- Streamlines are traced from injection wells
- The saturation equation is solved explicitly along the streamlines
- Saturation values are mapped back from the irregular grid (streamlined nodes) to the regular (finite difference) grid
- ***Fluids are redistributed on the FD grid by a corrector step***

Results

The permeability field is presented in Figure 1. White color represents high permeability zones, black color – low permeability zones. This simulation is performed with a set of Corey type [14] relative phase permeability curves and “North Sea type” Leverett function, shown in Figure 2.

Figure 3 contains two saturation profiles obtained without capillary forces (0.3 and 0.5 pore volumes injected) and three saturation profiles (0.1, 0.3 and 0.5 PVI) obtained with the capillary forces present.

Saturation profiles for capillary-dominated displacement obtained by Eclipse and streamline simulator have visual differences. Eclipse predicts strong end-effects remaining on the vertical permeability borders for a long time, while the streamline simulation tends to sweep these end-effects rather quickly. On another hand the streamline simulator predicts slower propagation of the front in the capillary-dominated regime.

This difference can be explained from several points of view. Not only the sources of the numerical errors are different for these two simulators, but the flow paths are different themselves. Eclipse flow path is a straight line, connecting centers of two neighboring blocks, while streamline is much closer to the physical flow path.

I believe that streamline simulators capture the displacement front behavior better than finite-difference methods.

Predicted oil production curves are presented in Figure 4. The streamline simulator predicts differences in oil production for the cases of viscous dominated (0 mN/m IFT) and capillary (10, 50 mN/m) dominated displacements. Indeed, simulations for both the surface tensions of 10 and 50 mN/m are capillary dominated and demonstrate the same displacement mechanism.

Production curves predicted by Eclipse have different behavior. Oil production and breakthrough time increases with increase of the interfacial tension from 0 to 10 mN/m, due to the redistribution of water. Further increase of the interfacial tensions leads to the

drop of oil production and decrease of breakthrough time as the result of increasing end-effects.

More results may be found in the papers presented in the publication list or on my web page.

Conclusions

- A streamline approach with capillary and gravity effects is developed. Capillary and gravity effects are introduced by the modification of pressure and saturation equations.
- Streamline method is demonstrated to predict oil – water displacements in wide range of capillary and gravity dominated flow regimes and in complex permeability fields.
- The predictions obtained by the streamline method support our physical intuition and are comparable to predictions obtained with Eclipse. The checkerboard simulation with 50 dynes/cm interfacial tension shows the biggest difference in the oil production predicted by Eclipse and CapSL. Even in this case the difference in the total amount of oil produced at two pore volumes of water injected is less than 6%.

Acknowledgements

I would like to acknowledge Franklin M. Orr Jr. and Kristian Jessen from Stanford University for cooperation and wonderful 6 months I have spent in SUPRI-C group, department of Petroleum Engineering, Stanford University.

Tables and Figures

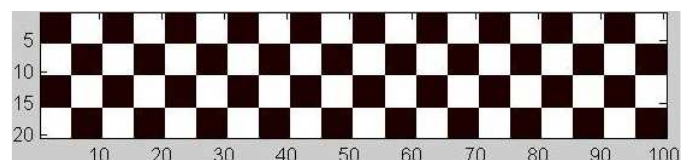


Figure 1: Permeability “checkerboard” field

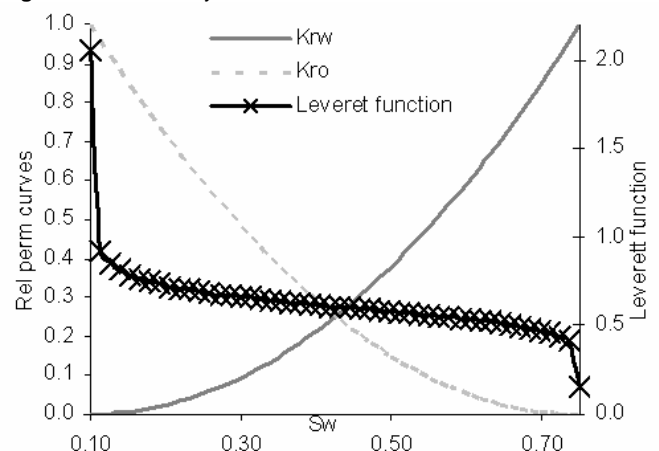


Figure 2: Relative permeability curves and Leverett function of the test run 4

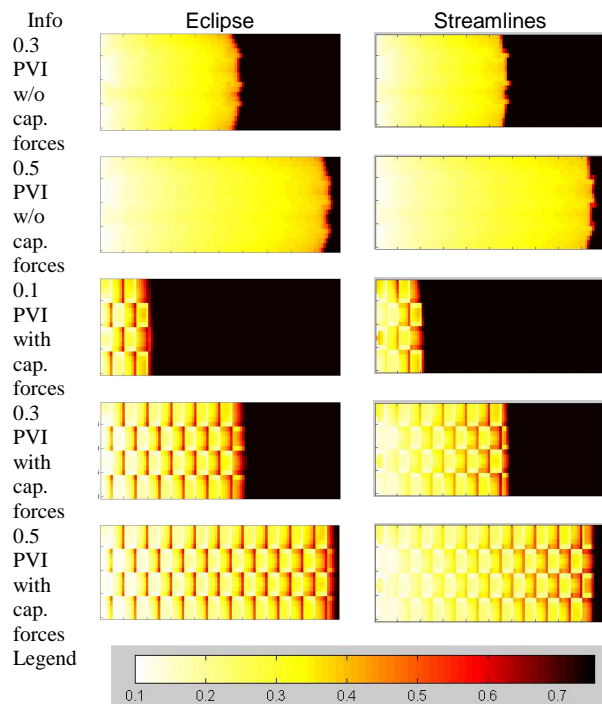


Figure 3: Checkerboard simulation

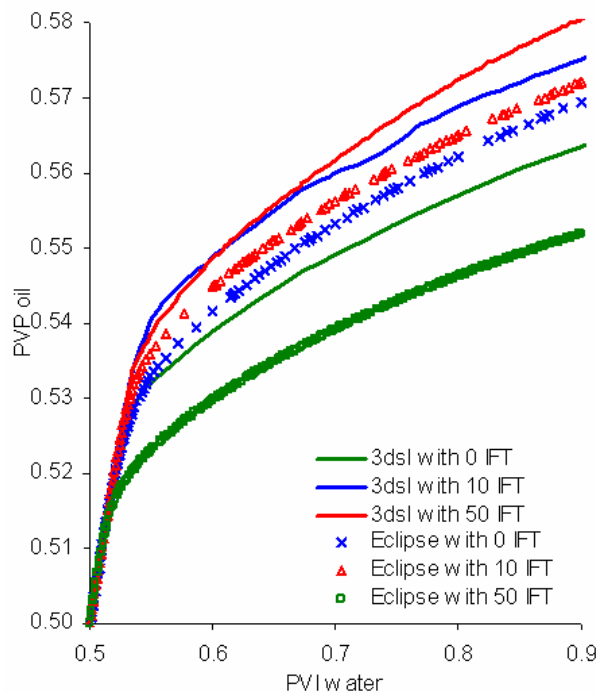


Figure 4: Oil production curves for checkerboard simulation

References

1. Bratvedt, F., Gimse, T. and Tegnander, C.: "Streamline computations for porous media flow including gravity" *Transport in Porous Media* (Oct. 1996) 25(1).
2. Trangenstein, J.A.: *Numerical Analysis of Reservoir Fluid Flow, Multiphase Flow in Porous Media: Mechanics, Mathematics and Numerics, Lecture notes in Engineering*. Springer Verlag (34).

3. Aziz, K. and Settari, A.: *Petroleum Reservoir Simulation*, Elsevier applied science publishers. London and New York, 1979.
4. Thiele, M.R.: "Streamline simulation" *Proceedings of 6th international forum on reservoir simulation 2001*
5. King, M.J. and Datta-Gupta, A: "Streamline Simulation: A Current Perspective", *In Situ* (1998) 22(1).
6. Batycky, R.P.: "A Three-Dimensional Two-Phase Field Scale Streamline Simulator." Ph.D. Thesis. Department of Petroleum Engineering, School of Earth Science, Stanford University, Stanford, California, 1997.
7. Buckley, S.E. and Leverett, M.C.: "Mechanisms of Fluid Displacement in Sands," *Trans. AIME* (1941) 249.
8. Pollock, D.W.: "Semianalytical Computation of Path Lines for Finite-Difference Models," *Ground Water* (Nov-Dec 1988) 26(6)
9. King, M.J. *et. al.* "Rapid Evaluation of the Impact of Heterogeneity on Miscible Gas Injection" *SPE26079 proceedings of the Western Regional Meeting, Anchorage* (1993)
10. Thiele, M.R. *et.al.*: "Simulating flow in Heterogeneous Media Using Streamtubes and Streamlines," *SPE Reservoir Engineering* (February 1996) 10.
11. Batycky, R.P. *et.al.*: "A 3D Field-scale Streamline-based Reservoir Simulator," *SPE Reservoir Engineering* (1997).
12. Rapoport, L.A. and Leas, W.J.: "Properties of linear waterfloods," *Trans. AIME*, (1953) 198.
13. Osako, I. and Datta-Gupta, A.: "Time step selection during streamline simulation via transverse flux correction," paper SPE 79688 presented at 2003 SPE reservoir simulation symposium, Houston, Feb. 3-5.
14. Lake, L.: *Enhanced Oil Recovery*, Prentice Hall, Englewood Cliffs, 1989.
15. Leverett, M.C.: "Capillary Behavior in Porous Solids," *Trans. AIME* (1941) 142.

List of Publications

1. Berenblyum, R.A., Hansen, J.H., Shapiro, A.A., Stenby, E.H. Modeling acid restimulation of carbonate fractured injection wells in the north sea. Accepted for publication in the *Petroleum Science and Technology*, 2003.
2. Berenblyum, R.A., Shapiro, A.A., Jessen, K., Stenby, E.H., Orr, F.M., Black oil streamline simulator with capillary effects. SPE 84037
3. Berenblyum, R.A., Shapiro, A.A., Jessen, K., Stenby, E.H., Orr, F.M., Black oil streamline simulator with capillary effects. 24th annual workshop and symposium collaborative project on enhanced oil recovery. International Energy Agency. 2003

**Suzan Biran**

Address: CHEC, Dept. of Chemical Engineering
Building 229, Office 104
Technical University of Denmark
Phone: (+45) 45 25 29 20
Fax: (+45) 45 88 22 58
e-mail: sb@kt.dtu.dk
www: www.chec.kt.dtu.dk

Supervisor(s): Anker Jensen
Søren Kiil
Poul Bach, Novozymes A/S

Ph.D. Study

Started: 1 September 2003
To be completed: August 2006

Stability of Enzymes in Granular Enzyme Products for Laundry Detergents

Abstract

Powdered laundry detergents contain granular materials consisting of surfactants, builders, bleaching agents, enzymes, etc. Although used in a small amount (1-2%), enzymes have an important role in the cleaning power of the detergent. Being fragile biomolecules, enzymes are losing their activity during storage due to the contact with harsh chemicals present in the detergent. The mechanism of inactivation is not completely understood. In this project, it is aimed to investigate the factors responsible for the deactivation of enzymes and propose new formulations and protective components to improve stability of granulates.

Introduction

Enzymes are used today in a wide range of industrial processes and in consumer products. The largest application of industrial enzymes is in detergents. The detergent industry absorbs about 45% of enzyme sales in western Europe and more than 25% of the total worldwide enzyme production [1]. After being produced by submerged microbial fermentation, enzymes are recovered and sold as either powder or liquid products for industrial use. In powdered laundry detergents, they are granulated and covered with a protective coating to prevent dust allergies and increase the stability of enzymes.

The main enzyme activity in biological laundry detergents is protease, which acts on organic stains such as grass, blood, egg and human sweat. However, it has become more common in recent years to include a "cocktail" of enzyme activities including lipases and amylases. Lipases are effective on stains resulting from fatty products such as oils and fats, while amylases help remove starchy food deposits. More recently, color enhancing and "anti-bobbling" washing powders have been developed which contain cellulases. The mode of action of such cellulases is to remove detached cellulose fibrils, which cause a progressive dulling of the color as dirt is trapped on the rough surface of the fabric.

Laundry detergents typically consist of a mixture of separate granular materials including surfactants, builders, bleaching agents and enzymes. The surfactants

are the main cleaning agent, while the builders provide alkalinity and ionic strength to the wash liquor. Bleaching agents are added to provide a white shine and remove stains on the fabric. A modern bleaching agent is Sodium Percarbonate (SPC), which decomposes in water and releases hydrogen peroxide, being the actual bleaching chemical. In addition to these, powdered laundry detergents contain soil anti-deposition polymers, anti-corrosion agents, perfumes etc.

Enzymes are very fragile biomolecules. They can lose their activity in environments, like detergents, where harsh chemicals are present. In practice the enzymes lose a significant part of their activity over a time period of several weeks. To overcome this problem, manufacturers prefer to add more enzyme granules in their products to have satisfactory wash performance. However, this results in an increase in the production cost of the laundry detergent. Partly to obtain a better stability during storage, the enzyme containing particles are typically coated by layers of salts, polymers and/or waxes. This reduces the rate of diffusion of aggressive species into the particles where reaction with the enzymes may cause deactivation. Furthermore, the particles are often formulated with anti-oxidants, such as thio-sulfates, to minimize deactivation reactions. For the enzymes in laundry detergents, the deactivation is mainly related to the release of hydrogen peroxide from the bleaching

chemicals in a moisture-containing atmosphere. Moreover, humidity, autolysis of enzymes, high local pH in granule, oxygen, defects in granulate structure and other detergent components are some of the factors affecting the granulate stability during storage.

The present understanding of inactivation mechanism of detergent enzymes during storage [2] involves diffusion of water vapor through bleaching particles, where SPC is “activated” and hydrogen peroxide present in its structure is released. The subsequent diffusion of hydrogen peroxide vapor in the enzyme granule results in oxidation of methionine and tyrosine residues in the enzyme. The sulfur in methionine, found in the active site of Savinase (protease), can be oxidized to sulfoxide and further to sulfone by hydrogen peroxide. The fact that enzyme activity is reduced significantly even in non-bleach containing detergents implies that other mechanism(s) are also involved in deactivation of granulates.

Specific Objectives

The objective of this project is to understand the inactivation mechanism of detergent enzymes during storage. It is also aimed to investigate the effect of different detergent ingredients on the granulate stability. According to the new findings, the previously proposed mechanism can be confirmed or modified. In light of the results, new stability-enhancing components or coatings will be proposed and tested for their efficiency in reducing enzyme deactivation in powdered detergents.

Future Work

The concentration and actual composition of the gases released during storage in the detergent box will be investigated. An accurate method for measuring the gaseous hydrogen peroxide will be established. Since the conventional test methods are very time consuming (4 or 12 weeks), a quick assay, lasting few days, for prediction of enzyme inactivation under controlled storage conditions will be applied. Deactivation mechanism of enzyme granulates will be investigated as a function of single or combination of detergent components, relative humidity and presence of coating layers and antioxidants. As a mean of obtaining a better understanding of the results, the transport and reaction phenomena in enzyme granules will be modeled. Finally, new enzyme formulations will be tested for development of products with higher stability.

Acknowledgements

I would like to thank to Novozymes Bioprocess Academy for supporting this project.

References

1. G. Broze (Edr.), Handbook of Detergents, Part A: Properties, Surfactant Science Series Vol. 82, Marcel Dekker, Inc. New York, 1999, p.639.
2. O. Simonsen, FT Status of Bleach Stability Mechanism Studies, Report no: 1999-08218-01, Enzyme Development and Applications Formulation Technology, Novozymes A/S, 1999.

**Astrid Boisen**

Address: Haldor Topsøe A/S
Nymøllevej 55
DK-2800 Kgs. Lyngby

Phone: (+45) 45 27 26 80

Fax: (+45) 45 27 29 99

e-mail: asb@topsoe.dk

www: www.haldortopsoe.com

Supervisor(s): Ib Chorkendorff
Søren Dahl, Haldor Topsøe A/S

Ph.D. Study

Started: 1 July 2002

To be completed: July 2005

Study of Alloy Catalysts for Use in Production of Hydrogen

Abstract

In recent years, there has been a renewed interest in the water-gas shift reaction due to its potential use in conjunction with the hydrogen-based fuel-cell power generation. Improving the catalysts used in the water-gas shift process is important to make hydrogen production via on-board reforming competitive. Therefore the rate of the water-gas shift reaction is studied. To gain insight into the overall trends of the reaction rate the reaction is studied over a series of transition metal catalysts. This will be used in order to single out the interesting alloy catalysts.

Introduction

A widely studied reaction of considerable industrial importance is the water-gas shift reaction where water and carbon monoxide produce carbon dioxide and hydrogen:



$$\Delta H = -41.2 \text{ kJ/mol}, \Delta G = -28.6 \text{ kJ/mol}$$

In general, the water-gas shift reaction can take place whenever carbon monoxide and water are present and therefore it is an important step or side reaction in a lot of processes. Most frequently, it is used in the production of hydrogen following the steam reforming of hydrocarbons, e.g. methane.



Due to the moderate exothermicity of the reaction the equilibrium constant, K_p , decreases with increasing temperature in accordance with Le Chateliers principle. The water-gas shift reaction is equilibrium controlled and the equilibrium constant is independent of pressure.

$$K_p = \frac{P_{\text{CO}_2} \cdot P_{\text{H}_2}}{P_{\text{CO}} \cdot P_{\text{H}_2\text{O}}},$$

which means that there is a trade off between favorable equilibrium and rate of reaction.

Industrially, the water-gas shift reaction is run as a staged process. The first stage is the high-temperature reaction typically carried out at 310-450°C. The catalyst used is an iron oxide, Fe_3O_4 , catalyst structurally promoted with chromium oxide in order to inhibit sintering. In this step, the CO content in the gas is reduced to typically ca. 3%. Subsequently, medium-temperature and low-temperature shifts are used to further convert the remaining CO. The low-temperature reaction is typically run at 210-240°C. The catalyst used is a $\text{Cu/ZnO/Al}_2\text{O}_3$ catalyst [1]. The low-temperature WGS reaction is limited by kinetics and can therefore be considered the area where the current demand for advanced catalysts is the greatest [2].

In recent years, there has been a renewed interest in the water-gas shift reaction due to its potential use in conjunction with the hydrogen-based fuel-cell power generation. Often the hydrogen feedstock will be obtained by on-board reforming. However, the carbon monoxide formed by the reforming reaction needs to be completely converted both because it is a pollutant and because it poisons the platinum electrodes in polymer electrolyte membrane (PEM) based fuel-cells, thus hampering the fuel-cell performance. Here, the aim of the water-gas shift reaction is both to reduce the level of carbon monoxide as well as to produce more hydrogen. In order to make hydrogen production via on-board reforming competitive, it is crucial to improve the

water-gas shift catalyst to be able to function at even lower temperature.

The reverse water-gas shift reaction has attracted relatively little attention. This is partly due to alcohol or hydrocarbon by-products over many catalysts.

Specific Objectives

Within the last couple of years, detailed knowledge has been acquired concerning why alloy catalysts sometimes are better catalysts than the individual alloy components. The aim of this project is to investigate alloy catalysts for the Water-gas shift process. Trends in the water-gas shift activity of the single-metal catalysts will be studied to give a better understanding of the system and to single out the interesting alloy catalysts.

Results and Discussion

The kinetics of the reverse water-gas shift reaction, catalyzed by the $MgAl_2O_4$ -spinel supported group VIII, VII and IB metals, were investigated. The reverse Water-gas shift reaction was carried out at atmospheric pressure in a fixed-bed flow reactor in the 180-360°C temperature range and at 1:1, 1:5, and 5:1 CO_2/H_2 feed-gas compositions.

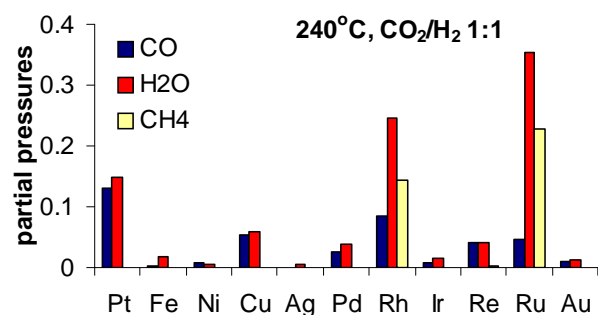


Figure 1: Partial pressures of CO, H₂O and CH₄ gas produced in the reverse Water-gas shift reaction over various $MgAl_2O_4$ -spinel supported transition metal catalysts.

Using ruthenium and rhodium catalysts produced substantial amounts of methane via the methanation reaction (the reverse steam reforming reaction).

The experimental data obtained were interpreted by using a simple power-law rate equation:

$$r_0 = A \cdot \exp\left(\frac{-E_a}{RT}\right) \cdot p_{CO_2}^\alpha \cdot p_{H_2}^\beta \cdot p_{CO}^\chi \cdot p_{H_2O}^\delta,$$

where r_0 is the rate of the reaction in the limit of “zero”

conversion $\left(0.005 \leq \frac{p_{CO} \cdot p_{H_2O}}{p_{CO_2} \cdot p_{H_2} \cdot K} \leq 0.3\right)$, A is

called the pre-exponential factor, E_a is the activation energy (in units kJ/mol), R is the gas constant and p_x is the partial pressure of component x .

With respect to preparation of alloy catalysts, which is the aim of the project, it is useful to observe periodic trends of the activity of various transition metals. For the reverse water-gas shift reaction it would be reasonable to expect a relation between the activity of the metal catalyst and the dissociative adsorption of CO_2 , which is the most likely rate-limiting step [3]. Plotting the rate against the calculated chemisorption energy of CO_2 dissociation [4] on step sites on the corresponding fcc metal surfaces gives a volcano shaped curve.

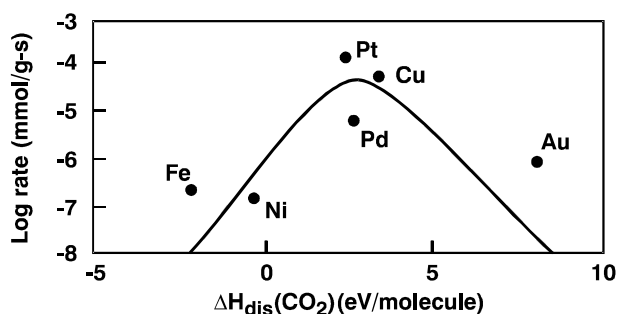


Figure 2: A volcano-shaped relationship between metal activity at 240°C and the chemisorption energy of CO_2 dissociation.

Only the metals at the top of the volcano curve can dissociate CO_2 reasonably well without binding reaction products and intermediates so they cannot be released again. The metals to the right are inferior catalysts because they are not able to dissociate CO_2 fast enough. The metals to the left are inferior catalysts because they bind reaction products and intermediates too strong. Such a volcano-shaped relationship has previously been reported for the forward Water-gas shift [5].

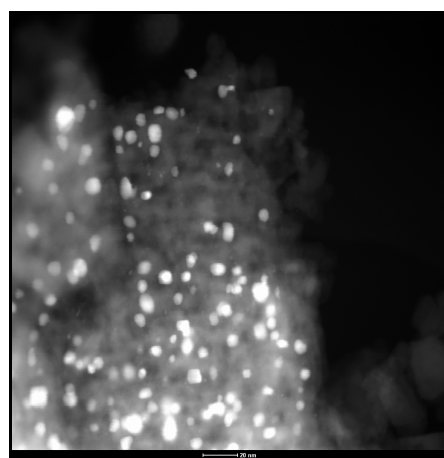


Figure 3: STEM image of platinum particles (bright) on a $MgAl_2O_4$ support

By making an alloy of a metal to the right in the volcano curve with a metal to the left in the volcano

curve a catalyst lying at the top of the volcano curve can be obtained.

The activity data above are correlated to the overall mass of the catalyst sample. Scanning transmission electron microscopy (STEM) measurements are performed in order to obtain information about the relation between catalyst activity and the surface area of the metal particles. From the STEM images, information about particle size distribution of the metal particles can be obtained.

The single-metal catalysts are currently tested in the forward water-gas shift reaction. Trends in the water-gas shift activity of the single-metal catalysts are studied in order to single out the interesting alloy catalysts.

Acknowledgements

The Danish Research Council in the context of the program "Towards a Hydrogen based Society" is supporting the project.

References

1. Rhodes, G. J. Hutchings, A. M. Ward, *Catal. Today* 23 (1995) 43.
2. G. Jacobs, L. Williams, U. Graham, G. A. Thomas, D. E. Sparks, B. H. Davis, *Appl. Catal. A: General* 252 (2003) 107
3. G. C. Wang, L. Jiang, X. Y. Pang, Z. S. Cai, Y. M. Pan, X. Z. Zhao, Y. Morikawa, J. Nakamura, *Surface Science* 543 (2003) 118-130
4. "The Brønsted-Evans Polanyi relation and the volcano curve in heterogenous catalysis" T. Bligaard, J. K. Nørskov, S. Dahl, J. Mathiesen, C. H. Christensen, J. S. Sehested. To be published.
5. D. C. Grenoble, M. M. Estadt, D. F. Ollis, *J. Catal.* 67 (1981) 90-102

List of Publications

1. Krogh, M. M. Andreasen, A. Boisen, I. Schmidt, M. Brorson, S. Dahl, C. J. H. Jacobsen: "Fra grafit til Nanomaterialer" *Dansk Kemi* nr. 9-2001, s. 24-28
2. A. Boisen, A. Hazell, C. J. McKenzie: "Structural characterisation of the H-bonded $[\text{Mn}^{\text{II}}(\text{OH}_2)_2 \dots (\text{OCH}_3)_2 \text{Mn}^{\text{III}}]$ motif: A model for resting state hydroxylic solvent coordination in Mn(II)-Mn(III) enzymes" *Chem. Commun.* (2001) 2136-2137
3. Schmidt, A. Boisen, E. Gustavsson, K. Ståhl, S. Persson, A. Carlsson, C. J. H. Jacobsen: "Carbon Nanotube Templated Growth of Mesoporous Zeolite Single Crystals" *Chem. Mater.* 13 (2001) 4416-4418
4. J. H. Jacobsen, S. Dahl, A. Boisen, B. S. Clausen, H. Topsøe, A. Logadottir, J. K. Nørskov: "Optimal Catalyst Curves: Connecting Density Functional Calculations with Industrial Reactor Design and Catalyst Selection" *J. Catal.* 205 (2002) 382-387
5. A. Boisen, S. Dahl, C. J. H. Jacobsen: "Promotion of Binary Nitride Catalysts: Isothermal N_2 Adsorption, Microkinetic Model and Catalytic Ammonia Synthesis Activity" *J. Catal.* 208 (2002) 180-186
6. U. G. Nielsen, A. Boisen, M. Brorson, C. J. H. Jacobsen, H. J. Jakobsen, J. Skibsted: "Aluminium Orthovanadate (AlVO_4): Synthesis and Characterization by ^{27}Al and ^{51}V MAS and MQMAS NMR Spectroscopy" *Inorg. Chem.* 41 (2002) 6432-6439
7. J. H. Jacobsen, I. Schmidt, M. Brorson, A. Boisen, T. W. Hansen, S. Dahl: "Non-crystallographic Nanopores in Single Crystals: A New Approach in Nanomaterials Chemistry" *European Powder Diffraction EPDIC 8, Materials Science Forum*, 2003, p. 217
8. Boisen, I. Schmidt, A. Carlsson, S. Dahl, M. Brorson, C. J. H. Jacobsen: "TEM stereo-imaging of mesoporous zeolite single crystals" *Chem. Commun.* (2003) 958-959
9. C. J. H. Jacobsen, I. Schmidt, A. Boisen, K. Johannsen "Katalytisk kemi. Et spørgsmål om miljø og ressourcer" *Holte Bogtrykkeri*, 2002, ISBN 87-986802-7-7



Dennis Bonn 
Address: CAPEC, Dept. of Chemical Engineering
Building 227, Office 25
Technical University of Denmark
Phone: (+45) 45 25 28 08
Fax: (+45) 45 93 29 06
e-mail: db@kt.dtu.dk
www: www.capec.kt.dtu.dk
Supervisor(s): Sten Bay J rgensen

Ph.D. Study
Started: August 2000
To be completed: January 2004

Data Driven Modeling of Batch Processes for State Estimation, Control and Optimization

Abstract

The non-stationary and most often nonlinear dynamic behavior of batch processes can be approximated with sets of interdependent linear models. These models can be obtained from sparse historical production data and the model sets will approximate batch processes sufficiently well for them to be successfully applicable for the design of model-based state estimation and control tools such as the Kalman filter, Model Predictive Control and Iterative Learning Control. Moreover, as a simulation tool, the models can aid the search for a better or optimal batch recipe.

Introduction

Most often the complex and nonlinear dynamics of continuously operated processes can be approximated with a moderate set of local Linear Time-Invariant (LTI) models, each of which describes a characteristic region in the operation window. These regions described by local models will often be characterized by a set of active constraints. For batch and semi-batch processes (from here on, batch will cover both batch and semi-batch processes) however, the set of active constraints will change as the batch progresses. In fact, to operate a batch process in an optimal fashion, a specific sequence of constraints is tracked during operation. This means that local approximations of characteristic regions are not sufficient to describe batch operation. The transitions between these locally approximated characteristic regions are also needed to provide a complete description of batch operation. Furthermore, even if specific sets of constraints were active for longer periods; local LTI models can not be expected to describe the time variation due to changing hold-ups and/or compositions.

The periodic nature and the finite horizon of batch processes however, make it possible to model the evolution from each sample point to the next in a batch with one grid-point LTI model. In this fashion, both the time variation within the characteristic regions and the transitions between these may be approximated with a grid of grid-point models. Thus, such a model set gives a complete description of a batch. The finite horizon of

batch processes means that the model set will be finite. The periodic way in which the same recipe is repeated batch after batch means that several measurements from the individual sample points are available for identification. That is, the time evolution of a process variable is measured at specific sample points during the batch operation and as the batch operation is repeated, several measurements are collected from every sample point. With multiple data points/measurements from one specific sample point a grid-point model can be identified for this sample point. Explicitly, in addition to the time dimension, data from batch processes also evolve in a batch index dimension.

Multiple ARMAX Modeling

Given the discussion above, batch processes are modeled with sets of dynamic grid-point LTI models. Such a set of grid-point LTI models could also be referred to as a Linear Time Varying (LTV) batch model. These grid-point LTI models can be parameterized in a number of ways -- e.g. as Output Error (OE) models, AutoRegressive models with eXogenous inputs (ARX), State Space (SS) models, etc. In the present contribution an AutoRegressive Moving Average model with eXogenous inputs (ARMAX) parameterization was chosen. This choice of parameterization offers a relatively good multivariable system description with a moderate number of model parameters.

As operation of a batch progresses, different inputs and outputs may be used depending on the current phase of the batch and hence in order to model batch operation it is convenient to define the following variables and references for each time step t :

1. Input variable $u_t \in \mathcal{R}^{n_u(t)}$ with reference $\bar{u}_t \in \mathcal{R}^{n_u(t)}$
2. Output variable $y_t \in \mathcal{R}^{n_y(t)}$ with reference $\bar{y}_t \in \mathcal{R}^{n_y(t)}$
3. Disturbance variable $w_t \in \mathcal{R}^{n_y(t)}$

Using an ARX model parameterization, the output deviation $\bar{y}_t - y_t$ at time t may be given as a weighted sum of $n_A(t)$ past output deviations and $n_B(t)$ past input deviations

$$\begin{aligned} \bar{y}_t - y_t = & -a_{t,t-1}(\bar{y}_{t-1} - y_{t-1}) - \dots \\ & -a_{t,t-n_A(t)}(\bar{y}_{t-n_A(t)} - y_{t-n_A(t)}) \\ & + b_{t,t-1}(\bar{u}_{t-1} - u_{t-1}) + \dots \\ & + b_{t,t-n_B(t)}(\bar{u}_{t-n_B(t)} - u_{t-n_B(t)}) + w_t \end{aligned}$$

where $n_A(t), n_B(t) \in [1, \dots, t]$ are the grid-point ARX model orders and $a_{i,j} \in \mathcal{R}^{n_y(i), n_y(j)}$ and $b_{i,j} \in \mathcal{R}^{n_y(i), n_u(j)}$ are the (possibly) structured grid-point ARX model parameter matrices. The fact that the model parameter matrices may be structured implies that $n_A(t)$ and $n_B(t)$ should be considered as the highest model orders at time t . Note, as the grid points are modeled with individual grid-point models, the sample points do not have to be equidistantly spaced in time. Let N be the batch length/(number of samples) and define the input \mathbf{u} , output \mathbf{y} , shifted output \mathbf{y}^0 , and disturbance \mathbf{w} profiles as

$$\begin{aligned} \mathbf{u} &= [u_0' \ u_1' \ \dots \ u_{N-1}']' \\ \mathbf{y} &= [y_1' \ y_2' \ \dots \ y_N']' \\ \mathbf{y}^0 &= [y_0' \ y_1' \ \dots \ y_{N-1}']' \\ \mathbf{w} &= [w_1' \ w_2' \ \dots \ w_N']' \end{aligned}$$

Note, not all initial conditions y_0 are measurable and/or physically meaningful --- e.g. off-gas measurements. Thus the ARX model set may be expressed in matrix form

$$\bar{\mathbf{y}} - \mathbf{y} = -\mathbf{A}(\bar{\mathbf{y}}^0 - \mathbf{y}^0) + \mathbf{B}(\bar{\mathbf{u}} - \mathbf{u}) + \mathbf{w}$$

where \mathbf{A} , \mathbf{B} are structured lower block triangular matrices. The profile \mathbf{w} is a sequence of disturbance terms caused by bias in the reference input profile $\bar{\mathbf{u}}$, the effect of process upsets, and the modeling errors from linear approximations. This means that the disturbance \mathbf{w} contains contributions from both batch wise persistent disturbances, such as recipe/input bias, model bias, and erroneous sensor readings, as well as from random disturbances, which occur with no batch wise correlation. It thus seems reasonable to model the disturbance profile \mathbf{w} with a random walk model with respect to the batch index k

$$\mathbf{w}_k = \mathbf{w}_{k-1} + \Delta \mathbf{w}_k$$

where the increment disturbance profile $\Delta \mathbf{w}_k$ is modeled with a Moving Average (MA) model with respect to time

$$\Delta \mathbf{w}_{k,t} = v_{k,t} + c_{t,t-1}v_{k,t-1} + \dots + c_{t,t-n_C(t)}v_{k,t-n_C(t)}$$

with model order $n_C(t) \in [1, \dots, t]$. In matrix form the disturbance model is expressed as

$$\Delta \mathbf{w}_k = \mathbf{C} \mathbf{v}_k$$

where the sequence $\mathbf{v}_k = [v_{k,1}' \ v_{k,2}' \ \dots \ v_{k,N}']'$, $v_{k,t} \in \mathcal{R}^{n_y(t)}$, represents batch wise non-persistent disturbances that are assumed to be zero-mean, independent and identically distributed. Considering the difference between two successive batches

$$\begin{aligned} \Delta \mathbf{y}_k &= \mathbf{y}_k - \mathbf{y}_{k-1} \\ &= \mathbf{A} \mathbf{y}_k^0 - \mathbf{B} \Delta \mathbf{u}_k + \mathbf{C} \mathbf{v}_k \end{aligned}$$

A batch ARMAX that is independent of the reference profiles and batch wise persistent disturbances has been obtained. With such a batch ARMAX model the path is prepared for multivariable, model-based monitoring, control, optimization, and of course simulation.

Application Specific Models

Depending on the task the batch ARMAX model is to be applied to, it is convenient to convert the batch ARMAX model into different representations. If the task at hand is to predict (or simulate) the behavior of a batch before it is started the following form is convenient

$$\Delta \mathbf{y}_k = \mathbf{H} \Delta \mathbf{y}_{k,0} - \mathbf{G} \Delta \mathbf{u}_k + \mathbf{F} \mathbf{v}_k$$

Note that the disturbance matrix \mathbf{F} models the propagation of batch wise non-persistent disturbances --

- including batch wise non-persistent model-plant mismatch. The initial condition $\Delta y_{k,0}$ can be considered as either an input/control variable or a disturbance. The distinction between the two possibilities will of course depend on the information on and control of the outputs prior to a batch. If the initial conditions are considered disturbances, it is necessary to model them. The initial output deviation from the reference is also modeled as a random walk with respect to batch index, which means that the initial condition is given as a zero-mean random variable.

The model representation above is also convenient for the task of classification/monitoring (e.g. normal or not) of a batch after it has been completed. Furthermore, the model representation can be used to determine open-loop optimal recipes in the sense of optimizing an objective for the batch. If such an objective is to minimize the deviations $\mathbf{e} = [e_1' \ e_2' \ \dots \ e_N']'$, $e_t \in R^{n_y(t)}$, from a desired trajectory then the model can be modified into

$$\mathbf{e}_k = \mathbf{e}_{k-1} - \mathbf{H}\Delta y_{k,0} + \mathbf{G}\Delta \mathbf{u}_k - \mathbf{F}\mathbf{v}_k$$

There are two important points to be made about the trajectory tracking model form above. First of all, as the error profile in batch k depends on the error profile from batch $k-1$, the effects of the batch wise persistent disturbances are integrated with respect to batch index. This means that a properly designed controller can reject the effects of the batch wise persistent disturbances asymptotically with respect to batch index --- e.g. removing the effects of recipe and model bias. Secondly, given the above mentioned asymptotic behavior and as the control moves/actions generated by such a controller are deviations from the control/input profile realized in the previous batch, the control actions due to batch wise persistent disturbances will converge asymptotically to zero with respect to batch index. In literature it is said that the controller learns to reject the batch wise persistent disturbances --- i.e. the resulting controller is an Iterative Learning Control (ILC) scheme. A more accurate formulation would be that both output and input errors are modeled using integrators with respect to batch index.

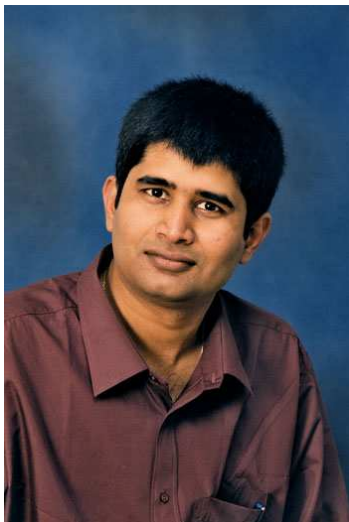
The two forms above of the batch ARMAX model above are applicable to off-line or inter-batch type applications. For on-line estimation, monitoring, feedback control, and optimization however, it is convenient to use a state space realization of the batch ARMAX model. To achieve such a realization it is necessary to simplify the batch ARMAX model structure with the assumption that the number of outputs is constant. In an observer canonical form the state space realization is given as

$$\begin{aligned} x_{k,t} &= \mathbf{A}_t x_{k,t-1} + \mathbf{B}_t \Delta \mathbf{u}_{k,t-1} + \mathbf{E}_t v_{k,t} \\ y_{k,t} &= \mathbf{C} x_{k,t} \end{aligned}$$

with the SS model dimension n_x and initial condition $x_{k,0} = \mathbf{C}'\Delta y_{k,0}$. The SS model matrices contain the corresponding block columns in the batch ARMAX model. Just as above, the SS model form is convenient for prediction, monitoring, and optimization type applications, but also facilitates on-line implementations of these. Furthermore, the SS model form is particularly well suited for closed-loop or feedback control applications. For tracking control applications the SS model form can be modified into

$$\begin{aligned} x_{k,t} &= \mathbf{A}_t x_{k,t-1} + \mathbf{B}_t \Delta \mathbf{u}_{k,t-1} + \mathbf{E}_t v_{k,t} \\ e_{k,t} &= e_{k-1,t} - \mathbf{C} x_{k,t} \end{aligned}$$

Following the discussion above, a multivariable feedback controller properly designed using the trajectory tracking SS model form above, will reject the effects of the batch wise persistent disturbances asymptotically with respect to batch index. That is, due to the output and input error integration in the model framework, a controller designed to reject disturbances with respect to time in one batch at a time will also asymptotically reject the effects of batch wise persistent disturbances with respect to batch index.



Debasish Chakraborty

Address: ICAT, Dept. of Chemical Engineering
Building 312
Technical University of Denmark

Phone: (+45) 45 25 31 25

Fax: (+45) 45 93 23 99

e-mail: dc@kt.dtu.dk

www: www.icat.dtu.dk

Supervisor(s): Tue Johannessen
Hans Livbjerg
Ib Chorkendorff

Ph.D. Study

Started: 1 April, 2003

To be completed: March 2006

One Step Flame Synthesis of Direct Methanol Fuel Cell Catalyst

Abstract

Flame synthesis is studied as a one-step preparation method of catalysts for direct methanol fuel cells (DMFC) by combustion of Ru-acetylacetonate and Pt-acetylacetonate in a quenched-cooled flame reactor. The structure, surface and morphology of the catalysts were investigated by x-ray photoelectron spectroscopy (XPS), transmission electron microscopy (TEM), and Scanning Auger microscopy (SAM). Transmission electron microscopy observation showed that particles with diameter less than approximately 5 nm were produced. XPS studies revealed that there were possibly three different oxidation states of Pt in the PtRu/C catalyst. SAM studies showed how the Pt containing particles were deposited on the fibres of the carbon support.

Introduction

Direct methanol fuel cell (DMFC) has the potential to replace the combustion engine in vehicular applications. The device uses a liquid fuel, which means that the existing fuel supply, storage, and delivery systems could be used possibly with a few minor modifications. Also methanol can be produced from natural gas, coal or biomass. Compared to the hydrogen fuel cell, which is also in consideration as a future energy supplying device, direct methanol fuel cell has the advantages of ease of fuel supply and storage [1]. DMFC can be operated at lower temperature than the internal combustion engine (ICE) and this will certainly reduce the polluting nitrogen oxides produced by ICE. DMFC offers another unique advantage for city driving; its efficiency increases as the load on the fuel cell decreases, which is exactly the opposite of the heat engines.

However, it has not yet been possible to develop DMFC of acceptable cost, which can give performance comparable to that of its main competitor, i.e. heat engines. The cost of DMFC depends mainly on the electrolyte membrane and the Pt based catalysts, that has the highest activity for methanol oxidation [2]. The cost of the membrane can be reduced by the growth of the market, but the only way to lower the cost of the catalyst is to reduce the amount of Pt used without sacrificing the performance [3]. Therefore, it is necessary to improve the catalyst performance.

In DMFC carbon supported Pt-Ru catalyst is used. Substantial enhancements in activity were found for platinum modified with a second metal like ruthenium. One hypothesis for this enhancement of activity is that the second component such as Ru acts as a redox co-catalyst with the methanol adsorbing and dehydrogenating on the Pt whilst the poisoning residue was chemically oxidized on the co-catalyst. The other explanation is that the second component acts as an agent which weakens the adsorption of residues on Pt via a ligand effect and/or promoting the electrosorption of water at lower potentials and thus accelerating the removal of residues [1]. Whichever is the mechanism, it might be concluded that for improved performance, it is necessary to have a well-mixed Pt-Ru bimetallic alloy as catalyst. The general ways of making catalyst are co-impregnation, sequential impregnation, co-precipitation, absorbing alloy colloids or surface organometallic chemistry techniques. However, it could be difficult to achieve the desired close proximity of the active components by the conventional methods as the active components might deposit on different sites on the support. Moreover, all of these processes need several stages for making active catalyst. Flame pyrolysis can be a viable alternative to replace the wet processes with a one step continuous process.

Flame pyrolysis has been successfully used to produce catalysts [4]. In flame pyrolysis, precursors are rapidly evaporated as they are exposed to high flame

temperatures resulting in vapours that react forming intermediate and product molecules and clusters that quickly grow to nano-sized particles by coagulations and/or surface reaction [5]. The precursors and the products have very high chances to mix intimately before the particles are formed. This intimate mixing can result in higher degree of alloying and greater proximity of active elements of the catalysts.

The work presented here describes very preliminary results of our effort to develop a one step synthesis method of DMFC catalyst. It will be seen that nano-sized particles can be very easily deposited on the gas diffusion layer of the fuel cell. This is a very important result in terms of preparing catalyst with very high dispersion.

Experimental

The flame synthesis setup is shown in Figure 1.

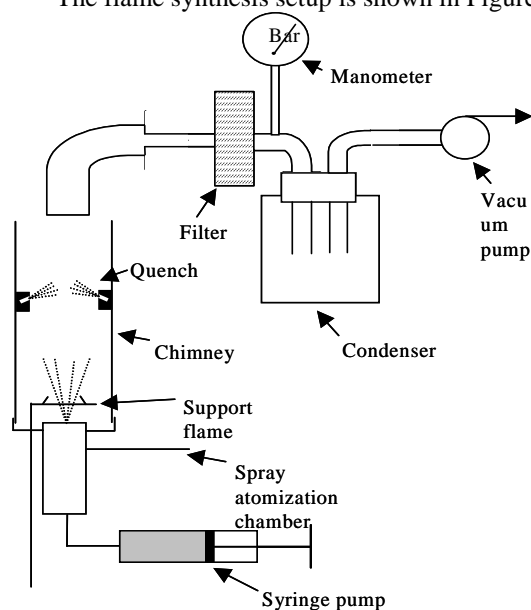


Figure 1: Outline of the flame synthesis equipment

The precursors, ruthenium (III) acetylacetonate ($\text{Ru}(\text{acac})_3$, Sigma-Aldrich) and platinum (II) acetylacetonate ($\text{Pt}(\text{acac})_2$, Aldrich Chem.Co), were dissolved in solvent containing isooctane and tetrahydrofuran at a volume ratio of 4 to 1. The solution was pumped through a nozzle to spray the precursor solution to the flame. The dispersion and combustion gas was introduced through a slit surrounding the nozzle. Supporting hydrogen flames were also created by introducing hydrogen horizontally of the main flame. The product particles were collected on the carbon-based fuel cell gas diffusion layer (GDL) by passing the flame outlet aerosols through it.

Based on collaboration with IRD Fuel A/S, a test fuel cell was built (Figure 2). The graphite bipolar plates had machined flow structures with serpentine flow pattern, capable of accommodating electrodes of maximum $4,9 \text{ cm}^2$.



Figure 2: Photograph of the test fuel cell

The system is equipped with two humidifiers for humidifying the inlets to anode and cathode. The inlet to the anode and cathode sections of the fuel cell travelled along serpentine channels and picked up water coming from the humidifiers separated from the flow by Nafion membranes.

Results and Discussion

Scanning Auger Micrographs of a metal deposited carbon sheet showed the structures of the support (Figure 3.a). When the sample was scanned for Pt, almost uniform deposition of Pt containing particles on the fibres was observed (Figure 3.b).

Figure 4(a) and 4(b) are the TEM images depicting the morphology of the particles on a TEM grid produced by the combustion of the precursors. Figure 4(a) shows the particle size ranges from $\sim 2 \text{ nm}$ to $\sim 5 \text{ nm}$. Figure 4(b) is a close-up picture of one particle. It shows a spherical morphology with lighter region near the periphery and darker inside region. This might be due to the segregation of lighter elements (i.e. Ru or RuO) to the outer surface of the sphere. In that case the inner surface will be mostly Pt or Pt compounds.

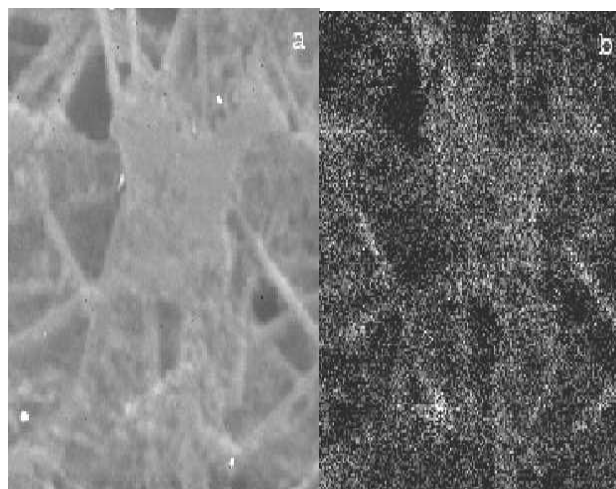


Figure 3: Scanning Auger Micrographs of the whole sample (a), showing the presence of Pt as bright spots (b)

Table 1. Relative intensities of different species from curve fitted spectra

	Pt/C	PtRu(3:1)/C	PtRu(1:1)/C
1 st component	71.5ev	71.66 ev	71.78 ev
2 nd component	72.48 ev	73.1 ev	73.2 ev
3 rd component	74.9 ev	74.55 ev	74.65 ev

Table 2. Relative intensities of different species from curve fitted spectra

	Pt/C	PtRu(3:1)/C	PtRu(1:1)/C
1 st component	45.8%	44.6%	36.3%
2 nd component	50%	52%	60%
3 rd component	4.2%	3.4%	3.7%

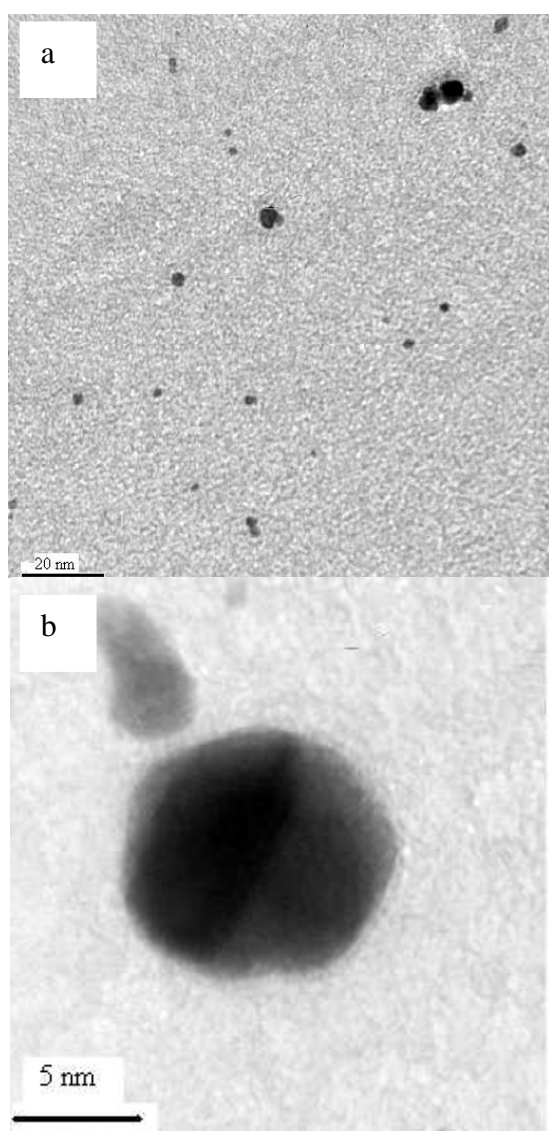


Figure 4: TEM micrographs of particles (a), and a single particle (b), produced by the flame.

To characterise the electronic states of the deposits, X-ray photoelectron spectroscopy was carried

out on several samples. The spectra showed the presence of Pt and Ru in the deposits. Furthermore, in order to understand the effect of alloying of Pt by Ru in the catalyst, the Pt 4f region has been investigated in detail (Figure 5). The spectra could be deconvoluted into three components. Considering the fact that higher oxidation states of Pt will have higher binding energies, the three peaks could be attributed to Pt⁰, Pt²⁺, and Pt⁴⁺ [6]. The binding energies and area ratios of different components are shown in Table 1 and Table 2. It is worthwhile to mention that we could not get enough information for Ru by this method because its binding energy lies in close proximity to binding energy of C, which has more intensive peaks in this case.

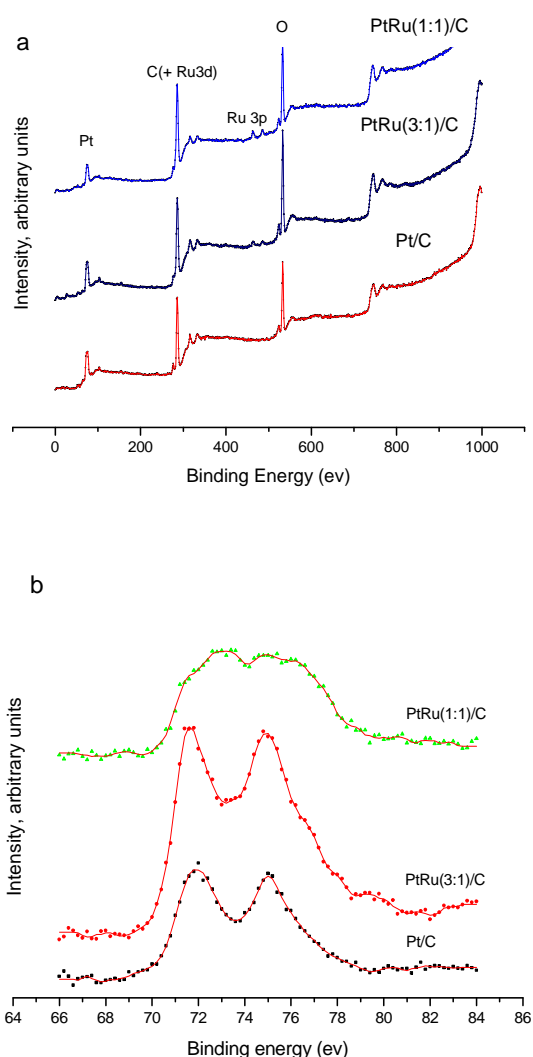


Figure 5: X-ray photoelectron spectra of different catalysts showing all possible peaks (a), and Pt 4f peaks (b).

Conclusion

We have presented the initial results of a one-step method for synthesis of a DMFC catalyst. The characterization of the catalysts made at the preliminary stage showed that nano-particles were produced and also the presence of both Pt and Ru in the catalyst was confirmed by XPS studies. We think that the preliminary results are promising and further research could result in an effective one step method for DMFC catalyst preparation.

Acknowledgement

The authors wish to thank the Technical University of Denmark for supporting the project with a Ph.D. scholarship. We are also thankful to IRD Fuel Cells A/S for providing the carbon support and input for making the test fuel cell unit.

References

1. McNicol B.D, Rand D.A.J., Williams KR., J. of Power Sources 83, 1999, 15-31.
2. Carrette L, Friedrich KA, Stimming U., CHEMPHYSICHEM 1, 2000, 162-193.
3. Cha S.Y, Lee W.M., J. of Electrochem. Soc., 146(11), 146, 4055-4060.
4. Johannessen T., Koutsopoulos S., J. Catal., 205(2), 2002, 404-408.
5. Pratsinis S.E., Prog. Energy Combust. Sci., 24, 1998, 197-219.
6. Aricò A.S., Creti P., Kim H., Mantegna R, Giordano N., Antonucci V., J. Electrochem. Soc. 143(12), 1996, 3950-3959.



Mikkel Stochkendahl Christensen
Address: CHEC, Dept. of Chemical Engineering
Building 229, Office 112
Technical University of Denmark
Phone: (+45) 45 25 28 30
Fax: (+45) 45 88 22 58
e-mail: mch@kt.dtu.dk
www: www.chec.kt.dtu.dk
Supervisor(s): Kim Dam-Johansen
Anker Degn Jensen
Martin Skjøth-Rasmussen
Ph.D. Study
Started: 1 September 2003
To be completed: September 2006

Computational Fluid Dynamics in Chemical Engineering

Abstract

Commercial CFD (Computational Fluid Dynamics) codes are expected to manage chemical reactions in a multitude of chemically reacting systems and among these; combustion systems. However in these systems the governing equations describe changes, which span over many magnitudes making the problem stiff. In order to circumvent this problem, it is expected to decouple these equations and model some of the coupling separately. This modeling will then be used in numerical experiments, which will be compared to real physical experiments in the laboratory. Virtual reality visualization of the numerical simulations is also anticipated.

Introduction

Commercial CFD (Computational Fluid Dynamics) codes are expected to manage chemical reactions in a multitude of chemically reacting systems and among these; combustion systems. For industrial applications involving (gaseous) combustion particularly, the turbulent-diffusion systems are relevant to industrial modelers. However, a mathematical modeling of these turbulent-diffusion systems presents a number of challenges. The main difficulties of the numerical simulation of a turbulent-diffusive reactive flow phenomena lies in the physical complexity of the properties to be modeled, and the wide range of space and time scales in which they occur. The time scale, needed for a given property to equilibrate, varies for the chemical reactions from the fast chemistry (10^{-5} sec. or lower) to the slow - frozen chemistry (10^{-2} to 100 sec.), whereas the typical time scale for physical motion is in the order of 10^{-5} to 10^{-2} sec {1}. Typically in combustion processes, the fast chemical reactions are those related to the ignition behavior of a mixture, while the formation of pollutants such as NO_x , SO_2 , PAH (Polycyclic Aromatic Hydrocarbons) and soot is a result of the slow chemistry.

In modern combustion chemistry characteristics such as: ignition behavior, flammability, flame propagation, quenching and the emission of pollutants are described using DCK (Detailed Chemical Kinetic) mechanisms {2}. The DCK mechanisms are molecular-

level, kinetic mechanisms for the combustion of hydrocarbons, and consist of a complex set of elementary reactions, which incorporates a considerable number of possible intermediate species and reactions {3}. During the past decades a significant effort has aimed toward the development of DCK mechanisms, which can describe the chemical processes that occurs when a hydrocarbon is combusted, and mechanisms for the combustion of various hydrocarbons are available in the literature {1,4} or via the internet {5}. The literature also offers DCK mechanisms that can be used to simulate the formation of different pollutants such as NO_x {6}, SO_2 {7}, PAH {4,8}, even models for soot formation that can be added on top of DCK mechanisms are available from the literature {9} or via the internet {10}.

Chemistry Modelling in CFD Simulations

Ideally, the simulation of a practical combustion device would simply involve a compilation of the needed chemical-kinetic scheme from the available DCK mechanisms and use the newly compiled mechanism in a CFD simulation. However, to restrict the error on the calculation of the composition and the parameters of state of the fluid, the integration step must be shorter, at least by a factor of two, than the time scale of the fastest interaction in a direct numerical simulation of a problem. Thus, the grid resolution in the CFD simulation must be fine enough to resolve the fastest chemical reaction. Alternatively, progress in reacting

systems in static simulation can be approximated using well described mixing-reaction interaction models such as *mixed-is-burnt*, *probability density function*, *eddy break-up* and *eddy dissipation models*, or *flamelet library models*, which for increasing details, all increases the computational demand to the typically already challenging CFD simulation {11}.

The mixing-reaction interaction models all impose a number of difficulties to the chemistry modeling in CFD codes, since they all relate the chemical progress term to one or two parameters from the turbulence modeling. Doing so the simple mixing-reaction interaction models assume that the chemical kinetics are infinitively fast and that the progress of chemical reactions is controlled by turbulent mixing. However, the formation of some trace element pollutants i.e. NO_x, SO₂, PAH and soot, which result from the frozen chemistry, will be allowed a too fast progress of their chemical reactions when the turbulent mixing controls the progress. Alternatively, the chemistry models in the CFD codes must allow additional rate expressions to describe the chemical reactions that apply the frozen chemistry. Nevertheless, this alternative evokes a second difficulty imposed by chemistry modeling in CFD simulations. CFD codes were originally developed to handle fluid flow modeling without the influences of chemical reactions, thus the CFD solvers have been optimized to solve the equations for physical motion that span 3 to 4 orders of magnitude in time scale. When equations for the frozen chemistry is added to a CFD simulation, suddenly the solver must span over up to 8 orders of magnitude in time scale or more, which is problematic to the solvers in the CFD codes despite newly developed coupled solvers {12} and segregated solvers {13}. This is also a problem for the fast chemistry, but for the fast chemistry the previously mentioned grid resolution represents a more severe problem, while grid resolutions that are fine enough to obtain grid independent solutions for the equations of physical motion also will be fine enough to obtain grid independent solutions for the equations used to model the frozen chemistry.

Considering the outlined difficulties imposed by mixing-reaction interaction model to CFD simulations, alternative methods to apply DCK mechanisms to CFD simulations remains an important issue to simulations of practical combustion devices with complex geometries. Whilst the DCK mechanisms are important means to understand the formation process and emission of the trace element pollutants from industrial combustion processes.

Project Idea and Goals

Primary goals of and the expected output from the present project are enumerated below:

- Single cell reactor model for use in detailed chemical kinetic post-processing of CFD simulations

- Experimental work in laboratory reactor for model verification
- Virtual-Reality visualization of CFD data

while more details on the scientific goals and challenges and the development goals are outlined in the following subsections

Scientific Goals

The scientific challenge is the development of a qualitative and quantitative model or method that describes the interaction between chemical reaction, and macro and micro mixing applicable to both laminar premixed flow reactors and high-pressure turbulent diffusion flames.

Important aspects in modeling will include the macro mixing of chemical species, the reaction of these in the bulk phase, and particularly on the micro mixing and the reactions in the micro mixing level.

To generally increase the understanding of the behavior of combustion chemistry, and the interaction with the flow pattern in a reactor (e.g. such as combustion chambers in practical combustion devices) CFD modeling, in particular using Fluent[®] is foreseen. The objective of the project is that the developed models or methods can be incorporated into commercial CFD software, and may be used in combination with this for analysis of the flow patterns in the combustion zone of practical combustion devices.

The project will contribute to an increased fundamental understanding of combustion processes, particularly the influence of the interaction between chemical reaction and macro and micro mixing on combustion processes, which is of interest to the design of boilers, engines and motors, gas turbines and other devices that involve combustion processes will be emphasized. Finally, the project will also increase the understanding of the formation of trace element pollutants in practical combustion devices, and may furthermore contribute to an optimization of the combustion in practical combustion devices while minimizing the formation and emission of harmful trace element pollutants.

Development Goals

The interpretation and industrial application of results from experiments in conjunction with modeling using in particular CHEMKIN[®] and CFD should result in a model or method, which can be used to predict the formation of trace element pollutants in practical combustion devices under various stoichiometries, pressures and temperatures.

The project will contribute to the knowledge on the interaction between chemical reaction and macro and micro mixing and the chemistry and formation of trace element pollutants in practical combustion devices at

the CHEC Research Centre at the Department of Chemical Engineering, DTU, and to the center's industrial partners.

A final development goal is to set up a method for advanced visualization of CFD data in the Virtual Reality Theater at DTU.

References

1. Jürgen Warnatz, Ulrich Mass and Robert W. Dibble *Combustion* Springer-Verlag, Berlin, New York, 1995
2. Frédérique Battin-Leclerc, René Fournet, Pierre-Alexandre Glaude, Valerie Warth, Guy-Marie Côme and Gérard Scacchi *Modeling of the Gas-Phase Oxidation of n-Decane from 550 to 1600 K*, Proceedings from The International Combustion Symposium, Vol. 28, The Combustion Institute, Chicago, IL, USA, 2000, pp. 1597-1605
3. Martin Skov Skjøth-Rasmussen *Modelling of Soot Formation in Autothermal Reforming* Ph.D. Thesis, Department of Chemical Engineering, Technical University of Denmark Kgs. Lyngby, Denmark, September, 2003
4. Martin S. Skjøth-Rasmussen, Peter Glarborg, Martin Østberg, Tue Johannessen, Hans Livbjerg, Anker D. Jensen and Thomas S. Christensen *Formation of PAH and Soot in Fuel-Rich Oxidation of Methane in a Laminar Flow Reactor* Combustion and Flame, (2003), accepted for publication
5. Gregory P. Smith, David M. Golden, Michael Frenklach, Nigel W. Moriarty, Boris Eiteneer, Mikhail Goldenberg, C. Thomas Bowman, Ronald K. Hanson, Soonho Song and William C. Gardiner Jr., Vitali V. Lissianski and Zhiwei Qin *GRI-Mech 3.0 Database* http://www.me.berkeley.edu/gri_mech/ The Gas Research Institute, Chicago, IL, USA, 2000
5. Peter Glarborg, Maria U. Alzueta, Kim Dam-Johansen and James A. Miller *Kinetic Modeling of Hydrocarbon/Nitric Oxide Interactions in a Flow Reactor* Combustion and Flame, Vol. 115, pp. 1-27, (1998)
6. Jan-Erik Johnsson and Peter Glarborg *Sulphur Chemistry in Combustion I - Sulphur in Fuels and Combustion Chemistry in Christian Vovelle (ed.) Pollutants from Combustion - Formation and Impact on Atmospheric Chemistry NATO ASI Series C Mathematical and Physical Sciences - Advanced Study Institute, Vol. 547, Kluwer Academic Publishers B.V, Dordrecht, The Netherlands, 2000, pp. 263-282*
7. Jörg Appel, Henning Bockhorn and Michael Frenklach *Kinetic Modeling of Soot Formation with Detailed Chemistry and Physics: Laminar Premixed Flames of C₂ Hydrocarbons* Combustion and Flame, Vol. 121, pp. 122-136 (2000)
8. Michael Frenklach and Hai Wang *Detailed Mechanism and Modeling of Soot Particle Formation* in Henning Bockhorn (ed.) *Soot Formation in Combustion - Mechanisms and Models* Springer Series in Chemical Physics, Vol. 59, Springer-Verlag, Heidelberg, Berlin, 1994, pp. 165-189
9. Michael Frenklach *Soot Code* <http://www.me.berkeley.edu/soot/> The Frenklach Group, University of California, Berkeley, CA, USA, 2002
10. Ivar S. Ertesvåg *Turbulent Strøyming og Forbrenning* Tapir Akademisk Forlag, Trondheim, Norway, 1999
11. AEA-Technology *CFX-4.2 Solver Manual* CFX International, Harwell, UK, 1997
12. Fluent-Inc. *Fluent 5 User's Guide* Fluent Incorporated, Lebanon, NH, USA, 1998



Søren Gregers Christensen

Address: IVC-SEP Dept. of Chemical Engineering
Building 229, Office 210
Technical University of Denmark

Phone: (+45) 45 25 28 63
Fax: (+45) 45 88 22 58
e-mail: sgc@kt.dtu.dk
www: www.ivc-sep.kt.dtu.dk
Supervisor(s): Kaj Thomsen
Jørgen Møllerup

Ph.D. Study
Started: 1 September 2001
To be completed: August 2004

Modeling of Ion Exchange Processes in both Dilute and Concentrated Solutions

Abstract

Ion exchange equilibria have been modeled using the mass action law. The results show, that under the given assumptions, the model gives good results in both binary and multi component systems. Experiments are performed studying the absorption of water and salt from concentrated electrolyte solutions in different types of ion exchange resins. These experiments hopefully lead to a data material that could be used in developing a more complex model describing the complete distribution of ions and solvent between an aqueous phase and an ion exchange resin. The parameters of the Extended UNIQUAC have been extended to acidic systems. The model is now capable of describing the dissociation of both H_3PO_4 and HNO_3 in aqueous solutions and of describing the solubility of several different salts in aqueous solutions of these two acids.

Introduction

Ion exchange resins have been used commercially for more than a century and are at present time used extensively in the industry for separation and purification processes. One of the reasons for the growing interest in ion exchange processes is, that in many instances ion exchange technology can successfully substitute large-scale industrial separation/concentration processes, which do not satisfy modern ecological standards.

One of the most important controlling factors governing ion exchange as a separation method is the distribution of ions between the resin and the solution phase. Therefore, description of the equilibrium between a multi ionic solution and an ion exchanging material is essential for the development and optimization of ion exchange processes. Especially the choice of design and operating conditions require a detailed knowledge of the ion exchange selectivity. The amount of experimental data necessary for describing the ion exchange equilibria increases tremendously with each exchanging ionic species added to the system. Theoretical models that allow the prediction of multicomponent equilibria from corresponding binary experimental equilibria data are therefore very useful when designing ion exchange processes. At present time most attention has been paid to equilibrium of ion exchange concerning diluted solutions. However, a

general model capable of describing and predicting exchange equilibrium under a range of conditions does not exist at present time.

Specific Objectives

One of the main objectives of the project is to validate existing traditional models for the use in describing the equilibrium between an ion exchange resin and both dilute and concentrated aqueous electrolyte solutions.

Besides, the effect on the efficiency of the ion exchange of aspects such as the degree of cross linking within the ion exchange resin and the uptake of solvent and solutes should be considered. The amount of these kinds of data in literature is rather limited. Therefore experiments should be carried out concerning the absorption of salt and water in ion exchange resins with a varying amount of cross linking agent. The obtained results should be modeled using the Extended UNIQUAC model and a suitable affinity network model. One of the systems of interest is the ion exchange between $\text{K}^+ - \text{H}^+$ and Ca^{++} in both nitrate and phosphate systems. However, no parameters exist for the Extended UNIQUAC model in the presence of the acidic solutions. Therefore the parameters of Extended UNIQUAC model should be extended to apply in aqueous solutions of HNO_3 and H_3PO_4 .

Results and Discussion

Validation of Traditional Models

Usually two different approaches to the description of the ion exchange phenomenon are seen in the literature. In one of the approaches the ion exchange process is described as an osmotic equilibrium and in the other as a heterogeneous reaction. Usually the osmotic approach gives more rigorous models and a higher degree of information of the ion exchanger phase. However, due to lack of data, works dealing with the osmotic approach often are forced to use assumptions from the heterogeneous approach.

A common assumption is that the maximum uptake of ions by an ion exchanger is limited to the number of functional groups in the ion exchanger. Besides, it is often assumed that there is no uptake of ions with same charge as the functional groups and that the amount of solvent in the ion exchanger is independent on the ionic form of the exchanger, *i.e.* the swelling is constant during the exchange reaction. Introducing these assumptions makes it possible to model the equilibrium using the simple mass action law. This type of approach is useful for prediction and correlation of equilibria between ion exchangers like zeolites and resins with high degree of cross linking and aqueous solutions with low to moderate concentrations of ions.

The equilibria constant for the ion exchange reaction of several different systems of ionic species has been modeled using the common mass action law. The model has been used both with the assumption of ideality in both phases and with an activity coefficient model coupled with one or both phases. In the solution phase both the Pitzer and the Extended UNIQUAC has been used with similar results. In the resin phase the Wilson model has been applied taking into account the non-ideality. One example is given in figure 1 where the equilibrium between Ca^{++} and Na^+ on a Dowex ion exchange resin is shown.

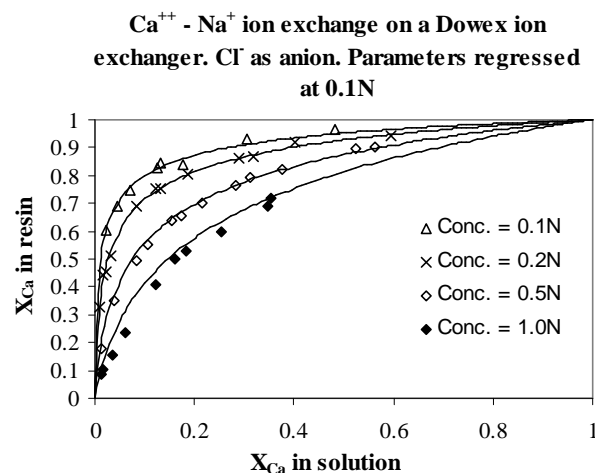


Figure 1.

The model is easily extended to multicomponent systems using only parameters obtained from the binary systems. An example of the models capabilities is shown in figure 2 where the Na^+ - Mg^{++} - Zn^{++} exchange is predicted from the corresponding binary systems.

The conclusion on the work is that the mass action law gives somewhat reasonable results for correlating the equilibrium isotherms of the different systems investigated. The accuracy of the model could be improved if introducing activity coefficient models for the two phases. However, the model does not give any information about the solvent uptake in the resin phase nor the effect of the resin structure (degree of crosslinking) on the ion exchange equilibrium.

Na^+ - Mg^{++} - Zn^{++} exchange on amberlite resin in aqueous chloride media.

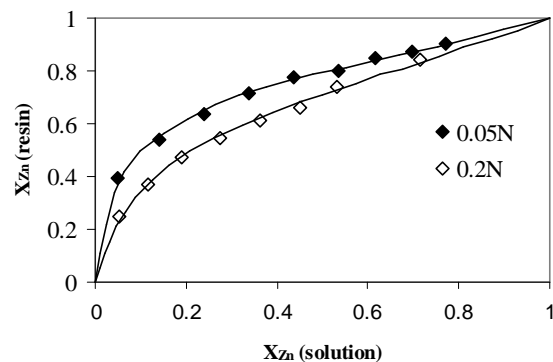


Figure 2.

Experiments Concerning the Absorption of Solvent and Solutes

At present time experiments are carried out at the Rohm & Haas production plant, Chauny, France. The experiments concern the ion exchange equilibrium between concentrated electrolyte solutions and different types of ion exchange resins.

The experiments cover 3 different gel type and 3 different macroporous type of ion exchange resins. The concentration of electrolyte in the bulk solution is varied between 0.5 and 3 molal.

The results show that the degree of cross linking in the ion exchange resin has a high influence on the absorption of salt and of the change in volume of the ion exchange resin during the absorption. Examples are given in figure 3 and 4.

IR120 is a gel type ion exchange with app. 7% cross linking agent while the Amberjet 1600 is a gel type resin with app. 16% cross linking. The figures shows that the higher degree of cross linking the less volume changes and the absorption of salt. However, the results

also show that even for the resin with very inelastic matrix the sorption of salt is relatively large.

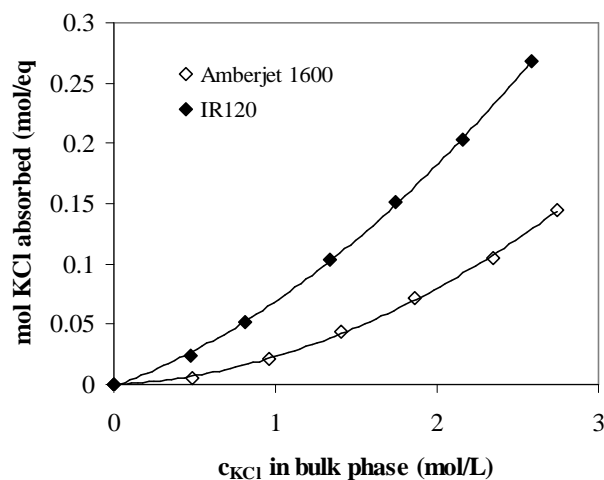


Figure 3

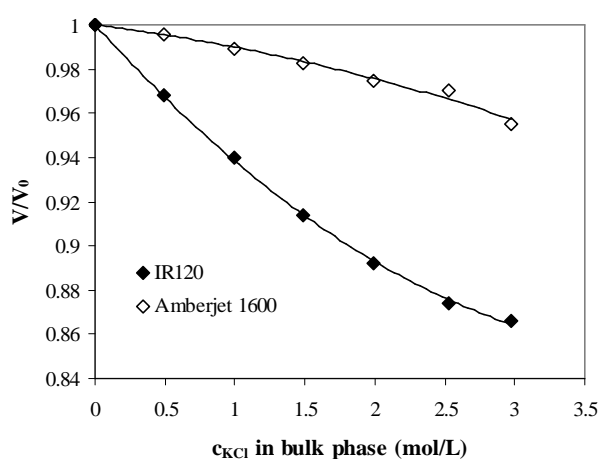


Figure 4

Extension of the Parameters of the Extended UNIQUAC Model to Aqueous Solutions of HNO_3 and H_3PO_4

The scope of this work is to describe the phase behavior (VLE, SLE) and thermal properties of aqueous solutions of ions like (K^+ , Na^+ , NH_4^+ , Ca^{2+} , Cl^- , NO_3^-) in the presence of phosphoric acid (H_3PO_4 , H_2PO_4^- , HPO_4^{2-}) by means of the Extended UNIQUAC model.

In this work we consider three different kinds of equilibria in order to describe the phase behavior of the aqueous electrolyte systems. The three different kinds are:

- *Solid-liquid equilibria, e.g.:*
 $\text{NaH}_2\text{PO}_4(s) \leftrightarrow \text{Na}^+(aq) + \text{H}_2\text{PO}_4^-(aq)$
- *Vapour-liquid equilibria, e.g.:*
 $\text{H}_2\text{O}(l) \leftrightarrow \text{H}_2\text{O}(g)$
- *Speciation equilibria, e.g.:*
 $\text{H}_3\text{PO}_4(aq) \leftrightarrow \text{H}^+(aq) + \text{H}_2\text{PO}_4^-(aq)$

The vapour-liquid equilibria is only considered for water. Except for the phosphoric and nitric acid, all electrolytes considered in this work are regarded as strong electrolytes meaning that they are completely dissociated at the involved concentrations.

Data used in the parameter optimization is taken from the IVC-SEP electrolyte databank which consists of more than 90000 data points.

The following type of data is included in the parameter optimization:

- SLE data
- Osmotic coefficients
- Mean ionic activity coefficients
- Excess heat capacity
- Heat of dilution
- Apparent molal relative heat capacity
- Specific heat
- Heat of solution
- Degree of dissociation

Model parameters are evaluated on the basis of more than 4000 experimental data points and the model shows good agreement between calculated and experimental data points in the temperature range from 0-110°C and concentrations up to 12 mol ($\text{kg H}_2\text{O}$)⁻¹ of phosphoric acid. The results show that the Extended UNIQUAC model successfully could have been applied to describe the phase behavior and thermal properties of various acidic aqueous solutions of electrolytes over a wide range of temperatures. The model is capable of describing the dissociation of both H_3PO_4 and HNO_3 in aqueous solutions and of describing the solubility of several different salts in aqueous solutions of these two acids. In addition the model reproduces the thermal properties of these solutions with high accuracy. One example of the model capabilities is given in figure 5 where the solubility of KH_2PO_4 in aqueous solutions of H_3PO_4 is shown.

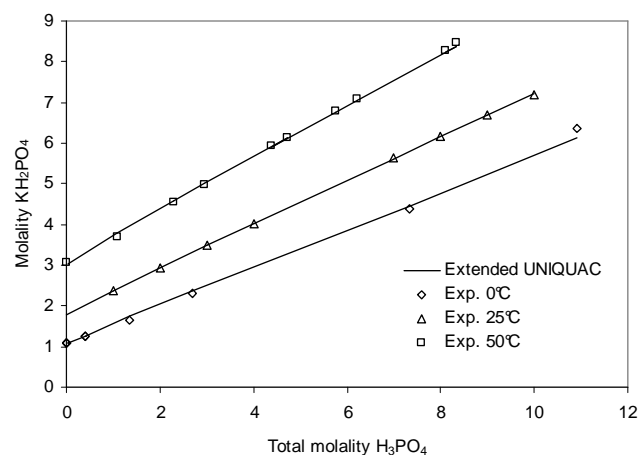


Figure 5

Conclusions

The conclusion on the work using the mass action law for describing ion exchange equilibria is that the method gives reasonable results for correlating the equilibrium isotherms of the different systems investigated. The method is relatively simple and could be used for both binary and multi component systems. However, the model does not give any information about the solvent and solute uptake in the resin phase nor the effect of the resin structure.

Experiments are currently performed concerning the ion exchange equilibrium between concentrated electrolyte solutions and different types of ion exchange resins. The results hopefully give a deeper understanding of the effect of ion interactions and matrix structure on the absorption of salt in the resin phase.

The work has included an extension of the parameters of the Extended UNIQUAC model to acidic aqueous solutions. The model is now capable of describing the dissociation of both H_3PO_4 and HNO_3 in aqueous solutions and of describing the solubility of several different salts in aqueous solutions of these two acids.

List of Publications

1. Søren Gregers Christensen and Kaj Thomsen, "Produktion af gødningssalte", Dansk Kemi, 83 (2002), p. 18-19
2. Søren Gregers Christensen and Kaj Thomsen, "Modeling of Vapor-Liquid-Solid Equilibria in Acidic Aqueous Solutions", Ind. & Eng. Chem. Res. 42 (2003) p. 4260 - 4268.
3. Søren Gregers Christensen and Kaj Thomsen, "Modellering af ligevægte i ionbytningsprocesser", Dansk Kemi 84 (2003) p. 21 – 23.



Loïc d'Anterrodres
Address: CAPEC, Dept. of Chemical Engineering
Building 227 Office 266
Technical University of Denmark
Phone: (+45) 45 25 29 11
Fax: (+45) 45 93 29 06
e-mail: loa@kt.dtu.dk
www: www.capec.kt.dtu.dk
Supervisor(s): Rafiqul Gani

Ph.D. Study
Started: September 2002
To be completed: August 2005

Group Contribution Based Process Flowsheet Synthesis, Design and Modelling

Abstract

The core idea is to apply the group contribution approach for property estimation to the synthesis, design and modelling of a flowsheet, with groups (or atoms, etc.) representing units, bonds representing streams, rules for molecule feasibility representing flowsheet feasibility and sum of group contributions representing the performance of the flowsheet.

Introduction

Modelling and simulation of a process flowsheet usually involve identifying the structure of the flowsheet, deriving model equations to represent each operation, and solving the resulting total model equations according to one of various available simulation strategies. The flowsheet synthesis problem determines the type of operations and their sequence needed to achieve the conversion of raw materials to some specified set of products. The flowsheet design problem determines the optimal values for the conditions of operation and other operation/equipment related variables for the synthesized flowsheet. The flowsheet modelling, synthesis and design problems are related since for generation and screening of alternatives, some form of flowsheet models are needed. Also, flowsheet models are needed for verification of the synthesis/design problem solution.

In contrast, a group-contribution (GC) based pure component property estimation of a molecule requires knowledge of the molecular structure and the groups needed to uniquely represent it. The needed property is estimated from a set of *a priori* regressed contributions for the groups representing the molecule. Having the groups and their contributions together with a set of rules to combine groups to represent any molecule therefore provides the possibility to “model” the molecule and/or a mixture of molecules. This also means that the reverse problem of property estimation, that is, the synthesis/ design of molecules having desired properties can be solved by generating chemically feasible molecular structures and testing for

their properties. This reverse problem is also known as computer aided molecular design.

Let us now imagine that each group used to represent a fraction of a molecule could also be used to represent an operation in a process flowsheet. Just as in chemical property estimation, groups may have one or more free attachments, in flowsheet “property” estimation, process-groups may also have similar number of free attachments, for example, connecting streams. In this way, a set of process-groups representing different types of operations may be created and the “properties” of a specified flowsheet may be estimated by first identifying the process-groups that will uniquely represent it and then by computing their contributions to the needed “property”.

Flowsheet Modelling and Design through Process-groups

To apply a group contribution method for flowsheet synthesis, design and modelling, a process-group representation of a flowsheet, a “property” model for flowsheet and the reverse “property” calculations for flowsheets have been developed.

Definitions

Process-group: A process-group is the representation of a unit operation or a set of units. It has at least one inlet stream and one outlet stream as connections.

Structure or flowsheet structure: A structure or a flowsheet structure is defined as the ensemble composed by the process-groups and the connections between the process-groups.

Flowsheet or process: A flowsheet or process is a flowsheet structure and additional parameters like stream composition, flowrate, pressure, temperature so that all the needed information for a rigorous simulation are available.

Process-group based representation of a flowsheet

A group representing the separation of components A, B, C and D in two outlet streams containing A and B, and, C and D, is named (AB)(CD). Special groups representing a process inlet or a process outlet are defined as iABCD and oAB, for an inlet with the 4 components and an outlet with only A and B.

From the list of available groups like iABC, (A)(BC), (B)(C) and the pure process outlets, a feasible flowsheet structure can be created as shown in figure 1. The process-groups are not component dependent, but component property dependent, thus the ability to use the same group with different components having similar properties.

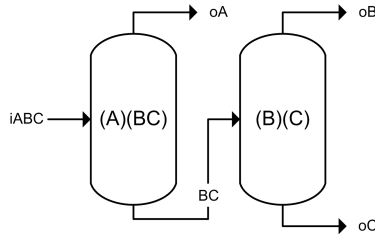


Figure 1: Example of a flowsheet structure based on simple process-groups

Reverse problem formulation

As developed by Erik Bek-Pedersen[1] the design of distillation columns can be based only on the driving force between the two key components. Two of the conclusions of the driving force model for distillation columns is that the driving force is inversely proportional to energy consumption and that in a distillation train the easiest separation, i.e., where the maximum driving force is available, must be performed first. From the driving force which is difference in composition between two co-existing phase (Eq. 1) it is possible to back calculate all the design parameters of the distillation columns.

A generalized driving force model based on the assumptions of the driving force for distillation column has been developed. Thus the ability to back calculate, reverse problem, the design parameters of any separation process that can be modelled in terms of driving force.

$$D_i = \frac{x_i \alpha_i}{1 + x_i (\alpha_i - 1)} - x_i = y_i - x_i \quad (1)$$

The main breakthrough in the driving force based modelling is that any model or experimental data can be used to obtain α_i .

Now, by associating a driving force to each process-groups it is possible to describe a flowsheet with process-groups without any over simplification of the unit models. The driving force model provides the back calculation capabilities to get the process design details from the flowsheet structure.

A flowsheet property model

A flowsheet “property” model (Eq. 2) has been defined to calculate the energy consumption of a flowsheet.

$$E = \sum_{k=1}^{n=NG} \frac{1 + p_k}{d_{ij}^k} \times a_k + A \quad (2)$$

where E is the energy consumption of the flowsheet (MkJ/hr), NG is the number of process-groups, p_k the penalty, d_{ij}^k the maximum driving force of the process-group k, a_k the contribution of the process-group k and A a constant.

$$p_k = \sum_{i=1}^{nt} Df_i \quad (3)$$

where nt is the number of tasks that should be performed before the task k in the ideal case and Df_i the driving force of task i.

The contribution of the process-groups a_k are regressed from experimental data. Every unit operation has a position in the flowsheet where it can “attain” the theoretical maximum driving force. At any other position, the unit operation is able to attain a lower driving force than the maximum. The penalty, p_k , is a function of the attainable driving force.

Flowsheet Synthesis

Using the same approach as Computer Aided Molecular Design[2] it is possible from the process-groups combination rules to generate flowsheet structures, evaluate them and find the best alternative matching the targets.

Process-group combination rules and feasible structure generation

Considering a group (ABC)(DE) this group has:

- 1 inlet defined as iABCDE
- 2 outlets defined as oABC and oDE

The inlet of the process-group (ABC)(DE), iABCDE, can only be connected to a corresponding oABCDE outlet from another group, or to a general iABCDE of the flowsheet. In the same way, the outlets oABC and oDE, can only be connected to a corresponding iABC or iDE of another process-group, or to a general outlet of the flowsheet oABC or oDE. Any other combination is not allowed. Respecting the combination rules ensure, from the definition of the process-groups to have a feasible structure.

From the process-groups involved in the problem, apply the combination rules to all the process-groups to generate all the feasible flowsheet alternatives. The “property” of each alternative can easily be calculated, thus the ability to do a rigorous simulation only with the most promising flowsheets.

Multi-property target flowsheet synthesis

In the case of the synthesis of alternatives with more than one “property” target, all the alternatives are computed, then a linear optimisation is performed to get the best alternatives with respect to a desired optimisation function. This can for example be used to balance energy consumption and risk, if a risk property model is available for the process-groups.

Results

The methodology has been successfully applied and the results from a simple illustrative problem involving the separation of a multi-component mixture with or without azeotropic pairs is presented here.

Considering the separation of a 5 component mixture into pure streams at optimal operational cost is the objective of this synthesis problem. The energy “property” model is used for prediction of the process energy cost and the necessary process-groups and their contribution (Table 2) are needed for prediction are already available. The details of the synthesis problem needed to solve this problem are given in table 1.

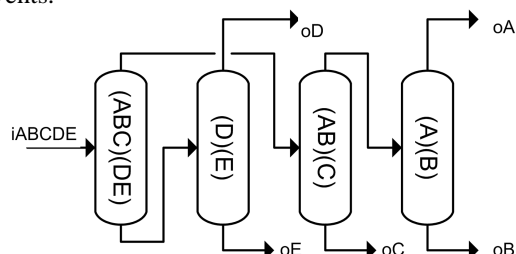
Table 1: Properties of the components and inlet definition

Component	Flow rate (kmol/hr)	Normal boiling point (K)	Relative volatility	Product purity specification
A	45.4	231	7.98	0.985
B	136.1	261	3.99	0.965
C	226.8	273	3.00	0.985
D	181.4	301	1.25	0.980
E	317.5	309	1.00	0.980

With the process-groups and their “property” model parameters available, the first step is to generate feasible “structures” that satisfy the product purity specification using the process-group combination rules. The next step is to predict the energy “property” of each generated flowsheet. Finally, the reverse problem is solved for any selected flowsheet to obtain the corresponding design variables that match the design target (attainable driving force for any operation in the flowsheet). The optimal flowsheet together with the minimum energy is shown in figure 2. If the compounds A-E are taken as Propane, i-Butane, n-Butane, i-Pentane and n-Pentane, then this solution can be compared with that given by Biegler et al.[3]. Note that the same solution is obtained without any process-model based numerical optimisation. The design targets for each operation in terms of attainable driving force is given in

table 3. Applying now the algorithm of Bek-Pedersen (2003), the design variables can be obtained (not shown here).

It should be noted that the solution provided is valid for any mixture of 5 components that have similar relative volatilities as given in table 1. Also, for azeotropic pairs, they are valid if the solvent-free relative volatility is the same. In this way, it also provides the design target for solvents.



$$E = \frac{9.1854}{0.2898} + \frac{4.1216}{0.1015} + \frac{2.5133}{0.0805} + \frac{9.7417}{0.2707} = 184.89 \text{ GJ/hr}$$

Figure 2: Best alternative for the 5 component separation

Table 2: Process-group parameter table for energy “property”

Process-group	Contribution
a _{(A)(BCDE)}	7.4146
a _{(AB)(CDE)}	2.4225
a _{(ABC)(DE)}	9.1854
a _{(ABCD)(E)}	2.79454
a _{(A)(BCD)}	9.8414
a _{(B)(CDE)}	2.3182
a _{(AB)(CD)}	2.2835
a _{(ABC)(D)}	11.3013
a _{(BC)(DE)}	10.1391
a _{(BCD)(E)}	2.6829
a _{(A)(BC)}	11.4227
a _{(B)(CD)}	2.8731
a _{(AB)(C)}	2.5133
a _{(BC)(D)}	12.0868
a _{(C)(DE)}	12.1721
a _{(CD)(E)}	2.4254
a _{(A)(B)}	9.7417
a _{(B)(C)}	3.3387
a _{(C)(D)}	10.8515
a _{(D)(E)}	4.1216
A	36.9301

Conclusion

This new method offers important benefits over the traditional ones. The method is truly predictive and is component independent as far as generation of alternatives are concerned. The ability to generate from the groups all the feasible alternatives of a given process without the need for rigorous models another advantage. It opens the possibility to screen a lot of alternatives very quickly and with good accuracy. The method is also an “integrator” in the sense that by adding new

process-groups it is possible to simultaneously model, design and synthesize products and processes that can produce them.

Current work is creating more “property” models for the process groups and the representation of complex unit operations such as the divided wall columns. Work is also going on to generate model flowsheets with reaction and separation.

Table 3: Driving force of the separation tasks at T=300K and P=1atm

Separation	Maximum driving force
A/B	0.2707
B/C	0.0805
C/D	0.2898
D/E	0.1015

References

1. Erik Bek-Pedersen, 2003, Synthesis and Design of Distillation based Separation Schemes. PhD thesis, Technical University of Denmark.
2. Peter M. Harper, 2000, A Multi-Phase Multi-Level Framework for Computer Aided Molecular Design. PhD thesis, Technical University of Denmark.
3. L. T. Biegler, I. E. Grossmann and A. W. Westerberg, 1997, Systematic Methods of Chemical Process Design, Prentice Hall.



Mario Richard Eden

Address: CAPEC, Dept. of Chemical Engineering
Building 227, Office 264
Technical University of Denmark

Phone: (+45) 45 25 29 10
Fax: (+45) 45 93 29 06
e-mail: mre@kt.dtu.dk
www: www.capec.kt.dtu.dk

Supervisor(s): Sten Bay Jørgensen
Rafiqul Gani

Ph.D. Study
Started: June 1999
To be completed: December 2003

Property Based Process and Product Synthesis and Design

Abstract

This thesis describes the development of a general framework for solving process and product design problems. Targeting the desired performance of the system in a systematic manner relieves the iterative nature of conventional design techniques. Furthermore, conventional component based methods are not capable of handling problems, where the process or product objectives are driven by functionalities or properties rather than chemical constituency. The framework is meant to complement existing composition based methods by being able to handle property driven problems.

Introduction

In recent years the chemical engineering design community has moved towards the development of integrated solution strategies for simultaneous consideration of process and product design issues. By doing so, the complexity of the design problem increases significantly. Mathematical programming methods are well known, but may prove rather complex and time consuming for application to large and complex chemical, biochemical and/or pharmaceutical processes. Model analysis can provide insights that allow for simplification of the overall problem as well as extending the application range of the original models. In principle, the model equations representing a chemical process and/or product consist of balance equations, constraint equations and constitutive equations. The nonlinearity of the model, in many cases, is attributed to the relationships between the constitutive variables and the intensive variables. The model selected for the constitutive equations usually represents these relationships. By decoupling the constitutive equations from the balance and constraint equations a conventional process/product design problem may be reformulated as two reverse problems. The first reverse problem is the reverse of a simulation problem, where the process model is solved in terms of the constitutive (synthesis/design) variables instead of the process variables, thus providing the synthesis/design targets. The second reverse problem (reverse property prediction) solves the constitutive equations to identify unit operations, operating conditions and/or products by matching the synthesis/design targets. Since the reverse

problem formulation technique extends the application range of the numerical solvers as well as the models themselves, it is possible to identify alternative designs that conventional methods are not capable of finding. Thus business decision making can be facilitated, as the methodology allows for easy screening of alternatives and identification of candidate designs that should be selected for further, more rigorous investigation.

The links between the two reverse problems are the constitutive variables. One representation of such variables is the physical properties of the components and streams in the system. The design targets, which are identified by the first reverse problem, describe specific property values that need to be matched when solving the second reverse problem. Therefore a framework capable tracking properties in a systematic manner is called for. Such a framework should also be able to handle problems that are driven by properties rather than chemical constituency. An example of such a problem is the design of paper of a specified quality, where the performance of the paper machine, i.e. the quality of the paper, can not be described by composition based methods alone, since paper consists primarily of cellulose. The properties of paper, that determine whether or not the quality is acceptable, e.g. reflectivity, opacity etc., depend on the physical properties of the paper, e.g. fiber length, fibrocity etc.

Recently, the concept of property clustering has been introduced for systematic tracking of properties throughout chemical processes. These clusters allow for systematic representation of process streams and units from a property perspective. In this thesis, the property

clustering techniques are incorporated into the reverse problem formulation framework, thus providing a representation of the constitutive variables. The clusters are tailored to have the attractive features of intra-stream and inter-stream conservation, thus enabling the development of consistent additive rules along with their ternary representation. The combined reverse problem formulation and property clustering framework is used to solve several property driven problems in a targeted manner.

General Problem Formulation

A general process/product synthesis and/or design problem can be represented in generic terms by the following set of equations:

$$F_{Obj} = \min(A^T y + f(x)) \quad (1)$$

$$\text{s.t. } h_1\left(\frac{\partial x}{\partial z}, x, y\right) = 0 \quad (2)$$

$$h_2(x, y) = 0 \quad (3)$$

$$g_1(x) > 0 \quad (4)$$

$$g_2(x, y) > 0 \quad (5)$$

$$B \cdot y + C \cdot x > d \quad (6)$$

In the above equations, F_{Obj} is the objective function that needs to be minimized or maximized in order to satisfy the desired performance criteria; x and y are the optimization real and integer variables respectively; h_1 represents the process model equations including the transport model; h_2 represents process equality constraints; g_1 and g_2 represent other process/product related inequality constraints, while equation (6) represents structural constraints related to process as well as products. Although the model equations themselves may be static, the transport model will most likely consist of ordinary differential equations. Furthermore, the model structure given by equation (2) is limited to simple transport models, where there is no coupling between the constitutive equations and the flow field. If spatial gradients are negligible, then equation (2) reduces to:

$$h_1(x, y) = 0 \quad (7)$$

It is important to point out, that all synthesis/design problems may be described using this generalized set of equations. Depending on the specific problem some terms and equations may be omitted, e.g. determination of only feasible solutions will not require equation (1). It must be emphasized however, that regardless of the problem a process model represented by equation (2) is needed and it is the model type and validity ranges that defines the application range of the solution. Hence heuristic and graphical methodologies resulting in a feasible but not necessarily optimal solution, as well as mathematical programming techniques that determine optimal solutions can be formulated and solved by defining equations (1)–(7).

The ease of solution of the overall problem as well as the attainable solutions is governed primarily by the complexity of the process model. Therefore it is reasonable to investigate if the solution of the process model can be simplified.

Reverse Problem Formulation Framework

In principle, the model equations representing a chemical process and/or product consist of balance equations, constraint equations and constitutive equations. The nonlinearity of the model, in many cases, is attributed to the relationships between the constitutive variables and the intensive variables. The model selected for the constitutive equations usually represents these relationships, therefore it would seem appropriate to investigate how to rearrange or represent the constitutive models.

By decoupling the constitutive equations from the balance and constraint equations the conventional process/product design problems may be reformulated as two reverse problems. The first reverse problem is the reverse of a simulation problem, where the process model is solved in terms of the constitutive (synthesis/design) variables instead of the process variables, thus providing the synthesis/design targets. The second reverse problem (reverse property prediction) solves the constitutive equations to identify unit operations, operating conditions and/or products by matching the synthesis/design targets. An important feature of the reverse problem formulation is that as long as the design targets are matched, it is not necessary to resolve the balance and constraint equations.

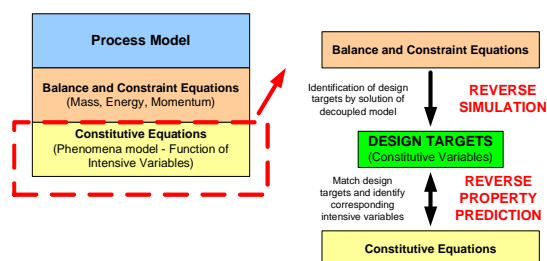


Figure 1: Decoupling of constitutive equations

The model type and complexity is implicitly related to the constitutive equations, hence decoupling the constitutive equations from the balance and constraint equations will in many cases remove or reduce the model complexity. Since the constitutive equations (property models) contain composition terms, it is beneficial to solve for the constitutive variables directly, thus removing the composition dependency from the problem.

Property Clustering

Standard techniques for process design are based on individual chemical species. Therefore, tracking, manipulation, and allocation of species are key design

tools starting with component materials balances to process modeling equations that are based on targeted species. But, should components always constitute the basis for process design and optimization? Interestingly enough, the answer is no! Many process units are designed to accept or yield certain properties of the streams regardless of the chemical constituents. For instance, the design and performance of a papermaking machine is based on properties (e.g., reflectivity, opacity, and density to name a few). A heat exchanger's performance is based on the heat capacities and heat transfer coefficients of the matched streams. The chemical identity of the components is only useful to the extent of determining the values of heat capacities and heat transfer coefficients. Similar examples can be given for many other units (e.g., vapor pressure in condensers, specific gravity in decantation, relative volatility in distillation, Henry's coefficient in absorption, density and head in pumps, density, pressure ratio, and heat capacity ratio in compressors, etc.).

Since properties (or functionalities) form the basis of performance of many units, it will be very insightful to develop design procedures based on key properties instead of key compounds. The challenge, however, is that while chemical components are conserved, properties are not. Therefore, the question is, whether or not it is possible to track these functionalities instead of compositions? The answer is yes!

The essence of this novel approach is to develop conserved quantities called clusters that are related to the non-conserved properties. The clusters can be described as functions of the raw physical properties themselves. The clusters are obtained by mapping property relationships into a low dimensional domain, thus allowing for visualization of the problem. The clusters are tailored to possess the two fundamental properties of inter- and intra-stream conservation, thus enabling the development of consistent additive rules along with their ternary representation.

To overcome the limitations encompassed when trying to track properties among process streams and units, the use of property-based clusters has been proposed. The clusters are obtained by mapping property relationships into a low dimensional domain, thus allowing for visualization of the problem. The clusters can be described as functions of the raw properties. The clustering approach utilizes property operators defined as:

$$\psi_j(P_{jM}) = \sum_{s=1}^{N_s} \frac{F_s}{\sum_{s=1}^{N_s} F_s} \cdot \psi_j(P_{js}) = \sum_{s=1}^{N_s} x_s \cdot \psi_j(P_{js}) \quad (8)$$

In equation (8), $\psi_j(P_{js})$ is an operator on the j 'th property P_{js} of stream s . The property operator formulation allows for simple linear mixing rules, i.e. the operators correspond to the actual properties, or the operators may describe functional relationships of the properties, e.g. for density, where the resulting property

of mixing two streams is given as the inverse of the summation over the reciprocal property values multiplied by their fractional contribution (x_s). The property operators are converted to dimensionless variables by division by an arbitrary reference, which is appropriately chosen such that the resulting dimensionless properties are of the same order of magnitude:

$$\Omega_{js} = \frac{\psi_j(P_{js})}{\psi_j^{ref}} \quad (9)$$

An Augmented Property index (AUP) for each stream s is defined as the summation of all the dimensionless property operators:

$$AUP_s = \sum_{j=1}^{NP} \Omega_{js} \quad (10)$$

The property cluster for property j of stream s is defined as follows:

$$C_{js} = \frac{\Omega_{js}}{AUP_s} \quad (11)$$

A cluster based mixer model from original composition based balance equations has been developed. The mixer model is given in equations (12) and (13):

$$C_{jMIX} = \sum_{s=1}^{N_s} \beta_s \cdot C_{js}, \quad \beta_s = \frac{x_s \cdot AUP_s}{AUP_{MIX}} \quad (12)$$

$$AUP_{MIX} = \sum_{s=1}^{N_s} x_s \cdot AUP_s \quad (13)$$

Incorporating these clusters into the mass integration framework enables the identification of optimal strategies for recovery and allocation of plant utilities. Process insights are obtained through visualization tools based on optimization concepts. Since the clusters are tailored to maintain the two fundamental rules for intra- and inter-stream conservation, lever-arm analysis may be employed extensively to identify recycle potentials. For visualization purposes the number of clusters is limited to three, however when using mathematical programming this limitation is removed.

It should be noted that even though for visualization purposes the number of clusters is limited to three, this does not imply that the number of properties describing each stream is also limited to three. Assuming that the necessary number of properties describing the process streams is 5, then a one-to-one mapping to property clusters would yield 5 clusters. If it is desired to visualize this problem, then it is necessary to reformulate the property operator descriptions in such a

way that total number of operators is 3, i.e. a property operator can be a function of several properties.

Case Study – Recycle Opportunities in Papermaking

To illustrate the usefulness of constitutive or property based modeling, a case study of a papermaking facility is presented. Wood chips are chemically cooked in a Kraft digester using white liquor (containing sodium hydroxide and sodium sulfide as main active ingredients). The spent solution (black liquor) is converted back to white liquor via a recovery cycle (evaporation, burning, and caustification). The digested pulp is passed to a bleaching system to produce bleached pulp (fiber). The paper machine employs 100 ton/hr of the fibers. As a result of processing flaws and interruptions, a certain amount of partly and completely manufactured paper is rejected. These waste fibers are referred to as broke. The reject is passed through a hydro-pulper followed by a hydro-sieve with the net result of producing an underflow, which is burnt, and an overflow of broke, which goes to waste treatment. It is worth noting that the broke contains fibers that may be partially recycled for papermaking.

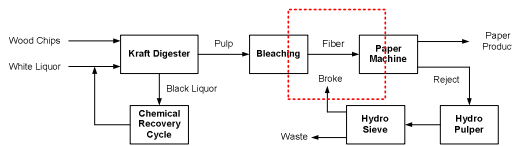


Figure 2: Schematic of pulp and paper process

The objective of this case study is to identify the potential for recycling the broke back to the paper machine, thus reducing the fresh fiber requirement and maximize the resource utilization. Three primary properties determine the performance of the paper machine and thus consequently the quality of the produced paper:

- Objectionable Material (OM)
- Absorption coefficient (k)
- Reflectivity (R_{∞})

In order to convert property values from raw property data to cluster values, property operator mixing rules are required. The property relationships can be described using the Kubelka-Munk theory. The mixing rules for objectionable material (OM) and absorption coefficient (k) are linear, while a non-linear empirical mixing rule for reflectivity has been developed.

Since the optimal flowrates of the fibers and the broke are not known, a reverse problem is solved to identify the clustering target corresponding to maximum recycle. In order to minimize the use of fresh fiber, the relative cluster arm for the fiber has to be minimized, i.e. the optimum feed mixture will be located on the boundary of the feasibility region for the paper machine. The cluster target values to be matched by mixing the fibers and broke are identified graphically and represented as the intersection of the mixing line and the feasibility region in figure 3.

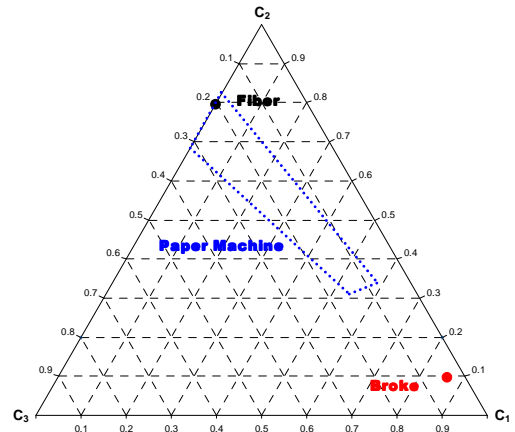


Figure 3: Ternary cluster diagram

Direct recycle does not achieve the minimum fiber usage target. Therefore the properties of the broke will have to be altered to match the maximum recycle target. For the same mixing point, the required interception can be calculated and is shown graphically in figure 4. This clustering result can then be converted back to a set of property targets.

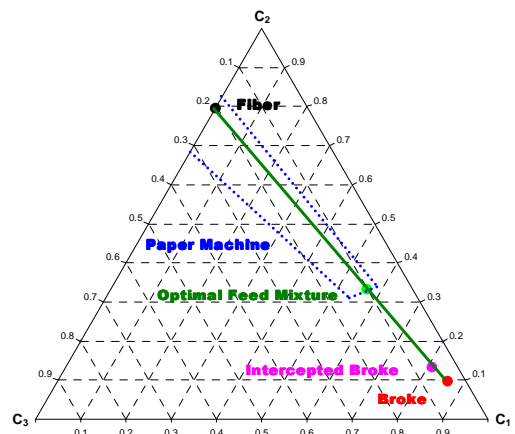


Figure 4: Identification of property interception targets

Note that for each mixing point on the boundary of the feasibility region, a clustering target exists for the intercepted broke, so the reverse problem formulation technique is actually capable of identifying all the alternative product targets that will solve this particular problem.

Synthesis and Design of Formulations

Formulation, the mixing of materials to achieve a new or improved product, is practiced in many different industries, including paints and dyes, foods, personal care, detergents, plastics, and pharmaceutical development. Often the formulations are selected based on qualitative engineering knowledge and/or experience; however the effectiveness of such an approach is determined by the available data and absence of bias towards specific solutions. The

prevailing methodology for formulation design utilizes Design Of Experiments (DOE) software, which is based on rigorous optimization routines. When applied to the synthesis of a three component mixture problem, the data can be visualized using ternary diagram, where each of the vertices represents the pure components or mixtures to be used in the formulation. As functions of composition the property values are plotted as contour plots and for each desired property of the formulation a new ternary diagram must be generated. Furthermore this has to be repeated for all candidate ternary mixtures attainable from the pure component set. This approach will quickly suffer combinatorial problems if the number of candidate components/mixtures increases. Thus there is a need for fast, reliable and systematic screening methods capable of identifying candidate formulations without suffering from combinatorial explosion. A framework capable of handling multiple candidate components/mixtures is needed to synthesize promising formulations.

In this work, a new simple, yet effective, systematic method to synthesize and design formulations has been developed. For any formulation design problem, the target and the raw materials are identified on the ternary property cluster diagram. Since formulation design involves only mixing operations, the optimal formulation is easily determined together with all possible solutions by determining the mixing operations that will match the target. It should be noted that the design of the formulation and the simulation of the mixing operation are performed simultaneously. Since all mixing operations are straight lines within the ternary diagram it is possible to visually identify the binary, ternary and multi-component mixtures, which are capable of matching the desired target properties. Lever-arm analysis can be employed to optimize the fractional contributions from each stream in terms of e.g. cost, environmental impact or any other performance indicator. Thus business decision making can be facilitated, as the methodology allows for easy screening of alternatives and identification of candidate formulations that should be selected for further, more rigorous investigation including laboratory trials. The significance of this method is that irrespective of how many components and or mixtures are handled, the problem is solved visually on a ternary diagram. Also, the same method (but with different cluster properties) is applicable to wide range of problems, such as, solvent mixtures, oil blends, coatings for paints, additives for drugs and many more.

Case Study – Visual Mixture Formulation

To illustrate the use of the property cluster based formulation design method, a simple visual “mixture” design is presented. The objective of this investigation is to identify binary and ternary mixtures of pure components resulting in a target mixture with a solubility parameter of approximately $18.5 \text{ MPa}^{1/2}$ and a target set of properties. In order to identify candidate components that would be feasible constituents

matching the target formulation, a database search was performed. The search space was limited to compounds with solubility parameters between 18.0 and $19 \text{ MPa}^{1/2}$, thereby ensuring mutual miscibility of all the compounds found. The search yielded many compounds and the 25 compounds with solubility parameters closest to $18.5 \text{ MPa}^{1/2}$ have been considered. For illustrative purposes, however only 6 of those components are highlighted in this study. The components were selected solely based on their relative placement on the ternary diagram to ensure a reasonable spread in order to illustrate the formulation synthesis.

The property data is converted to property cluster values for ternary representation. The resulting diagram is given in figure 5, where the individual components are denoted by small dots along with the component ID, while target is shown as a slightly larger dot. Drawing straight lines between the pure component points through the target cluster, the candidate formulations can be identified. The feasible binary and ternary candidate formulations are shown in figures 6 and 7.

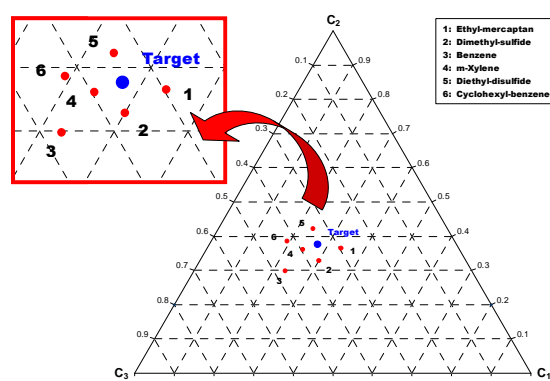


Figure 5: Visualization of formulation synthesis

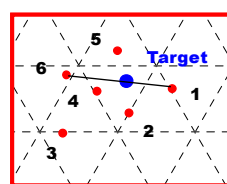


Figure 6: Binary candidates

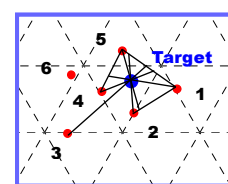


Figure 7: Ternary candidates

It must be emphasized that matching the cluster target is a necessary but NOT sufficient criterion for matching the property targets. The AUP values of the formulated mixture and the target must also match in order to match the property targets. In the following the validation procedures for binary and ternary mixture formulations are presented. The procedures can be extended to quaternary and multi-component formulations using visual as well mathematical optimization techniques. The first step is visual identification of the candidate constituents for e.g. a quaternary mixture, thus reducing the search space by screening out inherently infeasible combinations. Next

the feasible mixture compositions are identified by evaluating the AUP values of the formulated mixtures and finally a performance criterion is added to identify the optimal mixture.

Conclusions

The primary contributions of the work presented in this thesis are two-fold, i.e. first, by the introduction of the reverse problem formulation concepts, the inherent iterative nature of solving design problems is relieved for a large class of problems. Secondly, the use of property based clusters allows for solution of problems that are driven by properties rather than chemical constituency. A key advantage of the reverse problem formulation framework presented in this thesis, is the ability to identify optimum solutions to process and product design problems much easier than by solving the conventional forward problem. Furthermore, the property clustering technique represents an extension to conventional composition based methods, as it enables the solution of problems where conventional methods are not capable of describing the problem adequately.

Acknowledgements

Financial support from the Nordic Energy Research Program (Process Integration Section) and the Danish Department of Energy is highly appreciated. External research was conducted at Auburn University, USA. The fruitful research collaboration and friendship of Dr. Mahmoud M. El-Halwagi is held in the highest regard.

List of Publications

1. Jørgensen S.B., Gani R., Jonsson G., Eden M.R. (1999): "Development of Alternative Energy Efficient Separation Processes", *Journal of Danish Chemistry*, Teknisk Forlag.
2. Eden M.R., Koggersbøl A., Hallager L., Jørgensen S.B. (2000): "Dynamics and Control During Startup of Heat-integrated Distillation Column", *Computers and Chemical Engineering*, **24**, pp. 1091-1097.
3. Eden M.R., Andersen T.R. (2000): "Computer Aided Process Engineering for Process Integration and Design", Scandinavian Simulation Society (SIMS) 2000 Proceedings, Lyngby, Denmark.
4. Andersen T.R., Eden M.R. (2000): "Computer Aided Process Engineering for Operational Analysis and Control Design", Scandinavian Simulation Society (SIMS) 2000 Proceedings, Lyngby, Denmark.
5. Eden M.R., Gani R. (2002): "Computer Aided Process/Product Design – Issues, Needs and Solution Approaches", Proceedings of WWDU 2002, Berchtesgaden, Germany, 2002.
6. Eden M.R., Jørgensen S.B., Gani R., El-Halwagi M.M. (2002): "A New Component-Free Approach for Simultaneous Process and Product Design through Property Integration", Proceedings for CHISA 2002, 15th International Congress of Chemical and Process Engineering, Prague, Czech Republic.
7. Eden M.R., Jørgensen S.B., Gani R., El-Halwagi M.M. (2002): "Property Integration – A New Approach for Simultaneous Solution of Process and Molecular Design Problems", *Computer Aided Chemical Engineering* **10**, 79-84, Elsevier.
8. Eden M.R., Jørgensen S.B., Gani R., El-Halwagi M.M. (2002): "A Novel Framework for Simultaneous Separation Process and Product Design", Proceedings of International Conference on Distillation and Absorption 2002.
9. Eden M.R., Gani R., Jørgensen S.B. (2002): "Development of Sustainable Chemical Products and Processes", *Journal of Danish Chemistry*, **10**, pp. 34-37, Teknisk Forlag.
10. Eden M.R., Gani R., Jørgensen S.B. (2002): "A Holistic Design Methodology", *Journal of Danish Chemistry*, **12**, pp. 29-32, Teknisk Forlag.
11. El-Halwagi M.M., Glasgow I.M., Eden M.R., Qin X. (2002): "Property Integration: Componentless Design Techniques and Visualization Tools", *AIChE Journal* (accepted for publication).
12. Eden M.R., Jørgensen S.B., Gani R., El-Halwagi M.M. (2003): "A Novel Framework for Simultaneous Separation Process and Product Design", *Chemical Engineering and Processing* (in press).
13. Eden M.R., Jørgensen S.B., Gani R. (2003): "A New Modeling Approach for Future Challenges in Process and Product Design", Proceedings of ESCAPE-13, *Computer Aided Chemical Engineering* **14**, 101-106, Elsevier.
14. Eden M.R., Jørgensen S.B., Gani R., El-Halwagi M.M. (2003): "Reverse Problem Formulation based Techniques for Process and Product Design", Proceedings of PSE-2003, *Computer Aided Chemical Engineering* **15A**, pp. 451-456, Elsevier.
15. Eden M.R., Jørgensen S.B., Gani R., El-Halwagi M.M. (2003): "Property Cluster based Visual Technique for Synthesis and Design of Formulations", Proceedings of PSE-2003, *Computer Aided Chemical Engineering* **15B**, pp. 1175-1180, Elsevier.



Søren Søndergaard Frederiksen

Address: IVC-SEP, Dept of Chemical Engineering
Building 229, Office 217
Technical University of Denmark

Phone: (+45) 45 25 29 78

Fax: (+45) 45 88 22 58

e-mail: ssf@kt.dtu.dk

www: www.ivc-sep.kt.dtu.dk

Supervisor(s): Jørgen M. Møllerup,
Michael L. Michelsen
Ernst Hansen

Ph.D. Study

Started: March 2001

To be completed: February 2004

Modelling of the Adsorptive Properties of Whey Proteins on Anion Exchangers

Abstract

Chromatographic separations are of singular importance to the biotechnological industry because they deliver high purity, are relatively easy to develop at the laboratory scale and can be scaled linearly to the desired production level in most cases. Hence one reason for the ubiquity of chromatographic steps in preparative protein purification steps is that they provide a relatively efficient means to meet manufacturing goals of the pharmaceutical biotechnology industry. Development of chromatographic purification processes for new pharmaceutical proteins has to proceed very rapidly in order to produce material for the clinical trials. Once these trials have been performed the process cannot easily be changed because the process characterise the product. Ultimately new clinical trials must be performed for obtaining approval of the process changes. Therefore, the purification process must be developed at an early stage of development when very little material is available.

Introduction

To enable efficient process development rational strategies for screening and selection of chromatographic media and process conditions must be developed where one combines the experimental experience with theoretical considerations and model calculations. A chromatographic separation is developed through a number of steps including screening of different media and techniques to select appropriate candidates to investigate the retention behaviour in dependence of the possible process variables that usually comprise particle size, pH, type and concentration of salt, solvents and additives, and temperature. When more material becomes available capacities must be estimated. Process optimisation includes column size and column aspect ratio, flow rate, buffer composition and gradient length. All this can of course be performed by the trial and error method but ultimately a model-assisted development shall be beneficial.

Whey proteins may serve as an excellent model mixture to investigate the use of simulation tools in the development and optimisation of chromatographic separations. In the work presented we have determined and correlated gradient and isocratic retention volumes for the whey proteins α -lactalbumin, β -lactoglobulin A

and B, and BSA at a pH from 6 to 9 at various NaCl concentrations on the anion exchangers Q-Sepharose XL, Source 30Q, Merck Fractogel EMD TMAE 650 (S) and Ceramic Q-HyperD F. A model for simultaneous correlation of the isocratic and gradient elution data is presented. An integral part of this model is the model for the distribution ratio in the linear range that shall be obtained from a non-linear isotherm model as the limit of the distribution ratio at zero protein concentration.

The Isotherm

The Steric Mass Action (SMA) model [1] is a three-parameter model:

$$\frac{q_i}{c_i} = A_i \left(1 - \frac{\sum (\zeta_j + z_{p\text{protein}_j}) q_j}{\Lambda} \right)^{v_i}$$

where

$$A_i = K_i \left(\frac{\Lambda}{c_{\text{salt}} z_{\text{salt}}} \right)^{v_i}$$

is the distribution ratio in the linear range of the isotherm, that is at low protein concentrations. q is the protein concentration, c the mobile phase concentration, Λ is ligand density (eq/L pore volume), ζ a steric

hindrance factor, z_{protein} the binding charge of the protein, and $v = z_{\text{protein}}/z_{\text{salt}}$ is a charge ratio, z_{salt} is the charge of the counterion and K the equilibrium ratio

$$RT \ln K_i = -\Delta G_{\text{protein},i}^0 + v_i \Delta G_{\text{counterion}}^0$$

Δ is the difference between G^0 in the adsorbed state and the solute state. The distribution ratio A is determined from the isocratic retention volume V_R

$$V_R = V_{\text{column}} [\varepsilon + (1-\varepsilon) \varepsilon_p k_d (1+A)]$$

ε is the interstitial porosity, ε_p is the porosity of the particle and k_d is an exclusion factor that is 1 for the salt and less than one for large molecules. The retention volume at linear gradient elution is

$$V_{R_{\text{gradient}}} = V_{R_{\text{salt}}} + \frac{1}{G} \left[GB \left(\frac{\Lambda}{z_{\text{salt}}} \right)^v (v+1) + c_{\text{salt}_{\text{start}}} \right]^{v+1} - \frac{c_{\text{salt}_{\text{start}}}}{G}$$

$$G = \frac{c_{\text{salt}_{\text{end}}} - c_{\text{salt}_{\text{start}}}}{V_{\text{gradient}}},$$

$$B = V_{\text{column}} (1-\varepsilon) \varepsilon_p k_d K \text{ and}$$

$$V_{R_{\text{salt}}} = V_{\text{column}} [\varepsilon + (1-\varepsilon) \varepsilon_p]$$

G is the change in salt concentration divided by the gradient volume.

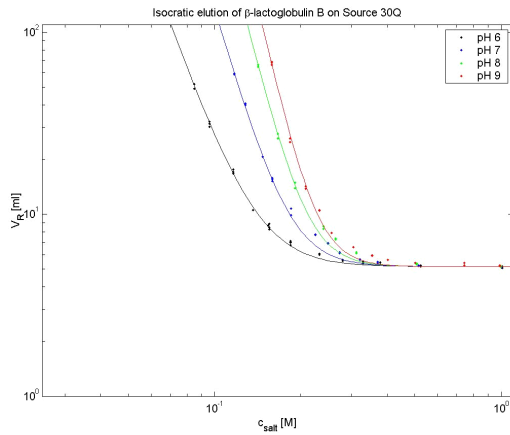


Figure 1: Experimental and correlated isocratic retention volumes for β -Lactoglobulin on Source 30Q.

Results

Figures 1 and 2 show experimental and correlated isocratic retention volumes (top) and experimental and predicted gradient elution volumes (bottom) for β -Lactoglobulin on Source 30Q and Ceramic Q-HyperD F. Further details are given elsewhere [2, 3].

The parameters for the Source 30Q column are: $\Lambda=0.308$ equiv/l pore volume, $\varepsilon=0.4$, $\varepsilon_p=0.57$, $k_d=0.70$, $L=10$ cm and $d_{\text{column}}=1$ cm. The binding charge at the various pH values is:

pH	6	7	8	9
v	4.29	5.50	6.56	7.31

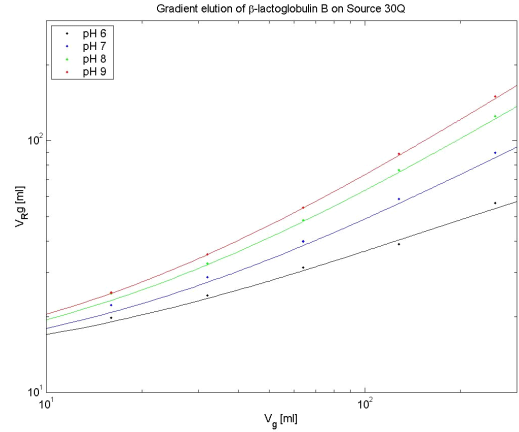


Figure 2: Experimental and correlated gradient elution volumes for β -Lactoglobulin on Source 30Q. The gradient volumes were 16, 32, 64, 128, & 256 ml.

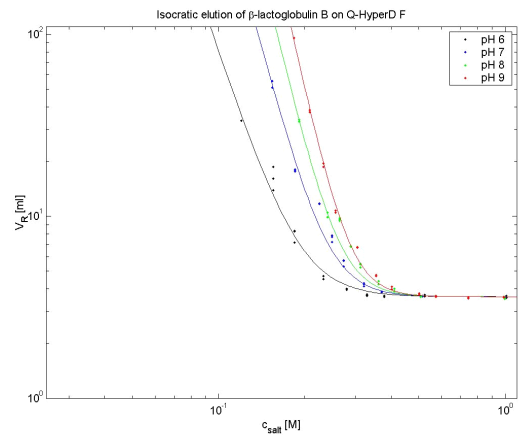


Figure 3: Experimental and predicted isocratic retention for β -Lactoglobulin on Ceramic Q-HyperD F.

The parameters for the Ceramic Q-HyperD column are: $\Lambda=0.777$ equiv/L pore volume, $\varepsilon=0.4$, $\varepsilon_p=0.68$, $k_d=0.18$, $L=10$ cm and $d_{\text{column}}=1$ cm. The binding charge at the various pH values is:

pH	6	7	8	9
v	4.63	5.84	6.57	7.28

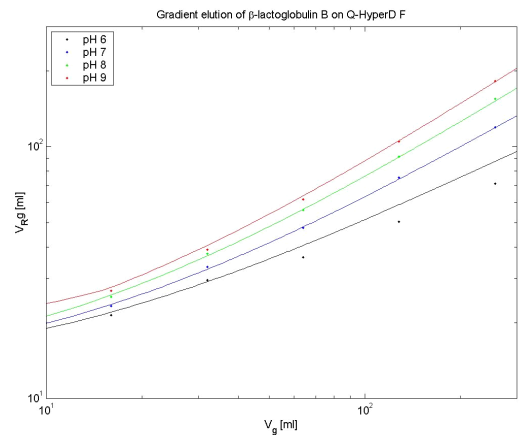


Figure 4: Experimental and predicted gradient elution volumes (bottom) for β -Lactoglobulin on Ceramic Q-HyperD F. The gradient volumes were 16, 32, 64, 128, & 256 ml.

Table 1: Initial and final salt concentrations for gradient experiments

pH	$C_{\text{salt,start}}$ [M]	$C_{\text{salt,end}}$ [M]
6	0.063	0.280
7	0.061	0.323
8	0.051	0.313
9	0.042	0.305

Scale-Up

Figure 3 shows that the peak shape and retention behaviour is independent of the column dimensions when the flow rate, the gradient volume and the load are scaled to the column volume.

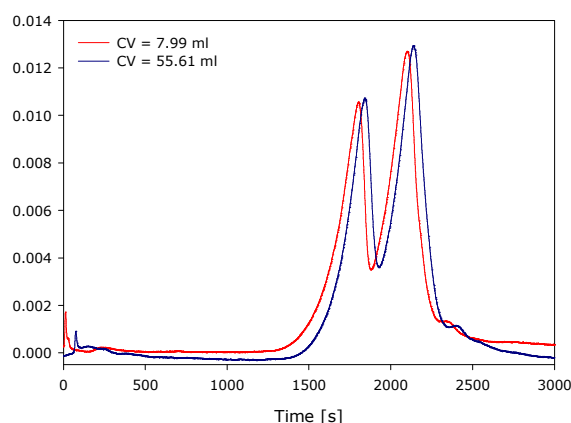


Figure 5: Scale up of a β -Lactoglobulin separation on Source30Q. The flow rate is 0.5 column volumes. The column dimensions are (diameter x length) 1x10 and 2 x17 cm, respectively

References

1. Brooks, C. A. and S. M. Cramer, *AICHE Journal*, 38, (1992) 1969-1978
2. L. Pedersen, J. M. Mollerup, E. Hansen and A. Jungbauer, *J. Chrom B* 790 (2003) 161-173
3. Linda Pedersen: A Modelling Retention Volumes, Isotherms and Plate Heights for Whey Proteins in Anion-Exchange Chromatography, Ph.D. Dissertation, DTU, 2002



Lusi Hindiyarti

Address: CHEC, Dept. of Chemical Engineering
Building 229, Office 130
Technical University of Denmark

Phone: (+45) 4525 2824
Fax: (+45) 4588 2258
e-mail: lh@kt.dtu.dk
www: www.chec.kt.dtu.dk

Supervisors: Peter Glarborg
Hans Livberg
Flemming Frandsen

Ph.D. Study
Started: 1 September 2003
To be completed: August 2006

Gas Phase Sulfur, Chlorine, and Alkali Metal Chemistry in Biomass Combustion

Abstract

The high-temperature sulfur/chlorine/potassium chemistry has important implications for sulfur/chlorine emissions (SO_2 , HCl), aerosol formation (KCl, K_2SO_4) and deposits formation in combustion. Significant efforts in the past have focused on chlorine and sulfur chemistry, but little is known about alkali metal chemistry or the interaction between S, Cl and K. The S/Cl/K chemistry in combustion involves both gas phase and condensed phase reactions. A better understanding of the gas phase chemistry of these components may facilitate development of more efficient methods to minimize emission and operation problems in biomass or waste combustion systems.

Background

Combustion and gasification of renewable fuels (biomass, waste) involves a number of chemical reactions, which are important for emissions, aerosol formation and deposition/corrosion. The high-temperature sulfur/chlorine/potassium chemistry has important implications for sulfur/chlorine emissions (SO_2 , HCl), aerosol formation (KCl, K_2SO_4) [1,2] and deposits formation in combustion [3]. Significant efforts in the past have focused on chlorine and sulfur chemistry, but little is known about alkali metal chemistry or the interaction between S, Cl and K. The S/Cl/K chemistry in combustion involves both gas phase and condensed phase reactions [4]. Despite the practical importance of Cl/S/K-interactions, few attempts have been made to understand the detailed kinetics of the system. Current modeling is largely limited to chemical equilibrium calculations. Such calculations do not account for kinetic limitations, which are known to be important for conversion of HCl to Cl_2 or SO_2 via SO_3 to H_2SO_4 . Conversion of KCl until formation of K_2SO_4 , a critical step in aerosol formation, is presumably also kinetically limited but little is known.

A better understanding of the gas phase chemistry of these components may facilitate development of more efficient methods to minimize emission and operation problems in biomass or waste combustion systems.

Objective

The objective of this project is to develop a fundamental knowledge of the gas phase chemistry that is important for emissions, aerosol formation or deposit formation in combustion of biomass and waste. The aim is to develop a detailed chemical kinetic model for conversion of chlorine, sulfur and alkali-containing species and their interaction. Such a chemical description can be implemented in reactor models and used to simulate effect of fuel and process parameters on emissions and operation.

Project

Presently, existing kinetic models develop at our institute and elsewhere; provide a fairly good description of hydrocarbon oxidation and nitrogen chemistry in high temperature processes. Also a significant knowledge about sulfur and chlorine chemistry is available. In the proposed project, these mechanisms/databases should be extended with subsets for alkali metal chemistry and S/Cl/K/Na interactions. This is done through an interaction between experimental and modeling work that step-by-step attempt to extend our knowledge of this chemistry. The experiments will take place in a laboratory flow reactor under well-controlled reaction conditions and perhaps also in an entrained flow reactor (larger scale, alkali metals difficult to handle in small scale). The

experimental results are interpreted in terms of a detailed reaction mechanism, using the CHEMKIN software package.

Future work

In the beginning of the project a literature study is being done, it will be followed by:

- Establishment of laboratory flow reactor to study the system
- Experimental investigation of gas phase alkali metal chemistry, development of detailed chemical kinetic model
- Validation of the model with experimental data
- Assessment of practical implications through modeling

References

1. K.A. Christensen, H. Livberg, *Aerosols science and Technology*, (2000) 33, 470-489.
2. L.B., Nielsen, H. Livberg, *J. Aerosol Sci.* (1996), 27(I), S367-S368.
3. H.P. Michelsen, O.H. Larsen, F.J. Frandsen, K.D. Johansen, *Fuel Process. Technol.* (1998), 54, 95-108.
4. K. Iisa, Y. Lu, *Energy & Fuels* (1999), 13, 1184-1190.



Edgar Ramírez-Jiménez

Address: CAPEC, Dept. of Chemical Engineering
Building 227, Office 223
Technical University of Denmark

Phone: (+45) 45 25 29 12
Fax: (+45) 45 93 29 06
e-mail: erj@kt.dtu.dk
www: www.capec.kt.dtu.dk
Supervisor(s): Rafiqul Gani

Ph.D. Study

Started: 1 September 2002
To be completed: September 2005

Modeling, Design, Operability and Analysis of Reaction-Separation Systems with Recycle

Abstract

This overview presents a methodology for a systematic model-based analysis and the results obtained from it for an integrated design and analysis of reaction-separation systems with recycle that is under development within the Ph.D. project. This systematic approach consists of three stages where *stage 1* identifies the limiting values of the design/operation variables; *stage 2* identifies the goal/target values of a related set of design/operation variables and *stage 3* verifies/validates the result of stages 1 and 2. The methodology decomposes the problem in such way that every stage generates information (data) and resolves a sub-set of design and operational issues. This information generation is cumulative so that at the last stage all-important (and relevant) data of the process becomes known while all-important design and operation issues become resolved. Two reaction-separation systems have been chosen as preliminary case studies to illustrate the methodology.

Introduction

Processes with Reaction-Separation-Recycle (*RSR*) configuration are common in chemical industries and usually show high sensitivity to changes or disturbances in the design/operating variables. Some of the important causes for these behaviors are the nonlinearity of the process and kinetic models, the specified performance of the separation units and/or the amount of purge from the recycle streams (including mass or energy recycle).

The study of the behavior of *RSR* systems becomes relevant for an integrated design and (plantwide) control at the early stages of the conceptual design, so that not only the recycle structure of the flowsheet can be established but also the overall performance of the system can be assessed. On the other hand, for the design and control issues, it is important to find the most appropriate set of parameters and conditions, in order to identify the possible reasons for disturbances (sensitivity) so that the process can exhibit a better performance ([1]-[3]). The first important step, however, is to identify a reliable process model.

The objective of this Ph.D.-work is to develop a systematic integrated design/analysis approach for

Reactor-Separator-Recycle systems. In this overview, we will highlight the application of the methodology through examples of *RSR* processes reported in the literature.

Methodology

The methodology consists of three stages (see Fig. 1a for methodology and Fig. 1b for process flowsheet). In the *First stage* of the approach we derive a simple model and analyze its solutions. Through this analysis some important characteristics of the process, for example, critical parameters and constraints (such as critical conversion, bifurcation points, etc.) can be identified. This is feasible since idealized models can be used to characterize the process design/operation in terms of representative parameters that lump the main variables of a process. For example, in reactor design, the kinetic rate constant, the reactor volume and the feed flowrate are grouped into the dimensionless parameter known as the Damköhler number (*Da*). Since this number is usually employed to evaluate the reactor performance, consequently, the analysis in this stage is able to guide the user in making design decisions through such lumped variables (parameters).

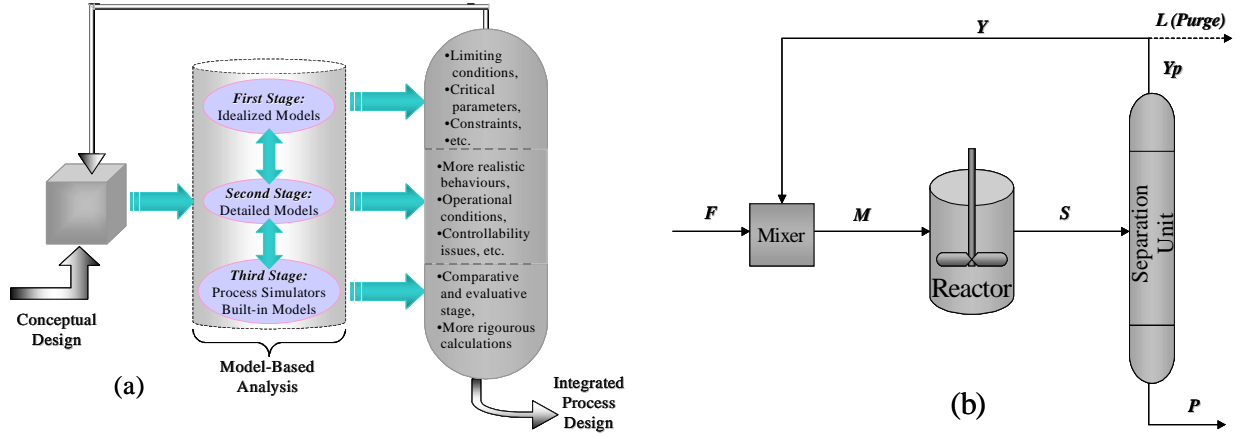


Figure 1: a) Methodology overview, b) Flowsheet considered for a reaction-separation-recycle system.

Once an initial identification of a selected set of key process features has been made, it is possible to perform an analysis with more detailed (delumped) models. Thereby, in this *Second stage*, a more detailed and realistic analysis is possible and characteristics that could not be seen in the first stage (for example, feed flowrate) are now identified. The model development can be as complex and complete, depending on the available process knowledge and understanding. The results from this stage will typically be design/operational variables such as feed flowrates, reaction yield, reactor volume, etc., that is, variables that define process flowsheet and/or its operation.

Finally, as a *Third model-based analysis stage* process simulations with rigorous built-in models are used as a means of comparison and verification of the results (design decision) from the two previous stages.

Case Studies

For this overview, we are highlighting the model-based approach through two well-known case studies. In this way we can confirm the results obtained previously as well as provide new insights.

Case Study 1

In this example, the second order reaction scheme $A + B \longrightarrow C$ is considered. The reaction takes place in an isothermal continuous-stirred-tank reactor (CSTR), the separation section is modeled as a *splitter* unit and some of the unreacted raw materials (mainly) are recycled back to the reactor through a *mixer* and also the possibility for a *purge* is considered. The modeling basis is a steady-state operation. Fig. 1b represents the flowsheet for a RSR system.

According to Fig. 1b, the following nomenclature is used: the molar flows of the feed of the system, reactor's feed and outlet, splitter's top and bottom and recycle stream and purge are F , M , S , Yp , P , Y and L , respectively. In general, sub indices will be used to refer to the components, while variables written in lower-case will represent flow rates on a dimensionless basis,

which is obtained with respect to the feed to the system of a component of reference (component A in the present example), for instance, $s_B = S_B/F_A$. Greek letters will represent flow ratios such as recoveries (e.g. $\alpha_{Y,S} = Y_A/S_A$).

Stage 1: Considering the recycling of unreacted components A and B ($\alpha_{Y,S} = \beta_{Y,S} = 1$), removal of all product C ($\gamma_{P,S} = 1$) and no purge ($\lambda = 0$) as in [4], the following simple steady state model is obtained in terms of a Da number of second order ($= k_1 \rho_A^2 V_R / F_A$) as the main variable of design as

$$Da = \frac{\left[\frac{(1-x_A)}{x_A} - v_B(y_B - 1) + v_C + v_D y_D \right]^2}{\frac{(1-x_A)}{x_A} v_B (y_B - 1)} = 0 \quad (1)$$

In Eq. (1) the value of the conversion of A , x_A , is calculated for specified values of Da with all other variables specified (given on a dimensionless basis: molar density of $B = v_B = \rho_B/\rho_A$; recycle of $B = y_B = Y_B/F_A$; molar density of solvent $D = v_D = \rho_D/\rho_A$). This quadratic model gives an *output* multiplicity (two values of conversion at the same Da number, as shown in Fig. 2. If Eq. (1) is differentiated with respect to x_A and set to zero, we can identify the critical design/operational parameters of the process in terms of x_A^{cr} and Da^{cr} , as given by Eqs. (2) and (3), respectively.

$$x_A^{cr} = \frac{1}{1 + v_B (y_B - 1) + v_C + v_D y_D} \quad (2)$$

$$Da^{cr} = \frac{4[v_B (y_B - 1) + v_C + v_D y_D]}{v_B (y_B - 1)} \quad (3)$$

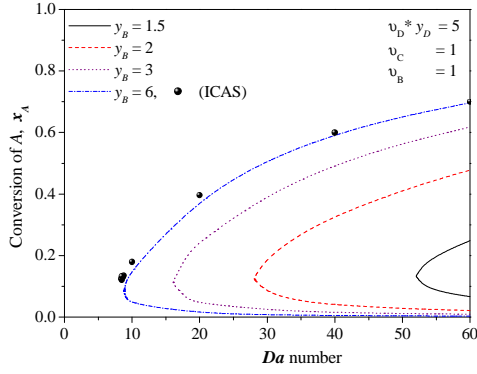


Figure 2: Results obtained from the Second-order reaction in CSTR-separator-recycle. Using Bildea's specifications

Stage 2: In this second stage, we now 'delump' the model from *Stage 1* by removing some of the assumptions used there. The recovery factors and the reactants feed ratio (flow of *B*/flow of *A*), f_B , now become variables of design. The new model takes the shape of Eq. (4), where x_A is calculated for specified values of F_A , F_B , V_R , k_1 and ρ_A . Note that the Da is now calculated as a function of the process conditions. As a consequence, instead of having an *output* multiplicity, an *input* multiplicity appears, where a single value of the recycle flow is obtained for three values of feed ratio (Fig. 3).

$$\frac{k_1 \rho_A^2 V_R}{F_A} = \frac{\sigma x_A}{\sigma - \alpha_{r,s}(1-x_A)} \times \left\{ \frac{\left(\frac{(1-x_A)}{\sigma - \alpha_{r,s}(1-x_A)} + \Psi \cdot v_b + \frac{x_A \cdot v_c}{\sigma - \alpha_{r,s}(1-x_A)} + v_D y_D \right)^2}{\Psi \cdot \left[\frac{(1-x_A)}{(\sigma - \alpha_{r,s}(1-x_A))} \right]} \right\} \quad (4)$$

$$\text{where } \Psi = \frac{f_B (\sigma - \alpha_{r,s}(1-x_A)) - \sigma x_A}{(\sigma - \beta_{y,s})(\sigma - \alpha_{r,s}(1-x_A))}$$

$$\sigma = 1/(1-\lambda)$$

From a controllability point of view, it can be stated that as the value of f_B approaches to 1 a high sensitivity to this parameter is observed and the possibility of the "snowball-effect" therefore increases. Note also the high recycle flow value in Fig. 3.

Stage 3: The objective of this stage is to verify the results from *stages 1* and *2* with rigorous simulation. For this purpose, simulations have been performed with ICAS ([5]) that provides a process simulation engine with in-house models trying to look for the two solutions (two values of conversion at a given value of Da) predicted by the simplified lumped model.

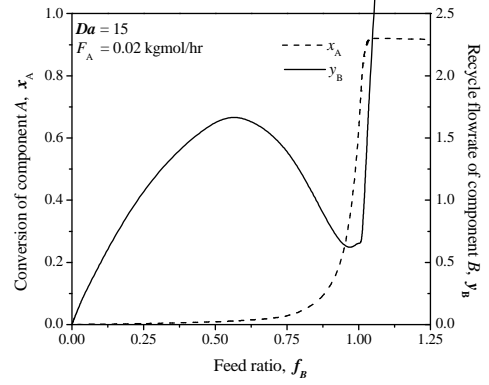


Figure 3: Methodology's stage 2: Conversion of component A and recycle of B with respect to the feed ratio.

The simulations, however, could only find one (higher conversion one) while the second (lower conversion) is only obtained by changing the feed flowrate specification of *B* (see Fig 2). This points to the risk of making design decisions with lumped parameters and that these need to be verified through delumped models. For this example, the Da is useful in identifying the operational limits, while the delumped variables are useful for defining the design/operation target(s). The presence of the "snow-ball effect" was also observed with the process simulator.

Case Study2

Let us consider now the isothermal first-order consecutive reaction system $A \xrightarrow{k_1} B \xrightarrow{k_2} C$, where the intermediate product *B* is the one of interest. The same flowsheet as in Fig. 1b is considered.

Stage 1: In this case neither the recycle of *B* ($\beta_{y,s} = 0$) nor purge ($\lambda = 0$) are considered and component *C* is taken out of the system ($\gamma_{p,s} = 1$). Again, as in the previous example, the system can be also characterized in terms of the Da (this time of first order) as design variable and the conversion of reactant *A* (see Eq. (5)).

$$Da - \frac{x_A}{(1-x_A)(1-\alpha_{r,s}(1-x_A))} = 0 \quad (5)$$

$$p_B = Da \cdot \frac{(1-x_A)^2}{(1-x_A)(1-k_2^*)}, \text{ where } k_2^* = k_2/k_1 \quad (6)$$

Figure 4 shows the effect of Da over the yield of the product *B*, p_B , as is also evident from Eqs. (5) and (6). It is clear that as the value of the Da increases the yield of component *B* should increase also until it reaches a maximum from where, it should decrease as the production of *C* is favored. It is important to note the positive effect of the recovery of component *A* on the value of p_B and how the location of its maximum moves towards low Da values as the recovery increases.

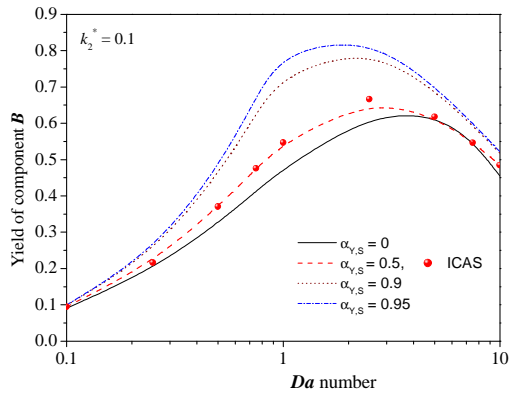


Figure 4: Yield of product B in the 'simple' model.

Stage 2: Having identified the effect of the Da and $\alpha_{y,s}$ over the conversion of A and the yield of B, as well as the locus of its maximum let us now consider the recovery of component B (even though this could be counterintuitive) and also the possibility of purge.

As in Case Study 1 the Da number is calculated from the design variables, being this time, mainly, the recoveries of components A and B and the inlet flowrate of A. Fig. 5 shows the effect of the recovery of B over the conversion of A and the yield of B as well as the recycle flowrate of B. Here it is important to remark that as $\beta_{y,s}$ approaches 1, the presence of the “snow-ball effect” is observed. Thus, this recycle is not advantageous since the more B is recycled the yield of B decreases (p_B).

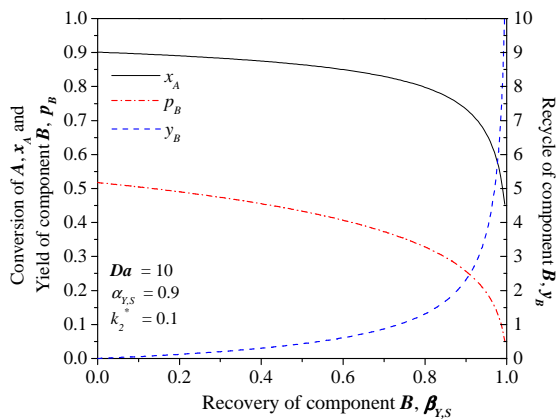


Figure 5: Results from Stage 2 for a consecutive-reaction system.

Stage 3: For the verification stage the simulations were again carried out in ICAS, confirming the results obtained from the two previous stages ('bullets' in Fig. 4).

Conclusions

As the recycle stream couples the reaction and separation units the behavior of the system can be significantly different from that of the individual units ([6]). Moreover, some of the previous works ([4], [6]) have considered only the recycling of some of the

reactants in a specific amount, but not variation of these. While these issues, obviously increases the complexity of modeling, through this three-stages model-based analysis of a process flowsheet it is possible to systematically identify the operational limits (through lumped variables) as well as conditions of operation (through delumped variables).

The results derived from the model-based analysis are useful not only to identify operational constraints and/or limiting conditions, but also to determine the appropriate control structure needed in order to maintain operational targets such as yields or conversion. This is feasible since according to the systematic model-based approach, the optimization variables in design are the manipulated variables in control while the state variables defining the condition of operation (in design) are the variables being controlled. Current and future work will highlight this aspect of the model-based analysis approach.

Acknowledgement– It is gratefully acknowledged the financial support from The National Council for Science and Technology of México (CONACYT) to this Ph.D. project.

References

1. W.L. Luyben, Ind. Eng. Chem. Res., 32 (1993) 466-475.
2. W.L. Luyben, Ind. Eng. Chem. Res., 33 (1994) 299-305.
3. J. Morud and S. Skogestad, J. Proc. Cont., 6 (1996) 145-165.
4. C.S. Bildea, A.C. Dimian and P.D. Iedema, Comp. Chem. Eng., 24 (2000) 209-215.
5. R. Gani, ICAS Documentation, CAPEC (2002).
6. S. Pushpavanam, and A. Kienle, Chem. Eng. Sc. 56 (2001) 2837-2849.

List of Publications

1. E. Ramírez and R. Gani, Analysis of Design and Operation of Processes with Reaction-Separation Systems, ECCE-4 Conference, Granada, Spain, 20-25 September, (2003),
2. E. Ramírez and R. Gani, Model-based Analysis of Reaction-Separation Systems with Recycle, AIChE Annual Meeting, San Francisco, Ca., USA, 16-21 November, (2003),
3. E. Ramírez and R. Gani, A Systematic Approach for the Design and Analysis of Reaction-Separation Systems with Recycle, ESCAPE-14 Conference, (Submitted),
4. E. Ramírez and R. Gani, A Methodology for the Analysis and Design for Reaction-Separation Systems with Recycle, FOCAPD 2004 Conference, (Submitted).



Johnny Johansen
Address: ICAT, Dept. of Chemical Engineering
Building 312
Technical University of Denmark
Phone: (+45) 45 25 31 96
Fax: (+45) 45 93 23 99
e-mail: joj@kt.dtu.dk
www: www.icat.dtu.dk
Supervisor(s): Tue Johannessen
Hans Livbjerg
Ph.D. Study
Started: 1 February 2003
To be completed: February 2006

Activation of Methane by Partial Oxidation in Membrane Reactors

Abstract

Ceramic membranes are made by flame synthesis where organo-metallic precursors are decomposed in a flame to produce nanometer sized particles. By depositing these particles on a porous substrate, it is possible to reduce the pore sizes from micrometer range to nanometer range in a one-step-process. This has in a previous study been done with MgO, Al₂O₃, and MgAl₂O₄ spinel achieving pore sizes down to approximately 2-5 nanometers. The produced membranes show good mechanical stability. For the present study, the aim is to produce dense or porous membranes, which can be applied in a membrane reactor for controlled partial oxidation of methane.

Introduction

Methane resources are often found in desolate areas, which make it difficult to exploit, since the transport expenses are prohibitive. Also, methane found together with oil is a hindrance, since the methane must be removed before the oil can be pumped to the surface. Therefore, the methane is - in some cases - flared in order to get to the oil. This represents an enormous contribution to the CO₂ emission and is energetically very undesirable. It is estimated that with the current level of methane consumption, the methane reserves would last approximately twice as long if all the methane could be exploited [1]. Much research has therefore gone into processes that convert methane into liquid products, which more economically can be pumped in pipelines and transported in ships. This can already be done by steam reforming, where syngas (CO and H₂) is formed from CH₄ and H₂O at high temperature. The syngas is a feedstock for the catalytic production of a variety of bulk chemicals such as ammonia and methanol. Unfortunately, the plant for reforming of methane is large and requires substantial investment, which is not viable for offshore applications or in remote areas. It is therefore necessary to find an alternative route for making liquid products from methane. For this reason partial oxidation of methane to methanol has become attractive, since this reaction is slightly exothermic and it therefore, in principle, can be done without any external heat source.

Membrane reactors where the outer wall acts as an oxygen separating membrane reactors has already been proven as a possible method for oxidation of methane to

syngas[2,3,4], but the fabrication of these membranes by the traditional thin-film techniques is difficult and the materials are expensive. Flame synthesis offers a potentially better and cheaper way to produce such membranes.

Specific Objectives

The scope of this Ph.D. project is to develop membranes that are selectively permeable to oxygen by flame synthesis. These membranes can then be coated with a catalyst layer to enhance the formation of the desired reaction product, in this case methanol.

Flame Synthesis

Flame synthesis of ceramic materials can be done by dissolving organo-metallic precursors in an organic solvent, which is then vaporized into a flame zone where the solvent and precursors evaporate and combust. This results in an oxidation of the metal precursors to metal oxides. The metal oxide molecules will nucleate due to the high supersaturation and initially formed particle nucleus will subsequently grow by coagulation and sintering. This variation of flame synthesis is called flame spray pyrolysis (FSP).

Flame synthesis can also be done by evaporating/sublimating a liquid/solid metal compound into a carrier gas, which is then fed to a hydrogen or methane flame. In this way the dissolving and vaporization steps are avoided and a more uniform product is normally achieved, but the method is less flexible, and the number of stable precursor molecules is limited.

Figure 1 shows the setup for flame synthesis by FSP. The setup consists of a syringe pump dosing the precursor solution to the nozzle where the air for atomizing the liquid also enters. The liquid is sprayed into the flame zone, which is sustained by supporting hydrogen flamelets.

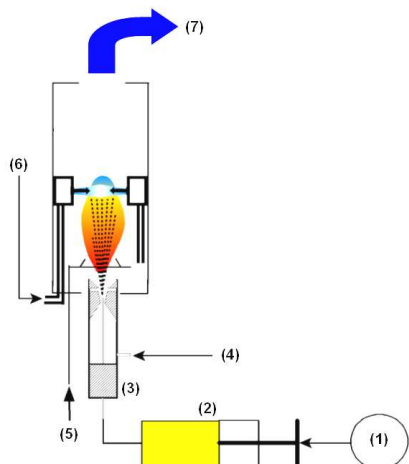


Figure 1: Drawing of FSP setup. 1) Precursor solution 2) Syringe mounted in syringe pump 3) Nozzle 4) Air inlet 5) Hydrogen for supporting flamelets 6) Air inlet for quench cooling ring 7) Particles suspended in gas.

At a given height it is possible to inject air into the flame zone and the product gas will then be quench cooled, thereby effectively freezing the sintering of collided primary particles. The outlet gas will contain suspended particles with morphologies ranging from completely spherical to dendritic aggregates depending on the experimental parameters.

Membrane Formation by Nano-Particle Deposition

Membrane layers can be formed by using a porous substrate tube (or surface) as a nano-particle filter [5]. The product gas from the flame reactor can be sucked through the porous substrate by a vacuum pump thereby creating a thin filter cake on the surface of the substrate. The top-layer can be deposited directly on a coarse pore structure ($>5 \mu\text{m}$) due to the “lack” of fluid forces on the particles compared with the forces in a liquid suspension when colloidal suspensions are applied.

Figure 2 shows the working principle of a membrane deposition unit. The particle containing gas from the flame reactor is sucked through the tube (axial) while at the same time suction is applied through the porous substrate (radial), thereby depositing particles onto the substrate.

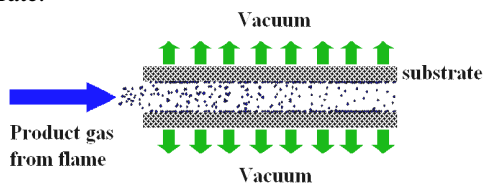


Figure 2: Deposition of particles on a porous substrate tube.

Results

Ceramic powders such as TiO_2 , MgO , Al_2O_3 , and MgAl_2O_4 -spinel have been produced by flame synthesis [6] with specific surface areas ranging from less than $1 \text{ m}^2/\text{g}$ to more than $300 \text{ m}^2/\text{g}$. This diversity makes the method well suitable for both production of the actual membrane layer and the catalyst layer that is intended to be deposited on the membrane wall.

Figure 3 shows a SEM picture of a MgO -membrane. It can be seen that the membrane layer does not penetrate into the substrate pore structure. A change from $8 \mu\text{m}$ substrate pores to a thin layer with Knudsen separation factor is obtained in one deposition step over the time-scale of an hour. The formed membrane layer has good mechanical stability and no additional thermal treatment is necessary.



Figure 3: A SEM picture of a MgO membrane. The coarse substrate structure is seen to the right.

Discussion

It is possible to operate the flame reactor, so that spherical particles are produced in different size ranges. This is exploited when producing membranes by deposition, but when the objective is to make dense oxygen conducting membranes this method has to be combined with some post treatment, which could be thermal treatment in order to sinter the top layer or it could be CVD on top of the nano-porous membrane.

It also remains to be shown that nano-porous membranes can in fact be produced with materials that conduct oxygen.

Conclusions

Nano-porous ceramic membranes can be made by flame synthesis in a one-step-process, but post treatment is needed to produce dense membranes needed in this study.

Acknowledgements

Special thanks to the STVF who has funded this PH.D.

References

1. P.N. Dyer et al., *Solid State Ionics*, 134, (2000), 21-33
2. T. Ishihara, Y. Takita, *Cat. Surv. Jap.* 4 (2), (2000), 125-133.
3. H. Dong et al., *Chin.Sci.Bull.* 45 (3), (2000), 224-226
4. Z. Shao et al., *Sep. Pur. Tech.* 25, (2001), 97-116
5. S.K. Andersen et al., *J. Nanoparticle Res.*, (2002), 4(5), 405-412.
6. J.R. Jensen et al., *J. Nanoparticle Res.*, 2000, 2, 363-370.



Kåre Jørgensen
Address: CHEC, Dept. of Chemical Engineering
Building 229, Office 114
Technical University of Denmark
Phone: (+45) 45 25 28 31
Fax: (+45) 45 88 22 58
e-mail: kj@kt.dtu.dk
www: www.chec.kt.dtu.dk
Supervisor(s): Anker Degn Jensen
Kim Dam-Johansen
Poul Bach, Novozymes A/S
Ph.D. Study
Started: 15 February 2002
To be completed: February 2005

The Effect of Formulation Ingredients on the Drying Kinetics and Morphology of Spray Dried Enzyme Suspension Particles

Abstract

In this work drying kinetics and morphology development of suspension droplets containing enzymes are investigated through drying of 200-300 μ m droplets in a Droplet Dryer. The droplets experience free fall in a heated drying tower (25-225°C) where the water content of the droplets is determined by in-line sampling through sampling ports in the tower walls. Morphology is determined by capturing the droplets in silicon oil or liquid nitrogen. Droplet drying kinetics and (possibly) morphology development will be built into a drying model, and suggestions for increasing the drying rate while retaining a solid, spherical, high-density particle with good friability will be given. The experimental set up is currently in the construction phase.

Introduction

This text will give a brief introduction to the field of suspension droplet drying kinetics and morphology development in relation to spray drying processes, product quality and development of improved product properties. The text will give the current status of the research performed in this PhD project.

Spray drying processes are used throughout numerous industries for the production of easy-to-handle, easily transportable, storage stable particulate solid products. A list of products where spray dryers are applied includes: Pharmaceuticals, foods, chemicals, cosmetics, detergents, ceramics, dyes and fertilizers [1].

Spray drying is characterised by being a unique way of producing a particulate solid product from a solution, suspension or paste in a single operation.

Studies into spray drying processes have traditionally focused on [2]:

1. Atomisation studies, where droplet size distributions, feed characteristics, atomiser design, pressure/rotational speed and throughput are investigated.
2. Studies of gas flow patterns and droplet/particle residence times.
3. Single droplet drying studies, which give information about the development of particle morphology.

4. Mathematical models to correlate experimental data to simulate whole dryer performance by predicting droplet drying rates and drying behaviour.

The increased application of spray drying to produce high value products e.g. for the pharmaceutical, cosmetics or food industries, where the cost of the spray drying stage is less important than for e.g. bulk foods such as milk powder, has greatly increased the focus on a detailed understanding of the droplet drying process.

With the introduction of computational fluid dynamics (CFD) to simulate gas and particulate motion in a spray dryer the interest in droplet/particle drying rate and its effect on particle morphology has increased further. The drying rate as well as the quality of a spray dried product, e.g. with respect to friability (i.e. mechanical strength), flowability, bulk and particle density, particle size distribution (PSD), low moisture content to ensure good storage stability of active ingredients (e.g. enzymes, flavour, aroma, etc.), is greatly dependent on the particle morphology [3,4].

The drying rate and the morphology of spray dried droplets/particles depend on both liquid suspension (i.e. formulation) and process conditions. Some parameters are – for the most common case where hot air is used to dry off solvent water:

- Formulation:

- Solid content, size and size distribution of primary particles in suspension, polymeric material with high molecular weight, inorganic salts which may lower the vapour pressure, initial droplet temperature, viscosity.

- Process conditions:
 - Temperature and relative humidity of drying air, air/liquid flow rate, droplet size, injection velocities of droplets, etc.

The desire to produce particulate products with specifically designed properties is great e.g. in the pharmaceutical and food industries. The only way to increase the knowledge about droplet drying and morphology development is to perform experiments and attempt to model the drying rate and morphology in dependence of the parameters just listed.

Specific Objectives

The primary objective of this PhD project is to increase the knowledge about the effect of formulation ingredients on the drying kinetics and morphology development in suspension droplets formed by atomisation.

Through experimental work on a new set up (see description in section “Experimental set up” and Fig. 1 and Fig. 2) data will be generated, which give information about drying kinetics and morphological development.

Experimental set up

The experimental set up used in this PhD project is named a Droplet Dryer and a preliminary set up can be viewed on Fig. 1 and Fig. 2. A picture of the droplet generator unit is seen on Fig. 1.

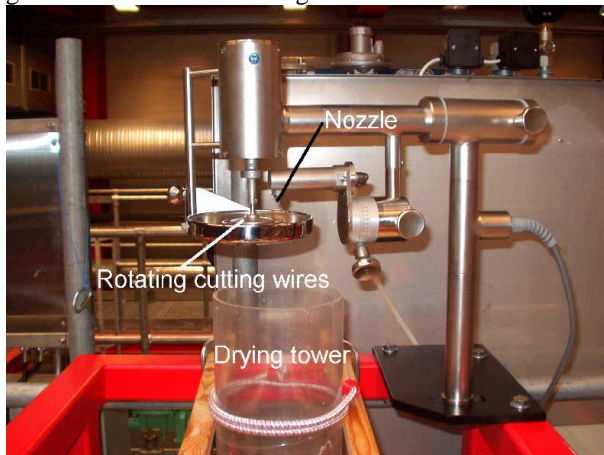


Figure 1: JetCutter[®] droplet generator

Droplets are generated by a JetCutter[®]. Forcing the formulated liquid through a nozzle of size 100-300 μm creates a liquid jet, which is cut into cylinders by a rotating cutting wire (48 wires, $\omega = 500\text{-}8500\text{rpm}$, $d_{\text{wire}} = 50/90\mu\text{m}$). The surface tension will then transform the cylinders into spherical droplets. A more detailed description of the JetCutter[®] technology is given in [5] and [6].

Liquid droplets now enter a heated drying tower (sketched on Fig. 2) where the air temperature can be

controlled from 25-225°C. The air introduced into the drying tower runs co-currently with the droplets in order to stabilise the droplet flow and allow for well-defined residence times.

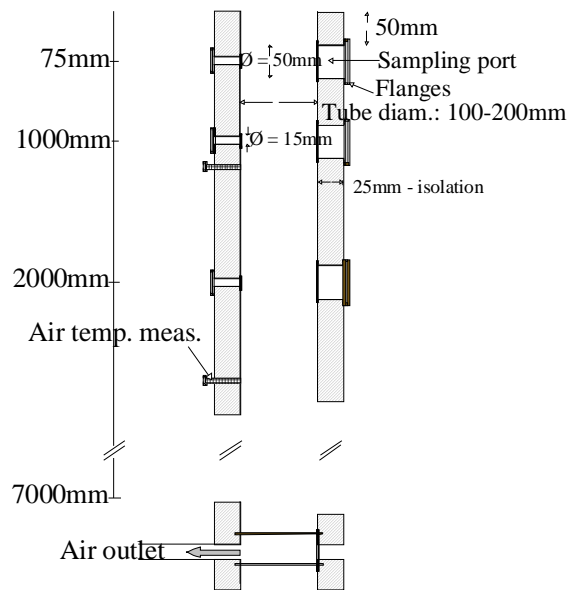


Figure 2: Sketch of basic design of drying tower. Droplets and drying air is introduced in the top and the droplets dry while falling downwards

Through the sampling ports in the stainless steel drying tower the droplets can be sampled and their water content determined by a method briefly described in the following:

Droplets can e.g. be collected in a cup in which the atmosphere is controlled and taken out for moisture removal and determination by drying on silica gel. The water remaining in droplets after the sampling is dried off in an oven giving the water content. Another possible water determination method is that of Karl Fischer where methanol and other chemicals are used to give the total water content – see e.g. [7].

For qualitative evaluation of the morphology of the drying droplets/particles, these are caught in e.g. neutrally buoyant silicon oil, which stops the evaporation by encapsulating the droplets. These can be isolated and the morphology determined by light or electron scanning microscopy.

Dry particles are also sampled from the Droplet Dryer experiments in order to evaluate their friability by exposing the particles to controlled impact and/or shearing conditions. The mechanical evaluation of the particle friability may be performed as described in the work of Jørgensen [8], who investigated different types of enzyme granules.

Examples of wet droplets and solid particles produced by the JetCutter[®] can be seen on Fig. 3 and Fig. 4. It is observed that the droplet distribution produced is relatively narrow, which is promising for future experiments.

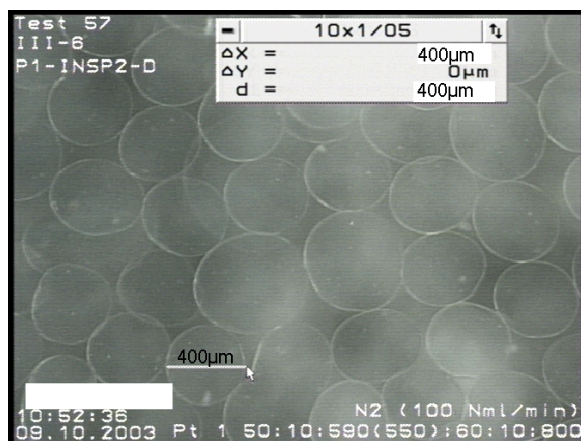


Figure 3: 2wt.% Na-alginate droplets caught in 2wt.% CaCl₂ solution. JetCutter settings: Rotational speed of cutting wires: 4000rpm; Flowrate through nozzle: 0.3g/s; Nozzle diameter: 200µm.



Figure 4: 2wt.% Na-alginate caught in 2wt.% CaCl₂ solution and dried in a Petri dish. JetCutter settings: Rotational speed of cutting wires: 4000rpm; Flowrate through nozzle: 0.3g/s; Nozzle diameter: 200µm.

Results and Discussion

So far no experiments have been conducted where the drying rate or morphology have been determined. Instead the spreading of the droplets after they have been formed by the JetCutter[®] is quantified in order to establish the necessary drying tower dimensions.

In a bulleted list the following plan is laid down for the work during autumn/winter of 2003/2004:

- Establish droplet flow pattern in order to specify the Droplet Dryer tube diameter (length is set at max. 7m by the height of the process hall building)
- Design air inlet, isolation of droplet generator from hot air stream in the drying tower.
- Final offer and purchase of “hot solution” for the drying tower, i.e. stainless steel tube, flanges, sampling ports, heating tape to maintain constant drying air temperature, initial heating and relative humidity of drying air.
- Air temperature profile determination inside the drying tower.

- Wet droplet collection and water content determination has to be implemented together with a sampling method for droplet/particle morphology determination.

Experiments will be performed on formulated suspensions containing undissolved particles together with different binders, inorganic salts, enzyme stabilisers, etc. These are all materials which have a decreasing effect on the drying rate since they lower the water activity or cause the droplet to form a skin through which water vapour from the wet droplet core slowly diffuses to the droplet surface and away.

The droplet and particle morphologies are very much dependent on the formulation ingredients. Polymeric materials have a strong tendency to form a skin around the drying droplet and thereby reduce the evaporation rate considerably due to the reasons just described [2]. As opposed to these (expected) skin-forming polymers and water-activity-decreasing salts, the undissolved suspension particles will give structure to the drying droplet and thereby increase the drying rate by allowing for capillary transport of liquid water to the droplet surface. This will prolong the period where the surface of the droplets is saturated with liquid and the evaporation rate therefore is high.

Modelling

A droplet dries in two phases. The *first phase* is usually termed the constant rate period (CRP). Here the droplet surface is saturated with liquid water and the drying rate is determined by the rate at which water vapour can be convectively transported away from the saturated surface, i.e. by the film resistance.

The existence of inorganic salts or other dissolved compounds in the formulation liquid will lower the vapour pressure at the surface and therefore decrease the evaporation rate. This may lead to a continuously decreasing evaporation rate during the CRP since the concentration of dissolved compound continuously increases when the water evaporates. This effectively questions the use of the term ‘constant rate’ period.

As an example a saturated solution of sodium chloride will have a water activity of 0.75 at 25°C, and saturated sodium sulphate solution has a water activity of 0.94 at 25°C and 0.88 at 37°C. Therefore, the effect of salts on the vapour pressure of water should not be blindly disregarded.

As a first approximation the vapour pressure decrease due to dissolved compounds is neglected during the *first phase* of drying and the mass balance for the drying droplet becomes:

$$\frac{dm_l}{dt} = k_m M_w S_i (C_{vi} - C_{v\infty}) \quad (1)$$

where m_l [kg] is the mass of liquid in the droplet; t [s] is the time; k_m [m/s] is the convective mass transfer coefficient for water vapour at the droplet surface to the bulk drying air; S_i [m²] is the droplet surface area ($=4\pi R_p^2$); R_p [m] the droplet radius; C_{vi} and $C_{v\infty}$ [mol/m³] are the water vapour concentration at the

droplet surface (index i for interface) and in the drying air bulk phase, respectively. M_w [kg/mol] is the molecular mass of water.

Since the droplet shrinks during the CRP the equation for the relation between the mass loss and the droplet radius is given:

$$\frac{dm_i}{dt} = 4\pi R_p^2 \rho_l \frac{dR_p}{dt} \quad (2)$$

where ρ_l [kg/m³] is the liquid density.

An energy balance for the suspension droplet is set up to account for the transport of heat to and from the droplet (including the assumption that the droplet has uniform temperature, i.e. the wet-bulb temperature)

$$(m_s C_{ps} + m_l C_{pl}) \frac{dT_p}{dt} = h S_i (T_\infty - T_p) + \lambda_w \frac{dm_i}{dt} \quad (3)$$

where m_s [kg] is the mass of solids within the droplet (most often safely assumed to be constant, i.e. no solid evaporates or is lost during drying); C_{ps} and C_{pl} [J/kg/K] are the heat capacities of the solid material and the liquid (water), respectively; T_p [K] is the temperature of at the droplet surface; T_∞ [K] is the bulk drying air temperature and λ_w [J/kg] is the latent heat of vaporisation of water at the droplet surface temperature.

The CRP can be described by the following model of the drying droplet (see Fig. 5).

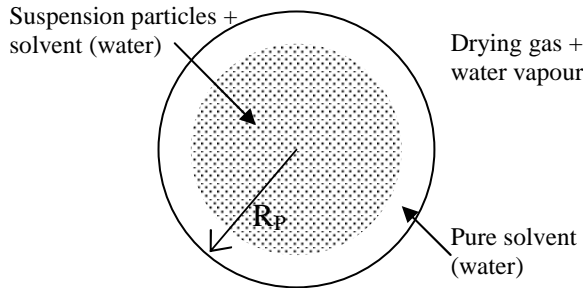


Figure 5: Model of drying of a slurry droplet during the first phase of drying (CRP) after [9]

During the *second phase* of drying the moisture transport through the porous structure to the droplet surface is no longer fast enough to ensure a surface that is saturated with water. Instead a solid crust/skin forms and a liquid-vapour interface recedes towards the centre of the drying particle, thus leaving a dried crust behind through which the water vapour produced at the interface by conduction of heat from the particle surface diffuses. Before the heat is conducted to the liquid-vapour interface it is transferred by convection from the bulk phase drying air to the outer surface of the crust/skin.

In the *second phase* of drying the resistance towards drying is typically controlled by the rate of diffusion of water vapour through the more or less porous crust/skin e.g. [1]. As sketched on Fig. 6 the drying particle is usually considered as a dry crust with a wet core, which shrinks as heat is transported to the wet core surface and water evaporates and diffuses through the crust/skin. The diffusion becomes slower as the crust thickens

thereby decreasing the evaporation rate and thus giving the alternative name for the second phase of drying, namely the *falling rate period*.

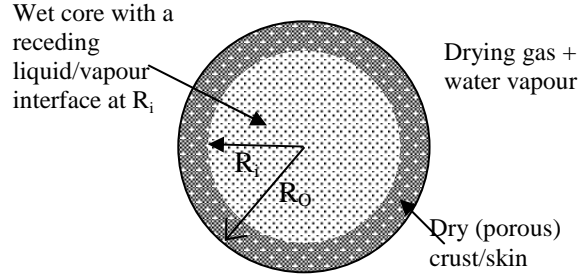


Figure 6: Model of drying of a slurry droplet during second phase of drying (falling rate period) after [9]

However, there are also results which indicate that the film resistance to mass transfer at the particle surface should not be neglected even in the second phase of drying [9]. It is very much dependent on the remaining formulation ingredients which influence the drying rate, whether film resistance is negligible during the second phase of drying.

The mass and energy balances for the second phase of drying can be described briefly with the introduction of a mass transfer resistance in the crust given by a Maxwell-Stefan type diffusion, which accounts for a flux which is unidirectional [9]

$$\frac{dm_i}{dt} = \left\{ \frac{M_w D_v P_T}{RT_{ave}} \ln \frac{P_T - P_{vi}}{P_T - P_{vo}} \right\} / \left\{ \frac{1}{4\pi\alpha^n} \left(\frac{1}{R_o} - \frac{1}{R_i} \right) \right\} \quad (7)$$

where D_v [m²/s] is the diffusion coefficient of water vapour in drying air; P_T [Pa] is total pressure of water vapour and air (=10⁵ Pa) in the drying air; T_{ave} [K] is the average temperature of the crust, i.e. somewhere between T_i and T_o , where T_i [K] is the temperature at the wet receding interface core surface and T_o [K] is the temperature at the crust (i.e. particle) surface. α [-] is the void fraction of the dry crust, and the exponent n is a parameter giving the relationship between the porosity and tortuosity of the crust and assumed to be equal to 1 [10]. P_{vi} and P_{vo} [Pa] are the partial pressure of the vapour at the inner and outer surfaces of the dry spherical crust, respectively. P_{vi} is assumed to be the saturation pressure of vapour at the wet core temperature. R_o [m] is the radius of the dry spherical crust, i.e. the particle diameter, while R_i [m] is the diameter of the wet core.

The heat flow to the wet core is transferred first by convection from the ambient air and then by conduction through the dry crust. Thus assuming quasi-steady state conditions the temperature of the outer and inner surface of the crust can be calculated. It is assumed that the temperature at the inner surface of the crust is equal to the temperature within the wet core since, since the thermal conductivity here is assumed to be much greater than the thermal conductivity within the porous crust. The inner surface temperature is calculated via a heat balance. The sets of ordinary differential equations in

order to reach droplet mass, diameter, temperature, and crust thickness as a function of time, ambient temperature, relative humidity, and initial droplet diameter can be solved using a fourth order Runge-Kutta method [9].

Only the most basic models have been presented here. Using FORTRAN programming more complex models for drying rate and implementation of possible morphology development description [11] will also be introduced and their validity discussed based on experimental data collected from the set up described in the 'Experimental set up' section.

Conclusions

A Droplet Dryer experimental set up is being constructed in order to investigate the effects of formulation ingredients and drying process conditions on the drying rate and morphology of spray dried suspension droplets, which may contain enzymes. Droplets are generated by rotating cutting wires, which cut a liquid jet into cylinders and surface tension then transforms the cylinders into spherical droplets. These droplets are dried in a 7m high drying tower where sampling ports allow for a determination of the drying rate and morphology development as a function of time. The temperature of the drying air in the tower can be controlled between 25 and 225°C.

The drying rate and morphology development is modelled using mass and energy balances and models for the formation of the crust. The crust formation separates the *first phase* of drying (CRP) where the droplet surface is saturated with water from the *second phase* of drying (falling rate period), where water vapour diffusion from a wet shrinking core inside the dry crust/skin is expected to control the drying rate.

By changing parameters such as

- Temperature and humidity of drying air;
- Solid content, size and size distribution of primary particles in suspension;
- Effects of adding polymeric material and inorganic salts;
- Viscosity of formulation

the investigation of how formulation ingredients and process conditions interact to give specific dried product qualities will be concluded.

The friability of the dried particles produced will also be tested since this is of crucial importance to the product quality.

Acknowledgements

CHEC is financially supported by Elsam, Elkraft, the Danish and the Nordic Energy Research Programmes, the Technical Research Council of Denmark and the Technical University of Denmark.

This project is carried out in collaboration with Novozymes A/S.

Financial support for this project from Novozymes A/S is gratefully acknowledged.

References

1. K. Masters, Spray drying handbook, 4th edition, George Godwin, London, 1985, pp. 76, 185, 481.
2. D.E. Walton, The morphology of spray-dried particles – A qualitative view, *Dry. Technol.* 18 (2000) 1943-1986.
3. C.J. King, Control of food-quality factors in spray drying, pp. 69-76 in Proceedings of fourth international drying symposium, Kyoto, Japan, 09-12 July, 1984, edited by R. Toei and A.S. Mujumdar.
4. T.M. El-Sayed, D.A. Wallack, C.J. King, Changes in particle morphology during drying of drops of carbohydrate solutions and food liquids. 1. Effects of composition and drying conditions, *Ind. Eng. Chem. Res.* 29 (1990) 2346-2354.
5. U. Prüße, B. Fox, M. Kirchhoff, F. Bruske, J. Breford, K.-D. Vorlop, The jet cutting method as a new immobilization technique, *Biotech. Techniques* 12 (1998) 105-108.
6. K.-D. Vorlop, J. Breford, Production of solid particles from a liquid medium, German Patent DE 4424998, 1994.
7. D.A. Skoog, D.M. West, F.J. Holler, Fundamentals of Analytical Chemistry, 7th edition, Saunders College Publishing, Orlando, FL, USA, 1996, p. 381.
8. K. Jørgensen, Design of a Shear and Impact Resistant Enzyme Granule, MSc Thesis, Department of Chemical Engineering, Technical University of Denmark, 2002.
9. Kadja, M., Bergeles, G., Modelling of slurry droplet drying, *Appl. Therm. Eng.* 23 (2003) 829-844.
10. Abuaf, N., Staub, F.W., Drying of liquid-solid slurry droplets, pp. 277-284 in *Drying '86 volume 1, Proceedings of the fifth international symposium on drying*, editor: Mujumdar, A.S., Springer-Verlag, Berlin, F.R. Germany, 1986.
11. Elperin, T., Krasovitev, B., Evaporation of liquid droplets containing small solid particles, *Int. J. Heat Mass Transfer* 38 (1995) 2259-2267.

List of Publications

1. K. Jørgensen, P. Bach, A.D. Jensen, Design of impact resistant enzyme granules, Oral presentation (O-13-004) at 1st European Symposium on Product Engineering, part of 4th European Congress of Chemical Engineering, Granada, Spain, 21-25 September 2003.
2. A.D. Jensen, K. Jørgensen, P. Bach, Test af mekanisk stabilitet af enzymgranulater til vaskepulvere, *Dansk Kemi* 10 (2003) 18-21.
3. K. Jørgensen, P. Bach, A.D. Jensen, Impact and attrition shear breakage of enzyme granules and placebo particles – application to particle design and formulation, *submitted to Powder Technol.*, 2003.



Jacob Nygaard Knudsen

Address: CHEC, Dept. of Chemical Engineering
Building 229, Office 116
Technical University of Denmark

Phone: (+45) 45 25 28 46

Fax: (+45) 45 88 22 58

e-mail: jnk@kt.dtu.dk

www: www.chec.kt.dtu.dk

Supervisor(s): Peter Arendt Jensen

Weigang Lin

Kim Dam-Johansen

Ph.D. Study

Started: 1. April 2001

To be completed: June 2004

Transformation of Ash-forming Elements during Thermal Conversion of Annual Biomass

Abstract

The usage of annual biomass as a fuel in combined heat and power plants has proven to be a technical challenge. This is among other things due to the fuel's high concentrations of the elements potassium, chlorine and sulfur. In this Ph.D. project, the transformation and release of Cl, K and S during thermal conversion of annual biomass are investigated at grate-combustion conditions. The influence of combustion temperature and ash composition on the quantity of Cl, K and S released to the gas phase are determined. The aim is to establish the release mechanisms of Cl, K and S and the parameters in control of the gas phase release.

Introduction

The use of annual biomass such as straw, stalks and shells in heat and power generation is an interesting option in order to provide renewable energy and to reduce the net CO₂ emissions. In Europe and North America, straw is the most available biomass resource with a yearly production around 800 million tons [1]. In Denmark, straw is a particularly interesting bio-fuel since it is an agricultural waste-product being available in surplus. However, the use of straw as a fuel in combined heat and power plants has proven to be a technical challenge. This is among other things, due to the relatively high concentrations of the elements: potassium, chlorine and sulfur. Formation of acidic pollutants and high mass loadings of aerosols together with deposition on heat transfer surfaces of potentially corrosive components are among the encountered problems [2-4].

The problematic behavior of the Cl-K-S system is linked to the volatile nature of the salts, KCl and K₂SO₄. During the conversion of annual biomass in grate-fired furnaces, Cl, K and S are partly released to the gas phase as illustrated in Figure 1. However, Cl, K and S may also be partially retained in the bottom ash and thus transported straight through the system. Clearly, the extent of Cl, K and S release to the gas phase is directly related to the problems mentioned above. In order to predict the impacts of a given fuel in the combustion system, the release of Cl, K and S as a function of

combustion conditions and fuel composition needs to be investigated.

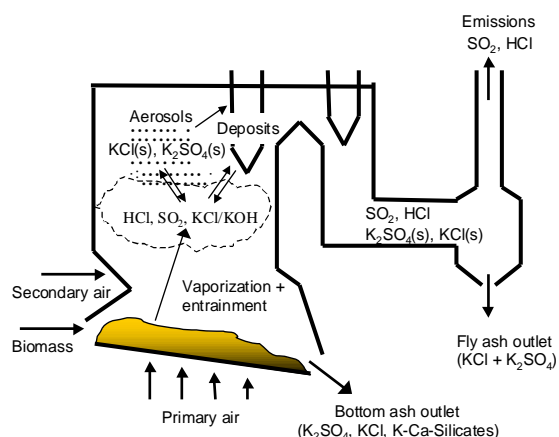


Figure 1: Illustration of the release and fate of Cl, K and S in a biomass-fired grate-furnace.

Specific objectives

The objectives of the present Ph.D. project are to investigate the transformations and release-mechanisms of ash-forming elements during thermal conversion of annual biomass. This includes:

- Quantitative assessment of the Cl, K and S release to the gas phase from various biomass fuels

- Investigating the influence of secondary reactions of inorganic species in the fuel-bed
- Identification of the parameters which control the gas phase release
- Development of a release-model for the major inorganic species (Cl, K and S)

Results and Discussion

Quantification of Cl, K and S release: Using a laboratory scale reactor in investigating the release behavior, the combustion conditions can be carefully controlled. To simulate the heating rate of an industrial boiler, an experimental procedure is utilized where the biomass sample is inserted into a hot reactor. The release of Cl, K and S from the sample can be quantified by a chemical analysis of the residual ash and a mass balance on the system. Information about the release kinetics of Cl and S may be obtained by online measurements of the gas phase concentrations of HCl and SO₂. This procedure is illustrated in Figure 2.

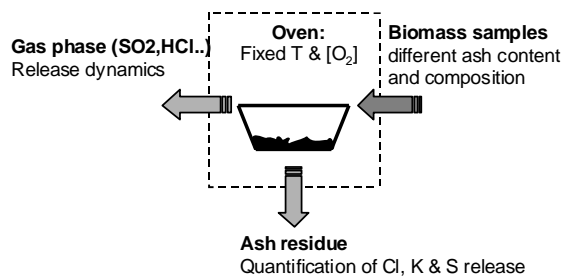


Figure 2: Schematic illustration of the experimental procedure for the Cl, K and S release quantification.

In case of a series of experiments at different temperatures and oxygen concentrations are conducted, it is possible to quantify the release as a function of combustion conditions. The influence of other elements on the release such as Ca, Si and P may be investigated by conducting experiments with biomass fuels of different mineral content and composition.

Four biomass fuels with a distinctive different ash composition were selected for the release investigation. As seen in Table 1, the concentration range of Cl, K, S and Si is particularly broad.

Table 1: Characteristics of the annual biomass fuels applied in the experimental investigation.

Fuel	Wheat	Oat	Barley	Carinata
Moisture (%)	8.4	7.8	8.5	7.3
Ash (% , dry)	4.8	3.8	6.9	4.9
Ca (% , dry)	0.35	0.72	0.34	0.60
Cl % , dry)	0.27	0.05	0.79	0.05
K (% , dry)	1.2	0.55	2.3	1.4
S (% , dry)	0.17	0.14	0.20	0.26
Si (% , dry)	0.79	0.27	0.81	0.05

The experimental release investigation revealed that both the combustion temperature and the ash composition had severe impact on the extent of Cl, K and S release to the gas phase at grate combustion conditions.

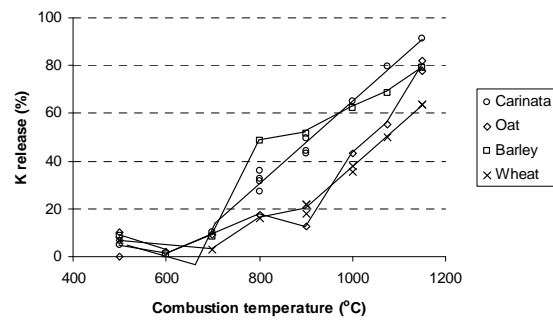


Figure 3: Release of potassium as a function of temperature.

Potassium: It is seen in Figure 3 that the release of potassium to the gas phase increases with the applied combustion temperature for all biomass fuels regardless of the ash composition. Between 20 and 50% of the total potassium has been released at 900°C. At temperatures above 900°C the relative potassium release increases almost linearly with temperature until 60 to 90% is released at 1150°C. The local temperature on the grate in grate-fired furnaces is fluctuating, but frequently above 900-1000°C [5]. This implies that significant amounts of the fuel-potassium are released to the gas phase during grate combustion of annual biomass.

It is furthermore seen in Figure 3 that the release of potassium is greatly affected by the ash composition. The biomass fuels with the higher Si and lower Cl content relative to K (oat and wheat straw) display the lower potassium release. Potassium can be incorporated into silicate structures [6]. The vapor pressure of potassium fixed in silicate structures is relatively low, which reduces the release of potassium to the gas phase. On the other hand, a high concentration of chlorine relative to potassium may increase the volatility of potassium, due to the relatively high vapor pressure of KCl at combustion relevant temperatures. Thus, chlorine promotes the release of potassium to the gas phase. This effect is evident for the barley straw, which contain substantial silicon but exhibits a relatively high release of potassium due to the promoting effect of chlorine.

In summary, the experimental investigation indicates that the release of potassium to the gas phase will be considerable for biomass fuels containing high amounts of chlorine and/or potassium relative to silicon. On the contrary, the potassium release is expected to be low for high-silicate fuels with low chlorine content.

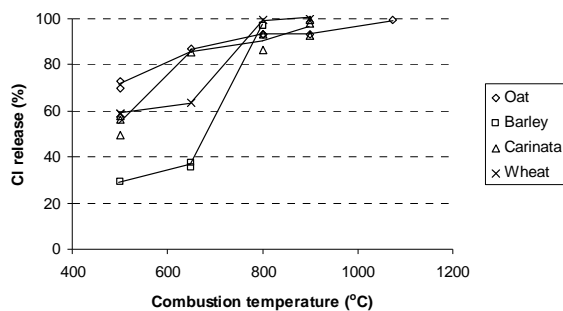


Figure 4: Release of chlorine as a function of temperature.

Chlorine: It appears in Figure 4 that chlorine is released in two steps for the samples which contain substantial Cl (barley and wheat). Between 30 and 60% is released in the first step below 500°C. The remaining Cl is released in the second step between 650 and 800°C. The observed two-step chlorine release is in agreement with observations in the literature [6]. It has been demonstrated that chlorine is released as HCl during the fuel devolatilization at 200-400°C. The second release-step of chlorine is linked to the evaporation of KCl [6], which mainly occurs between 700 and 800°C as seen in Figure 4. This is consistent with the observed increase in the potassium release between 700 and 800°C for the fuels rich in chlorine as shown in Figure 3.

For the samples which have a relatively low Cl content (oat and carinata), the chlorine release is gradually increasing as a function of combustion temperature. In general a higher fraction of the fuel-chlorine appears to be released at lower temperatures for the low-chlorine fuels. This is most likely an effect of concentration rather than a true mechanistic difference. Significantly less KCl must be evaporated from the low-chlorine fuels, thus the evaporation rate becomes important at lower temperatures.

Nevertheless, the investigation indicates that combustion of annual biomass above 800°C results in nearly complete release of Cl to the gas phase. The ash composition or the absolute Cl content of the fuel does not affect this fact. The temperature on the grate in grate-fired furnaces is typically significantly above 800°C [5], which implies that most fuel-chlorine will be released to the gas phase during grate-combustion of annual biomass.

Sulfur: In contrast to the observed release behavior of Cl and K, Figure 5 reveals that the sulfur release appears to be more sensitive to the ash composition than the combustion temperature. In case the biomass fuel contains relatively high amounts of Ca and K compared to Si, (oat and carinata), approximately 50% of the sulfur is released almost independently of the applied combustion temperature. On the other hand, if the Si concentration is high, the sulfur release increases with combustion temperature. Calcium and potassium are the elements facilitating sulfur capture in the residual ash. It appears in Table 1, that the content of Ca and K in the

fuels is sufficient to retain all fuel-sulfur. However, in the high-silicate fuels, calcium and potassium are to a large extent incorporated into glassy silicate structures. The retention of sulfur in Ca-K-silicates is low, hence, the sulfur release to the gas phase is observed to be higher for high-silicate fuels.

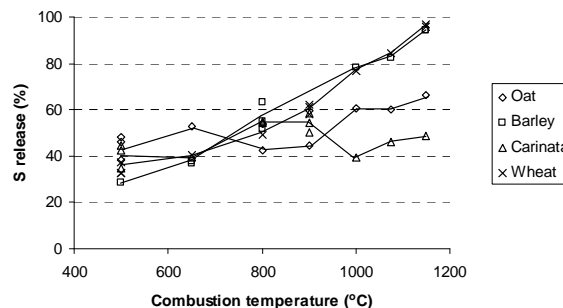


Figure 5: Release of sulfur as a function of temperature.

It appears in Figure 5 that the sulfur release is greater than 40% at all temperatures and for all of the investigated biomass fuels. This is related to the occurrence of substantial amounts of volatile organic sulfur in annual biomass. Earlier work [7] has indicated that annual biomass fuels contain both organic sulfur and inorganic sulfate. The organic sulfur is released to the gas phase during devolatilization at 200-400°C, whereas the inorganic sulfate is retained in the char.

Altogether, the experimental work indicates that the sulfur release in grate-fired boilers is controlled by the organic-to-inorganic sulfur ratio in the fuels and the accessibility of potassium and calcium. The accessibility of potassium and calcium is largely determined by the relative concentration of silicate.

Influence of secondary reactions in the fuel-bed: In an industrial grate-fired boiler, the height of the fuel-bed is several times higher than in the laboratory reactor. This indicates that there could be an effect of scaling on the interactions between inorganic species in the gas phase and unconverted fuel. In Figure 6, the idealized grate-firing process is illustrated.

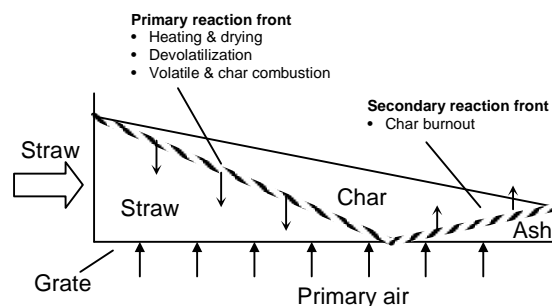


Figure 6: Schematic illustration of the idealized grate-combustion process [5].

According to Figure 6, a primary reaction front propagates downwards from the top of the bed. In this narrow zone, the fuel undergoes heating and drying

followed by devolatilization and partial combustion of volatiles and char. Depending on the operating conditions, a char-layer of varying thickness remains on top of the fuel-bed. The inorganic species released to the gas phase during devolatilization are transported up through the char-layer by the primary air. This indicates that secondary reactions may occur between char and inorganic species such as HCl and SO₂ contained in the gas phase.

The reactions of HCl and SO₂ with biomass char have been investigated in the laboratory. Char samples have been exposed to a mixture of N₂-SO₂ or N₂-HCl at different temperatures as illustrated in Figure 7.

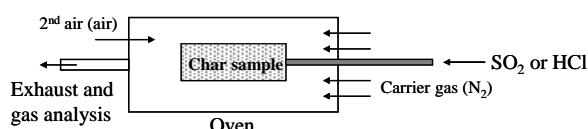


Figure 7: Sketch of experimental absorption procedure.

In order to evaluate the absorption efficiency of biomass char, the fraction of HCl/SO₂ absorbed in the char is determined as a function of temperature. The results are shown in Figure 8.

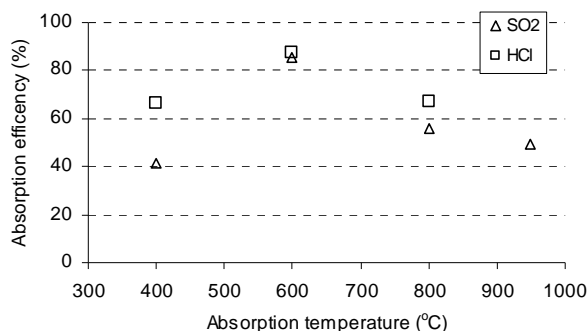


Figure 8: Percentage of SO₂ and HCl absorbed in biomass char as a function of temperature.

Figure 8 reveals that HCl and SO₂ are efficiently captured by biomass char in the entire investigated temperature range. This indicates that secondary reactions (recapture) of chlorine and sulfur with char could be important during grate-combustion of biomass. More work is needed to establish the exact influence of secondary reactions on the overall release behavior.

Conclusions

The objectives of this Ph.D. project were to investigate the transformation and release of Cl, K and S during grate-combustion of annual biomass. An experimental quantification of the Cl, K and S release to the gas phase was conducted. The investigation revealed that both the combustion temperature and the ash composition had great impact on the extent of Cl, K and S release to the gas phase at grate combustion conditions. The release of K was largely determined by the fuels content of chlorine and silicon along with the combustion temperature. The sulfur release was controlled by the

accessibility of Ca and K. Additional experiments suggested that HCl and SO₂ may be recaptured by char in the fuel-bed. Although this is an ongoing investigation, the current results provide the first important steps in establishing the release mechanisms of Cl, K and S at grate-combustion conditions.

Future

This is ongoing work. Effort is being made to establish the release mechanisms of Cl, K and S. An important part in the future work is to develop a reliable model to predict the release of Cl, K and S as a function of the applied combustion conditions and the inorganic composition of the fuel.

Acknowledgements

This Ph.D. project is kindly sponsored by, the Danish and the Nordic Energy Research Programmes.

References

1. D.O. Hall, R.P. Overend, Biomass Regenerable Energy, John Wiley & Sons, London, 1987, chap.4.
2. H.P. Michelsen, F.J. Frandsen, K. Dam-Johansen, O.H. Larsen, Fuel Processing Technology, 54 (1998) 95-108.
3. B. Sander, N. Henriksen, O.H. Larsen, A. Skriver, C. Ramsgaard-Nielsen, J.N. Jensen, K. Stærkind, H. Livbjerg, M. Thellefsen, K. Dam-Johansen, F.J. Frandsen, R. van der Lans, J. Hansen, Emissions, Corrosion and Alkali Chemistry in Straw-Fired Combined Heat and Power Plants, 1st World Conference on Biomass for Energy and Industry, Sevilla, Spain, June 2000.
4. K.A. Christensen, M. Stenholm, H. Livbjerg, Journal of Aerosol Science, 29 (1998) 421-444.
5. R. Van der Lans, L.T. Pedersen, A. Jensen, P. Glarborg, K. Dam-Johansen, Biomass and Bioenergy 19 (2000) 99-208.
6. P.A. Jensen, F.J. Frandsen, K. Dam-Johansen, B. Sander, Energy & Fuels 14 (2000) 280-1285.
7. J.N. Knudsen, W. Lin., F.J. Frandsen, K. Dam-Johansen, Sulfur Transformations during Thermal Conversion of Biomass, Power Production in the 21st Century, Engineering Foundation Conference, Snowbird, Utah, USA, 28 Oct. - 2 Nov. 2001.

List of Publications

1. J.N. Knudsen, W. Lin, F.J. Frandsen, K. Dam-Johansen, Experimental Investigation of Sulfur Release during Thermal Conversion of Wheat Straw and its Application to Full-scale Grate Firing, Proceedings vol. 3, 6th Int. Conf. on Tech. and Combust. for a Clean Environment, July 2001, Porto, Portugal.
2. J.N. Knudsen, W. Lin., F.J. Frandsen, K. Dam-Johansen, Sulfur Transformations during Thermal Conversion of Biomass, Power Production in the 21st Century Engineering Foundation Conference, October 2001, Snowbird, USA.



Irene Kouskoumvekaki
IVC-SEP, Dept. of Chemical Engineering
Building 229, Office 212
Technical University of Denmark

Address: IVC-SEP, Dept. of Chemical Engineering
Building 229, Office 212
Technical University of Denmark

Phone: (+45) 45 25 28 64
Fax: (+45) 45 88 22 58
e-mail: ik@kt.dtu.dk
www: www.ivc-sep.kt.dtu.dk
Supervisor(s): Georgios M. Kontogeorgis
Michael L. Michelsen

Ph.D. Study
Started: 1 February 2001
To be completed: February 2004

A Predictive Equation of State for Paints

Abstract

With focus on developing a predictive equation of state that could be applied to paint systems, a variety of activity coefficient models (ACM) and one equation of state (EoS) were evaluated against experimental data in asymmetric alkane and polymer systems. It was shown that it is essential for the ACM to contain a free volume (FV) term that takes into account the difference in size between the two components. The Entropic-FV (EFV) model was found to be the most successful among all the evaluated ACMs and its behavior has been further improved by optimizing the FV expression against activity coefficient experimental data of short and long alkanes in asymmetric systems. The evaluation of EOS was focused on the recently presented Perturbed Chain Statistical Associating Fluid Theory (PC-SAFT) and its modification developed recently by our group. PC-SAFT was evaluated against experimental data of different equilibrium types: vapor-liquid equilibrium (VLE), liquid-liquid equilibrium (LLE) including both upper critical solution temperature (UCST) and lower critical solution temperature (LCST), in a variety of binary and ternary polymer systems with non-polar, polar and associating solvents. The overall behavior of PC-SAFT has been in most cases very good in both predicting and correlating the above systems with a small interaction parameter, which makes the model very promising for further evaluation in complicated cases such as aqueous polymer systems, associating polymer systems and blends etc.

Introduction

Paints are complex materials comprising of one or more polymers dissolved in one or more solvents, while other compounds are also typically present (additives, pigments). Typical polymers employed as binders by the Danish Paint Industry are acrylics, epoxies, phenolics and alkyds. These require water-based or water-organic mixed solvents. The proper choice of solvent is crucial in specific applications, for financial and environmental reasons. The latter have now become increasingly more important with the pressure for substituting or reducing the volatile organic content (VOCs) of paints. Moreover, the polymer-mixed solvent system is usually miscible at the formulation stage but may phase separate during the drying/curing phases. Thus, temperature may have an influence. Traditional methods employed in the paint industry e.g. Hansen solubility parameters are simple and adequate in many cases but require substantial experiments and are sufficient only for yes/no answers (soluble/non-soluble). As apparent from the above discussion, the prediction of phase diagrams as a function of temperature, pressure,

composition and polymer molecular weight will substantially assist the paint formulator.

The purpose of this project is to develop a simple equation of state for predicting multicomponent / multiphase equilibria of complex polymer solutions. Such systems are of direct application in the paints and coatings industry, of major importance in the Danish society. Better understanding of their thermodynamic behavior may help in improving existing and developing new user-friendly paints achieving at the same time the targeted properties.

Specific Objectives

The introductory phase of the project includes an investigation of various combinatorial and free-volume expressions, which appear in thermodynamic models, for polymer solutions.

The purpose of this phase is two-fold: First, to investigate the performance of EFV [1], Unifac-Free Volume (UFV) [2], Unifac-ZM [3] and Flory-FV [4] models for various -nearly- athermal systems: alkane-alkane and polymer solutions. The evaluation is carried

out by direct comparison of results against VLE [5-11], solid-liquid equilibrium (SLE) [12] experimental data, as well as extrapolated data generated with molecular simulation methods [13].

Second, to attempt to improve the performance of Entropic-FV by adjusting the hard-core volume V^* of the free-volume term ($V^* = aV_w$, where $a=1$ in original Entropic-FV). The target is to investigate whether a single, unique a -value can be adopted for all the athermal solutions considered, covering both solvent and polymer activities and whether this value is of physical significance.

Furthermore, the ability of the Unifac-FV and Entropic-FV models to predict phase equilibria for dendrimer systems has been also investigated. Dendrimers constitute a new type of complex polymeric molecules, where the predictive performance of free-volume models that use the group contribution approach has not been extensively evaluated so far.

The following phase of the project includes evaluation of the PC-SAFT in polymer systems. PC-SAFT is a non-cubic, segment-based equation of state which was designed specifically to deal with systems containing polymers and associating fluids. The performance of the original [14] and a modified version developed by the group [15] have been evaluated in the following areas of application:

- obtaining pure component parameters of polar (ketones, chloroform etc.) and associating (water, alcohols, amines) compounds
- predicting and correlating VLE and LLE of complex, branched polymers such as polystyrene (PS), polyvinyl acetate (PVAc) and polyisobutylene (PIB), in alkane, polar and associating solvents
- predicting and correlating binary and ternary systems of nylon 6, ϵ -caprolactam and water that are present during the manufacturing process of nylon 6. This part of the project was contacted during the external stay at Dutch State Mines (DSM) company in Holland and was initiated by the need of the company for such a tool.

Results and Discussion

The basic conclusions from the evaluation of the various combinatorial and free-volume expressions are that the models perform well for the activity of the short-chain alkane (γ_1) but not for the activity of the long-chain one (γ_2).

The proposed modification of the Entropic-FV model was based on optimizing the relation of the hard-core volume to the van der Waals (vdW) volume, considering the statement of Bondi [16] that due to the packing of molecules, a higher than V_w 'inaccessible' volume represents more adequately the hard-core volume. This leads to an expression of the type $V^* = \alpha V_w$ ($1 < \alpha < 2$). Values of the a -parameter in this range were introduced in the equation $V^* = \alpha V_w$ and the results of the evaluation are shown in Figures 1-2. Although a

completely unique value for all systems and both γ_1 and γ_2 is difficult to obtain, a value of $a = 1.2$ is a reasonable compromise. The Entropic-FV model for $a = 1.2$ becomes now the best model in all situations.

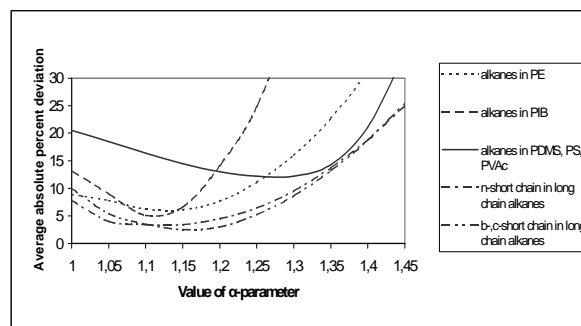


Figure 1: % Absolute Average Deviation between experimental and calculated solvent infinite dilution activity coefficients, versus the a -parameter in Entropic-FV ($V_f = V - aV_w$)

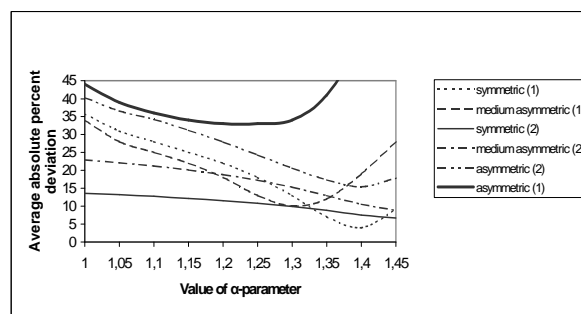


Figure 2: % Absolute Average Deviation between experimental and calculated solute infinite dilution activity coefficients versus the a -parameter in Entropic-FV ($V_f = V - aV_w$)

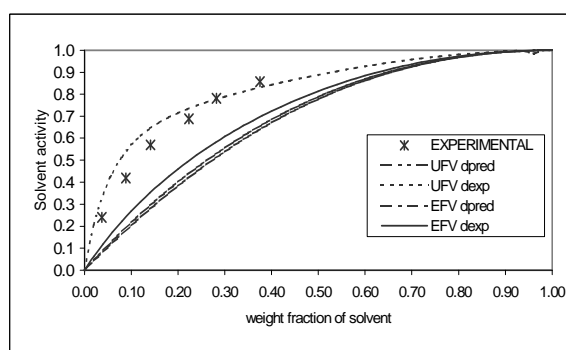


Figure 3: Experimental [18] and predicted activities of methanol in Polyamidoamine of Generation 2 (PAMAM-G2) with the Entropic-FV and the Unifac-FV models.

In dendrimer systems, the Entropic-FV and the Unifac-FV models, with no extra fitting parameters, can predict the solvent activity with acceptable accuracy in many cases. However, due to the special structure of

dendrimers, dependable tools such as the van Krevelen method [17] are necessary for the prediction of their molar volume, which is a parameter that influences significantly the overall performance of free-volume models. The Unifac-FV model is more sensitive to the value of density than the Entropic-FV model (Figure 3), which indicates deficiencies in these cases of the free-volume expression derived from the Flory equation of state.

Table 1: Comparison of the performance of the simplified against the original PC-SAFT in predicting vapor-liquid equilibria of polymer solutions ($k_{ij}=0$ in all cases). Average absolute percentage deviation (%AAD) between experimental and predicted equilibrium pressure curves.

%AAD	PC-SAFT	
	(Simplified)	(Original)
<i>Cyclic hydrocarbons</i>		
PS-cyclohexane	13	16
PS-benzene	28	13
PS-ethyl benzene	3	6
PS-m-xylene	25	16
PS-toluene	18	7
PVAc-benzene	6	10
<i>Chlorinated hydrocarbons</i>		
PS-carbon tetrachloride	18	12
PS-chloroform	30	11
PP-dichloromethane	59	74
PP-carbon tetrachloride	55	47
<i>Esters</i>		
PS-propyl acetate	5	21
PS-butyl acetate	3	25
PVAc-methyl acetate	3	2
PVAc-propyl acetate	19	18
<i>Ketones</i>		
PS-acetone	6	26
PS-diethyl ketone	7	28
PS-methyl ethyl ketone	14	12
PVAc-acetone	4	7
PP-diethyl ketone	16	27
PP-diisopropyl ketone	4	11
PVAc-methyl ethyl ketone	7	6
<i>Amines</i>		
PVAc-propylamine	4	3
PVAc-isopropyl amine	17	16
<i>Alcohols</i>		
PVAc-1-propanol	56	54
PVAc-2-propanol	84	73
PVAc-1-butanol	59	59
PVAc-2-butanol	39	36
PVAc-2methyl-1propanol	29	29
Overall	23	24

In the more difficult case of liquid-liquid equilibria, a novel method, which has been called ‘the method of alternating tangents’ (Figure 4), has been developed for tracing the liquid-liquid equilibria in binary polymer-

solvent systems. The algorithm is robust and traces the full temperature composition curve for both UCST and LCST type systems through the critical solution temperature.

When it comes to the evaluation of the original and the modified version of the PC-SAFT EoS, it has been shown that the applied simplification is not at the expense of the accuracy of equation of state (table 1), while the computational time and complexity are significantly reduced, especially for associating systems. For this reason, our focus has been directed to the further evaluation of the simplified PC-SAFT only. With no binary interaction parameter, simplified PC-SAFT is able to predict vapor-liquid equilibria of polymers with non-associating solvents. In the case of associating solvents, a small binary interaction parameter k_{ij} is usually needed for the satisfactory correlation of the experimental data.

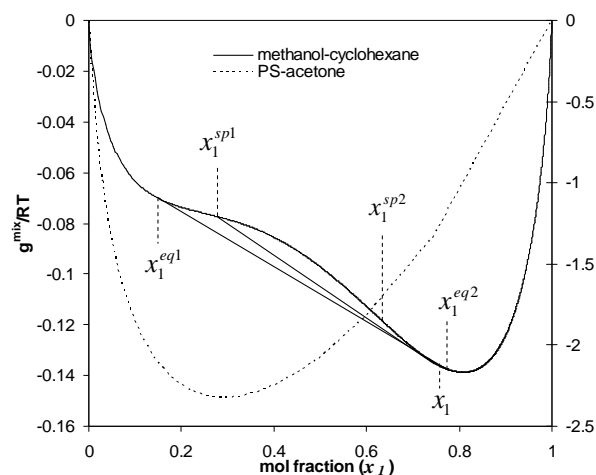


Figure 4: Illustration of the method of alternating tangents. The solid line is the system methanol (1)-cyclohexane (2). The dotted line is the system PS (1)-acetone. The two spinodal points are indicated by x_1^{sp1} and x_1^{sp2} . The equilibrium (binodal) points are indicated by x_1^{eq1} and x_1^{eq2} . Starting from a spinodal point, the equilibrium values can be calculated by solving for only one point at a time.

In general, the simplified PC-SAFT is successful in modelling LLE, successfully predicting the correct behaviour in many systems exhibiting upper, lower or both critical solution temperatures. Where predictions are not accurate, a small value of the binary interaction parameter is required to correlate the experimental data (Figure 5).

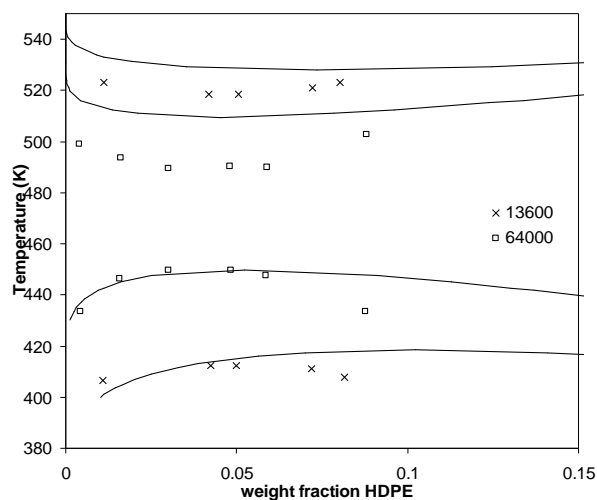


Figure 5: Liquid-liquid equilibrium in the system High Density Polyethylene (HDPE)-butyl acetate. The system displays both upper and lower critical solution temperature behaviour. The experimental data are from Kuwahara et al. [19] for molecular weights 13 600 and 64 000. Lines are simplified PC-SAFT correlations with $k_{ij} = 0.0156$ for both molecular weights.

Finally, the application of the model to the nylon 6 manufacturing process shows that the five pure component parameters of ϵ -caprolactam can be used as initial estimates for the parameters of polyamide 6, while σ is fitted to the pure polymer PVT data. It was also found that there is a linear dependency of the segment size parameter σ to the linear polyethylene segment fraction of the polyamide, so other polyamide types can be similarly modeled (Figure 6).

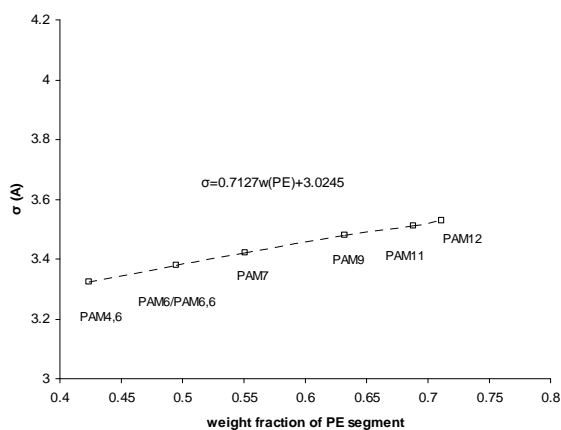


Figure 6: Optimum σ values against the weight fraction of linear polyethylene segment in the polyamide chain for seven polyamide types.

Based on experimental data of the three binary systems, the ternary system nylon 6 – ϵ -caprolactam – water has been successfully correlated (Figure 7).

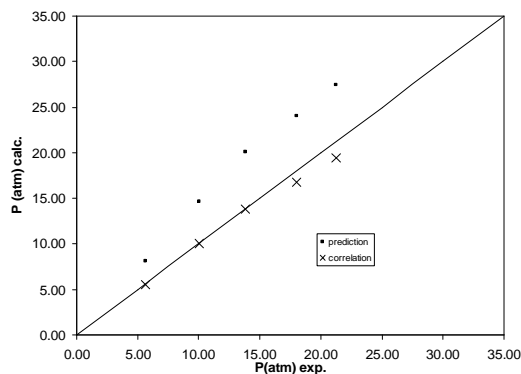


Figure 7: Comparison of experimental pressure data [20] with prediction and correlation results with PC-SAFT at 543.15K, for the ternary system polyamide 6 (1) - ϵ -caprolactam (2) – water (3) (binary interaction parameters: prediction: $k_{12}=-0.07$, $k_{13}=-0.04$, $k_{23}=-0.011$, correlation: $k_{12}=-0.07$, $k_{13}=-0.11$, $k_{23}=-0.011$).

Conclusions

In the recent years, there has been an industrial need to come up with a thermodynamic tool that would be able to describe complex, multicomponent polymer mixtures that are present in paints. This tool could be either an advanced activity coefficient model or a simple equation of state that would be able to handle the difference in the free volume and size between the large polymer molecule and the small solvent. It should be able to predict satisfactorily pure compounds as well as two-phase binary systems. Furthermore, it should be successful in correlating the more complex multicomponent, multiphase systems that are more representative of paint solutions. Our investigation has shown that activity coefficient models have limitations when it comes to describing highly asymmetric systems, liquid-liquid equilibria or processes under high pressures. A new FV model has been developed to correct for the first limitations.

On the contrary, modern equations of state such as the modified PC-SAFT we have proposed, can be very successful in describing with good accuracy and limited empirical assumptions (when it comes to estimation of parameters) all kinds of equilibria in binary and ternary complex polymers solution with polar or associating solvents. This observation makes PC-SAFT a very promising EoS for further evaluation to complex systems such as aqueous polymer solutions, associating polymer systems and blends.

Acknowledgements

The author wishes to thank J. C. Hempel foundation for financial support, as well as the Danish Technical Research Council (STVF) for financial support of this work in the framework of a grant entitled: ‘*Thermodynamic properties of polymer solutions related to paints and coatings*’. The author wishes furthermore to thank Georgios Kontogeorgis and Michael Michelsen for their supervision, as well as Thomas Lindvig, Nicolas von Solms and Samer Derawi

for having contributed significantly in the presented work, with many valuable ideas and discussions.

References

1. H.S. Elbro, Aa. Fredenslund and P. Rasmussen, *Macromolecules* 23 (21) (1990) 4707.
2. T. Oishi and M. Prausnitz, *Ind. Eng. Chem. Process Des.* 17 (3) (1978) 333.
3. C. Zhong, Y. Sato, H. Masuoka and X. Chen, *Fluid Phase Equilibria* 123 (1996) 97.
4. P.J. Flory, *Discuss. Farad. Soc.* 49 (1970) 7.
5. K. Kniaz, *Fluid Phase Equilibria*, 68 (1991) 35.
6. K. Kniaz, *J. Chem. Eng. Data*, 36 (1991) 471.
7. R.N. Lichtenhaler, D.D. Lieu and J.M. Prausnitz, *Ber. Bunsenges. Phys. Chem.* 78 (1974) 470.
8. J.F. Parcher, P.K. Weiner, C.L. Hussey and T.N. Westlake, *J. Chem. Eng. Data* 20 (1975) 145.
9. Y.B. Tewari, D.E. Martire and J.P. Sheridan, *J. Phys. Chem.* 74 (1970) 2345.
10. J.D. Newman and J. M. Prausnitz, *J. Paint Technol.* 45 (1973) 33.
11. W. Hao, H.S. Elbro and P. Alessi, *Polymer Solution Data Collection Part 1-2, DECHEMA, Chemistry Data Series XIV*, 1992.
12. E.N. Polyzou, P.M. Vlamos, G.M. Dimakos, I.V. Yakoumis and G.M. Kontogeorgis, *Ind. Eng. Chem. Res.* 38 (1999) 316.
13. G.M. Kontogeorgis, E. Voutsas and D. Tassios, *Chem. Eng. Science*, 51 (12) (1996) 3247.
14. J. Gross and G. Sadowski, *Ind. Eng. Chem. Res.* 40 (2001) 1244.
15. N. von Solms, M.L. Michelsen and G.M. Kontogeorgis, *Ind. Eng. Chem. Res.* 42 (2003) 1098.
16. A. Bondi, *Physical Properties of Molecular Crystals, Liquids and Glasses*, Wiley, New York, 1968.
17. Van Krevelen, *Properties of polymers. Their correlation with chemical structure; their numerical estimation and prediction from additive group contributions*. Elsevier, 1990.
18. C. Mio, S. Kiritsov, Y. Thio, R. Brafman, J. Prausnitz, C. Hawker,; E.E. Malmstrøm, *J. Chem. Eng. Data*. 43 (1998) 541.
19. N. Kuwahara, S. Saeki, T. Chiba and M. Kaneko, *Polymer* 15 (1974) 777.
20. C. Giori, B.T. Hayes, *Journal of Polymer Science: Part A-1*, 8 (1970) 351.
5. I.A. Kouskoumvekaki, G. Krooshof, M.L. Michelsen, G.M. Kontogeorgis, Application of the Simplified PC-SAFT Equation of State to the Manufacturing Process of Polyamide 6 (submitted for publication).
6. N. von Solms, I.A. Kouskoumvekaki, T. Lindvig, M.L. Michelsen, G.M. Kontogeorgis, A Novel Approach to Liquid-Liquid Equilibrium in Polymer Systems with Applications to Simplified PC-SAFT (submitted for publication).

List of Publications

1. I.A. Kouskoumvekaki, M.L. Michelsen, G.M. Kontogeorgis, *Fluid Phase Equilibria* 202 (2) (2002) 325-335.
2. G.M. Kontogeorgis, I.A. Kouskoumvekaki, M.L. Michelsen, *Ind.Eng.Chem.Res.* 41 (18) (2002) 4686-4688.
3. I.A. Kouskoumvekaki, R. Giesen, M.L. Michelsen, G.M. Kontogeorgis, *Ind.Eng.Chem.Res.* 41 (19) (2002) 4848-4853.
4. I.A. Kouskoumvekaki, N. von Solms, M.L. Michelsen, G.M. Kontogeorgis, *Fluid Phase Equilibria* 214 (2) (2003) 279-290.



Anne Krogh

Address: ICAT, Dept. of Chemical Engineering
Building 312, Office 083
Technical University of Denmark

Phone: (+45) 45 25 31 96
Fax: (+45) 45 93 23 99
e-mail: ak@kt.dtu.dk
www: www.icat.dtu.dk
Supervisor(s): Ib Chorkendorff
Claus Hviid Christensen
Søren Dahl, Haldor Topsøe A/S

Ph.D. Study
Started: 1 July 2003
To be completed: July 2006

From Step-sites on Single Crystals to Technical Catalysts

Abstract

The structure of the active sites in catalytic hydro- and dehydrogenation of hydrocarbons has never been elucidated. Identifying the active sites on a single crystal catalyst of transition metal will give knowledge on how to optimize technical industrial catalysts. Surface science studies will be performed by using the UHV/HPC technique to investigate the reaction mechanism and the active sites in the relevant reactions. These studies will complement catalytic testing of technical catalysts in micro reactors. By optimizing the catalysts, larger selectivities might be obtained and the unwanted hydrogenolysis of the hydrocarbons can be avoided.

Introduction

Hydrogenation and dehydrogenation of hydrocarbons is one of the most important chemical reactions. Reactions like dehydrogenation of ethane to ethene, ethylbenzene to styrene or hydrogenation of benzene to cyclohexane are widely used in the chemical industry. Ethylene, which is mainly used for polymerization in the production of polyethylene (PE), is nowadays produced from thermal cracking of hydrocarbon feedstocks such as ethane or naphtha [1], but can be produced by dehydrogenation of ethane. PE is the major plastic produced on weight basis in the world, 45·10⁶ tons were produced in 1995 [1]. Other examples of hydro-/dehydrogenation reactions are hydrogenation of benzene to cyclohexane, which is used in the production of nylon, and dehydrogenation of ethylbenzene to styrene, which is the monomer of polystyrene.

Hydrogenation of olefines on metal catalysts was discovered by Sabatier and Senderens in 1897. Since then, several catalysts have been developed and the hydrogenation of olefins is today one of the most studied chemical processes, especially the hydrogenation of ethene on Pt(111) [2]. Even though hydrogenation of olefins is a widely studied process not every aspect of the catalysts role has been discovered.

Hydrogenation, Dehydrogenation, and Hydrogenolysis

These hydro- and dehydrogenating reactions are often not very selective because of the competing hydrogenolysis, where a scission of the C-C bonds occurs.

Extensive studies on hydrogenation and dehydrogenation reactions have been carried out by J. H. Sinfelt [3]. Group VIII metals were found to be excellent catalysts for hydro- and dehydrogenation reactions as well as hydrogenolysis. Combined with IB metals, the hydrogenolysis was suppressed. Sinfelt explains this as a reduction of surface sites when adding IB metal onto the VIII metal. These surface sites were not further identified. The importance of surface sites such as steps, kinks, and terraces on catalytic activity has later been shown [1]. Therefore the effect from group IB metals was not explained in detail by specific surface properties by Sinfelt.

Surface science studies on well defined single crystals can be used to identify active surface sites in catalysis and give knowledge on reaction kinetics for various reactions [4]. Studies have shown that blocking the surface atomic steps on the surface of a ruthenium single crystal lowered the probability of dissociative adsorption of nitrogen with 9 orders of magnitude [5].

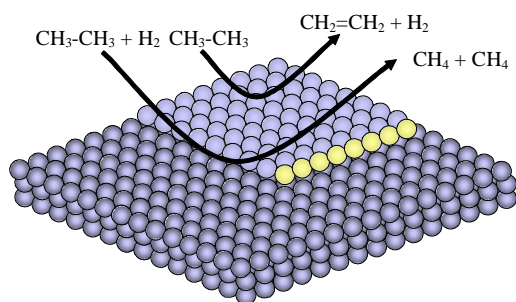


Figure 1: Schematic drawing of a ruthenium crystal surface terrace (dark atoms) and a step to the next terrace (lighter atoms). On the terraces dehydrogenation of ethane takes place. On the step to the left hydrogenolysis is catalyzed. Gold atoms block the step on the right so that no hydrogenolysis takes place.

The poisoning of the steps might have the same effect on the hydrogenolysis as on the dissociative adsorption of nitrogen, since both adsorption and dissociation are involved in the two reactions [6]. In order to minimize the scission of the C-C bonds in the hydrocarbons, blocking the step sites on the single metal crystals with well-defined surface structure is investigated (see Fig. 1). Thereby it is possible to increase the olefin selectivity and avoid the hydrogenolysis.

Investigating reactions on the surface of a single crystal can shed light on the reaction mechanism of the hydrogenating and dehydrogenating reactions. Results from this research will give a valuable and detailed insight into the optimization of real time catalysts.

Experiments

So far extensive alterations have been done in order to obtain equipment specifically designed for this project (see Fig. 2).



Figure 2: Inside the UHV chamber. The ruthenium single crystal is seen in the center of the copper house. A tungsten wire wrapped with gold for evaporating Au onto the surface of Ru, is seen under the crystal.

The first experiment to be performed is hydrogenation of ethane on a ruthenium single crystal. Evaporating gold onto the step sites of the Ru crystal will block these. The surface of the single crystal is to be investigated in an Ultra High Vacuum (UHV) chamber by Auger Electron Spectroscopy (AES) as well

as Temperature Programmed Desorption (TPD) of CO using Quadrupole Mass Spectroscopy (QMS). The catalytic activity of the ruthenium crystal with blocked step sites in the dehydrogenation of ethane is to be investigated in the High Pressure Cell (HPC) in connection with the UHV chamber. The results are to be compared with the catalytic activity of a non-manipulated ruthenium single crystal.



Figure 3: A catalytically tested 2wt% Ru/spinel for the dehydrogenation of ethane. The catalyst is placed in a quartz tube reactor with quartz wool plugs at the ends of the catalyst.

Real catalysts are also to be investigated by impregnating a support with the active catalytic metal, blocking the active steps in the hydrogenolysis, and subsequently testing the modified catalysts in a plug flow reactor simulating the actual industrial reaction. Therefore, in parallel to the UHV/HPC experiments, a ruthenium impregnated support is catalytically tested in a plug flow reactor. The catalyst is placed in a quartz tube reactor (see Fig. 3) and heated in an oven to 823 K while the reacting gas is led through the catalyst bed. Hereby a technical catalyst is tested and the products are identified in the effluent gasses using a Gas Chromatograph equipped with a Thermal Conductivity Detector (TCD) and a Flame Ionization Detector (FID).

Conclusions

The combined results from the experiments will improve our understanding of the area of hydrogenation/dehydrogenation reactions and identify the active sites in the catalysis making it possible to obtain a higher selectivity by suppressing the unwanted hydrogenolysis.

Acknowledgements

The PhD project is financed by the Technical University of Denmark, Haldor Topsøe A/S and Copenhagen Graduate School for Nanoscience and Nanotechnology.

References

1. Ullmann's Encyclopedia of Industrial Chemistry, Release 2003, 7th Edition.
2. F. Zaera, T.V.W. Janssens, H. Öfner, Surf. Sci. 368 (1996) 371-376.
3. J. H. Sinfelt, Bimetallic Catalysts, Discoveries, concepts, and applications, Wiley & Sons, New York, USA, 1983.
4. G.A. Somorjai, Introduction to Surface Chemistry and Chemistry, John Wiley & Sons, Inc., NY, USA, 1994.
5. S. Dahl et al., Phys. Rev. Lett., 83 (9) (1999) 1814-1817.
6. A. Michaelides, Z-P Liu, C.J. Zhang, A. Alavi, D.A. King, P. Hu, J. Am. Chem. Soc. 125 (2003) 3704-3705.



Morten Boberg Larsen

Address: CHEC, Dept. of Chemical Engineering
Building 229, Office 050
Technical University of Denmark

Phone: (+45) 45 25 28 29

Fax: (+45) 45 88 22 58

e-mail: mbl@kt.dtu.dk

www: www.chec.kt.dtu.dk

Supervisor(s): Kim Dam-Johansen

Lars Skaarup Jensen, F.L. Smidth A/S

Ph.D. Study

Started: 1 October 2003

To be completed: October 2006

Combustion Mechanisms Using Waste as a Fuel in Cement Production

Abstract

This project will analyze the combustion of wastes on the Hotdisc, which is a unit for combustion of waste in the production of cement. The analysis will be based on mathematical modeling of the different processes on the Hotdisc and comparison to experimental results. This will give a fundamental understanding of the processes prevailing during combustion of waste. A successful model can be used to optimize the Hotdisc and lower emissions of NO_x and CO.

Introduction

The use of waste as a fuel in kiln-systems for cement production is an economically and environmentally feasible way to get rid of waste and use its heat content to replace fossil fuel.

In the recent years, the use of waste in cement production has increased. Approximately 12% of the total fuel-usage in the production of cement is covered by use of waste in the EU. In Germany this figure has increased from 4% in 1987 to 30% in 2001. At some cement-plants more than 90% of the fuel-usage comes from waste. The different kind of waste employed at this moment in kiln-systems for cement production, are used tires, municipal waste, plastics and biomass [1]. In the future, it is expected, that the ability to use waste as fuel in the cement-industry will become even more important.

The Hotdisc-technology, which is developed at F.L. Smidth A/S, is used for combustion of wastes in the cement-industry. Figure 1 shows a schematic drawing of the Hotdisc-unit, which consists of a rotating plate, at which the combustion of the waste takes place.

A part of the raw-meal, which primarily consists of CaCO₃, Fe₂O₃, Al₂O₃, and SiO₂ with portions of MgCO₃ and other minor components,

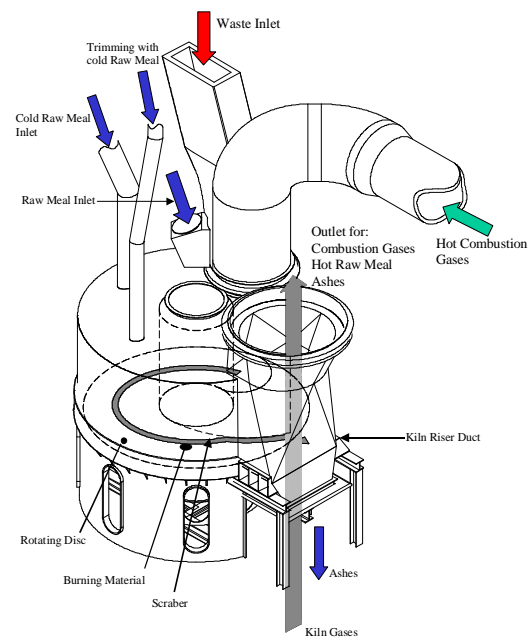
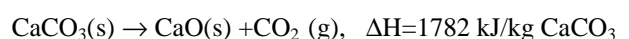


Figure 1: Schematic drawing of the Hotdisc.

is admitted to the Hotdisc, where it undergoes calcination according to the reaction scheme:



This endothermic reaction is the most energy consuming process in cement kilns, which uses approximately 65% of the energy input [2]. Different elements in the waste, as Fe, Al and Si, are implemented into the cement in their oxidized forms (Fe₂O₃, Al₂O₃,

SiO₂). Waste and ashes, which is not burned completely at the Hotdisc enters the rotary kiln.

Specific Objectives

This project will deal with further development of the existing Hotdisc-technology for combustion of wastes.

Mathematical modeling will be used to gain a further understanding of the processes prevailing during the combustion of the wastes. Some of the processes analyzed will be:

- Heating of waste followed by pyrolysis.
- Combustion of the volatiles in the gas phase followed by release of energy. Here, it is investigated whether turbulent mixing of reactants or finite rate chemistry is controlling the combustion. Furthermore, formation and reduction of NO_x is investigated.
- Conversion of char, ash and other inorganic compounds, e.g. Fe.
- Influence on the quality of the produced cement as a function of the waste composition of inorganics, as Fe and ash.
- The use of CaCO₃ to control the temperature on the Hotdisc.

A coupled analysis of the above, should ultimately lead to a better understanding of the combustion-mechanisms prevailing on the Hotdisc. Furthermore this analysis will contribute to the development of a realistic mathematical model. The model-predictions are compared to measurements made at a pilot-scale- or a real cement-production plant.

Conclusion

A successful mathematical model can be used to increase the performance of a Hotdisc. Furthermore this model can be used as a tool to predict emissions from the production of cement.

References

1. Smith, I., Co-utilization of coal and other fuels in cement kilns. IEA Clean Coal Centre, August 2003.
2. Andersen, P.S., Cementfabrikken (In Danish). F.L. Smidth, January 1981.



Hong Wen Li

Address: CAPEC, Dept. of Chemical Engineering
Building 227, Office 226
Technical University of Denmark

Phone: (+45) 45 25 29 09
Fax: (+45) 45 93 29 06
e-mail: lhw@kt.dtu.dk
www: www.capec.kt.dtu.dk
Supervisor(s): Sten Bay Jørgensen
Rafiqul Gani

Ph.D. Study
Started: 11 January 2001
To be completed: May 2004

Modeling for Design and Predictive Control of Integrated Process Plant

Abstract

The project purpose is to investigate the potential of integration of modelling, design and control for energy efficient operation of process plants. In particular, an integration of design and control will be investigated on an energy integrated process. This development is especially pronounced on operability of process integrated plants, and is centered around increasing understanding of the model and the optimization problem for model based control. The most significant energy reduction is expected from model-based control.

Introduction

Chemical Process plant design and operation of systems based on mathematical models and computer science has the potential to significantly increase the efficiency of manufacturing systems by integrating the operations and decision making of these systems. This integration aims at supporting development of sustainable processes and products. Full economic potential of such novel integrated processes is only exploited if they can be operated efficiently. An undesirable effect of process integration is the introduction of more complex nonlinear dynamics. In a linear perspective these dynamics can be interpreted as movement of poles and zeros of the transfer functions towards and into the right half plane. In a nonlinear perspective complex dynamics can be interpreted as bifurcation phenomena, which can give rise to highly undesirable behaviors. Thus it is essential to be able to investigate and classify the nonlinear behavior types. Through such a classification it is possible to distinguish between the types that can be handled through advanced model based control design versus the types. This project focuses upon the types of nonlinear behaviors for which an improved performance can be obtained using nonlinear model predictive control design. The principal objective of this study is to investigate and develop methodologies for optimizing control of integrated sub-plants.

Specific Objective

The efficiency of manufacturing systems can be significantly increased through diligent application of

control based on model analysis thereby enabling more tight integration between decision-making and process operation. The principal objective of this study is to investigate the nonlinear behavior, which is relevant for designing optimizing control of a heat integrated distillation pilot plant. The nonlinear dynamic behavior is investigated in terms of a bifurcation analysis. First, a simple dynamic model capable of capturing the important non-linear behavior has been derived and solved through a computer aided modeling toolbox (ICAS-MOT). Next, the position of control valves, which plays an important role in moving the operation points around within the operation range of the integrated column, is first used as bifurcation parameters. The focus is on revealing and understanding the possible nonlinear behaviors and their influence upon the further decisions behind the experimental design for validating the process model in the region around optimal operation.

Process Description and Process Model

The heat integrated distillation pilot plant, shown in Figure.1 [1], contains two main parts, a distillation column section and a heat pump section. It separates a mixture of methanol and isopropanol, which contains low concentration water as impurity. The column has 19 sieve trays. The heat pump section is physically connected to the distillation column through the condenser at the top and the reboiler at the bottom of the column. Two control valves α_{CV8} and α_{CV9} control the

operation region is on the part of low vapour flow rate when α_{CV9} is kept constant at 0.4 because the bifurcation points B and C are far beyond the high pressure safety limit (see Figure 3) of the distillation pilot plant.

Sensitivity Analysis of Bifurcation

The theoretical and qualitative analysis of bifurcation diagram Figure 2 is the following. The slope of $\partial V/\partial \alpha_{CV8} = \partial V/\partial P_H \partial P_H/\partial \alpha_{CV8}$ changes sign through infinity at bifurcation points A, B and C. It is known that both column pressure and vapor flow rate in the column are sensitive to the high and low pressures in the heat pump section, where high pressure P_H on the heat pump section has positive gain to vapor flow rate in the column [3], i.e. $\partial V/\partial P_H > 0$. Thus the sign of $\partial V/\partial \alpha_{CV8}$ should follow the sign of $\partial P_H/\partial \alpha_{CV8}$, which is the slope of high pressure with respect to α_{CV8} (see Figure 3). The total energy balance for the energy integrated distillation pilot plant is:

$$d(M_{tot} \cdot H_{tot})/dt = F \cdot H_{feed} - D \cdot H_{top} - B \cdot H_{bot} + W_{comp} - Q_{cool} - Q_{loos}$$

Where $M_{tot} \cdot H_{tot}$ is the total plant enthalpy, H_{feed} , H_{top} and H_{bot} is enthalpy of feed, top and bottom product, Q_{cool} is heat transfer rate out through the air coolers, and W_{comp} is work introduced by the compressor. Q_{loos} is the heat loss rate through equipment and tube surfaces. This latter term can be neglected by ensuring proper insulation of all surfaces.

When valve position α_{CV8} decreases, this will immediately affect the high pressure P_H such that P_H begins to increase. Thereby the compression work is increased, but the cooling rate will also gradually increase as the temperature gradient in the secondary condenser and in the air coolers will increase with P_H . The increase in the high pressure affects vapor flow rate in the column, and consequently the heat pump low pressure P_L also increases when α_{CV9} is kept constant. The increased in low pressure P_L tends to reduce the compression work. If the resulting effect of P_H and P_L on W_{comp} is positive the energy flux into the system increase further. And if the compressor work increases faster than the sum of all the outgoing heat flows, the behavior of the entire plant may become unstable, i.e. reach the bifurcation points. So the sign of $\partial P_H/\partial \alpha_{CV8}$ depends on difference between the increase of compressor work and the sum of all the outgoing heat flows.

Bifurcation Diagram with Cascade Control

From the bifurcation results in Figure 2 one can see that branch AB is unstable. So to compare the nonlinear behavior with and without control of the high pressure P_H , a cascade control loop is added into the model, where the control valve α_{CV8} now controls the high pressure P_H , whose set point is given by the vapor flow control loop. Then the bifurcation analysis is done with vapor flow rate set point as a bifurcation parameter

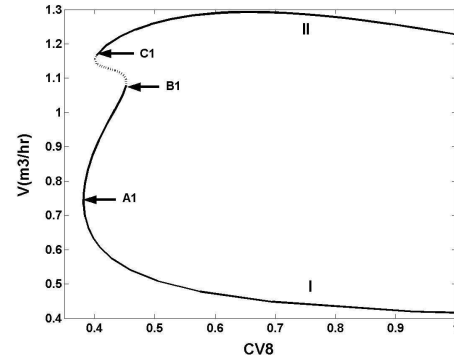


Figure 4: Bifurcation diagram with cascade loop control

shown in Figure 4. Comparing Figures 4 and 2 one can see that the branches A1B1 and C1II become stable (solid line) while B1C1 becomes unstable (dotted line) when cascade control loop is implemented. The largest eigenvalue corresponding to Figure 4 is shown in Figure 4.2 (not shown) where the branch B1C1 is much further into the right half plane than branch AB in figure 2.2 (not shown). This means that the controller improve the stability of the process within the feasible operating region.

Sensitivity Investigation to Valve α_{CV9}

The sensitivity of the bifurcations to α_{CV9} in Figure 5 shows that the vapor flow rate increase as valve α_{CV9} open from 0.4 to 0.5 with the above cascade control

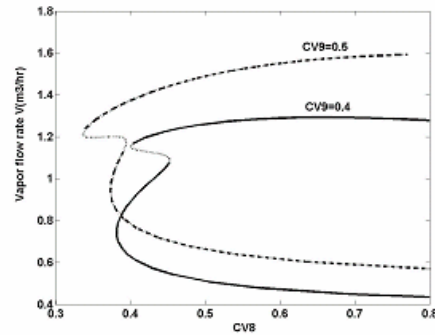


Figure 5: Bifurcation diagram sensitivity to α_{CV9} with cascade control

loop implemented. Consequently the low pressure P_L will decrease. This is in agreement with the finding that the low pressure P_L has negative gain to column vapour flow rate (3).

Sensitivity Investigation to Heat Transfer (area) Coefficients of the Reboiler and Condenser

The sensitivity of two uncertain parameters, i.e. heat transfer (area) coefficients in the reboiler and condenser are investigated with the same cascade control loop. The results of different heat transfer (area) coefficients in the reboiler are shown in Figure 6. Clearly the bifurcation

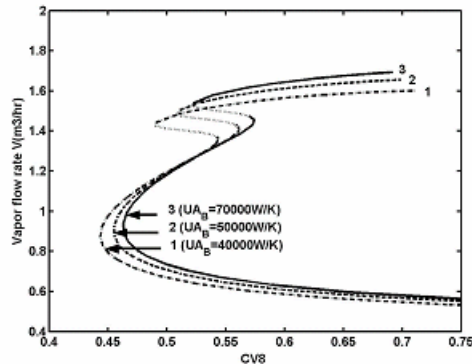


Figure 6: Sensitivity to UA_B with cascade control

curves are somewhat sensitive to the reboiler heat transfer (area) coefficient, whereas it is not sensitive to the condenser heat transfer (area) coefficient (these results are not given in this paper).

Conclusions and Future Work

A bifurcation analysis has been performed on a heat-integrated distillation column. The parameters chosen as primary bifurcation parameter in this investigation are the heat pump control valves and set point of the vapour flow rate. The bifurcation analyses are done with and without control loop implemented to the high pressure on the heat pump side. The results from the bifurcation

analysis furthermore indicate that complex dynamic behaviour occurs in this heat-integrated distillation pilot plant and reveals that a fold bifurcation exists and controller can improve the stability of the system within the feasible operating range. Thus special precautions have to be taken to verify the modelled behaviour before implementing optimising model predictive control on the actual plant. Based on this analysis, a sequence of experiments involving the distillation pilot plant has been planned to validate the model and the plant performance in the region around optimal productivity. Predictive control for optimal operation of the energy integrated distillation pilot plant will be carried out.

References

1. J. Hansen, S.B. Jørgensen, J. Heath and J.D. Perkins, 1998, J. Proc. Contr. 185-195,8
2. M.R. Eden, A. Koggersbøl, L. Hallager and S.B. Jørgensen, 2000, Comp. and Chem.Eng.1091-1097, 24.
3. H. W. Li, R. Gani and S. B. Jørgensen, 2003, Ind. Eng. Chem. Res. 4620-4627, 42.
4. M. Ipsen and I. Schreiber, 2000, Chaos, 791-802, 10(4).
5. B.M. Russel, J.P. Henriksen, S. B. Jørgensen and R. Gani, 2000, Comp. Chem. Eng. 967-973, 24(2).

List of Publication

1. H.W. Li, R. Gani and S.B. Jørgensen, Ind. Eng. Chem. Res. 42 (2003) 4620-4627.



Simone C. van Lith
Address: CHEC, Dept. of Chemical Engineering
Building 229, Office 116
Technical University of Denmark
Phone: (+45) 45 25 28 46
Fax: (+45) 45 88 22 58
e-mail: sl@kt.dtu.dk
www: www.chec.kt.dtu.dk
Supervisors: Peter Glarborg
Flemming J. Frandsen
Peter Arendt Jensen
Ph.D. Study
Started: 1 January 2002
To be completed: December 2004

Release of Inorganic Metal Species, Sulfur and Chlorine during Combustion of Woody Biomass on a Grate

Abstract

The main objective of this Ph.D. project is to improve the understanding of the release of inorganic metal species, S and Cl from the fuel bed during combustion of woody biomass on a grate. This understanding is essential for the development of models for aerosol and fly-ash formation and behavior, aiming to find solutions for the ash-related problems occurring during combustion of woody biomass in power plants. The release of inorganic metal species, S and Cl during combustion of specific woody biomass fuels has been quantified by lab-scale experiments under well-controlled conditions, simulating a grate-fired system. The results obtained so far indicate that the release of the studied elements is strongly dependent on the temperature and the inorganic composition of the fuel.

Introduction

World wide, there is an increasing interest in using biomass as an energy source, due to the important advantages of using biomass fuels compared to fossil fuels: (1) biomass constitutes a renewable resource and (2) the net emission of CO₂ is reduced. However, there are also a number of problems related to biomass combustion. First of all, environmentally harmful gases (e.g. SO₂ and HCl) are emitted during the combustion of biomass. Another important problem is the emission of particulate matter (aerosols and fly-ashes) that is formed during biomass combustion. Inside combustion units, the formation aerosols and fly-ashes causes deposit formation on superheater tubes, which in turn leads to a reduction of the heat transfer efficiency to the water/steam system and corrosion of the superheater tubes. Furthermore, practically all aerosols formed during combustion of biomass are emitted with the flue gas during combustion, which may cause environmental and health problems.

Woody biomass is an attractive fuel, since it is easily available and relatively cheap on most locations. Furthermore, woody biomass fuels generally have a low ash content compared to other biomass fuels, and are therefore thought to be 'less problematic fuels' considering the ash-related problems mentioned above. However, the ash-related problems are also observed in

wood-fired boilers, and especially the aerosol formation during combustion of wood is a serious problem.

Specific Objectives

In order to be able to address the ash-related problems mentioned above, an understanding of the release of inorganic elements from the fuel during combustion is needed. The objectives of this Ph.D. study are to quantify the release of inorganic metal

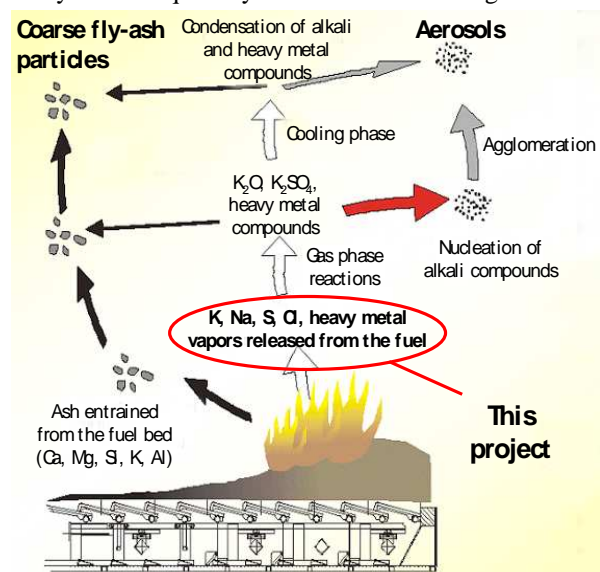


Figure 1: Study area of the Ph.D. project [1].

species, S and Cl during combustion of woody biomass on a grate and to investigate the mechanisms by which the release takes place. Figure 1 indicates the specific study area in relation to aerosol and fly-ash formation.

The quantitative and qualitative release data to be obtained in this study are essential for the modeling of aerosol formation and behavior, and for the subsequent development of solutions for problems involving aerosol and fly-ash formation and emissions of gaseous pollutants during the combustion of woody biomass.

Literature Investigation

Most wood types contain 0.2 to 1.0 wt% ash, which is very low compared to straw (5-10 wt%) and coal (often > 10 wt%). Furthermore, woody biomass generally has a low concentration of potassium, sulfur and chlorine compared to straw and coal. However, the amount of calcium and heavy metals (such as zinc, copper and lead) are relatively high in most woody biomass fuels; especially bark contains a relatively high amount of calcium, and waste wood contains a relatively high amount of heavy metals.

Inorganic matter in biomass can be present in four general forms: (1) easily leachable salts, (2) inorganic elements associated with the organic matter of the biomass, (3) minerals included in the fuel structure, and (4) inorganic material added to the biomass during fuel processing [2]. Information about the association of inorganic elements in biomass fuels can be found in the biochemical literature, but can also be obtained by using advanced fuel characterization techniques, such as Scanning Electron Microscopy (SEM) and Chemical Fractionation (CF).

In the biochemical literature, it was found that the inorganic elements in biomass can be divided into three groups, according to their growth requirement: (1) macronutrients, which have a high growth requirement; (e.g. Ca, K, S, Mg, N, and P), (2) micronutrients, which have a low growth requirement (e.g. Zn, Fe, Mn, Cu, and Cl), and (3) beneficial elements, which stimulate growth, but are not essential (e.g. Na, Si and Al) [3].

The distribution of the inorganic elements in the plant cells and the way in which the elements are bound are related to the function of the elements in the plant [3]. Figure 2 shows an example of the distribution of calcium in plant cells.

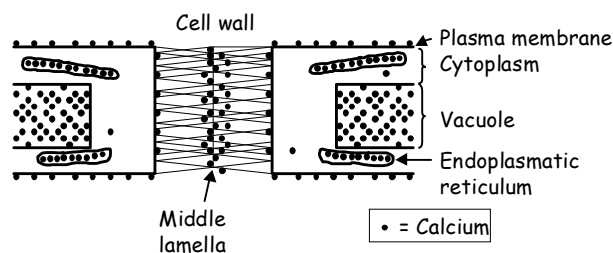


Figure 2: Schematic drawing of two adjacent plant cells, in which the distribution of Ca is indicated [3].

SEM provides visual information about the fuel or char structure and gives information about the structure

and chemistry of inorganic species in the fuel. CF is a technique based on leaching with increasingly acidic solvents, and provides information about the reactivity / association of inorganic elements in the fuel. A combination of the use of both techniques can give valuable information about the association of inorganic elements in biomass, which is important for the understanding of the release mechanisms of inorganic elements from the fuel during combustion.

Some information was found on the release of inorganic elements during wood combustion, but no quantitative data could be found in the literature. Most of the studies reported in the literature were based on the release of alkali metals during pyrolysis and char combustion. The general finding is that potassium is released in two steps. A small amount is released during the pyrolysis phase, at low temperatures (below 500°C), whereas the major part of the release takes place in the high temperature region (above 500°C) during the char combustion and ash cooking phases. It was also observed that in the case of woody biomass combustion, potassium is mainly released as potassium hydroxide (KOH) and potassium sulfate (K₂SO₄), which is due to the low chlorine content of woody biomass fuels.

The results of thermal equilibrium studies reported in the literature give an indication of the species being released during biomass combustion, as a function of temperature. The data suggest that the release of potassium from woody biomass fuels starts around 600°C, the release of sulfur between 750 and 900°C, and the release of chlorine around 500°C. Furthermore, it is predicted that the total amount of potassium present in the fuel will be released at 1050°C, whereas all of the chlorine will already be released around 650°C.

Experimental Equipment and Procedure

The main part of the experimental work is focused on the quantification of the release of inorganic metal species, sulfur and chlorine during wood combustion. The first challenge was to design an experimental set-up and develop an appropriate method for performing lab-scale combustion experiments that would provide accurate and reproducible release data. An experimental set-up has been built up (see Figure 3), consisting of an electrically heated oven (max. 1200°C) with an alumina tube inside, in which a fuel sample (max. 45 g) can be inserted and a gas (max. 10 Nl/min) can be introduced in order to provide a pyrolysis or combustion atmosphere around the fuel sample. A gas conditioning system and gas analyzers make it possible to measure the contents of O₂, CO and CO₂ in the flue gas in order to monitor the pyrolysis and combustion behavior and to determine if the fuel sample is completely combusted and the remaining ash residue can be assumed to contain inorganic elements only. The release is quantified by performing accurate weight measurements and chemical analysis of the fuel samples and ash residues, and performing mass balance calculations.

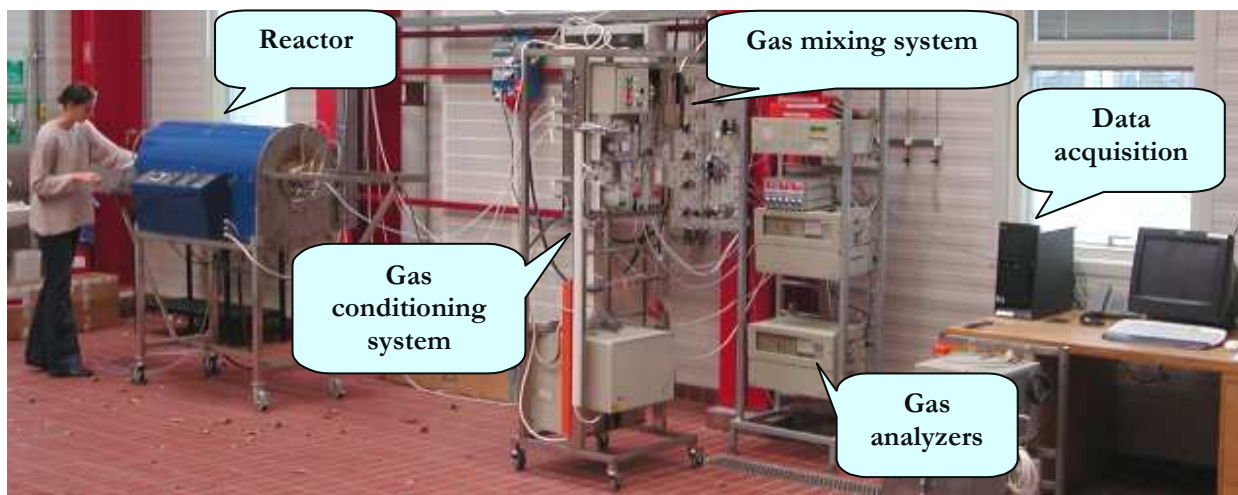


Figure 3: Experimental set-up for studying the release of inorganic elements from a burning wood sample.

Various experimental methods have been tested and compared in order to find the most appropriate method for obtaining accurate quantitative release data.

Table 1: Chemical characteristics of the woody biomass fuels to be investigated.

Fuel type	Ash content (wt% d.b.)	Chemical characteristics
Spruce	~ 1	Very low concentrations of Cl and S; low concentration of metals.
Beech	~ 0.5	Very low concentrations of Cl, and S; low concentration of metals; very low concentration of Si.
Bark 1	~ 4	High concentration of K; very high concentration of Ca.
Bark 2	~ 10	Very high concentrations of Si, Al, and Fe.
Waste wood	~ 3	High concentrations of Cl and S; very high concentrations of heavy metals.
Fibreboard	~ 1	Very high concentration of Ti; low concentration of K.
Fibreboard coated	~ 1	Very high concentration of Ti, but lower than fibreboard.

Fuel Characterization

The woody biomass fuels to be investigated in this study consist of both untreated fuels (spruce, beech and two types of bark) and treated fuels (waste wood and two types of fibreboard). Each fuel type has a characteristic ash content and inorganic composition, as summarized in Table 1. This means that the influence of ash content and inorganic composition on the release of inorganic elements during combustion can be investigated by using the different fuels in the lab-scale experiments.

Besides the chemical composition, the various woody biomass fuels also differ in structure. Samples of the different fuel types have been studied using SEM. This study showed the differences in structure between the fuel types and the occurrence of mineral particles both inside and outside the fuel structure. Especially the bark contains large amounts of calcium-rich minerals inside the fuel structure (see Figure 4). These observations are important for the understanding of the association of inorganic elements in biomass and the release during combustion.

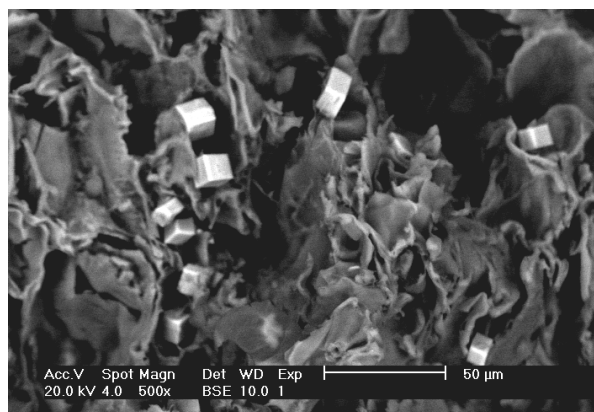


Figure 4: SEM picture of bark, showing calcium-rich crystals (white cubes) inside the fuel structure.

Information about the association of the inorganic elements in some of the fuels is available from CF analysis and can be compared to the experimental release data.

Experimental Results and Discussion

The release of inorganic elements during combustion of spruce and fibreboard has been investigated in the temperature range 500-1150°C. The original contents of Cl, S and K in these two fuels are shown in Figure 5 to compare with the release trends for these elements as a function of temperature for the range 500-850°C presented in Figure 6. In this temperature range, a very high release of Cl (~100%) and S (~75%) and a low release of K (up to ~30%) were

observed for spruce (see Figure 6). The release of other metal species was also investigated and indicated a high release of Cd (~100%), and a low release of Mg (up to ~15%), and Cu (up to ~25%), starting at ~500-550°C. For Zn and Pb, the release increased from ~0 to ~100%, whereas for Si, Al and Ca no release was observed. Similar release trends were observed for fibreboard, although the release of S and K was lower in this case.

When comparing Figure 5 and 6, it is seen that the release of inorganic elements from the fuel during

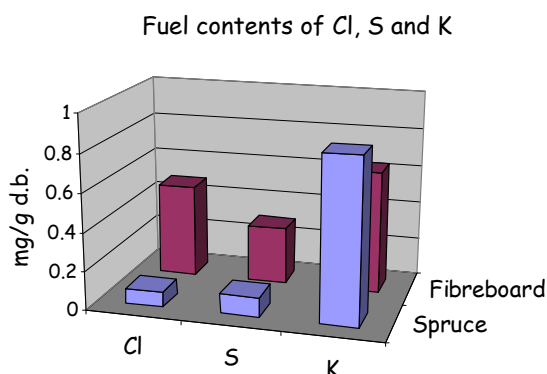


Figure 5: Contents of Cl, S and K in spruce and fibreboard.

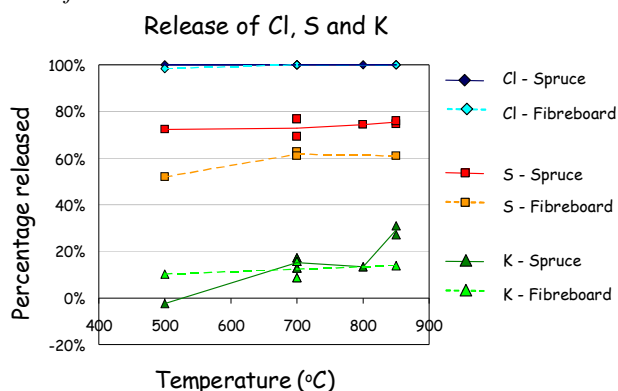


Figure 6: Release of Cl, S and K from spruce and fibreboard as a function of temperature.

combustion cannot be explained by looking at the quantities of these elements in the fuel only; the presence of other inorganic elements in the fuel have an influence on the volatility of certain elements as well. For example, in the case of fibreboard, the high content of titanium present in the fuel from the pigments in the coating may have an influence on the release of other elements. This will be studied in more detail.

Conclusions

Unless the lack of quantitative data on the release of inorganic elements during wood combustion in the literature, important information was found on the distribution, function and association of inorganic elements in plants. This information is valuable for the interpretation of the release data in terms of the possible

mechanisms by which the elements are released from the fuel during combustion.

The main objective for this Ph.D. study is to quantify and understand the release of inorganic metal species, S and Cl during combustion of woody biomass on a grate. An experimental set-up has been built up to investigate the release under well-controlled conditions and the results indicate that the experimental method is suitable to obtain an accurate quantification of the release during the combustion of various types of woody biomass fuels. The release was found to be strongly dependent on the temperature and on the fuel composition.

Future Work

In the remaining part of the project, the experimental work will be extended to obtain quantitative release data of the other woody biomass fuels available and to investigate the influence of other parameters (such as particle size, residence time, etc.). Furthermore, the fuels, as well as the ashes obtained after the combustion experiments at different temperatures will be physically and chemically characterized in detail. This will provide information on the association of the inorganic elements in the fuel and the speciation in the ash, which will give a better understanding of the release mechanisms. A specific thermodynamic equilibrium study of the various woody biomass fuels is also planned, in order to provide insight into the inorganic transformations taking place during combustion.

The ultimate aim is to develop a model for the release of inorganic metal species, S and Cl during combustion of woody biomass on a grate.

Acknowledgements

This Ph.D. project is funded by the Danish Technical Research Council (STVF). Weigang Lin, Jacob Knudsen, Jørn Hansen, Thomas Wolfe and the people from the KT workshop are acknowledged for their help with the build-up of the experimental set-up and technical support. Violeta Alonso Ramírez is acknowledged for her contribution to the experimental work.

References

1. I. Obernberger, T. Brunner and M. Jöller, Characterisation and Formation of Aerosols and Fly-ashes from Biomass Combustion, Report EU Project 'Aerosols from Biomass Combustion', 2001.
2. M. Zevenhoven-Onderwater, Ash-forming Matter in Biomass Fuels, Ph.D. dissertation Åbo Akademi, Finland, 2001, p. 88.
3. H. Marschner, Mineral Nutrition of Higher Plants, Second Edition, Academic Press, London, U.K., 2002, p. 889.



Oleg Medvedev
Address: IVC-SEP, Dept. of Chemical Engineering
Building 229, Office 260
Technical University of Denmark
Phone: (+45) 45 25 28 89
Fax: (+45) 45 88 22 58
e-mail: om@kt.dtu.dk
www: www.ivc-sep.kt.dtu.dk
Supervisor(s): Alexander Shapiro

Ph.D. Study
Started: 1 November 2001
To be completed: October 2004

Transport Properties in Free Space and in Porous Media

Abstract

The main task of the Ph.D. study is to improve the existing models and/or to create a new model for the diffusion coefficients for the multicomponent mixtures. Study of the transport properties in multicomponent liquid mixtures and high-pressure gases is an important and challenging scientific problem. It has special importance for petroleum engineering, for study of the geological-scale migration processes and distributions of hydrocarbon mixtures in porous rock of petroleum reservoirs.

Introduction

Multicomponent diffusion is the governing mechanism in many natural phenomena, as well as in industrial processes, like those of chemical and petroleum engineering. Diffusion in an n -component mixture is determined by $n(n-1)/2$ independent coefficients, by the number of interactions between individual fluxes of different components. While the theory of diffusion is well developed, the values of the diffusion coefficients in realistic multicomponent mixtures remain a problem.

Only several models for the diffusion coefficients of multicomponent mixtures may be found in the literature. The experimental data on multicomponent diffusion is scarce, since the corresponding experiments are difficult to perform. Only few reports with the values of the diffusion coefficients in ternary mixtures are available and to the best of our knowledge, there is no available experimental data on diffusion coefficients for systems with more than three components.

The experimental data on ternary diffusion is normally reported on the four independent Fickian diffusion coefficients. However, most of the models operate with different systems of thermodynamic variables, where the number of independent transport coefficients is reduced due to the Onsager reciprocal relations. For the ternary mixture this gives three independent transport coefficients.

Transformation from Fickian to Onsager coefficients requires knowledge of the thermodynamic functions (the derivatives of chemical potentials with regard to molar fractions). These functions may be evaluated on the basis of the certain thermodynamic model: the

equation of state or the activity coefficient model. The fact that the number of independent coefficients is reduced during such a transformation makes it possible to verify the consistency and the accuracy of the experimental data, as well as the applicability of the existing thermodynamic models to modeling the transport properties.

The idea behind the first part of the study is to apply Onsager reciprocal relations to verification of available experimental data on diffusion coefficients and thermodynamic models for multicomponent mixtures.

After verification of the experimental data and thermodynamic models, the modeling part follows. The modeling part provides the rigorous physical framework for future modeling. Such a framework is constructed by means of the theory of fluctuations around an equilibrium state, described both by the methods of the statistical mechanics and by the theory of Markov processes.

It was proved that the rate of diffusion in the mixture may be described in terms of three factors: 1) *The thermodynamic factor*, determined by the structure of the mixture and "the system of thermodynamic coordinates", in which diffusion is expressed, 2) *the kinetic factor*, or the rate of the molecular motion, and 3) *the resistance factor*, determined by the fact that other molecules may serve the obstacles on the way of a given molecule. These factors are differently expressed and combined in different models for diffusion coefficients.

Besides modeling of diffusion coefficients the study of the transport mechanisms inside the porous media is performed. The stochastic and averaged models for the

process of particle suspension flow in the porous media are created. This work is performed in cooperation with Prof. Pavel Bedrikovetski from UENF, Brazil. The process of filtration of the particle suspension in the porous media is of great interest for petroleum industry, mainly with regard to offshore waterflooding and permeability damage.

Specific Objectives

Consistency Check

Modeling of the diffusion coefficients in the multicomponent mixtures requires knowledge of volumetric and caloric thermodynamic functions. Thus specific thermodynamic models are required. Also the experimental data should be validated with regard to its consistency for future modeling and fitting.

That can be done in the framework of the Onsager reciprocal relations. The experimental data on the diffusion is mainly presented in the terms of Fick diffusivities:

$$\mathbf{J} = \mathbf{D}\nabla\mathbf{C} \quad (1)$$

where \mathbf{J} denotes the $(n-1)$ vector of diffusive molar fluxes of the species, \mathbf{D} is the $(n-1) \times (n-1)$ matrix of Fick diffusion coefficients and \mathbf{C} is the vector of molar densities. The Fick diffusion coefficients are normally measured and reported in the literature. It should be mentioned that the Fick diffusion matrix \mathbf{D} is not necessarily symmetric:

$$D_{ij} \neq D_{ji} \quad (2)$$

With the help of the formalism of non-equilibrium thermodynamics it is possible to express the entropy production in the different sets of thermodynamic coordinates and by that to recalculate the Fick matrix of diffusion coefficients into the Onsager diffusion coefficients (intermediate derivations skipped):

$$\mathbf{D} = \frac{1}{z_n T} \mathbf{A}_{\mathbf{U}} \mathbf{L} \frac{\partial \boldsymbol{\mu}}{\partial \mathbf{c}} = \frac{1}{z_n n T} \mathbf{A}_{\mathbf{U}} \mathbf{L} \frac{\partial \boldsymbol{\mu}}{\partial \mathbf{z}} \quad (3)$$

where the transformation matrix is:

$$\mathbf{A}_{\mathbf{U}} = \frac{1}{z_n} \begin{bmatrix} 1-z_1 & -z_1 & \dots & -z_1 \\ -z_2 & 1-z_2 & \dots & -z_2 \\ \vdots & \vdots & \ddots & \vdots \\ -z_{n-1} & -z_{n-1} & \dots & 1-z_{n-1} \end{bmatrix} \quad (4)$$

and \mathbf{L} is $(n-1) \times (n-1)$ symmetrical matrix of the Onsager coefficients, $\boldsymbol{\mu}$ is vector of components chemical potential and \mathbf{z} is vector of the molar amounts.

Solving system of linear equation (3) provides connection between Fick matrix and Onsager matrix. Since Onsager matrix is symmetrical the procedure can verify the consistency of the experimental data and thermodynamic models, used for calculation of the chemical potential [1].

Modeling Framework

The modeling of the diffusion coefficients in the multicomponent mixtures requires rigorous theoretical

background, since there is no available experimental data for multicomponent mixtures to build empirical models. We should be sure about theoretical basis and extrapolational abilities of the model in order to apply it for multicomponent mixtures.

The theoretically rigorous framework for transport coefficients was proposed by Alexander Shapiro [2]. It was shown that the matrix of the diffusion coefficient can be estimated in terms of the so called *transfer* matrix:

$$\mathbf{L}_{Tr} = \mathbf{L}_K \mathbf{L}_R \mathbf{L}_T \quad (5)$$

In the last equation $\mathbf{L}_K (n \times n)$ is the *kinetic* matrix:

$$\mathbf{L}_{K,ij} = \delta_{ij} C_j, C_j = \left(\frac{8RT}{\pi M_j} \right)^{1/2}, (i, j = 1 \dots n) \quad (6)$$

The *thermodynamic* matrix $\mathbf{L}_T, (n+1) \times n$ is expressed in the terms of the following thermodynamic values:

$$F_{ij} = \frac{\partial^2 S}{\partial N_i \partial N_j}, F_{n+1, n+1} = \frac{\partial^2 S}{\partial U^2}, \quad (7)$$

$$F_{i, n+1} = F_{n+1, i} = \frac{\partial^2 S}{\partial N_i \partial U}.$$

The *thermodynamic* matrix is negative minor of the inversed matrix:

$$\mathbf{L}_{T,ij} = -f_{ij}, \mathbf{f} = \mathbf{F}^{-1} \quad (8)$$

The *resistance* matrix is expressed in the terms of *penetration lengths* $Z_i(\mathbf{N}, U), i = 1 \dots n$. The *penetration length* is the newly introduced property. That is the characteristics of the molecular motion and it means the length after which the molecule of component “forgets” its initial velocity:

$$L_{R,ij} = \delta_{ij} Z_i(\mathbf{N}, U) - N_i \frac{\partial Z_i(\mathbf{N}, U)}{\partial N_j} \quad (9)$$

$$L_{R,i, n+1} = -N_i \frac{\partial Z_i(\mathbf{N}, U)}{\partial U}$$

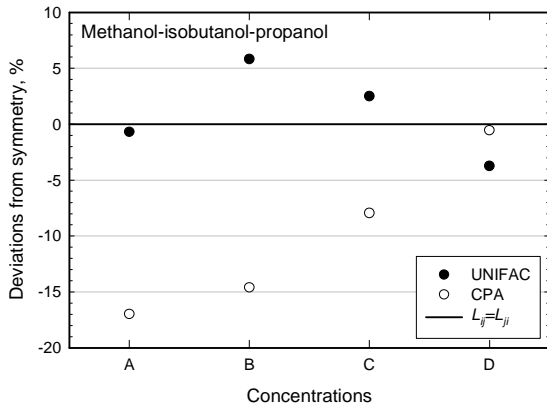
Thus the problem of estimation the matrix of diffusion coefficients for the multicomponent mixture reduces to the problem of estimation the vector of the penetration lengths $Z_i(\mathbf{N}, U)$. The penetration length either can be determined by means of the molecular dynamics simulation, as value connected to the velocity time correlation function, either by some kinetic considerations. As a first step we get the penetration lengths by fitting of the experimental data on binary diffusion. And analyze them for future modeling.

After estimation of the transfer matrix the matrix of diffusion coefficients can be derived in the following way:

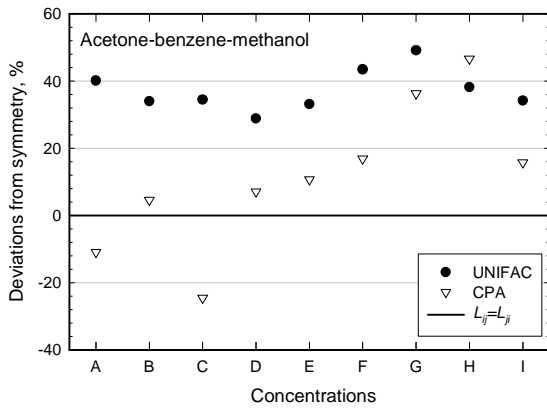
$$\mathbf{L}_D = \mathbf{G} \bar{\mathbf{L}}_{Tr} \mathbf{G}^T, \bar{\mathbf{L}}_{Tr} = \frac{1}{2} (\mathbf{L}_{Tr} + \mathbf{L}_{Tr}^T) \quad (10)$$

The matrix \mathbf{G} transfers the matrix of diffusion coefficients from the diffusion-convective system of coordinates to Maxwell Stefan system and vice versa.

Thus, the fitting of the diffusion coefficients requires knowledge of the thermodynamic properties for the determination of the *thermodynamic* matrix. The majority of existing thermodynamic models is optimized and developed for calculation of phase equilibria properties. Thus the estimation of the caloric properties requires also some empirical dependencies for caloric properties of the pure components. The method of estimation of the thermodynamic matrix was proposed and used for fitting diffusion coefficients of selected binary mixtures. Some of the results of modeling the binary mixtures are presented in Results section.



Concentrations: A - (0.2941; 0.3533); B - (0.1487; 0.1493); C - (0.1478; 0.7016); D - (0.6995; 0.1504)



Concentrations: A - (0.350; 0.302); B - (0.766; 0.114); C - (0.553; 0.193); D - (0.400; 0.500); E - (0.299; 0.150); F - (0.206; 0.548); G - (0.102; 0.795); H - (0.120; 0.132); I - (0.150; 0.298)

Figure 1: Deviations from the Onsager reciprocal relations for the systems containing associating fluids. Experimental data from [8,9].

Suspension Flow in the Porous Media

During the external Ph.D. stay in the group of Professor Pavel Bedrikovetski (UENF, Brazil) the model for Deep Bed Filtration was developed. Deep Bed Filtration – is the process of particle suspension filtration in the porous media [3]. It is of particular interest for petroleum industry, since of offshore oil production. During injection of the sea water the

particles, suspended in the water can plug the pores and reduce the permeability and porosity of the porous media. The permeability damage and porosity reduction can highly affect water injection and oil production. Also, description of the suspension flow in the porous media can be of great interest for membrane technologies and for bioscience.

Here we investigate the particle suspension flow in the porous media with particles, captured by the pores by some adhesive forces. Thus, the problem can be described on the stochastic level by considering the probabilities of the particle to be plugged by pore. That is the extension of the newly developed stochastic approach for Deep Bed Filtration [4].

The stochastic system of equation describes flow of the particles suspension, accounting for plugging rate and porosity change. Also, the equation for the pore plugging kinetics on stochastic level was derived. The process of the plugging of the pore is described by Markov chain and resulted equation is similar by its type to Boltzmann equation of fluid kinetics.

Before deriving the system of the model equations, let us introduce the key variables. We distinguish the two concentrations of the particles of the size r_s :

$C(r_s, x, t)$ - the suspended concentration;

$\Sigma(r_s, x, t)$ - the deposited concentration.

Also we introduce the amount of the free pores of some specific size r_p : $H(r_p, x, t)$.

After deriving of the stochastic system of equations we are interested in deriving the averaged model system in the terms of the averaged values, which is of the practical interest for the industrial applications:

$$\begin{aligned} c(x, t) &= \int_0^{\infty} C(r_s, x, t) dr_s \\ \sigma(x, t) &= \int_0^{\infty} \Sigma(r_s, x, t) dr_s \\ h(x, t) &= \int_0^{\infty} H(r_p, x, t) dr_p \end{aligned} \quad (11)$$

Also, we are interested in deriving equations for porosity and permeability change due to the process of plugging.

Results and Discussions

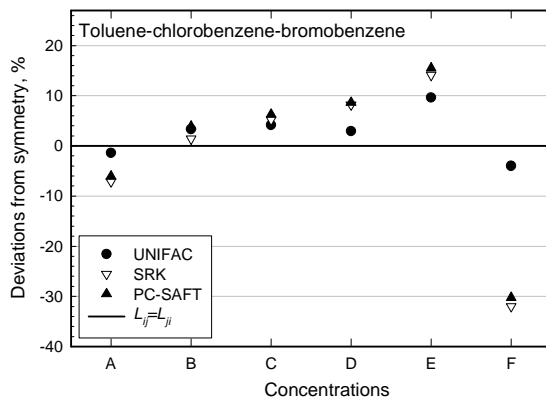
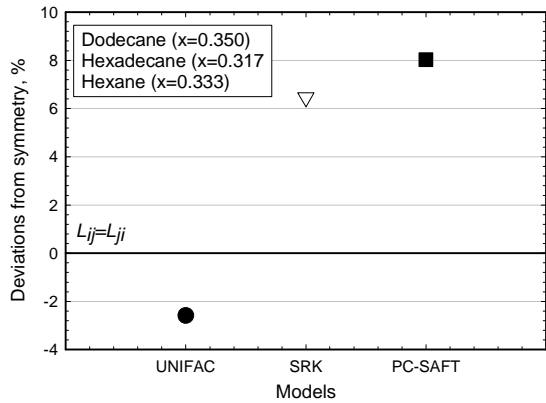
In that section some up-to-date results are presented and discussed. Also we discuss the possible subjects and points for further investigation.

Consistency Check

In that section we present the results of the consistency check of the experimental data on the diffusion coefficients and thermodynamic models. The more extended results can be found in [1].

The thermodynamic models used in the consistency check are: UNIFAC [5], SRK, CPA[6] and PC-SAFT[7].

And below are some results, obtained using three thermodynamic models.



Concentrations: A - (0.250; 0.500); B - (0.260; 0.030);
C - (0.700; 0.150); D - (0.150; 0.700); E - (0.450;
0.250); F - (0.180; 0.280)

Figure 2: Deviations from the Onsager reciprocal relations for the systems modeled by the three thermodynamic models. Experimental data from [10,11].

The experimental Fick diffusion coefficients were recalculated to the Onsager diffusion coefficients, using eq.(3). The deviations between diagonal Onsager diffusion coefficients were analyzed. Below deviations from symmetry are plotted for selected mixtures and some thermodynamic models.

So, we have shown that checking the symmetry of Onsager coefficients is necessary and nontrivial. Of the data tested, the most problematic system is that of acetone-benzene-methanol. This system exhibits high non-ideality, and the abnormally high cross-diffusion coefficients are reported for it. Both thermodynamic models applied to this system produce high and rather different deviations from symmetry. The nature of these deviations may require further analysis.

Apart from this system, all the models considered behave rather similarly, UNIFAC being slightly (but uniformly) better. An important fact is that the models are either consistent or fail simultaneously on the same points. This shows that verification of the symmetry is a

good method for checking the consistency of the experimental data on ternary diffusion.

It should be noted that most of the thermodynamic models have been designed for and fitted to the problems of phase equilibria. However, verification of the symmetry requires such “exotic” properties as derivatives of chemical potentials. Our analysis probably indicates that the existing thermodynamic models (especially UNIFAC) are well adjusted to calculation of these properties also. However, further work on improvement of the existing thermodynamic models is required for more reliable prediction of the partial molar properties, in connection with the transport-related problems.

Diffusion Modeling Framework

As it was shown before the problem of modeling diffusion coefficients is reduced to the problem of estimation the *thermodynamic* matrix and *resistance* matrix. Our current goal is to estimate the *resistance* matrix from diffusion data on binary mixtures.

It can be shown from thermodynamic transformations that thermodynamic matrix can be determined as (here expressions are for binary mixture):

$$\mathbf{L}_{T,ij} = -f_{ij}, \mathbf{f} = \mathbf{F}^{-1}$$

where

$$F_{ij} = - \left. \frac{\partial(\mu^j/T)}{\partial N_i} \right|_{U,V,N} = - \frac{1}{T} \left. \frac{\partial \mu^j}{\partial N_i} \right|_{U,V,N} + \frac{\mu^j}{T^2} \left. \frac{\partial T}{\partial N_i} \right|_{U,V,N};$$

$$F_{i,n+1} = F_{n+1,i} = \left. \frac{\partial(1/T)}{\partial U} \right|_{U,V,N} = - \frac{1}{T^2} \left. \frac{\partial T}{\partial N_i} \right|_{U,V,N};$$

$$F_{n+1,n+1} = \left. \frac{\partial(1/T)}{\partial U} \right|_{U,V,N} = - \frac{1}{T^2} \left. \frac{\partial T}{\partial U} \right|_{U,V,N}.$$

Since we are using thermodynamic models, such as cubic EoS or PC-SAFT we have normally (T,P,\mathbf{N}) as a set independent variables. We use the following equations to calculate required values, using our set of independent variables:

$$\left. \frac{\partial T}{\partial U} \right|_{U,V,N} = \left[\left. \frac{\partial U}{\partial T} \right|_{T,V,N} \right]^{-1} \quad (12)$$

$$\left. \frac{\partial T}{\partial N_i} \right|_{U,V,N} = - \frac{\left. \frac{\partial U}{\partial N_i} \right|_{T,V,N}}{\left. \frac{\partial U}{\partial T} \right|_{T,V,N}} \quad (13)$$

and the following for chemical potential:

$$\left. \frac{\partial \mu^j}{\partial N_i} \right|_{U,V,N} = \left. \frac{\partial \mu^j}{\partial N_i} \right|_{P,T,N} -$$

$$\left. \frac{\partial \mu^j}{\partial T} \right|_{P,T,N} \frac{\left. \frac{\partial U}{\partial N_i} \right|_{T,V,N}}{\left. \frac{\partial U}{\partial T} \right|_{T,V,N}} -$$

$$\left. \frac{\partial \mu^j}{\partial P} \right|_{P,T,N} \left(\left. \frac{\partial P}{\partial N_i} \right|_{T,V,N} - \left. \frac{\partial P}{\partial T} \right|_{T,V,N} \frac{\left. \frac{\partial U}{\partial N_i} \right|_{T,V,N}}{\left. \frac{\partial U}{\partial T} \right|_{T,V,N}} \right)$$

Now we need the expression for the internal energy and chemical potential in the coordinates (T,V,\mathbf{N}) . We

define these properties in the set (T, P, \mathbf{N}) and transfer them to desired coordinates by numerical solving of the EoS $V = V(P, T, \mathbf{N})$.

The internal energy defined in the following way:

$$U = U^{id} + U^{res}$$

The ideal part is:

$$U^{id} = \sum N_i h_0^i(T) - NRT$$

$$h_0^k(T) = H^0 + \Delta h_f^k(298.2K) + \int_{298.2}^T C_p^k(T) dT$$

The residual part is:

$$U^{res} = -RT^2 \left[\sum N_i \frac{\partial \ln \phi^i(T, P, \mathbf{N})}{\partial T} + N \left(\frac{\partial z(T, P, \mathbf{N}) / \partial T}{Z} - \frac{\partial z(T, P, \mathbf{N})}{\partial T} \right) \right]$$

where z is the compressibility.

And the chemical potential defined as:

$$\mu^k = RT \ln \phi^k + RT \ln(z^k P / P_0) + h_0^k(T) - Ts_0^k(T)$$

$$s_0^k(T) = S^0 + \Delta s_f^k(298.2K) + \int_{298.2}^T \frac{C_p^k(T)}{T} dT$$

Thus, we can determine *thermodynamic* matrix, using some thermodynamic models, as cubic EoS, PC-SAFT or some modifications of cubic EoS, such as CPA. Also we need some caloric information about the components, which is available in some databases, for instance in DIPPR database [12].

Determination of the resistance matrix requires knowledge of the penetration lengths $-Z(U, V, \mathbf{N})$. The simplest expression for the penetration length comes from simple linear Vignes rules for diffusion in binary mixture:

$$Z_i = \sqrt{\frac{M_i}{M_{12}}} Z, Z = A \exp(-v_1 N_1 - v_2 N_2) \quad (14)$$

Thus, we fit binary diffusion coefficient for obtain coefficients of the penetration lengths. Below you can see some results for selected mixtures. The thermodynamic model used was SRK with MHV1 (UNIFAC VLE) mixing rules.

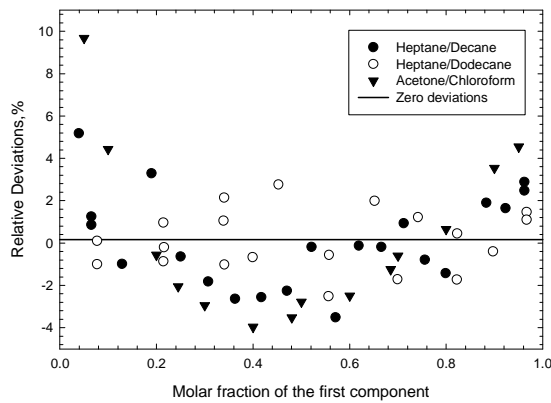


Figure 3: The deviations of the experimental data from the model for three binary mixtures. Experimental data from [13,14]

As you can see the deviations are rather low for the ideal mixtures (heptane/decane and heptane/dodecane) and slightly higher for acetone/chloroform mixture. That is because the used dependence for penetration length reproduces Vignes mixing rules, which are consistent only for ideal behaviour. However, the introduction of more advanced expression, for instance expression including cross-component interactions performs better for non-ideal systems. The further research is currently going on this subject. The coefficients of eq.(14), obtained from the fitting of the experimental data [13,14] are:

- for hexane/decane:

$$A = 2.11 \cdot 10^{-9}, v_1 = 2.82 \cdot 10^{-3}, v_2 = 4.43 \cdot 10^{-3}$$

- for hexane/dodecane:

$$A = 1.17 \cdot 10^{-9}, v_1 = 1.75 \cdot 10^{-3}, v_2 = 6.30 \cdot 10^{-3}$$

- for acetone/chloroform:

$$A = 3.89 \cdot 10^{-9}, v_1 = 2.20 \cdot 10^{-3}, v_2 = 2.27 \cdot 10^{-3}$$

The future work is to analyze the behavior of the penetration lengths for large scale of the binary mixture and establish the influence of the molecular structure on the values. Also, molecular dynamics simulations are planned to be used in order to get penetration lengths and compare them with the one, obtained from fitting.

Suspension Flow in the Porous Media

In this section we discuss the model of the Deep Bed Filtration. The formalism used here was developed in the works of the authors [4].

We aim in extension of the stochastic approach in investigation of the Deep Bed Filtration process. Here we describe the filtration of the particles in the porous media. The particles can be plugged by the porous media. The mechanism of the plugging is adhesive forces.

We developed the system of the stochastic model equations. The system contains three partial differential equations (PDE). The first equation describes the process of the flow and is nothing else like the particle conservation law in the porous volume. The second equation is the equation for the deposition rate. And the last equation is for the pore plugging kinetics. We do not present here the stochastic system for a matter of simplicity of the presentation.

However, in industrial applications, it is important to know the measurable averaged values, rather than some concentrations for specific pore or particle size. That's why the averaged model was deduced. Skipping intermediate derivations the final averaged system is the following:

$$\begin{aligned} \frac{\partial}{\partial t} \phi c(x, t) + \frac{\partial}{\partial x} U c(x, t) (1 - \alpha) &= -\frac{\partial}{\partial t} \sigma(x, t) \\ \frac{\partial}{\partial t} \sigma(x, t) &= \alpha l U c(x, t) \\ \frac{\partial}{\partial t} h(x, t) &= 0 \end{aligned} \quad (15)$$

The averaging procedure was performed rigorously; the only left stochastic value was presented as a “velocity reduction factor”:

$$\alpha = \frac{\int_0^{\infty} dr_s \int_0^{\infty} dr_p \left\{ \lambda(r_s, r_p) u_1(r_p) C(r_s, x, t) H(r_p, x, t) \right\}}{Uc(x, t)}$$

where we have:

$\lambda(r_s, r_p)$ - probability of particle to be plugged;

$u_1(r_p)$ - flow velocity through one pore.

The effect of incomplete plugging results in the last equation (15). The total amount of the pores remains unchanged, since pores don't disappear completely, just reduce their size.

The numerical solving of the system (15) allows get the distribution of the concentration and deposition in the porous media.

We are also interested in the equations for the permeability and porosity change. Such equations can be derived on the basis of the stochastic model. Unfortunately they cannot be averaged in the rigorous way due to high complicity. That's why we assumed that probability of particle to be plugged is the constant. After some simplifications and considerations we get the following system for practical applications (intermediate derivations are skipped):

$$\begin{aligned} \frac{\partial \phi(x, t)}{\partial t} &= -\beta_\phi c(x, t) U(x, t) \frac{k(x, t)}{\phi(x, t)} \\ \frac{\partial k(x, t)}{\partial t} &= -\beta_U U(x, t) c(x, t) \frac{k^2(x, t)}{\phi^2(x, t)} \end{aligned} \quad (16)$$

where we have two empirical coefficient, which came from procedure of averaging - β_U, β_ϕ .

The analytical solution of the system gives the following relations between permeability and porosity:

$$\frac{k(x, t)}{k_0(x)} = \left(\frac{\phi(x, t)}{\phi_0(x)} \right)^{\frac{\beta_U}{\beta_\phi}} \quad (17)$$

Here we have initial distributions at ($t = 0$):

$$k_0(x), \phi_0(x)$$

The sample numerical solution of the system (15), accounting for equations (16) and (17) is going to be performed in order to verify model system and to produce some recommendations for industrial applications.

References

1. O. Medvedev, A. Shapiro, Fluid Phase Equilibria, 208 (2003) 291-301.
2. A. Shapiro, Physica A 320 (2003) 211-234.
3. T. Iwasaki, J. Am. Water Works Ass., (1937) 1591-1602.
4. A. Santos, P. Bedrikovetsky, Transport in Porous Media (2003) (in press)
5. B.E. Poling, J.M. Prausnitz, J. O'Connell, *The Properties of Gases and Liquids*, McGraw-Hill Higher Education, Fifth Edition, New York, 2000.

6. I.V. Yakoumis, G.M. Kontogeorgis, E.C. Voutsas, D.P. Tassios, Fluid Phase Equilibria 130 (1997) 31
7. J. Gross, G. Sadowski, Ind. Eng. Chem. Res 40 (2001) 1244
8. F.O. Shuck and H.L. Toor, Chem. Eng. Sci., 67 (1963) 540-545
9. A. Alimadadian and P.C. Colver, Canadian J. Chem. Eng., 54 (1976) 208-213
10. J.K. Burchard and H.L. Toor, Chem. Eng. Sci., 66 (1962) 2015-2022
11. T.K. Kett and D.K. Anderson, J. Phys. Chem., 73 (1969) 1268-1274
12. R.P. Danner and M.S. High, Polymer Solution Handbook, Design Institute for Physical Property Data, American Institute of Chemical Engineers, 1992
13. H.Y. Lo, J. Chem. and Eng. Data, 19 (1974) 236
14. M.T. Tyn, W.F. Calus, J. Chem. and Eng. Data, 20, (1975) 310

List of Publications

1. Alexander A. Shapiro, Oleg O. Medvedev and Mariana G. Bagnoli, The conference proceedings of the International conference on the occasion of Lars Onsager's 100th birthday: "Transport, dissipation, and turbulence", Trondheim, Norway, June 1-5, 2003
2. M.G. Bagnoli, O.O. Medvedev and A.A. Shapiro, The conference proceedings of the 15th Symposium on Thermophysical Properties, Boulder, CO, USA, 2003
3. O. Medvedev, A. Shapiro, Fluid Phase Equilibria, 208 (2003) 291-301.
4. O. Medvedev, P. Zhelezny, V. Zhelezny, Fluid Phase Equilibria (2003) (in press).
5. O. Medvedev, A. Shapiro, The conference proceedings of the 19th European Conference on Applied Thermodynamics, Santorini Island, Greece, 2002
6. O. Medvedev, P.V. Zhelezny and V.P. Zhelezny, The conference proceedings of the 15th European Conference on Thermophysical Properties, London, UK, 2002
7. A.V. Chupakova, O.O. Medvedev and V.N. Buz, The paper was presented on the XIIIth School-seminar on Heat Exchange, St. Petersburg, Russia, 2001 (in Russian)
8. V.P. Zhelezny, E.G. Bisko and O.O. Medvedev, High Temperatures-High Pressures, 33 (2001) 685-692
9. V.P. Zhelezny, A. Yokozeki, P.V. Zhelezny, and O.O. Medvedev, The conference proceedings of the 14th Symposium on Thermophysical Properties, Boulder, CO, USA, 2000.
10. V.P. Zhelezny, A. Yokozeki, O.O. Medvedev, and M.V. Rybnikov, The conference proceedings of the 14th Symposium on Thermophysical Properties, Boulder, CO, USA, 2000.



Address:

Daniel Merino-García

IVC-SEP, Dept. of Chemical Engineering
Building 229, Office 250
Technical University of Denmark

Phone:

(+45) 45 25 29 70

Fax:

(+45) 45 88 22 58

e-mail:

dmg@kt.dtu.dk

www:

www.ivc-sep.kt.dtu.dk

Supervisor(s):

Simon I. Andersen

Ph.D. Study

Started:

February 2001

To be completed:

February 2004

Calorimetric Investigations of Asphaltene Self-Association and Interaction with Resins

Abstract

Asphaltenes are a complex fraction of crude oil known to cause severe problems in the extraction and refining of petroleum. Asphaltene research has been carried out for more than 60 years. Still, many fundamental questions are a matter of debate, such as the main mechanism of self-association and the average molecular weight of the fraction. This study is an attempt to shed some light on the aggregation behavior of asphaltenes in toluene, and the characterization of the interaction with another petroleum fraction, the resins. Resins are believed to act as natural inhibitors for asphaltene precipitation. The objective was to establish a procedure to apply Isothermal Titration Calorimetry to obtain experimental values of some of the parameters that are used to model and predict asphaltene behavior.

Introduction

Recovery and refinery processes face constant difficulties due to heavy fractions, namely well bore and pipeline plugging, de-stabilization in the mixing of crude oils, coke formation, and poisoning of catalysts [1,2]. Sometimes the damage is so severe that leads to the closing of the production [3]. Most of these problems are related to asphaltenes, waxes or mixtures of these fractions. This investigation has focused only on asphaltenes. They are defined as the fraction of crude that precipitates after the addition of an n-alkane (usually heptane) and that is soluble in an aromatic solvent (toluene). This loose definition allows the presence of very different molecules in terms of molecular weight and associating capacity. The number of different compounds inside the asphaltene fraction is estimated to be over 100,000. The amount of asphaltenes in crude oil varies in a wide range, from 0.1 to 17 wt% [1]. The fraction is highly aromatic: 20 to 50% of the carbon atoms are in aromatic rings [4]. The heteroatom content is very significant. Asphaltenes consist, as an average, of around 5-10% in weight of heteroatoms [1]. This implies that there may be around 4-6 heteroatoms per molecule, assuming a molecular weight of 1000 units. This gives this fraction a great tendency to associate, both through the polar moieties and the aromatic sheets.

The molecular structure of asphaltenes remains being a mystery, but there are evidences provided by NMR, IR, fluorescence spectroscopy, X-ray scattering, and mass spectroscopy that have led to the conclusion that asphaltene molecules contain fused rings linked by alkyl branches (archipielaço type, Figure 1).

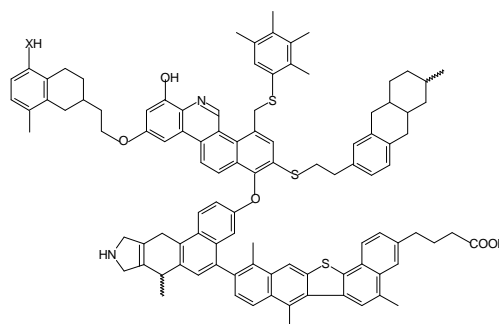


Figure 1: Hypothetical asphaltene molecule.

This project deals with the investigation of the state of asphaltenes in toluene solutions and the interaction with resins. The main technique used is Isothermal Titration Calorimetry (ITC). The calorimeter consists of a syringe and two cells, a reference and a sample cell. The device is placed inside a glove box to minimize the influence of the external conditions (Figure 2). The syringe solution is injected step by step in a series of injections of 5-10

μl . When the solution from the syringe is injected, there would be a re-arrangement of the equilibrium in the sample cell.

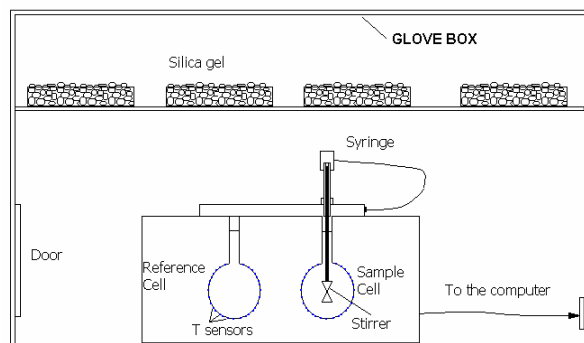


Figure 2: Schematic view of the ITC equipment.

The heat developed is recorded and displayed in the computer. The integration of the area below each peak gives the heat developed per injection (Figure 3). With the application of a suitable model, it is possible to determine the enthalpy of interaction of the substances injected from the cell with the ones present in the syringe.

Specific Objectives

The ultimate objective is to determine the enthalpy of interaction asphaltene-resin for several stable and instable crude oils. With this information, it would be possible to determine if resins have a critical influence in the stability of the crude oil. These experiments would also be useful for researchers that perform molecular simulations and develop models to describe asphaltene behavior, such as regular solution theory or SAFT equation. ITC is able to provide experimental enthalpies of asphaltene self-association and interaction with resins, together with the average number of interaction sites in asphaltene molecules. Thus, these values would help to reduce the number of unknowns in the modeling of asphaltene behavior, as they are usually considered as fitting parameters.

Results and Discussion

a) Asphaltene self-association

It is often useful to find simpler model substances that may help to understand the behaviour of complex fractions such as asphaltenes. It has been reported that asphaltenes stabilize water-in-oil emulsions, like surfactants and they also present surface activity. These evidences pointed the research about asphaltenes towards the determination of properties typical of surfactants. Surfactants usually consist of a polar head and a non-polar chain attached to it. In aqueous solutions, they tend to form micelles where the non-polar chains are protected from the solvent by the polar heads. This phenomenon starts to occur after a certain concentration is reached (Critical Micellar Concentration, CMC). In a calorimetric experiment, this CMC is easily calculated (Figure 3). The syringe is

filled with a concentrated solution of surfactant (30 g/l) to assure that it is in micellar state.

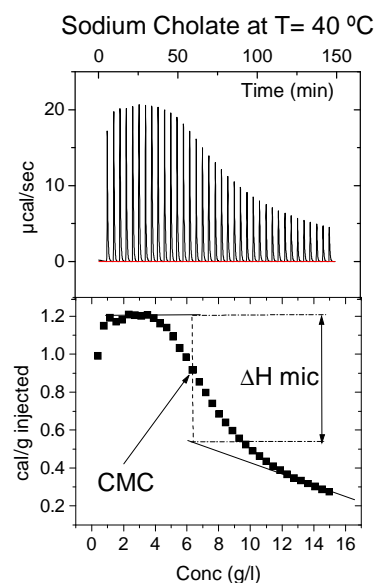


Figure 3: Determination of CMC of a surfactant

The solution is injected into the cell and the heat developed is recorded: in the first injections, the concentration in the cell is low and the micelles break completely into monomers. The breaking of micelles gives a high heat positive signal (endothermic), in this particular case. When the CMC is reached in the cell, the heat developed experiments a sharp decrease, as the micelles do not break any longer and the only heat recorded is the heat of dilution of the micelles. The inflexion point in the curve (6.11 g/l) is assigned to the CMC. There is good agreement between the literature and the data presented here (6.67 g/l, [5]). Several techniques [6] have been used in the past to obtain values of CMC of asphaltenes. This value would determine when asphaltenes started to self-associate.

Dyes are substances used in paint industry and have been used in fluorescence studies as model molecules for asphaltenes [7]. They are usually very aromatic and also contain a high number of heteroatoms. This leads to a complex mechanism of self-association, which results in aggregates of variable size. They are supposed to follow a step-wise mechanism of association. This means that they do not need a certain concentration in the solution to start forming stable aggregates. Instead, they form dimers, trimers and so on at all concentrations. Similarly to the ITC experiments with dyes (Figure not shown), the titration of asphaltenes into dried toluene showed that the heat developed decreases with increasing concentration in the cell (Figure 4). There is not a first region in which the heat developed is constant. The absence of this plateau suggests that asphaltenes do not have a CMC in this concentration region. The step-wise model seems to fit better the experimental evidences.

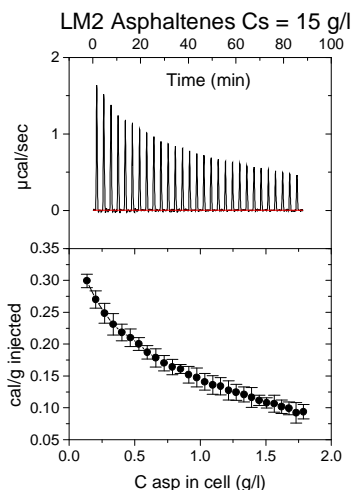
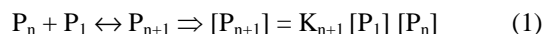


Figure 4: Titration of an asphaltene from Venezuela.

The concentration range studied was 1-10 g/l, as that is the region where most of the values of CMC are found in the literature. Ten different asphaltenes were tested to give more validity to the conclusions drawn. The behavior observed is the same for all of them, without a plateau at low concentrations and a continuous decrease of the heat developed.

Once the surfactant approach has been proven to be wrong, it is necessary to come up with a new way of interpreting asphaltene self-association. The approach followed is based on the chemical equilibrium theory. It assumes that the molecular aggregates are in equilibrium among themselves and with the monomers, following the same type of reaction as in polymer growth and in aggregation/stacking of aromatic molecules:



All the heat developed in the experiments is assigned to the formation of new species. After each injection, the concentration of the molecular aggregates changes and a new equilibrium has to be reached. The differences in concentration between the moment after the injection and the equilibrium allows the calculation of the number of association sites broken in the re-organization process and the total heat developed in each injection.

$$\text{Heat} = \text{Number of bonds broken (mol)} * (-\Delta H_a) \quad (2)$$

The parameters of the models are optimized by means of a non linear least square fitting of Equation 2. Four models have been used to fit the experimental data, all of them incorporating the step-wise growth mechanism. Equal K assumes that the equilibrium constants and the enthalpies are the same for all the reactions. The equilibrium concentration of the monomer is obtained by means of a mass balance analysis [9]. This model has been chosen over the other

because of its simplicity and overall good fits at all concentrations (Figure 5).

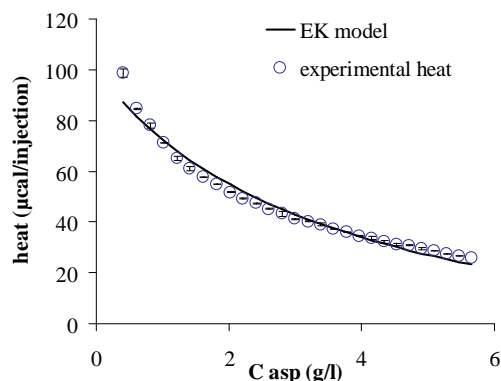


Figure 5: Fit of Equal K to KU asphaltenes (30 g/l).

The calculated values of ΔH_a are small (Table 1), a bit lower than the limit of the usual hydrogen bond (-8 to -40 kJ/mol, and smaller than the stacking of some pure aromatic compounds, such as pyrene (-15 kJ/mol,[8]). It must be taken into account that the model assumes that all molecules are equally active in the self-association. There are evidences that a significant fraction of asphaltenes do not take part in the self-association [9]. This may explain why the values of ΔH_a are so small.

Table 1: ΔH_a and K optimized by EK model.

	Cs = 5 g/l		Cs = 30 g/l	
	ΔH_a	K	ΔH_a	K
KU	-2.3	499.0	-2.9	122.2
Alaska 95	-4.7	340.3	-5.1	83.1
Yagual	-3.5	709.7	-4.5	118.5
Laggrave	-3.0	685.7	-4.0	101.4
LM2	-3.5	164.4	-4.7	63.5
Ca30	-2.1	795.5	-3.4	87.5
OMV	-2.7	419.9	-3.8	79.2
LM1	-3.1	566.1	-5.2	73.7

The choice of the model, however, is critical in the final value of ΔH_a and the average Mw affects greatly the values of the parameters. This is a deficiency of the model due to its simplicity compared to the complex mixture we are dealing with. The use of a more detailed model incorporating a distribution of Mw would imply an extensive study of methods to determine the molecular weight that is out of the scope of this project.

b) Alteration of asphaltene structure

Chemical alteration of asphaltenes was carried out to gain more insight on the importance of polar functionalities in the self-association of asphaltenes. First, polar acidic groups were blocked in two different reactions. Silylation affects only oxygen functionalities (hydroxyl and carboxylic) and substitutes the hydrogen by a trimethyl-silyl group. Methylation substitutes the hydrogen in acidic groups that contain not only oxygen but also nitrogen and sulphur. It is observed in ITC experiments that the heat developed decreases upon

alteration (Figure 6). There are fewer bonds broken, which implies that the capacity of self-association has been reduced after the reactions. The effect is greater in methylated samples, stressing the importance of nitrogen and sulphur groups in the associating capacity of asphaltenes.

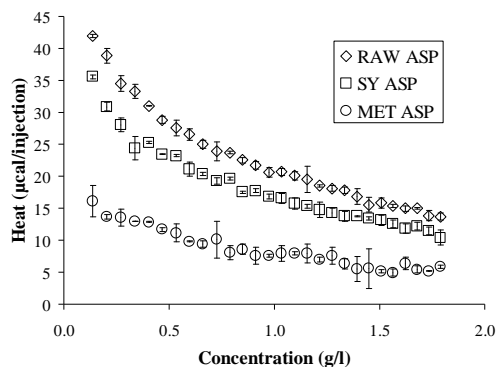


Figure 6: ITC of LM2 altered asphaltenes (10 g/l).

Fluorescence spectrum of methylated Alaska95 shows an increase in intensity at shorter wavelengths with respect to raw asphaltenes (Figure 7). This phenomenon is not observed in asphaltenes that did not show a substantial decrease in heat developed in ITC experiments.

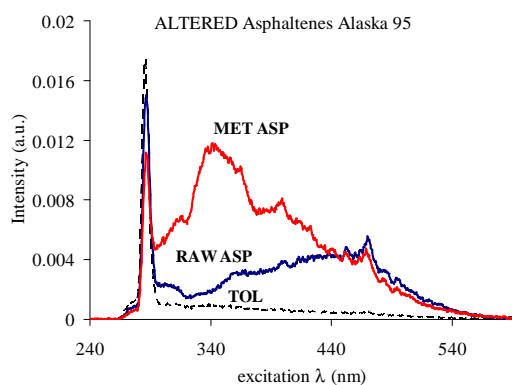


Figure 7: Schematic view of the ITC equipment.

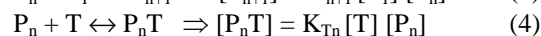
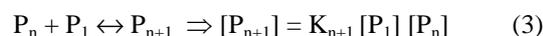
Emission at shorter wavelength would in principle imply the presence of smaller aromatic rings [11], but the reaction does not alter the core of asphaltene molecules. It is suggested that the emission is due to small molecules that were associated through hydrogen bonding in raw asphaltenes, as association is believed to quench the bands and also move them to longer wavelengths [12]. Two more reactions were carried out, in which oxygen and sulphur bridges were broken, decreasing the size of the molecules (Reduction). See reference 13 for a complete description of the process and the results obtained.

c) Interaction with model resins

To remediate asphaltene fouling, the concentration of resin-like material is increased by adding chemicals such as alkyl-phenolic surfactants. These molecules would act as synthetic resins that help in the

stabilization of asphaltenes. These experiments were intended to shed some light on the mechanism of stabilization by surfactants. They would also provide a solid background that will later be used in the interaction of native resins with asphaltenes.

Experiments were carried out by injecting a model resin, nonylphenol (NP) into an asphaltene solution in toluene. Reference tests were as well performed by injecting nonylphenol into pure toluene. The heat developed in the nonylphenol reference data was subtracted from the resin-into-asphaltene data. The resulting heat was assumed to be due to the interaction ASP-NP. The interaction between asphaltenes and nonylphenol is modeled as a Terminator-Propagator system. Asphaltenes are propagators of the growth of the aggregate. On the other hand, when a nonylphenol molecule is attached to the aggregate, the growth stops:



The calculated heat q is:

$$q = n_{A-N} (\text{mol}) * (\Delta H) + n_{A-A} (\text{mol}) * (-\Delta H_A) \quad (5)$$

n_{N-A} is the number of ASP-NP bonds formed and n_{A-A} is the number of ASP-ASP broken. The parameters of the models are optimized so that the heat calculated with Eq. 4 is as close as possible to the experimental heat.

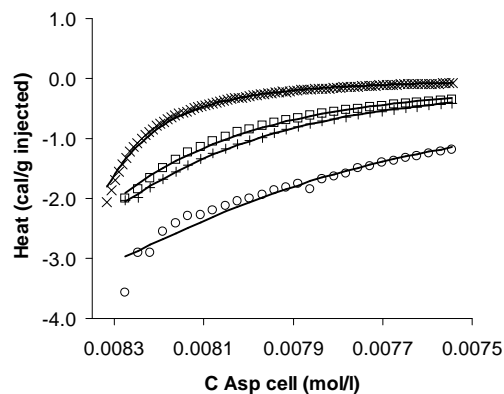


Figure 8: Fit of Model to LM1 10 g/l ASP titrated with NP Concentrations: (O) 5 g/l; (+) 20 g/l; (□) 40 g/l; (X) 100 g/l.

Figure 8 shows that the model is able to fit the experiments with different nonylphenol concentrations. The ΔH obtained are in the lower limit of hydrogen bonding (Table 2) and vary in a limited range. Nevertheless, the equilibrium constants K are rather concentration dependent. They tend to decrease as the concentration of nonylphenol increases. This could be interpreted in terms of affinity: at high nonylphenol concentration, it would have more tendency to self-associate than to interact with asphaltenes. At low concentrations of NP, the proportion of monomeric nonylphenol is higher, allowing a higher interaction

with asphaltenes that implies a higher value of the equilibrium constant K .

Table 2: Fitting results of asphaltene-nonylphenol interaction. ΔH (kJ/mol) and K in l/mol.

C_{NP} (g/l)	$C_{asp\ cell} = 10\ g/l$					
	LMI Asp.		KU Asp.		A95 Asp.	
	ΔH_i	K_i	ΔH_i	K_i	ΔH_i	K_i
5	-5.0	2433	-3.9	1913	-5.9	827
20	-5.1	285	-4.3	141	-6.5	108
40	-6.8	91			-6.7	93
100	-6.2	92				

C_{NP} (g/l)	$C_{asp\ cell} = 1\ g/l$					
	LMI Asp.		KU Asp.		A95 Asp.	
	ΔH_i	K_i	ΔH_i	K_i	ΔH_i	K_i
5	-2.4	275	-2.1	219	-5.7	121
20			-2.1	148	-5.9	73

In order to calculate the maximum capacity of interaction with asphaltenes, a high concentration of nonylphenol (300 or 468 mM) was injected into a low concentration of asphaltenes (1 g/l). This dilution assures that asphaltenes have a low aggregation state and most of the sites are available for the interaction with nonylphenol. The exothermic interaction NP-ASP is rapidly compensated by the high heat developed in the break of H bonds among nonylphenol molecules (Figure 9). The subtraction of the reference data (injection of NP into dried toluene) gives the heat developed in the interaction NP-ASP. This heat reaches a value of zero when all sites have been saturated.

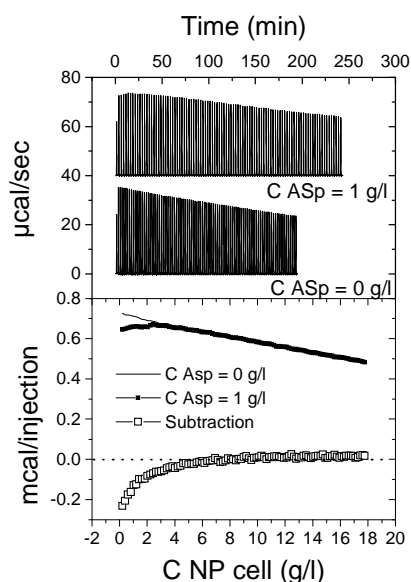


Figure 9: 100 g/l of NP into dried toluene and 1 g/l LM1 ASP.

The previous model assumed only one site per asphaltene molecule, so it is unable to provide the number of sites. A second approach is based on protein-ligand studies [14]. One Set of Independent Sites model (ONE) considers that asphaltenes contain a number of sites available for the interaction, and they all have the same affinity for nonylphenol. Besides, the binding of

one molecule is not affected by the neighbor sites. This means that two sites act as if there were very far from each other, even if they may be in the same molecule. It allows the calculation of the average number of interaction sites at the same time as the enthalpy of association. The fit is as well good (Figure 10) but the values of ΔH are extremely low. They are one order of magnitude lower than the ones obtained with the previous model. This is considered a deficiency of the model.

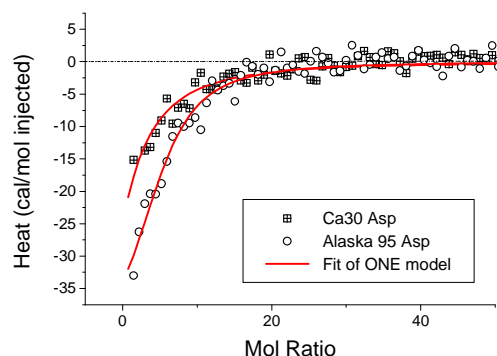


Figure 10: Fit of ONE model to NP-ASP experiments.

The number of sites ranges from 2.6 to 5.1 sites per kilogram. Elementary analysis shows that the amount of heteroatoms per kilogram of asphaltenes is also in that range. This may indicate that the hydroxyl group is mainly attached to asphaltenes through the heteroatoms by hydrogen bonds. Nevertheless, the capacity of nonylphenol to form bonds with the aromatic sheets through the free electrons of the π -orbitals cannot be neglected.

The average n obtained are in the same range as those reported by other researchers. Leon et al. [15] found 6.7 molecules of NP per asphaltene molecule asphaltene in adsorption studies on aggregates in n-heptane. Wu et al. [16] used 6 sites of interaction per asphaltene molecule in their SAFT calculations. Buenrostro-Gonzalez et al. [17] used 3-4 sites to successfully fit onset precipitation data with SAFT equation.

d) Interaction with native resins

Experiments with native petroleum resins have been performed as well. The heats developed are significantly lower than the ones of the interaction with Nonylphenol. Figure 11 shows that the fit of ONE model is still good. The average number of sites depends on the crude but is around 1 in all cases. The decrease with respect to NP may be due to steric hindrance: resin molecules are supposed to be bigger than nonylphenol; the binding of one molecule to a site might prevent other sites from being occupied if they are very close to each other. The contribution of the entropy to the free energy ΔG is much greater than that of the enthalpy, suggesting that the process is entropically driven.

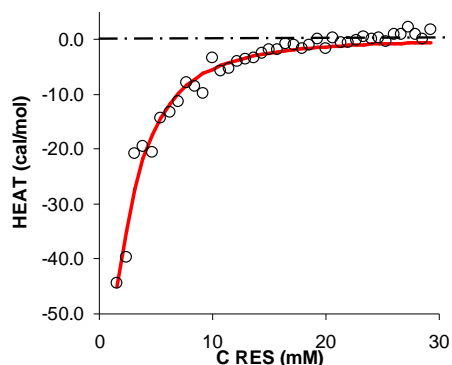


Figure 11: Titration of 1 g/l Ca30 ASP with 99 g/l RES. (o) Experimental (-) Fit of ONE model.

Table 3: ONE model fitting results on ASP-RES interaction. ΔH and ΔG in kJ/mol and ΔS in J/mol. K in l/mol.

Crude	C RES (g/l)	n	ΔH	K	ΔS	ΔG
A95	75.3	0.8	-2.8	257.3	37.0	-14.0
LM1	47.5	1.1	-0.5	753.5	53.3	-16.7
Ca30	99.0	1.5	-0.8	348.0	45.9	-14.7
	12.0	1.6	-0.7	1595.0	59.2	-18.6
YAGUAL	90.0	1.7	-0.8	381.6	46.7	-15.0
	65.6	1.8	-1.1	358.7	45.4	-14.8
	26.1	1.5	-0.6	2374.0	62.6	-19.6
LM2	94.0	1.6	-1.1	358.9	45.4	-14.8

Conclusions

ITC has been applied extensively to asphaltene solutions in toluene. The evidences presented here suggest that the aggregation of asphaltenes occurs in a step-wise manner at all concentrations. Asphaltenes have been altered to determine the importance of polar functionalities in the self-association. ITC experiments shows a significant reduction in aggregation capacity after the blockage of hydrogen bonding sites. The study of the interaction of asphaltenes with first a model molecule and then with native resins has been carried out. By means of a simple model, the average number of sites in an asphaltene molecule has been calculated, together with the enthalpy of interaction resin-asphaltene. These experimental values would be helpful in the improvement of the predicting capacity of the models that describe the behavior of asphaltenes by reducing the number of estimations or fitting parameters.

Acknowledgements

The author would like to acknowledge the help in the laboratory of Mr. Z. Teclé and Mr. D. Thoung. The work is financially supported by the Danish Technical Research Council (STVF via Talent Project).

References

1. J.G. Speight, *The Chemistry and Technology of Petroleum*, 3rd Ed., Marcel Dekker Inc., New York, 1999.
2. E.Y. Sheu, *Energy & Fuels* 16 (2002) 74-82.

3. S. Thou, G. Ruthammer, G. K. Potsch, 2002 Paper SPE 7832.
4. T.F. Yen, in: O.C. Mullins, E.Y. Sheu (Eds.) *Structures and Dynamics of Asphaltenes*, Plenum Press, New York, 1998.
5. S. Paula, W. Süss, J. Tuchtenhagen, A. Blume, *J. Phys. Chem.* 99 (1995) 11742-11751.
6. E. Rogel, O. Leon, G. Torres, J. Espidel, *Fuel* 79 (2000) 1389-1394.
7. H. Groenzin, O.C. Mullins, *J. Phys. Chem.* 103 (1999) 11237-11245.
8. R.B. Martin, *Chemical Reviews* 96 (8) (1996) 3043-3064.
9. S.I. Andersen, *Journal of Liquid Chromatography* 17 (19) (1994) 4065-4079.
10. C.Y. Ralston, S. Mitra-Kirtley, O.C. Mullins, *Energy & Fuels* 10 (1996) 623-630.
11. A.J. Pesce, C.-G. Rosen, T.L. Pasby, *Fluorescence Spectroscopy*, Marcel Dekker Inc., New York, 1971, p. 54.
12. P. Juyal, D. Merino-Garcia, S. I. Andersen, submitted to *Energy&Fuels*.
13. E. Freire, O.L. Mayorga, M. Straume, *Anal. Chem.* 62 (18) (1990) 950A-958A.
14. O. Leon, E. Rogel, A. Urbina, A. Andujar, A. Lucas, *Langmuir* 15 (1999) 7653-7657.
15. J. Wu, J.M. Prausnitz, A. Firoozabadi, *AIChE Journal* 44(5) (1998) 1188-1199.

List of Publications

1. J. Murgich, C. Lira-Galeana, D. Merino-Garcia, S.I. Andersen, J.M. del Rio-Garcia, *Langmuir* 18 (2002) 9080-9086.
2. D. Merino-Garcia, S. I. Andersen, *Petroleum Science and Technology* 21 (3&4) (2003) 507-523.
3. D. Merino-Garcia, J. Murgich, S. I. Andersen. Accepted for publication in *Petroleum Science and Technology*.
4. B.E. Ascanius, D. Merino-Garcia, S.I. Andersen. Submitted to *Energy&Fuels*.
5. D. Merino-Garcia, S. I. Andersen. Interaction Of Asphaltenes With Nonylphenol By Microcalorimetry. Submitted to *Langmuir*.
6. P. Juyal, D. Merino-Garcia, S. I. Andersen. Effect on Molecular Interactions of Chemical Alteration of Petroleum Asphaltenes (I). Submitted to *Energy&Fuels*.
7. P. Juyal, D. Merino-Garcia, S. I. Andersen. Effect on Molecular Interactions of Chemical Alteration of Petroleum Asphaltenes (II) Submitted to *Energy&Fuels*.
8. D. Merino-Garcia, S. I. Andersen. Interaction Of Petroleum Resins And Asphaltenes By Nanocalorimetry And Spectroscopy. Submitted to *Langmuir*.



Matías A. Monsalvo
Address: IVC-SEP, Dept. of Chemical Engineering
Building 229, Office 217
Technical University of Denmark
Phone: (+45) 45 25 29 78
Fax: (+45) 45 88 22 58
e-mail: mmo@kt.dtu.dk
www: www.ivic-sep.kt.dtu.dk
Supervisor(s): Sergio E. Quiñones-Cisneros
Alexander Shapiro
Ph.D. Study
Started: 1 November 2002
To be completed: November 2005

Phase Behaviour and Viscosity Modelling of Refrigerant-Lubricant Mixtures

Abstract

The understanding of thermophysical properties and phase behaviour of refrigerant-lubricant oil mixtures is highly important for optimal designing of refrigeration and air-conditioning systems. Refrigerant-lubricant mixtures may develop complex type of phase behaviour that must be considered when designing a cooling circuit. Such behaviour may include, open miscibility gaps, closed miscibility gaps, liquid-liquid-vapour equilibrium and even barotropic phenomena showing mass density inversions. This will also have a profound effect in the mixtures transport properties. This brings into consideration a multidisciplinary problem involving phase behaviour, dynamic behaviour, barotropic phenomena and, since cooling circuits operate around critical points, another important phenomenon: critical behaviour. Thus, given the complex behaviour that is intrinsic to refrigerant-lubricant mixtures, the development of models that accurately capture this type of behaviour is essential.

Introduction

The phasing out of chlorofluorocarbons (CFCs) has led to a major change in technology within the refrigeration and air conditioning industry. New high performance refrigerants, such as R134a (1,1,1,2 tetrafluoroethane) and their accompanying synthetic lubricants (such as polyalkylene glycols, polyol esters and alkylbenzenes), have been the result of intense and rapid technological development. This development has been based on a detailed understanding of the refrigeration application and the chemistry of refrigerants and lubricants. However, these mixtures, which are likely to have strong asymmetry, may develop complex type of phase behaviour. Thus, the understanding of thermophysical properties and phase behaviour of refrigerant-lubricant oil mixtures is highly important for optimal designing of refrigeration and air-conditioning systems under the various conditions of operation. Furthermore, for an optimal performance design, the phase and transport properties of the coexisting phases must also be taken into account. For instance, for the oil-rich condensed phase to smoothly flow back into the compressor, the viscosity should be appropriate and barotropic phenomena (density inversion) should be avoided [1].

As well as physical measurements of thermophysical properties of such mixtures, the accurate numerical modelling of the phase, barotropic, dynamic and critical

behaviour is essential. For many years, these different problems have been studied and a good amount of knowledge achieved. Yet, in order to be able to accurately model cooling cycles, to some degree, the used equations of state must take into account the non-analytical nature of the critical phenomena. Thus, the main research objective of this project is the development of a new type of equation of state applicable near the critical region and which can be used in conjunction with the recently developed friction theory (*f-theory*) [2] for refrigerant-lubricant mixtures.

Objectives

The main objectives of this project are:

1. The development of equations of state models capable of capturing the non-analytical nature of the critical region while at the same time having a mathematical structure simple enough for actual industrial applications.
2. The simultaneous development of an accurate *f-theory* viscosity model to be coupled to the new equations of state.
3. The accurate numerical modelling of the phase, critical, barotropic and dynamic behaviour observed in refrigerant-lubricant mixtures under wide ranges of temperature and pressure.

Results and Discussion

The type of phase behaviour that refrigerant-lubricant mixtures may develop, has been studied based on experimental information found after an extensive literature survey. In addition to larger immiscibility regions, it has been shown [3] that asymmetric mixtures such as refrigerant-lubricant mixtures may develop density inversions, as observed by Hauk and Weiner [1]. This complex behaviour can be modelled with reasonable accuracy with cubic equations of state and van der Waals mixing rules. The use of a cubic equations of state as simple as the Van der Waals EOS [4], or one of its more accurate empirical derivations such as the SRK EOS [5] or the PR EOS [6], represent a powerful tool for a better understanding of the complex phase behaviour patterns that may be found in fluid mixtures. To better illustrate this, a binary mixture has been analysed with the PR EOS. Figures 1-2 show the pressure-composition and the pressure-mass density phase diagrams for the HFC-134a + triethylene glycol (TRIG) mixture.

As shown in Fig. 1, multiple phase equilibria can be found, including the presence of a high pressure liquid-liquid immiscible region. Figure 2 shows the pressure-mass density diagram at 353.15 K. At this temperature, barotropic behaviour is observed.

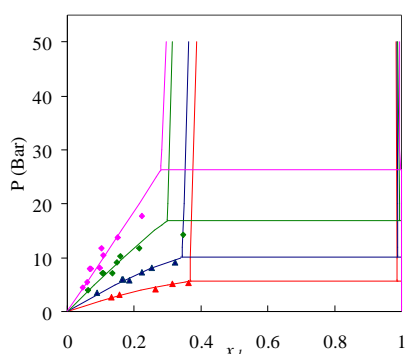


Figure 1: Example of solubility data correlation and VLE prediction for HFC (1) + TRIG, experimental data (Tseregounis and Riley, 1994) at 293.15 K (\blacktriangle), 313.15 K (\blacktriangle), 333.15 K (\blacklozenge), 353.15 K (\blacklozenge). Solid lines denote the calculated data by the PR EoS. Horizontal lines represent the predicted VLE region.

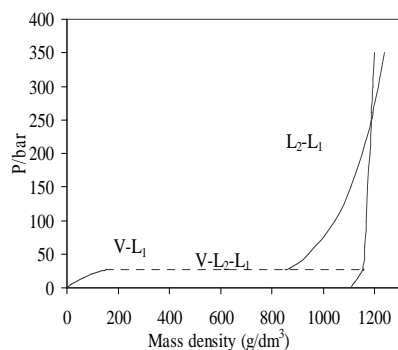


Figure 2: Pressure-density PR phase diagram of HFC134a + TRIG at 353.15 K.

Conclusions and Future Work

In spite of their simplicity, it appears that the PR EOS with the classical quadratic mixing rule may be appropriate for a description of the phase behaviour of complex systems such as HFCs + TRIG. Classical cubic EOS represent a powerful tool for the actual design of refrigeration cycles. This modelling approach can be used to prevent technical problems such as barotropic effects, decrease solubility-related compressor oil viscosity, among others.

The next step is to model the viscosity behaviour of refrigerants and refrigerant-lubricant mixtures by using the friction theory (*f-theory*).

Acknowledgments

The present study is supported by the Danish Research Council (project No. 26-01-0217).

References

1. Hauk and E. Weidner, Thermodynamic and Fluid-Dynamic Properties of Carbon Dioxide with Different Lubricants in Cooling Circuits for Automobile Application, *Industrial and Engineering Chemistry Research*, 39, (2000) 4646.
2. S.E. Quiñones-Cisneros, C.K. Zéberg-Mikkelsen and E.H. Stenby, The Friction Theory (*f-theory*) for Viscosity Modelling, *Fluid Phase Equilib.* 169, (2000) 249-276.
3. Quiñones-Cisneros, S.E., Phase and critical behaviour in type III phase diagrams, *Fluid Phase Equilib.*, 134, (1997) 103.
4. J.D. van der Waals, On the continuity of the gas and liquid state, Doctoral Dissertation, 1873.
5. G.S. Soave, Equilibrium Constants from a Modified Redlich-Kwong Equation of State, *Chem. Eng. Sci.*, 27, (1972) 1197-1203
6. D.-Y. Peng and D.B. Robinson, A New Two-Constant Equation of State, *Ind. Eng. Chem. Fundam.*, 15, (1976) 59-64.

List of Publications

1. S. E. Quiñones-Cisneros, J. García, J. Fernandez and M. A. Monsalvo, Phase and Viscosity Behaviour of Refrigerant-Lubricant mixtures, *Eurotherm 2003 Seminar N° 72*, Valencia (Spain), 2003, p. 323.
2. J. García, M. A. Monsalvo, S. E. Quiñones-Cisneros and J. Fernandez, Modelling Phase Equilibria and Viscosity for Refrigerant-Lubricant Oil Systems, *21st IIR International Congress of Refrigeration*, Washington D. C., 2003.
3. S. E. Quiñones-Cisneros, M. A. Monsalvo, J. García and J. Fernandez, Phase Behaviour of Refrigerant-Lubricant Mixtures, *20th European Symposium on Applied Thermodynamics*, Germany, 2003.



Jan Kamyno Rasmussen

Address: CAPEC, Dept. of Chemical Engineering
Building 227, Office 250
Technical University of Denmark

Phone: (+45) 45 25 28 01

Fax: (+45) 45 88 22 58

e-mail: jkr@kt.dtu.dk

www: www.capec.kt.dtu.dk

Supervisors: Sten Bay Jørgensen
Henrik Madsen, IMM-DTU
Henrik Steen Jørgensen, Novozymes A/S

Ph.D. Study

Started: 1 September 2003

To be completed: September 2006

Datadriven and Mechanistic Model based Control and Optimization of Fed-batch Fermentations

Abstract

Fed-batch processes are widely used in chemical and biochemical industry. Fermentations in biochemical industry are most often carried out as fed-batch processes. Operation of these processes is not possible using standard regulatory control schemes because of their non-linear nature and limitations in the production equipment. In this project a methodology for control and optimization of such processes will be developed based on the use of mathematical models.

Introduction

Fermentation processes are commonly used in biochemical industry for production of a wide variety of products. The true nature of these processes is rarely fully understood which makes the implementation of efficient control schemes very difficult. First principle engineering models are not used because the limited knowledge about the processes would make them very time consuming to develop.

Another promising strategy is to develop datadriven models entirely based on data from actual fermentations. When knowledge about the process is available a hybrid modeling approach to extract pertinent information from data can be applied.

The purpose of modeling these processes is to develop control structures that ensure uniform operation and optimize the productivity of the process.

This project is a part of the Novozymes Bioprocess Academy which is a newly established cooperation between Novozymes A/S, The department of Chemical Engineering and Biocentrum at DTU.

Specific Objectives

The objective of this project is to develop a methodology to identify mathematical models which can predict the behaviour of fed-batch fermentations in biochemical industry. Based on the identified models it is possible to control the fed-batch process. The models may also be developed for optimizing the process

performance. The results of the models will be validated against experimental data obtained on the plant and a control structure based on the models will be implemented in a pilot plant for validation purposes.

Results and Discussion

To begin with the approach will be to design a model based entirely on operational data, where a set of black-box models will be developed. The model will be able to predict the evolution of the process based on the given inputs. A methodology for generation of such models has already been developed in earlier projects [1]. It has been shown that this kind of datadriven models are able to account for disturbances that occur in the process. The advantage of datadriven modeling is that only limited prior information about the process is required. The disadvantage is that the resulting models do not have any physical interpretation and can not directly provide any information about the fermentation process.

The methodology uses a large number of linear time invariant models which each describe the behaviour of the process in a certain time interval. The combination of these linear models results in a model which covers the entire time span of the fermentation and approximates the highly non-linear behaviour of the process. Successful application of such models shows that the data contains sufficient information to predict the behaviour of future batches.

At a later point in the project knowledge about the microorganism and how the process is carried out can be combined with operational data in order to develop knowledge based models. A methodology for development of such knowledge based grey-box models has already been developed [2]. It is based on the use of stochastic differential equations which are well suited for combining first principle engineering models with data because they account for random uncertainty and noise.

The control structures used today are most often decentralized and lack the ability to account for limitations in the process equipment and microorganisms. Furthermore industrial operation often relies on the operators experience and can not be guaranteed to be uniformly reproducible. Uniformity in the production is important for the subsequent steps in the production facility. Development of models for control can be essential for reducing variations in product quality and can thereby improve the productivity of the overall process which is beneficial for economic reasons.

Conclusions

The limited knowledge about the nature of the fermentation processes used in industry makes it time consuming to develop first principle engineering models. An alternative is datadriven modeling based on process data. If some information about the process is available knowledge based grey-box models can be developed and efficiently used to uncover unknown functional relationships.

In this project both types of modeling will be explored and the results will be validated against actual plant data.

References

1. D. Bonné, S. B. Jørgensen, Datadriven Modeling of Nonlinear and Time-Varying Processes, IFAC SYSID 2003, 2003.
2. N.R. Kristensen, H. Madsen, S.B. Jørgensen, A Method for Systematic Improvement of Stochastic Grey-Box Models, Comp. & Chem. Eng., in print.



Nùria Muro Suñé

Address: CAPEC, Dept. of Chemical Engineering
Building 227, Office 218
Technical University of Denmark

Phone: (+45) 45252805
Fax: (+45) 45932906
e-mail: nms@kt.dtu.dk
www: www.capec.kt.dtu.dk
Supervisor(s): Rafiqul Gani

Ph.D. Study

Started: 1 August 2002
To be completed: August 2005

Prediction of the Solubility and Diffusion Properties of Pesticides in Polymers

Abstract

In the field of pesticide controlled release technology, a computer based model that can predict the delivery of the Active Ingredient (AI) from fabricated units is important for purposes of product design and marketing. A model for the release of an AI from a microcapsule device is presented here, together with a specific case study application to highlight its scope and significance. This paper also addresses the need for predictive models and proposes a computer aided modelling framework for achieving it through the development and introduction of reliable and predictive constitutive models.

A group-contribution based model for one of the constitutive variables (AI solubility in polymers) is presented together with examples of application and validation.

Introduction

There are many applications in agriculture, where protection from pests is required for extended periods of time. If control is required for periods of a year or more, then the conventional methods of delivering the pesticide compound (for instance, spraying a solution of the pesticide over the crop) may not be good enough because the pesticide might not be delivered at the specific desired site and also because it does not last long enough to accomplish the protection of the crop. Considerable improvement can be achieved by using controlled release systems for the pesticide delivery to the environment. Through the sustained release of the pesticide from these devices, the amount of pesticide used, as well as, the number of times it needs to be applied on the crop, is reduced. As the pesticide is usually encapsulated within a polymer membrane, there is also a reduction with respect to environmental hazards and human toxicity.

A great number of models exist for describing the wide variety of controlled release devices available, due to the attention that the sustained delivery of drugs has received in the past years. Our purpose at this level is to try and apply these models into the field of pesticide controlled release technology and to make them available through a computer aided system. As the controlled release devices consist basically of a pesticide (AI) that is encapsulated or incorporated within a polymer membrane, the most important

properties in these models are the ones that relate to the pesticide and the polymer. It is then appropriate to say that the solubility of the pesticide in the polymer and its diffusivity through the polymer membrane have a significant influence in the release of a pesticide from a controlled release device. This is where the models for prediction of the solubility of pesticides in polymers become important.

The main objective in this work is to make the current models predictive, flexible and robust so that they can be used to design and evaluate AI formulations and their delivery, rapidly and reliably. This implies being able to predict the properties that are critical to the controlled release mechanism through specially developed predictive property (constitutive) models. These property models when incorporated into the generic controlled release models will allow the study of the release of the pesticide molecule through the polymer. Thus, these computer models would be a valuable addition to the tools for both polymer and product design and analysis.

Model for Controlled Release

Controlled release technology presents several advantages over the conventional applications of pesticides; they are illustrated in Fig. 1. A comparison of the pesticide concentration in the environment over time obtained from a conventional pesticide application (—) with the concentration from a controlled delivery

system (—) is presented in this figure. It can be observed that with a conventional application a very high concentration is obtained initially, that can even be greater than the allowed toxicity level. This concentration decreases fast and is soon below the minimum effective level. On the other hand, the benefits of having a sustained pesticide delivery are immediately observed in the other concentration plot (—), due to the quick achievement of the desired concentration that is then maintained over time, this is obviously a more desirable scenario.

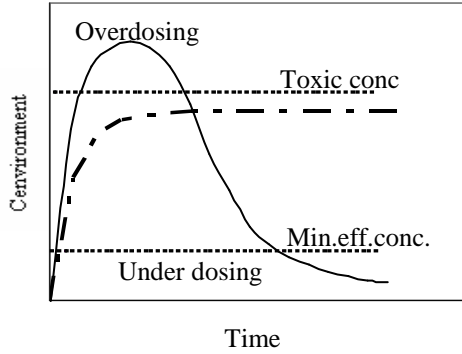


Figure 1: Common pesticide application (—) versus controlled release application (—)

Model Description

The field of controlled release technology offers a wide variety of devices with a similar final effect, one of the most common types being the microcapsules. A microcapsule is a reservoir system where the AI is enclosed within a polymer membrane, as is shown in Fig. 2. Several examples can be found in the market of microencapsulated pesticides (TopNotch, Fultime, etc.) with different properties and functionalities [1].

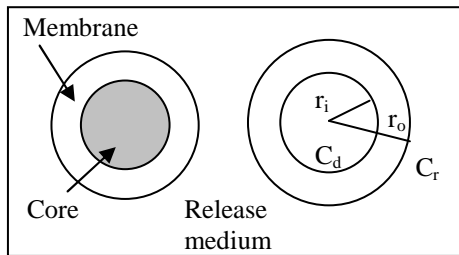


Figure 2: Microcapsule schematic representation

The process of AI release from a polymer can be described in most cases by Fickian diffusion, with the appropriate initial and boundary conditions. In the present work, a computer based model has been developed for the delivery of AI from microcapsule devices. This model accounts for the number of microcapsules and their size differences through a normal distribution function (Eq. 1). The controlled release is modelled with the equations for non-constant activity source (Eqs. 2 and 3, [2]), that are derived from Fick's law of diffusion and provide the concentration dependence with time.

This model applies for systems where the AI is available in solution below the solubility limit. In the microcapsules diffusion occurs through a thin film (of thickness h), thus the equation of diffusion can be considered in one dimension with respect to space.

$$f(r; \mu; \sigma) = \int_{-\infty}^{\infty} \frac{1}{\sqrt{2\pi}\sigma} \exp\left(-\frac{(r-\mu)^2}{2\sigma^2}\right) \quad (1)$$

$$\frac{dC_d}{dt} = \frac{DA}{V_b h} K_{m/d} \left[1 - \left(\frac{K_{m/r}}{K_{m/d}} + \frac{V_b}{V_d} \right) \right] C_{d,initial} \times \exp\left(-\frac{DA}{h} \left(\frac{V_d K_{m/r} + V_b K_{m/d}}{V_b V_d} \right) t\right) \quad (2)$$

$$\frac{dC_r}{dt} = \frac{DA}{V_b h} K_{m/d} C_{d,initial} \exp\left(-\frac{DAK_{m/d}}{V_b h} \left(\frac{K_{m/r}}{K_{m/d}} + \frac{V_b}{V_d} \right) t\right) \quad (3)$$

Equation 1 represents the normal distribution function that is applied to the microcapsule radius (r) in order to get a representation of the various sizes of microcapsules found in solution. This distribution is applied with a certain mean distribution value (μ) and a specific standard deviation (σ). Equation 2 represents the rate at which the concentration changes with time (t) in the donor compartment (C_d , g/cm^3), that is the “core”, as it is defined in Fig. 2. This concentration is affected by two properties related to the AI and the polymer: the diffusion coefficient (D , cm^2/s) of the AI within the polymer and the partition coefficients between the polymer membrane and the donor ($K_{m/d}$) and the one between the release medium and the polymer membrane ($K_{m/r}$). The geometric parameters of the microcapsule also have an effect on the release; these are the surface area through which diffusion takes place (A , cm^2), the volume of the microcapsule or donor volume (V_d , cm^3), and the thickness of the microcapsule wall (h , cm). Finally, the initial concentration in the core ($C_{d,initial}$, g/cm^3) and the volume of the release medium, or bulk volume (V_b , cm^3) are also present in this equation. In Eq. 3 the variation of the concentration in the receiver or release medium (C_r , g/cm^3) is represented over time and having mainly the same variables present in Eq. 2. In the total model, the radius distribution from Eq. 1 is used to calculate microcapsule volume and surface areas that appear in Eqs. 2 and 3.

Model Solution

In this section the model presented above is tested with some experimental data in order to assess its performance and suitability. The case study is selected so that the values of the model parameters and known variables required for the model equation solution are available from experiment. Shao et al. [3] have studied the release of a disperse dye solution from a microcapsule. This microcapsule is prepared by

complex coacervation and the dye solution is encapsulated with a gelatin and gum acacia membrane.

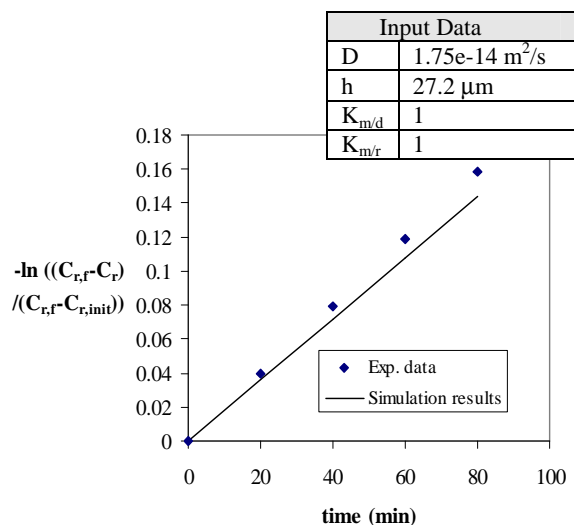


Figure 3: Comparison of model results with literature data [3]; where $C_{r,init}$ is the concentration of the receiver at time zero (g/cm^3) and $C_{r,f}$ is the concentration of the receiver at 24h (g/cm^3).

The model equations (Eqs. 2 and 3) are solved by setting values for the diffusion coefficient (D), the wall thickness (h) and the two partition coefficients ($K_{m/d}$, $K_{m/r}$) obtained from [3]. The available apparent diffusion coefficient includes the partitioning effect, therefore in our simulations the partition coefficients have been set to unity in order to avoid accounting for them more than once. The calculated values obtained from the simulation with the microcapsule release model are plotted together with the experimental values from the literature in Fig. 3. It can be observed that the model reproduces the release of the dye solution from the microcapsules reasonably well, even though the simulated values are somewhat lower than the experimental data. This small disagreement can be due to differences in the donor volume arising from the distribution of microcapsules sizes, which affects the amounts of AI released.

New Developments

Analyzing the microcapsule model presented in the previous section we observe that there are two parameters that are critical for the applicability of the model to a wide range of microcapsules and pesticides. These two parameters are the partition coefficient (related to the solubility of the pesticide in the polymer) and the diffusion coefficient. The first attempt, therefore, has been to select and implement a model for the prediction of the thermodynamic partition coefficient ($K_{pol/c}$) through activity coefficient calculations (Eq. 4). The challenge here is to use a simple model that is predictive and can then be extended to handle a wide range of complex molecules. The selected model is the ‘‘GC-Flory Equation of State’’ [4], which is a simple activity coefficient model based

on a group contribution approach, with an existing parameter table that provides accurate and predictive results.

$$K_{pol/c} = \frac{\Omega_c^\infty}{\Omega_{pol}^\infty} \quad (4)$$

In order to illustrate the possibility of having a completely predictive model for the controlled release of pesticides, some preliminary calculations related to the prediction of the partition coefficient are presented. In Table 1 the experimental values of activity coefficients at infinite dilution (Ω^∞) of two solutes in a polymer (Polystyrene, PS) are compared with the ones calculated with the GC-Flory EoS. It can be noted that good agreement has been obtained. After this initial test, the next validation test involved the calculation of partition coefficients of complex molecules in selected polymers. Table 2 highlights some of these results for three complex molecules (drugs are used as pesticide molecules being studied cannot be disclosed for reasons of confidentiality). These examples are selected so that the available parameter table of the GC-Flory EoS model can be used and the results compared with literature data, [5].

Although there are some differences between the experimental and calculated values we have to keep in mind that this has been pure prediction, that is, without any adjustment of parameters. We would like to note though, the qualitative goodness of the results.

Table 1: Comparison of experimental and calculated activity coefficients at infinite dilution, in weight-basis (Ω^∞)

Comp. 1	Comp. 2	T (°K)	Ω_1^∞ (exp)	Ω_1^∞ (calc)
1-propanol	PS (20000)	445.0	18.8	17.6
Benzene	PS (120000)	403.4	4.61	4.29

Table 2: Comparison of experimental and calculated drug partition coefficients between polymer and water ($K_{pol/w}^{AI}$), at 298 °K

Drug	Polymer	$\log K_{pol/w}^{AI}$ (calc)	$\log K_{pol/w}^{AI}$ (exp)
Androstenedione	EVA	2.61	2.182
Testosterone	EVA	2.66	2.217
Progesterone	EVA	3.01	3.210

Having the capabilities of the GC-Flory EoS model tested and verified, the next step has been to develop a modeling framework through which the group parameter table can be extended to handle a large range of pesticides and polymers. For example, with the partition coefficient of two well-known pesticides, Permethrin (52645-53-1) and Abamectin (71751-41-2), calculated through this model and the corresponding diffusion coefficients obtained either by experiment or predicted by a model, the controlled release can be

compared with different microcapsules and/or conditions of use. The results are, in principle, similar to the ones illustrated in Fig. 3.

Conclusions

A computer aided model has been developed that is able to reproduce the controlled release of an active ingredient from a microcapsule device, and it has been tested with available experimental data to evaluate its applicability. An extension of activity coefficient models for the prediction of solubility of the active ingredient in polymers is under development, and preliminary results indicate that it is feasible to create a predictive controlled release model. However, to make the system truly predictive, flexible and robust, a predictive model for the diffusivity of active ingredients within polymers is also needed and this is the subject of future work.

References

1. Scher, H.B., Rodson, M., Kuo-Shin, Lee, 1998, *Pesti. Sci.* 54, 394-400.
2. Comyn, J., 1985, *Polymer permeability*, Elsevier, NY.
3. Shao, Y., Fang, K., Zou, L., Wang, J., 1993, *J. of China Textile University (Eng. Ed.)*, 10, 2.
4. Bogdanic, G., Fredenslund, A., 1994, *Ind. Eng. Chem. Res.*, 33, 1331-1340.
5. Pitt, C.G., Bao Y.T., 1988, *Internac. Journal of pharmaceuticals*, 45, 1-11.

List of Publications

1. Muro, N., Gani, R., Bell, G., Cordiner, J., Computer Aided Modeling of Pesticide Uptake in Plants for Pesticide Formulation and Design, AIChE Annual Meeting, Indianapolis, 3-8 November 2002.
2. Muro, N., Gani, R., Extending property estimation methods to beyond their application range: property estimation for pesticide design, ESAT-2003, 9-12 October 2003.
3. Muro, N., Gani, R., Bell, G., Shirley, I., Computer-aided and predictive models for design of controlled release of pesticides, ESCAPE 14, 16-19 May 2004 (submitted).



Alfonso Mauricio Sales-Cruz
Address: CAPEC, Dept. of Chemical Engineering
Building 227, Office 266
Technical University of Denmark
Phone: (+45) 45 25 29 11
Fax: (+45) 45 93 29 06
e-mail: msc@olivia.kt.dtu.dk
www: www.capec.kt.dtu.dk
Supervisor(s): Rafiqul Gani

Ph.D. Study
Started: December 2002.
To be completed: November 2005.

Development of a Computer Aided Modeling System for Bio and Chemical Process and Product Design

Abstract

This project deals with the development of an advance computer aided modeling system (CAMS) that aids to model developer in model generation, model analysis, model identification and model solution in a fast, reliable and efficient manner. The advantages of using CAMS are highlighted through case studies in terms of reduction of modeling time and effort. Case studies are related to the optimization of a batch biogas reactor and the dynamic simulation of a semi-continuous copolymerization reactor. Up to now the results show that this contribution proposes an integrated modeling framework that allows understanding main characteristics of chemical processes.

Introduction

In general, modeling is one of the fundamental activities related to research and development of processes and/or products. There is an increasing trend to use computer- aided modeling systems (CAMS) and tools for integrated process analysis. CAMS provide the opportunity to reduce the time to market and investment costs through integrated product and process design with fast, reliable and efficient modeling steps. CAMS must ensure the integration of existing tools and models into a software environment to support model construction, analysis, solution, and validation.

The aim of this project is to highlight the use of a generic modeling framework for CAMS called ICAS-MoT [1], which is applicable to a wide range of modeling and associated problems. As a first case study, the modeling of an (experimental) anaerobic biogas reactor is considered, establishing a solution strategy that is divided into several sub-problems. Kinetic experiments have been carried out according to a predefined set of scenarios, and the available data have been used to estimate the unknown model parameters, using an off-line optimization approach and an on-line estimation approach. As a second case study, the dynamic evaluation of the monomer composition in the emulsion (aqueous and polymer particle) phases in a semi-batch reactor is presented. The dynamic simulations are verified and compared with earlier reported results.

Modeling Framework

The process of mathematical model building is a trial and error procedure. The iterative feedback/feedforward nature of this process is shown in Fig. 1. The model developer usually repeats the steps more than once. He gets closer reaching the model objectives with each cycle while, at the same time, refining the definition of the modeling purpose. The modeling approach can be subdivided into the following steps [2]: problem definition, system characteristics, problem data evaluation, model construction, model solution, model verification, and model validation. Usually all of these steps consume a lot of human resources and time. However, if the work is divided between human and computer, so that the computer assists to the model developer where it is efficient and leaving to the human the parts that require important decisions, then time and cost for model development can be significantly reduced.

The modeling framework used in this work is ICAS-MoT, which is an integrated modeling environment to build, analyze, manipulate, solve and visualize mathematical models. An important feature of ICAS-MoT is that the model developer does not need to write any programming codes to enter the model equations. Models are entered (imported) as text-files or XML-files, which are then internally translated. In model analysis step ICAS-MoT orders the equations into lower triangular form (if feasible), generates the

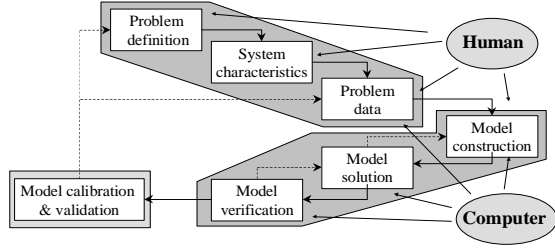


Figure 1: Modeling framework.

incidence matrix, verifies the degrees of freedom, and checks for singularity. After this interactive model analysis, the appropriate solver for the model equations is selected together with a corresponding solution strategy. As solver options, ICAS-MoT provides several solvers for AEs (algebraic equations), DAEs (differential algebraic equations) and numerical optimization methods.

Modeling and Identification of a Biogas Reactor

Process Description

Biogas processes are linked to methane production as a renewable and possibly also sustainable energy source, formed as the end product during biodegradation of organic waste material without oxygen. Recently, several steps have been taken towards establishing general purpose and comprehensive mechanistic models of bioprocesses, involving a large number of reactions with highly non-linear kinetics. However, as some of the kinetic parameters are not known, they must be identified and calibrated before the model can be used to optimize the process.

In particular, the anaerobic conversion of glucose to biogas carried out in a batch reactor is considered. The complex reaction scheme with five consecutive (Monod-type) reaction rates has been taken from a previous work [3], and experimental data collection has been performed to estimate the unknown model parameters. The kinetic mechanism (see Fig. 2) shows that the decomposition of glucose to methane and carbon dioxide passes through the production of lactic, acetic and propionic acid; while concentrations of other volatile fatty acids such as butyrate are negligible in comparison with those of acetate and propionate.

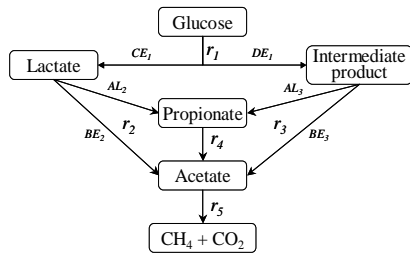


Figure 2: Kinetic mechanism for the anaerobic digestion of glucose

Model Construction

The behavior of the batch digester (anaerobic bioreactor) can be described by a set of non-linear first-order ordinary differential equations (mass balances) taking the form:

$$\frac{d[Gl]}{dt} = -r_1, \quad r_1 = \frac{m_{\max 1} [Gl] X}{k_{s1} + [Gl]} \quad (1)$$

$$\frac{d[Lac]}{dt} = CE_1 \cdot r_1 \cdot X - r_2, \quad r_2 = \frac{m_{\max 2} [Lac] X}{k_{s2} + [Lac]} \quad (2)$$

$$\frac{d[IP]}{dt} = DE_1 \cdot r_1 - r_3, \quad r_3 = \frac{m_{\max 3} [IP] X}{k_{s3} + [IP]} \quad (3)$$

$$\frac{d[Pr]}{dt} = AL_2 \cdot r_2 + AL_3 \cdot r_3 - r_4, \quad r_4 = \frac{m_{\max 4} [Pr] X}{k_{s4} + [Pr]} \quad (4)$$

$$\frac{d[Ac]}{dt} = BE_2 \cdot r_2 + BE_3 \cdot r_3 + Y_{Ac,Pr}^4 \cdot r_4 - r_5, \quad r_5 = \frac{m_{\max 5} [Ac] X}{k_{s5} + [Ac]} \quad (5)$$

Where $[Gl]$, $[Lac]$, $[IP]$, $[Pr]$ and $[Ac]$ are the glucose, lactate, intermediate product, propionate and acetate concentrations respectively. This model (Eqs. 1-5) is a DAE set with 18 unknown parameters $\{m_{\max 1}, m_{\max 2}, m_{\max 3}, m_{\max 4}, m_{\max 5}, k_{s1}, k_{s2}, k_{s3}, k_{s4}, k_{s5}, CE_1, DE_1, AL_2, AL_3, BE_2, BE_3, X, Y_{Ac,Pr}^4\}$, which have to be identified.

Model Identification Strategy

Model identification is necessary to be carried out together with a plan of experiments, which is designed such that first the total biomass concentration (X) is fixed, then several experiments are used as follows: (a) the parameters $m_{\max 1}$ and k_{s1} were calculated using Eq. 1 and experimental values of glucose concentration, (b) then $m_{\max 2}$, k_{s2} and CE_1 were calculated using Eqs. 1 and 2 and experimental values of glucose and lactate concentrations, considering $m_{\max 1}$ and k_{s1} as known, (c) then DE_1 and $Y_{Ac,Pr}^4$ were estimated by solving the carbon mass balance for the conversion of glucose to lactate, intermediate product and biomass. The results for the identification of these parameters are: $\{m_{\max 1}, m_{\max 2}, k_{s1}, k_{s2}, k_{s4}, k_{s5}, CE_1, DE_1, X, Y_{Ac,Pr}^4\} = \{197.94, 2.88, 46.0, 11.0, 14.0, 32.0, 0.137, 0.345, 14.0, 0.73\}$. Finally the identification of the missing (eight) kinetic parameters $\{m_{\max 3}, m_{\max 4}, m_{\max 5}, k_{s3}, AL_2, AL_3, BE_2, BE_3\}$ is done using all glucose, lactate, propionate and acetate concentrations together with Eqs. 1 - 5. This allowed the decomposition of the model identification problem into a set of sub-problems. In this paper, only the total model identification results are highlighted.

Two approaches are employed for the identification of the eight missing parameters: (a) off-line optimization by minimizing a least square function for a given set of experimental data and using the conventional NLP method (involving discretization of the DAEs), and (b) on-line estimation by using available experimental data and a non-linear dynamic estimator, whose algorithm add extra ODEs (one for each parameter to be estimated) to the reactor model. For

both cases, kinetic experiments were carried out and the available data were the four concentrations of *Gl*, *Lac*, *Pr* and *Ac*.

Off-line Parameter Optimization: In this test, we found the eight missing parameters by minimizing a least square function for a given set of experimental data. The minimization problem is stated as:

$$\min \sum_{i=1}^n \left\{ [Gl]_{exp}(t_i) - [Gl](t_i) \right\}^2 + \left\{ [Lac]_{exp}(t_i) - [Lac](t_i) \right\}^2 + \left\{ [Pr]_{exp}(t_i) - [Pr](t_i) \right\}^2 + \left\{ [Ac]_{exp}(t_i) - [Ac](t_i) \right\}^2 \quad (6)$$

Which is subject to Eqs. 1 - 5, and with bounds $[Gl](t) \geq 0$, $[Lac](t) \geq 0$, $[Pr](t) \geq 0$ and $[Ac](t) \geq 0$.

On-line Parameter Estimation: This approach was implemented by using an estimator [4], which requires the derivation of additional ODEs (one equation for each parameter to be estimated) to be solved simultaneously with the process model equations (Eqs. 1 - 5). Moreover, each parameter should be estimated from one on-line concentration measurement. For instance, taking into account the set of four available concentration measurements, then it is possible to estimate four parameters, so that the rest (four) of the unknown parameters are identified by off-line optimization. For purpose of illustration of the methodology, the set $\{AL_3, BE_3, m_{max4}, m_{max5}\}$ has been chosen for this on-line estimation approach since they have a linear dependency, leading to the following additional equations,

$$\frac{dAL_3}{dt} = g_{11} \cdot ([Gl]_{exp} - [Gl]) + g_{12} \cdot ([Lac]_{exp} - [Lac]) + g_{13} \cdot ([Pr]_{exp} - [Pr]) \quad (7)$$

$$\frac{dBE_3}{dt} = g_{21} \cdot ([Lac]_{exp} - [Lac]) + g_{23} \cdot ([Pr]_{exp} - [Pr]) + g_{24} \cdot ([Ac]_{exp} - [Ac]) \quad (8)$$

$$\frac{dm_{max4}}{dt} = g_{41} \cdot ([Gl]_{exp} - [Gl]) + g_{42} \cdot ([Lac]_{exp} - [Lac]) + g_{43} \cdot ([Pr]_{exp} - [Pr]) \quad (9)$$

$$\frac{dm_{max5}}{dt} = g_{51} \cdot ([Gl]_{exp} - [Gl]) + g_{52} \cdot ([Lac]_{exp} - [Lac]) + g_{53} \cdot ([Pr]_{exp} - [Pr]) + g_{54} \cdot ([Ac]_{exp} - [Ac]) \quad (10)$$

Where g_{ij} are non-linear functions obtained according Alvarez and Lopez [4]. In general, the estimator minimizes the error between the calculated concentrations and the experimental ones, such that at sufficiently long time, the ODEs (Eqs. 7 - 10) would be equal to zero meaning that the constant values of the parameters have been found.

Model Analysis

The classification of variables is done through ICAS-MoT, which allows the classification of all non-explicit variables. The variable classification for each identification strategy is as follows: (a) the off-line parameter optimization model has 30 equations (5 ODEs, 1 optimization equation, 24 explicit AEs) and 46 variables (5 Dependent, 8 Known, 10 Parameters, 23

Explicit), and (b) the on-line parameter estimation model has 33 equations (9 ODEs, 24 explicit AEs) and 46 variables (9 Dependent, 14 Known, 23 Explicit). The total number of data points (shown in Fig. 3) for both strategies is 22, but three of them (pointed out inside the dash circle in Fig. 3) were discarded because a large experimental error.

Model Identification and Simulation

Off-line Parameter Optimization: The optimization problem (Eqs. 1 - 6) was solved by the SQP-optimization method (included in ICAS-MoT) and using discretisation of the DAEs. The optimal kinetic parameters obtained were as follows: $\{m_{max3}, m_{max4}, m_{max5}, k_{s3}, AL_2, AL_3, BE_2, BE_3\} = \{4.48, 0.47, 2.88, 17.96, 0.0, 0.40, 0.46, 0.73\}$. Then, process simulation was performed by integrating the reactor model (Eqs. 1 - 5) with the BDF (Backward Difference Formula)-method (also included in ICAS-MoT) and using previous optimized parameters. The simulation results are shown in the Fig. 3, which are in accordance with the experimental data. The corresponding standard deviations were $\{\sigma_{Gl}, \sigma_{Lac}, \sigma_{Pr}, \sigma_{Ac}\} = \{29.7 \text{ mg/L}, 13.2 \text{ mg/L}, 12.2 \text{ mg/L}, 15.1 \text{ mg/L}\}$, and with a global correlation factor of 0.932.

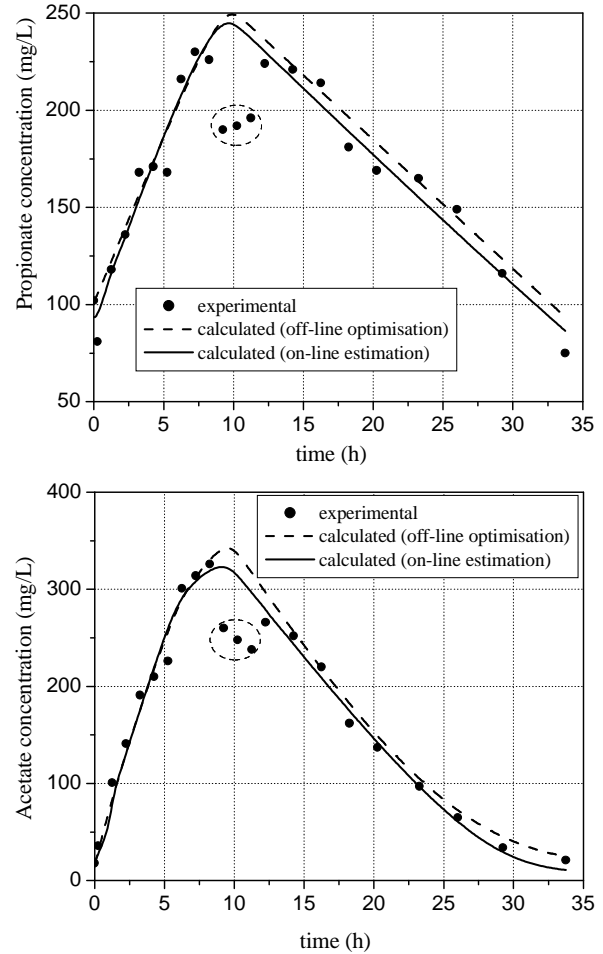


Figure 3: Concentration results for the biogas reactor.

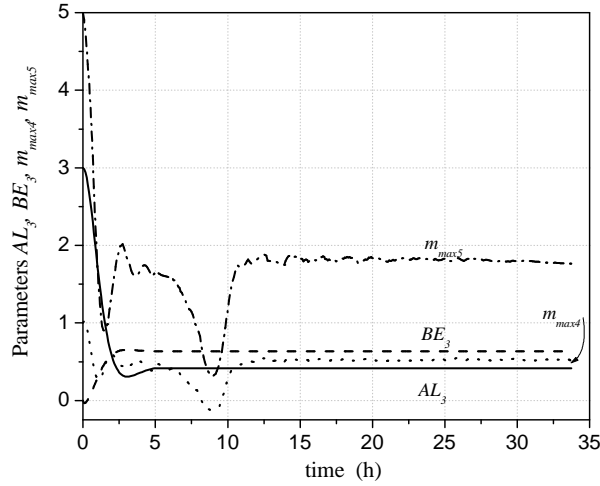


Figure 4: On-line parameter estimation for the biogas reactor.

On-line Parameter Estimation: To verify this approach, experimental data (taken originally in discrete form) was regressed as a time dependent function. Then the estimator model (Eqs. 1 – 5 and 7 - 10) were solved in ICAS-MoT (using BDF method) as an initial value integration problem. As aforementioned, four parameters were first identified by off-line optimization: $\{m_{max3}, k_{s3}, AL_2, BE_2\} = \{4.48, 17.96, 0.0, 0.46\}$. The results for the on-line estimated parameters are shown in Fig. 4, where it can be seen that their final values are: $\{AL_3, BE_3, m_{max4}, m_{max5}\} = \{0.41, 0.61, 0.519, 1.764\}$. The simulation results for concentrations are shown in Fig. 3, also in comparison with the off-line optimization results. The standard deviations were $\{\sigma_{Gl}, \sigma_{Lac}, \sigma_{Pr}, \sigma_{Ac}\} = \{22.7 \text{ mg/L}, 11.9 \text{ mg/L}, 9.1 \text{ mg/L}, 11.7 \text{ mg/L}\}$, the global correlation factor was 0.935. As can be seen both algorithms are quite good for the parameter identification of the biogas reactor.

Dynamic Simulation of a Polymerization Reactor

Process Description

Emulsion polymerization is currently the predominant process used in industry to produce a great variety of polymers of multiple uses (paints, adhesives, binders, etc.). Many applications of these polymer latexes require the formation of a continuous film with specific mechanical properties, which depend on the chemical composition of the polymer. However, the on-line measurement of composition in emulsion polymerization processes is still a difficult issue involving high cost of measuring and experimentation. Having this in mind, afterwards, the dynamic evaluation of the monomer composition in the emulsion (aqueous and polymer particle) phases for a semi-batch reactor is presented. In particular, the isothermal emulsion copolymerization of styrene (monomer 1) and methyl methacrylate (monomer 2) is considered, as shown in Fig. 5.

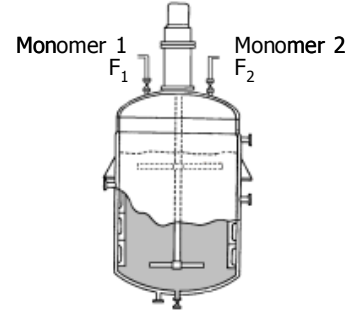


Figure 5: The emulsion copolymerization reactor.

Reaction mechanism: Free-radical polymerization involves in general four main steps: initiation, propagation, chain transfer and termination.

In the case of copolymerization system both monomers M_1 and M_2 will be activated to form free radicals, thus three initiation steps are considered with a terminal decomposing initiator. Propagation involves four distinctly different steps, neglecting penultimate effects. The monomer type in the penultimate position may also affect the rate of monomeric units addition to the growing polymer chain, but the importance of the penultimate effects has not been widely investigate. In the following it is assumed that penultimate effects can be neglected and the kinetic can be approximated by a first-order Markov process. Termination either by combination or disproportionation involves six steps, while transfer reactions can occur with a variety of chemical species including monomer, emulsifier, solvent, polymer and chain transfer agents.

Model Construction

Taking into account the preceding free-radical mechanism, the dynamic model is derived from balances of mass, volume and thermodynamic equilibrium. The details of modeling and parameters can be found in [5]:

$$\frac{d[M_1^p]}{dt} = g_1 \{ [M_1^p], [M_2^p], V_R, F_1, F_2, [I], \alpha_1, \alpha_2 \} \quad (11)$$

$$\frac{d[M_2^p]}{dt} = g_2 \{ [M_1^p], [M_2^p], V_R, F_1, F_2, [I], \alpha_1, \alpha_2 \} \quad (12)$$

$$\frac{d[I]}{dt} = g_3 \{ [M_1^p], [M_2^p], V_R, F_1, F_2, [I] \} \quad (13)$$

$$\frac{dV_R}{dt} = g_4 \{ [M_1^p], [M_2^p], F_1, F_2, [I] \} \quad (14)$$

$$\left(\frac{\Delta \bar{G}}{RT} \right)_1^p \{ [M_1^p], [M_2^p], \alpha_1, \alpha_2 \} = \left(\frac{\Delta \bar{G}}{RT} \right)_1^a \{ [M_1^p], [M_2^p], \alpha_1, \alpha_2 \} \quad (15)$$

$$\left(\frac{\Delta \bar{G}}{RT} \right)_2^p \{ [M_1^p], [M_2^p], \alpha_1, \alpha_2 \} = \left(\frac{\Delta \bar{G}}{RT} \right)_2^a \{ [M_1^p], [M_2^p], \alpha_1, \alpha_2 \} \quad (16)$$

Where $[M_1^p]$ and $[M_2^p]$ are the monomer concentrations in the polymer phase, $[I]$ is the initiator concentration, V_R is reactor volume, T is the reactor temperature, F_1 and F_2 are the feed flow rates of each monomer, α_1 and α_2 are the monomer partition coefficients, $(\Delta\bar{G})_i^p$ and $(\Delta\bar{G})_i^a$ are the partial molar free energies of monomers in polymeric (p) and aqueous (a) phases respectively, and g_i are nonlinear functions defined in [5].

Equations 15 and 16 correspond to the thermodynamic equilibrium, which is assumed to be quickly reached and maintained in the emulsion polymerization, since the monomer diffusion through the aqueous phase is fast. The thermodynamic equilibrium approach used in this model is based on Flory-Huggins theory [6].

Model Analysis

The model equations (Eqs. 11 - 16) form a set of stiff DAEs. The classification of equations and variables is done through ICAS-MoT as follows: the model has 114 equations (74 independent, out of which, 4 are ODEs, 2 are implicit AEs and 68 are explicit AEs) and there are 103 variables (sorting as 28 Parameters, 2 Unknown, 1 Known, 4 Dependent and 68 Explicit).

Model Simulation

The dynamic simulation based on the model (Eqs. 11 - 16) provides an estimate of the monomer concentrations in the different phases. The DAE set has been solved with the BDF-integration method included in ICAS-MoT. Fig. 6 shows the results for the dynamic behavior of the copolymerization of methyl methacrylate and styrene, considering a semi-continuous process operated under monomer-starved conditions. It can be seen that concentrations change throughout the course of the polymerization process and after the end of the monomer addition period, and a drop in the level of monomers in the polymer particles is observed followed by a drop in the aqueous-phase monomer concentrations. This basically demonstrates the diffusion of monomer from the aqueous phase into the polymer particles as modeled through the thermodynamic equilibrium approach (Eqs. 15 - 16).

It is worth of mentioned that these simulation results are in accordance with those reported by the authors [5].

Conclusions

The framework for a computer-aided modeling system has been presented and the modeling features related to model identification have been highlighted through two case studies. An important feature of the computer-aided system is that a model representing the process/operation can be imported into ICAS-MoT system and set up for identification and other applications without the user having to write any programming code. This makes the usually iterative model development and identification very efficient, fast and robust.

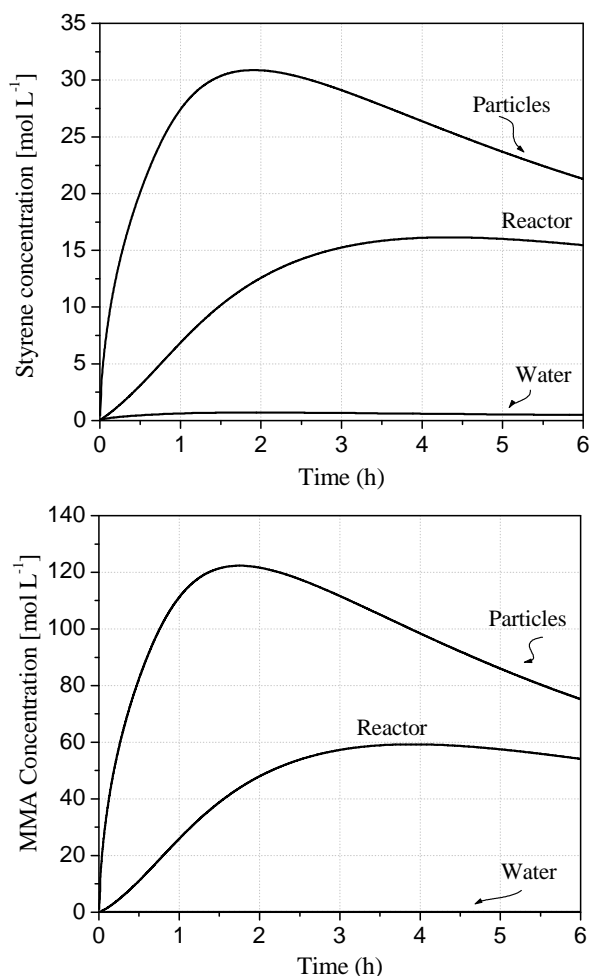


Figure 6: Dynamic evolution of monomer concentrations in the copolymerization reactor

Future work

Computer-Aided Modeling Framework

The ICAS-MoT system is being improved providing features for model analysis and model export in the form of CAPE-OPEN compliant COM-objects that can be used through external software. This makes the creation of a customized computer-aided system with validated models possible with a minimum of programming effort.

Another feature will be the addition of solvers for PDE (partial differential equation) and PDAE (partial differential algebraic equation) systems, since up to now ICAS-MoT can solve them but with a previous discretization.

Case Studies

For the anaerobic bioreactor, the ultimate objective is to provide the researcher with such a computer-aided tool so that future experiments can be designed and the bioreactor operated optimally. In particular, experimental designs are being carried out for a

complex biogas reactor used for the anaerobic treatment of sewage sludge.

For the emulsion copolymerization reactor, the modeling, operational analysis and process configurations will be considered. Several model/process configurations will be implemented in the same environment, for instance type of operation (batch, semi-batch or continuous), presence or absence of heat exchangers, thermodynamic equilibrium model, and use of different kind of polymer thermodynamics are considered. Further, dynamic simulation studies and the model analysis may help to identify process/operational sensitivities and to formulate control and optimization problems related to polymerization reactors.

References

1. M. Sales-Cruz, R. Gani, in: S.P. Asprey, S. Macchietto (Eds.), *Computer-Aided Chemical Engineering*, vol. 16: *Dynamic Model Development*, Elsevier, Amsterdam 2003, 209-249.
2. K. Hangos, I. Cameron, *Process Modeling and Model Analysis*. Academic Press, San Diego, CA, 2001.
3. I.V. Skiadas, H.N. Gavala, G. Lyberatos, *Water Res.*, 34 (2000) 3725-3736.
4. J. Alvarez, T. Lopez, *AIChE J.*, 45 (1999) 107-123.
5. J. Dimitratos, C. Georgakis, S. El-Aasser, A. Klein, *Comp. Chem. Eng.*, 13 (1989) 21-33.
6. P.J. Flory, *Principles of Polymer Chemistry*, Cornell University Press, New York, 1953.

List of Publications

7. M. Sales-Cruz, R. Gani, in: S.P. Asprey, S. Macchietto (Eds.), *Computer-Aided Chemical Engineering*, vol. 16: *Dynamic Model Development*, Elsevier, Amsterdam 2003, 209-249.
8. M. Sales-Cruz, I. Skiadas, I., R. Gani, *Proceedings ECCE-4 (4th European Congress in Chemical Engineering)*, EFCE-ANCHE Ed., Spain (2003), Vol. 9.
9. M. Sales-Cruz, R. Gani, I. Skiadas, *AIChE annual meeting*, to be held in San Francisco, CA, USA (November 2003), in press.
10. M. Sales-Cruz, R. Gani, *ESCAPE-14*, to be held in Lisbon, Portugal (May 2004), accepted.
11. M. Sales-Cruz, R. Gani, *FOCAPD'2004*, to be held in Princeton, NJ, USA (July 2004), submitted.



Sylvain Verdier
 Address: IVC-SEP, Dept. of Chemical Engineering
 Building 229, Office 262
 Technical University of Denmark
 Phone: (+45) 45 25 28 77
 Fax: (+45) 45 88 22 58
 e-mail: syv@kt.dtu.dk
 www: www.ivc-sep.kt.dtu.dk
 Supervisor(s): Simon I. Andersen
 Erling H. Stenby
 Ph.D. Study
 Started: 1 May 2003
 To be completed: May 2006

Experimental Study and Modelling of Asphaltene Precipitation Caused by Gas Injection

Abstract

Asphaltene precipitation in oil reservoirs is prejudicial to the economy of oil production. Many attempts have been carried out in order to model the behaviour and precipitation of asphaltenes, but the results have not been very successful yet. There is an important lack of experimental values for the main properties of asphaltenes, and this hinders the development of the modelling. This project especially aims at generating experimental data and at building a simple thermodynamic model based on these experiments and capable of predicting asphaltene precipitation caused by gas injection.

Introduction

Many models are available to describe precipitation of asphaltenes [1] but none of them is entirely satisfactory. Asphaltene are quite complex systems and simple parameters such as molecular mass remains doubtful and uncertain. A simple approach seems to be more relevant and may enable a good description of the various phenomena.

Specific Objectives

The first point we decided to investigate was the solubility parameter δ and its measurement, especially as a function of pressure. Indeed, the solubility parameter has a key role in the regular solution theory and its accurate determination remains problematic. The solubility parameter can be linked to the internal pressure with the following relationship:

$$\delta = \left(\frac{1}{n} \pi \right)^{1/2} \quad (1)$$

where π is the internal pressure and n is around the unity.

Internal pressure can also be linked to thermal properties such as thermal expansivity α and isothermal compressibility κ_T :

$$\pi = T \frac{\alpha}{\kappa_T} - P \quad (2)$$

Results and Discussion

This method has first to be calibrated with pure compounds such as hydrocarbons. Thermal expansivity is determined by means of microcalorimetry and the accuracy of the method developed is around 2% [2]. Density measurements are used so as to determine isothermal compressibility with Equation 3:

$$\kappa_T = -\frac{1}{V} \left(\frac{\partial V}{\partial P} \right)_T = \frac{1}{\rho} \left(\frac{\partial \rho}{\partial P} \right)_T \quad (3)$$

Density is determined quite accurately within 0.1% of deviation, by means of an Anton-Paar densimeter DMA 512 and isothermal compressibility can be calculated within 2.7% of deviation (these results will be published later). Thus, internal pressure is calculated for pure compounds as a function of pressure and compared to literature data at 1 bar [3]. Figure 1 shows the evolution of the solubility parameter as a function of pressure.

The deviation at 1 bar reaches at the most 1 MPa^{1/2} for cyclohexane. However, the link between internal pressure and solubility parameter is not as simple as described with Eq 1. Bagley et al. [4, 5] explains that internal pressure is only a measure of the cohesive energy density due to dispersion and polar forces.

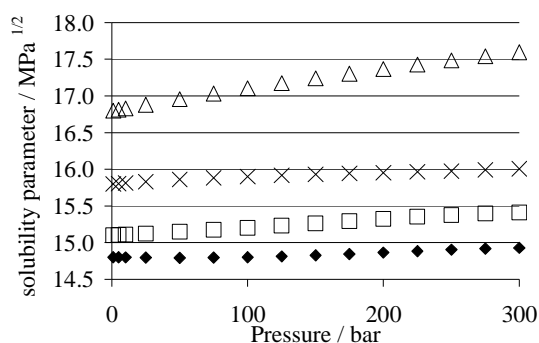


Figure 1: Solubility parameter of pure compounds at 303.15 K as a function of pressure. \blacklozenge , n-hexane; \square , n-heptane; \triangle , cyclohexane; \times , n-decane.

Once this method was validated, oils could be investigated. Figure 2 shows the solubility parameter of an oil (Yagual 3) as a function of pressure at 303.15 K. The solubility parameter is compared to a model based on SRK [6].

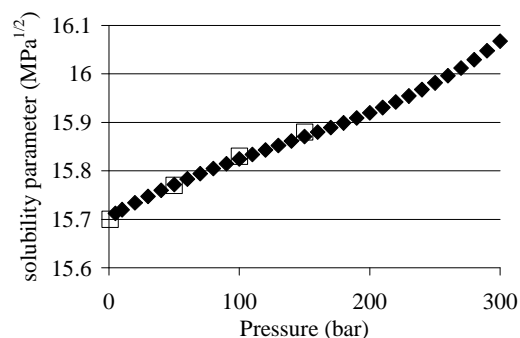


Figure 2: Solubility parameter of an oil at 303.15 K

The value of n is equal to 1.06. The model fits quite well the results of this work.

Conclusions

A method to measure internal pressure as a function of pressure was developed in this work and validated with pure compounds. Several dead oils were investigated and their solubility parameters were determined. From now on, the work will be focused on the determination of the solubility parameter of asphaltenes and its application in modelling. Gas injection experiments will be carried on, especially on live oils. Other points such as the structure of asphaltenes and a good characterization of oils will be investigated as well.

Acknowledgements

The authors appreciate the fruitful help of the technical staff of IVC-SEP and they would like to acknowledge the financial support of DONGs jubilæums fond for financial support.

References

1. S.I. Andersen, J.G. Speight, *J. Petrol. Sci. Eng.* 22 (1999), 53-66
2. S. Verdier, S.I. Andersen, *J. Chem. Eng. Data* 48 (2003), 892 – 897
3. A.F.M. Barton, *CRC Handbook of solubility parameters and other cohesion parameters*, CRC Press, Boca Raton, FL, 1983, 142 – 149
4. E.B. Bagley, T.P. Nelson, J.M. Scigliano, *J. Paint Technol.* 43 (1971), 35-42
5. E.B. Bagley, J.M. Scigliano, in: A. Weissberger (Ed.), *Techniques of Chemistry*, New-York, 1975, vol. viii, Part II, 437-485
6. G. Livberg, *Sound velocity in hydrocarbons*, Master Thesis, DTU (2000)

List of Publications

1. S. Verdier, S.I. Andersen, *J. Chem. Eng. Data* 48 (2003), 892 – 897



Ada Villafáfila García
Address: IVC-SEP, Dept. of Chemical Engineering
Building 229, Office 262
Technical University of Denmark
Phone: (+45) 4525 2864
Fax: (+45) 4588 2258
e-mail: aga@kt.dtu.dk
www: www.ivc-sep.kt.dtu.dk
Supervisor(s): Kaj Thomsen
Erling Stenby
Ph.D. Study
Started: 01 October 2002
To be completed: October 2005

Modeling of Mineral Scale Deposition in Geothermal and Oilfield Operations

Abstract

Scale formation is a common and expensive problem in many industrial processes, such as in oil and geothermal fields. Scale prevention is technically and economically more effective than re-dissolution once scale has formed. In this Ph.D. project we will focus on the prediction of mineral solubility in natural waters under conditions of varying brine composition, temperature and pressure. The Extended UNIQUAC model has been chosen for calculating solid-liquid-vapor equilibrium and crystallization. Both experimental data found in literature and measurements performed for the experimental part of this project will be used for parameter regression. As a conclusion of the work done until the moment it can be stated that Extended UNIQUAC is able of accurately represent the systems investigated.

Introduction

Mineral scale deposition is a problem encountered in oil production and geothermal power plants. It can be defined as the deposition of inorganic minerals from a brine. The precipitation of the minerals causes problems if it deposits onto a surface such as the inner wall of a pipe.

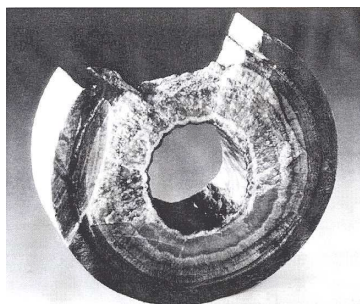


Figure 1: CaCO₃ Deposition in Tubing [2]

The amount and location of scale is influenced by many factors such as the degree of supersaturation, kinetics, pH, etc. One of the main causes of scale formation is the large changes in both pressure and temperature as the brine flows up the well. This sometimes leads to solid-phase deposition. Also the injection of so-called incompatible brines leads to scaling.

The consequences of scale deposition are serious damage in utilization systems, reduction of well porosity and reinjection capacity. All these effects lead

to a production decrease and to the consequent economical losses.

Specific Objectives

The first step towards scale deposition prevention is to have an appropriate tool to predict the behavior of scaling minerals in multi-component solutions at the temperature and pressure range of interest. A number of models to predict scale formation already exist, but as the problem becomes more severe, a better accuracy is required. One of the problems for the existing models is that they are based on a limited amount of data and therefore heavily rely on extrapolation.

This project will consist of a theoretical and an experimental part. In the experimental part, the solubility of different salts causing scale formation will be measured. Both binary and multi-component solutions will be analyzed, covering temperature and pressure ranges found in geothermal and oilfield wells. Such data are scarce or inexistent in literature.

In the theoretical part of the project a model for calculating solid-liquid-vapor equilibrium and the crystallization will be developed on the basis of the experimental data found in literature and the data obtained from the experimental part of this project. The Extended UNIQUAC model [1] is used to represent speciation, solid-liquid equilibrium, and gas-liquid equilibrium (gas fugacities are calculated from the SRK equation).

The most problematic scale minerals found in literature are calcite (CaCO_3), anhydrate (CaSO_4), gypsum ($\text{CaSO}_4 \cdot 2\text{H}_2\text{O}$), barite (BaSO_4) and celestite (SrSO_4). All of them are considered in this project, together with all the possible salts formed from the Na^+ - K^+ - Ca^{2+} - H^+ - Ba^{2+} - Sr^{2+} - Mg^{2+} - Cl^- - SO_4^{2-} - OH^- - HCO_3^- - CO_3^{2-} - CO_2 - H_2O system. Additional species could be added to the system if they are found to play an important role in the problem studied.

Extended UNIQUAC

There is a lack of data for scale minerals solubility in natural waters at high temperature and pressure conditions. Therefore, a method requiring limited amount of data but leading to accurate predictions for the solid-liquid-vapor equilibrium and crystallization processes for electrolyte solutions would be of great use. This is the case of the Extended UNIQUAC model, which only requires two parameters per species, plus two parameters per species pair. The temperature dependence is accounted for in the model equations. Two additional parameters have been introduced to the model presented by Thomsen [1] in order to account for the pressure dependence of the solubility. The results obtained through this modification are very satisfactory in the pressure range investigated (1 to 1000 bar).

Results and Discussion

The solid-liquid-vapor equilibrium for the systems BaSO_4 - H_2O , BaSO_4 - NaCl - H_2O , SrSO_4 - H_2O , SrSO_4 - NaCl - H_2O , CaSO_4 - H_2O , CaSO_4 - NaCl - H_2O and CaCO_3 - CO_2 - H_2O has been represented using the Extended UNIQUAC model. The liquid-vapor equilibrium for the system CO_2 - H_2O has also been studied. Some of the systems mentioned above are shown in figures 2 and 3, where the high accuracy of the Extended UNIQUAC model can be seen. The same close agreement between experimental data and Extended UNIQUAC calculations was observed for all the systems studied until the moment.

Figure 2 shows celestite solubility in water at 75°C and pressures up to 600 bar.

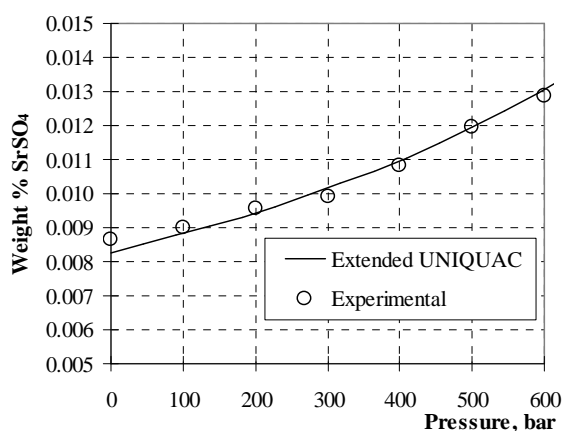


Figure 2: SrSO_4 Solubility in H_2O at 75°C

Barite solubility in water at 500 bar and temperatures up to 300°C is shown in figure 3. It is seen that barite solubility increases with temperature up to about 100°C, and it starts decreasing for higher temperatures. The Extended UNIQUAC model is able to accurately describe this solubility behavior. If a brine saturated with barite is pumped from a reservoir at 500 bar and 100°C to ambient pressure and temperature, barite will become supersaturated and will most likely precipitate from the brine.

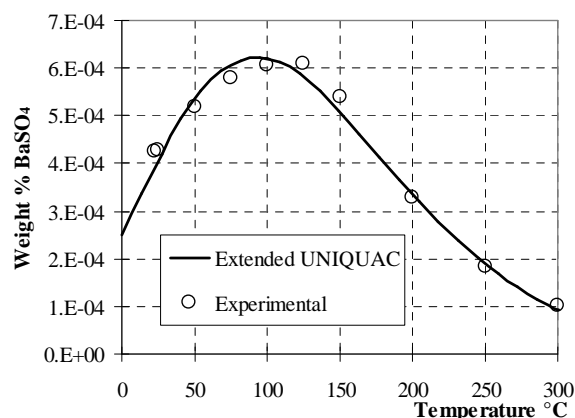


Figure 3: BaSO_4 Solubility in H_2O at 500 bar

Conclusions

The Extended UNIQUAC model as presented by Thomsen [1] modified with two additional parameters to account for the pressure dependency of the solubility has been used to represent solid-liquid-vapor equilibrium of different systems. The model is capable of representing accurately both binary and multicomponent systems, covering a wide range of temperature (up to 300°C) and pressure (up to 1000 bar).

Acknowledgements

I would like to thank Kaj Thomsen for his constant help and advice since the beginning of this work. I would also thank Simon Andersen and the IVC-SEP laboratory technicians for their support regarding the experimental part of the project.

References

1. K. Thomsen, P. Rasmussen, *Chemical Engineering Science* 54 (1999) 1787-1802.
2. B. Kaasa, *Prediction of pH, Mineral Precipitation and Multiphase Equilibria during Oil Recovery*, PhD thesis, Institutt for Uorganisk Kjemi, Norges Teknisk Naturvitenskapelige Universitet, Trondheim, Norway, 1998, p. 24.



Bjørn Winther-Jensen

Address: DPC, Dept. of Chemical Engineering
Building 423
Technical University of Denmark

Phone: (+45) 45 25 29 53
Fax: (+45) 45 88 21 61
e-mail: bwj@polymers.dk
www:

Supervisor(s): Jørgen Lyngaae Jørgensen
Keld West, Risø

Ph.D. Study
Started: 1 October 2001
To be completed: October 2004

Micro-Patterning of Conducting Polymers

Abstract

Conducting polymers has been around for the last 25 years but with a quite limited use in industrial applications. Stability and processability has been main difficulties for the actual use in larger scale. Since long Poly-3,4 ethylenedioxythiophene (PEDT) has been known as robust and high conducting among the conducting polymers. This project investigates the possibilities for micro-patterning of PEDT using lift-off and ink-jet technology. During this investigation it has been obvious that a lot of “building blocks” is necessary before micro-patterning is possible. Solving these “building blocks” (bonding to surfaces, high and stable conductivity, etc.) has to a large extent been achieved.

Introduction

With the aqueous suspension (Baytron P) from Bayer AG an easy access to PEDT is available. Unfortunately the conductivity of Baytron P is not expressing the full possibilities of PEDT compared to directly oxidative polymerised PEDT.

However, oxidative polymerisation of PEDT is not trivial when it comes to reproducible, homogenous films suitable for micro-patterning.

Bayer AG has developed and deliver the EDT monomer and an oxidative solution of Fe(III)TOS in butanol. By mixing these two ingredients PEDT is easily polymerised. But to get a homogenous film from the mixture requires a lot of skill and the pot-life of this mixed solution is only 10-20 min before the PEDT forms insolvable flocks (in the solution). This of cause makes practical use difficult.

This paper describes some of the problems and the solutions developed.

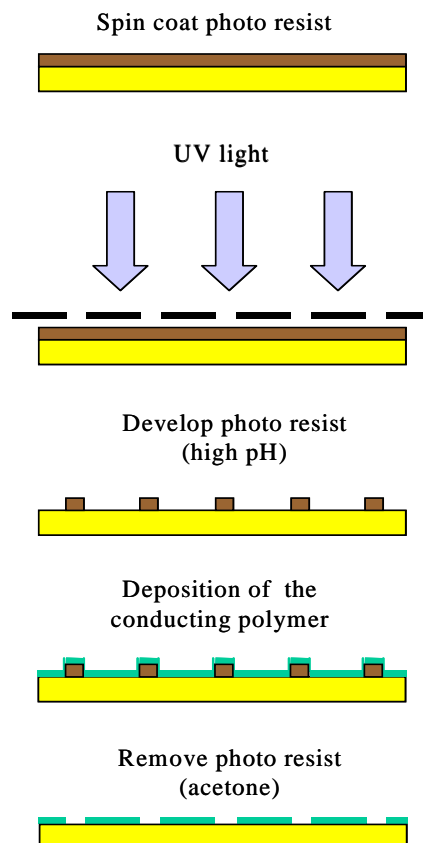
Micro-patterning by lift-off

If a lift-off procedure has to be useful for conducting polymers it has to fit into the existing production platform in the semi-conductor industry. This more or less fixes the route for the micro-patterning route (Fig.1).

A number of tasks are obvious:

1. Binding PEDT to the substrate (stand acetone ao.).

2. Uniform, controllable polymerization of Fig.1



PEDT.

3. PEDT have to stand high pH (> 13,5) for multi-layer patterning.

Ad 1)

A plasma polymerization process has been developed to bind PEDT (or other conducting polymers) to the substrate – normally Si-wafer. The plasma coating contains active groups where the PEDT can react during the oxidative polymerization process.

DTU is currently investigating if the plasma polymerization process can be patented.

Ad 2)

A base-inhibit oxidative polymerization of PEDT has achieved most of the requirements.

By adding pyridine as base to the monomer/Fe(III)Tos solution pH is raised to 2,5 (or more), this reduces the activity of the Fe(III) and the solution is stable for up till 3 days at room temperature. When printed or spin-coated the pyridine evaporates (before the monomer !) and the polymerization starts.

The method gives films with conductivity ~ 1000 S/cm, 2-3 times the conductivity achieved by PEDT with other methods.

Ad 3)

The PEDT films made by the method described in Ad 2) are surprisingly resistant to high pH.

Fig. 2 shows the resistant of a PEDT film exposed to pH 0,5 and 13,5 (measured after 2 hour) several times.

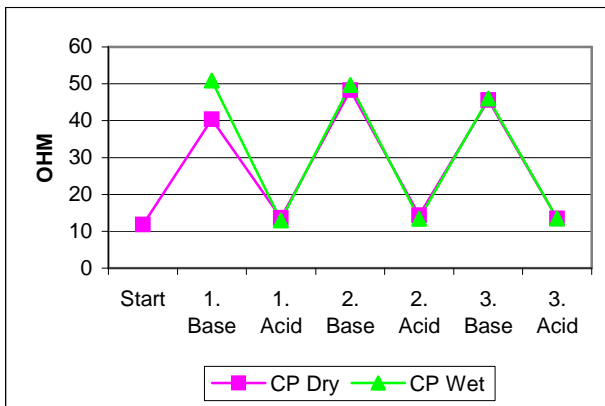
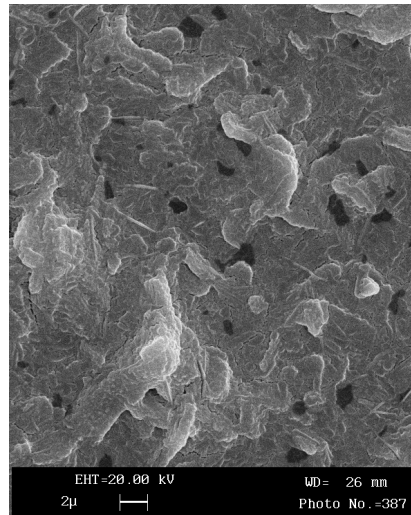
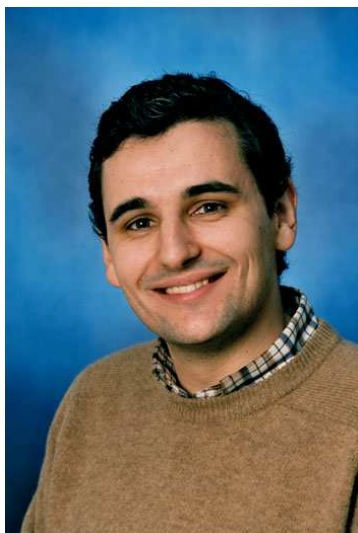


Fig.2

Most of the problems for the micro-patterning seems to be solved – the actual test during the winter and spring 2004 will show if we are right.



Diego Meseguer Yebra
Address: CHEC, Dept. of Chemical Engineering
Building 229, Office 130
Technical University of Denmark
Phone: (+45) 45 25 28 37
Fax: (+45) 45 88 22 58
e-mail: dmy@kt.dtu.dk
www: www.chec.kt.dtu.dk
Supervisor(s): Søren Kiil
Kim Dam-Johansen
Claus Erik Weinell, Hempel A/S
Ph.D. Study
Started: 1 May 2002
To be completed: May 2005

Efficient and Environmentally Friendly Antifouling Paints

Abstract

Antifouling paints are highly specialized coatings designed to combat the natural process of marine biofouling on immersed artificial structures. This project deals with the identification, characterization and quantification of the main processes responsible for the antifouling activity of an environmentally friendly system. Herein, the first results regarding the reactivity of some binder components with seawater are presented. Such information is part of the required experimental inputs to a mathematical model for a tin-free rosin-based self-polishing antifouling paint, whose structure is also outlined. A successful and innovative mathematical description of the paint activity is expected to speed up the paint design, testing and optimization.

Introduction

Marine biofouling is a natural and spontaneous process which involves tremendous economical losses on ocean-going ships. The most widespread preventive solution is to coat the underwater part of the vessel's hull with an antifouling (A/F) paint. In addition to the tight durability requirements inherent to paints exposed to such a harsh environment as seawater is, these products must release active compounds in a controlled manner during long periods of time (e.g. up to 5 years). Consequently, the design, optimization and testing of new products is a time-consuming and very complex tuning task.

An example of this was seen in the last years after the prohibition of the very efficient tin-containing coatings. Paint companies were urged to develop tin-free alternatives with similar performance to that of the toxic tin-based products. While the first granted patents related to some of today's commercially available products date back to the mid 80's [1], the moderate results of these technologies forced the marine paint companies to commercialize tin-containing products until the suggested date for the entry into force of the ban.

With the advent of new progressively stricter environmental regulations, there is a need for faster procedures for effective screening and development of promising environmentally benign alternatives. Kiil et al. [2] showed how the mathematical quantification of

some key processes in the A/F paint activity can result in reliable estimations of paint performance. Although originally based on a tin-based technology, the ideas underlying the model are directly applicable to any system based on a controlled reaction with seawater. The latter involves that the outputs of this research can be applied to a number of promising non-toxic A/F alternatives which are currently subjected to investigation elsewhere.

Project Objectives

The main goals of this research project are:

- o To characterize the main processes determining the activity of a tin-free A/F paint
- o To quantify and implement them into an advanced mathematical model
- o To analyze the influence of A/F paint components on the paint activity: (e.g. different (in)soluble pigments, (un)reactive binder components)
- o To develop fast testing methods based on model simulations and short rotary experiments
- o To adapt the model from artificial to natural seawaters in the extent possible.

The fulfillment of these objectives requires extensive rotary testing of different paint compositions, together with chemical reaction studies and mathematical modeling.

Working Mechanisms of Biocidal A/F Paints

All the currently marketed chemically-active tin-free alternatives are based on similar working principles (Figure 1).

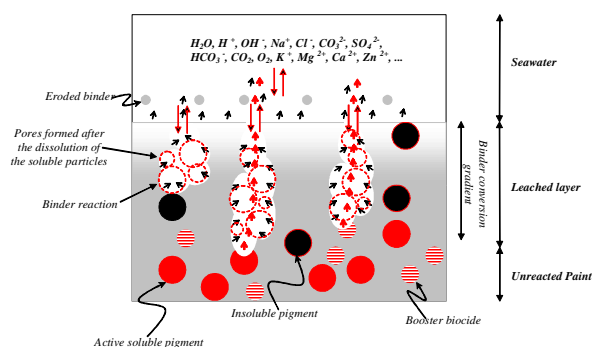
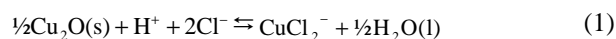


Figure 1: Schematic illustration of the working mechanisms of a chemically active A/F paint

Seawater and seawater ions diffuse to the paint surface where they rapidly react with the soluble pigments (typically Cu_2O):



The copper complexes formed diffuse out into the bulk seawater thereby forming a pore network in the paint (the so-called leached layer). At the paint surface and at the pore walls, seawater ions also react with the paint binder system. In the case of the rosin-based system of interest in this study, the following reaction takes place:

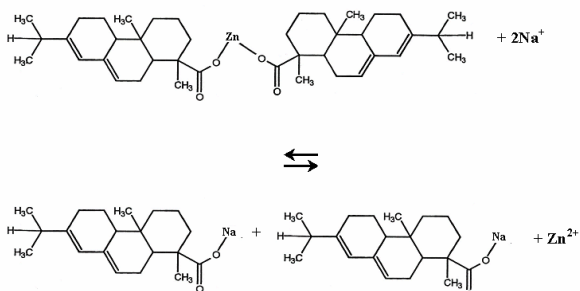


Figure 2: Alkaline hydrolysis reaction of the Zn carboxylate of abietic-acid with seawater. This mechanism has been characterized in this project by means of Fourier Transform IR Spectroscopy

This reaction results in the formation of very soluble soaps which diffuse out into the bulk seawater. If a biocidal compound is embedded in the binder, it will thus be exposed and released. Consequently, both the reaction with the pigments and the reaction with the binder lead to the release of active compounds which give rise to the A/F activity.

At a certain point in time, the binder at the pore walls of the leached layer will have different degrees of

reaction. The more converted binder will be that at the paint surface (longer contact time with seawater). The latter can be analyzed by means of Scanning Electron Microscopy coupled with Electron Dispersive X-Ray detectors (SEM-EDX) (Figure 3).

The model assumes that a very thin paint layer is released (polishing process) when the reaction at the paint surface has reached a certain conversion (X_{max}), thus exposing a less reacted binder surface. This parameter constitutes an innovative concept in A/F paint modeling and it is thought to depend strongly on the insoluble paint components, i.e. insoluble pigments and retardants.

The system must be designed in such a way that the release rate of the biocides are sufficient to prevent fouling throughout the paint's lifetime (typically 5 years). If it is intended to use a model-based approach to assist the design process, it is customary to determine the rate at which the reaction schematized in Figure 2 takes place. This is presented in the next section.

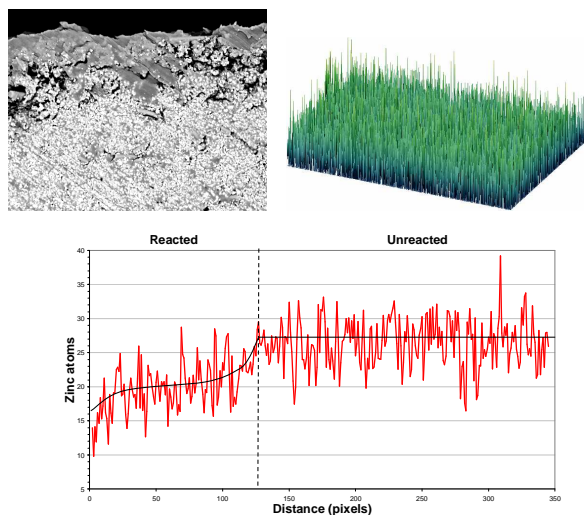


Figure 3: SEM picture and its corresponding EDX analysis showing the Zn atom signals (up). The intensity of the signal is processed by means of ImagePro, showing a distinct gradient from the unreacted paint to the paint surface (bottom).

Dissolution Rate Measurements

In this investigation, the zinc carboxylate of a refined and prereacted rosin compound is used. Natural rosin is distilled in order to eliminate impurities and subsequently hydrogenated. The resulting mixture consists mainly of tetrahydroabietic and dihydroabietic acids. Zinc resinates were prepared after reaction of the hydrogenated rosin dissolved in xylene 1:1 wt. with excess ZnO for two hours in a high speed disperser. The excess ZnO particles were removed by centrifugation (10min, 3000 r.p.m.). Clear separation between the different phases was observed. The supernatant liquid was extracted from the very upper part of the avoid contamination by ZnO particles and further filtered (0.45 μm). A Fourier Transform IR Spectroscopy analysis of the resulting mixture shows virtually 100% conversion to the dimeric carboxylate. The resinates

obtained in this way is brittle after solvent evaporation. Film cracking would result in uncontrolled exposed surface area. Thus, a water soluble polymeric plasticiser was added in the ratio 1:4 solids volume. A gravimetric method is chosen to follow the dissolution rate.

The samples were coated onto very thin glass panels of dimensions 2.4x6 cm. were used. Glass was found not to absorb water, unlike acrylic and polycarbonate materials, and it is thus appropriate for gravimetric studies (see Figure 4).

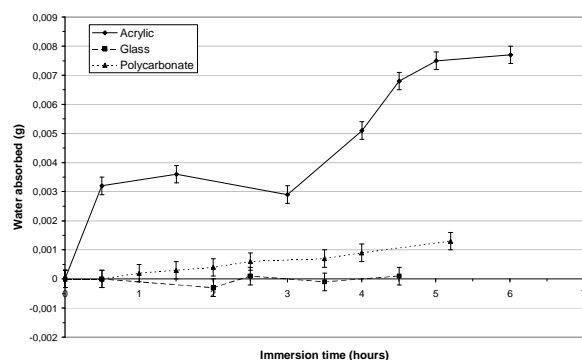


Figure 4: Water absorption of different materials as a function of immersion time

The panels were cleaned with xylene to remove potential surface contaminants. A surface area of 9.6 cm² was coated with binder by means of a Bird applicator. High wet film thicknesses were avoided in order to minimize crack failure due to poor cohesive strength of the binder. Overall, around 0.4 g of binder was applied to a ~0.53 g glass panel. The binder should be applied on a perfectly horizontal surface to avoid heterogeneous distribution. This was possible due to low viscosities and the absence of any flow or thixotropic additives which could impart a rheologic structure to the binder.

Results are only available in seawater at 25°C and a pH of 8.20±0.5. Consistent measurements of the dissolution rate of the mixture zinc resinate/plasticiser after 21 days of aging time in sea water have been obtained. The rate obtained is higher than those of the pure zinc resinate and hydrogenated rosin.

Future efforts will be directed towards the attainment of a kinetic expression to account for the effect of different seawater conditions on the dissolution rate of the zinc resinate and to the elucidation of the role of the plasticiser. New plasticizers will also be tested in order to optimize the binder dissolution rate without a loss of mechanical properties.

The Mathematical Model

As it comes from the discussion above, the basic phenomena modeled are (see Figure 5):

- o Cu₂O and binder kinetics
- o Seawater chemical speciation
- o Transport phenomena
- o A condition for paint polishing (X_{max})

Overall, the model describes the profiles inside the paint film for CuCl₂/CuCl₃²⁻, Cu²⁺, Na⁺, H⁺/OH⁻, Cl⁻, O₂, HCO₃⁻/CO₃²⁻, Zn²⁺/ZnCl⁺/ZnCl₂/ZnCl₃⁻/ZnCl₄²⁻ and Na resinate. The oxidation of Cu⁺ complexes to Cu²⁺ in the leached layer has been included for the first time according to the kinetics measured by Millero (2000) [3]. The incorporation of that process allows the study of the potential formation of insoluble Cu²⁺ salts, traditionally associated with rosin-based systems. An advanced numerical solution technique [4] is used to immobilize the moving boundaries (i.e. paint surface and pigment front) and allow the use of orthogonal collocation to solve the system of differential equations [5].

Regarding the seawater chemistry, the activity coefficients for the individual ionic species present within the leached layer and in the diffusive boundary layer are estimated by means of Extended UNIQUAC. This model is based on the addition of a Debye-Hückel term to the UNIQUAC expression of the molar excess Gibbs energy to account for the long-range interactions between the ionic species (electrostatic forces) as presented by Thomsen et al. [6].

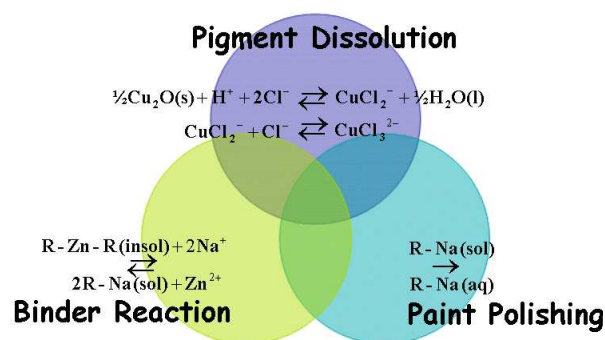


Figure 5: Scheme of the tin-free rosin-based (TFR) mathematical model. The main processes involved in the activity of the paint and their interactions are combined with chemical speciation calculations and transport phenomena.

A/F Paint Performance

The model outlined above has to be capable of reproducing the activity of model A/F paints. Such activity can be characterized by means of two experimental parameters (see Figure 6):

- o The degree of polishing
- o The thickness of the leached layer

To measure such parameters, a rotary set up (Figure 7) is available simulating the conditions experienced by the paint on a sailing ship's hull. By providing a Couette flow in the water around the paint samples, the shear stress could be adjusted to reach realistic values.

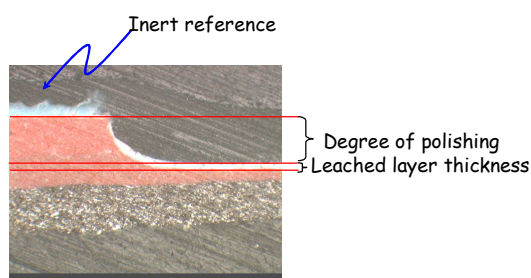


Figure 6: Measurement of the degree of polishing and leached layer thickness through optical microscopic analysis of the cross-section of exposed paints

Up to now, an important amount of rotary data is available studying the influence of different model paint compositions (e.g. Figure 8). It is presumed that the polishing process can be tailor-made through an identification of the individual roles of:

- o Insoluble pigments
- o Insoluble resins (retardants)
- o Pigment PSD
- o Pigments of controlled dissolution rate



Rotor with paint samples Tank of artificial seawater

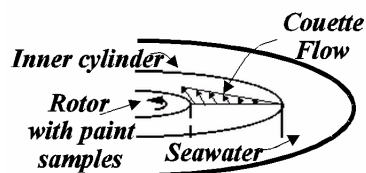


Figure 7: Rotary set-up (up). Inner cylinder and Couette flow regime (down)

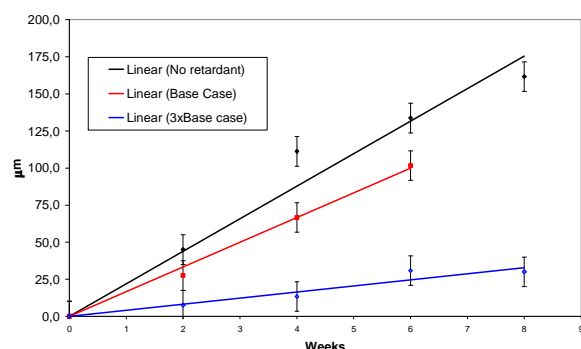


Figure 8: Influence of the amount of retardant on the paint polishing rate

Accelerated Paint Testing

Relatively simple experimental procedures can be designed to provide a fast estimation of the required input parameters for the model. Subsequent simulations can be used to select the most promising formulations

which should be subjected to more thorough testing. Future work will address the development of procedures for:

- o Fast estimation of binder and pigment kinetics.
- o Fast determination of X_{\max} (SEM/EDX)

The dissolution kinetics of ZnO and low leaching Cu₂O pigments are to be determined and verified by the use of the model and rotary experiments.

Conclusions

The use of A/F paints as a means of preventing the undesired settlement of marine organisms on the hulls of ocean going ships entails important economical benefits. Moreover, it involves reduced fuel consumption and, thereby, lower emissions of harmful compounds into the atmosphere. The prohibition of the very effective but environmentally harmful tributyltin-based coatings was the first of a series of expected restrictions which will regulate the A/F compounds that can be used on a bottom coating. The transition from the tin-based to the tin-free coatings has demonstrated the drawbacks of design and optimization processes based on trial and error tests after long-term rotary experiments. New approaches must thus be developed in order to adapt the current A/F products to the more environmentally friendly active compounds product in an efficient manner.

A mathematical model of the performance of a rosin-based tin-free alternative will soon be ready for validation against the rotary data already generated. The new binder reaction mechanisms and kinetics are yet to be fully determined.

If the model is proven successful, fast experimental procedures can be identified to provide the necessary input parameters for the model and allow a fast estimation of the performance without the need of too long rotary experiments. Ideally, the latter should only be performed with a few selected systems which have shown promising characteristics from the model analysis. In addition, information about the paint behavior under different seawater conditions could also be simulated, which is only feasible today at the expense of increasing testing costs.

The generic nature of the model, would make it extensible to innovative alternatives with the only condition of involving the release of active compounds. In this way, the development of non-biocidal chemically active alternatives would be eased.

Acknowledgements

The work presented in this article was carried out in the CHEC Research Centre in collaboration with Hempel's Marine Paints A/S.

Financial support from The Danish Technical Research Council and the J.C. Hempel Foundation is gratefully acknowledged.

I would like to thank Neel Winther-Hinge for her invaluable help with the SEM-EDX analysis, and Kaj Thomsen for providing the E UNIQUAC routines.

References

1. Yebra, D.M., Kiil, S., Dam-Johansen, K. Progress in Organic Coatings. Accepted for publication (2003)
2. Kiil, S., Weinell, C.E., Pedersen, M.S., Dam-Johansen, K. Ind. Eng. Chem. Res. 40 (18) (2001) 3906-3920.
3. Millero, F.J. The Physical Chemistry of Natural Waters, Wiley-Interscience, NY, U.S.A, 2001.
4. Kiil, S., Bathia, S.K., Dam-Johansen, K. Chemical Engineering Science 50 (17) (1995) 2793
5. Villadsen, J. and Michelsen, M.L. Solution of Differential Equations Models by Polynomial Interpolation, Prentice Hall, Englewood Cliffs, U.S.A, 1978.
6. Thomsen, K., Rasmussen, P., Gani, R. Chemical Engineering Science 51 (14) (1996) 3675-3683



Jacob Zeuthen

Address: Aerosol Lab., Dept. of Chemical Engineering
 Building 227, Office 122
 Technical University of Denmark

Phone: (+45) 45 25 29 64
 Fax: (+45) 45 88 22 58
 e-mail: jz@kt.dtu.dk
 www: www.aerosol.kt.dtu.dk
 Supervisor(s): Hans Livbjerg

Ph.D. Study
 Started: 1 August 2003
 To be completed: August 2006

Laboratory Investigation of Formation of Aerosols and Chemical Reactions in Flue Gas from Biomass- and Waste-Combustion

Abstract

The aim with this project is to investigate the formation of aerosol particles and deposits during combustion of the so-called CO₂-neutral fuels, biomass and waste. The kinetics of the chemical reactions leading to the formation of these particles and deposits, and the phase transitions involved, will be studied. In general, combustion aerosols should be avoided due to their harmful behavior in the environment. Particles from combustion of bio-fuels are particularly harmful due to their sticky and corrosive behavior in the process equipment.

This project involves experiments performed in a tubular furnace and also CFD (computational fluid dynamics) simulations using Fluent. The focus will be on developing a quantitative model based on experiments and simulations. The quantitative model can be used for design and control of Danish power plants using biomass and waste combustion in the future.

Introduction

Straw, some sorts of wood, and various kinds of waste contain considerable amounts of volatile inorganic salts, in particular the chlorides of sodium, potassium and zinc, which evaporate during combustion. When the flue gas cools down after combustion the inorganic vapors condense and form aerosol particles and deposits

on walls and super heater tubes. This phenomenon is much more pronounced for bio-fuels than for other fuels. Dealing with the problems caused by deposition of salts in the process equipment increases the cost of 'CO₂-neutral' combustion considerable. The aerosol particles and the deposits have previously been studied intensively by field-studies and the chemical

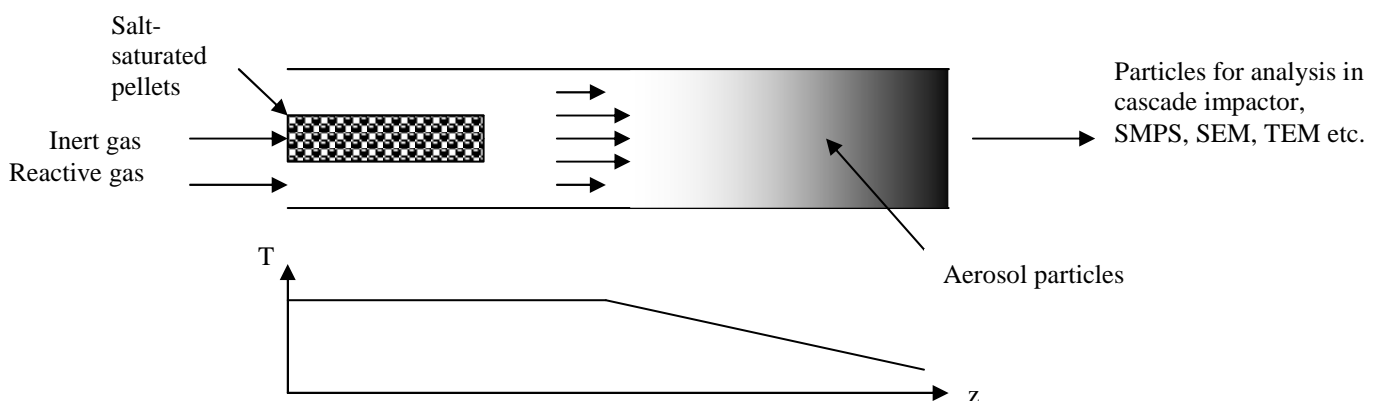


Figure 1: Schematic drawing of the tubular furnace. Gas enters the reactor in one end. The inert gas is led through a packing of pellets to be saturated with a volatile salt. The salt concentration of the gas is adjusted by changing the temperature of this part of the reactor. A temperature profile is applied on the reactor and particles are formed in the cooling zone by nucleation. The aerosol leaving the reactor can be studied by using a cascade impactor, SMPS (Scanning Mobility Particle Sizer), SEM (Scanning Electron Microscopy), TEM (Transmission Electron Microscopy) and other methods.

compositions of these have been found. However, the proposed qualitative models for the chemical reactions involved are not clear and are contradictory. Also, no quantitative models have been developed. Field-data are influenced by a highly varying chemistry of the fuel, by complicated distributions of residence times, temperatures and flow-patterns. Therefore it is not possible to develop quantitative models based on these data. In order to set up a quantitative model the important reactions involving the key chemical components must be studied separately. In this project a bench-scale tubular furnace with well-defined flue gas flow, temperature and gas-composition is used to establish a qualitative as well as a quantitative model for the formation of particles and deposits.



Figure 2: Experimental setup. To the left the SMPS system is placed and to the right the tubular furnace is seen.

Experimental work

For the experimental work a 173 cm long tubular furnace ($\varnothing=25$ mm) with laminar flow is used (see figure 1 and 2). It is possible to control the temperature up to ~ 1200 °C in nine separate axial sections along the flue gas flow direction. In the first part of the reactor an inner tube is placed. In this inner tube a flow of inert nitrogen passes pellets of inert alumina impregnated with the salt to be volatilized (e.g. NaCl or KCl). The nitrogen gets saturated and by changing the temperature of the pellets it is possible to adjust the salt-concentration in the gas (see figure 3). Other reactive gases (SO_2 , H_2O , NO and O_2 /air) enter the reactor on the outside of the salt-containing alumina pipe. The temperature is kept constant in the first part of the reactor and is then decreased in the flow direction after a given length. Using this technique, it is possible to study effects of different temperature gradients, flow velocities and chemical compositions on the formation of particles and deposits. It is also possible to introduce particle seeds with the inlet gas to study the effect of foreign seeds in the flue gas. These will serve as nucleation sites for further growth of inorganic materials and may serve to suppress homogeneous nucleation. Homogeneous nucleation leads to sub-

micron particles ($D_p < 1\mu\text{m}$), which are the most harmful particles for the environment, spreading over larger distances and with harmful impact on the human lungs. These particles are also more difficult to separate from the flue gas.

Modeling

Mathematical models will be used to describe the experiments performed. The models should account for the kinetics of chemical reactions involving the volatilized ash species, homogeneous nucleation, coagulation, particle growth by condensation, and particle transport by thermophoresis and diffusion. By applying the models the experimental results will be analyzed and alternative mechanisms will be compared and fitted to the experimental data. The modeling will be made by Computational Fluid-particle Dynamics using the programme package Fluent.

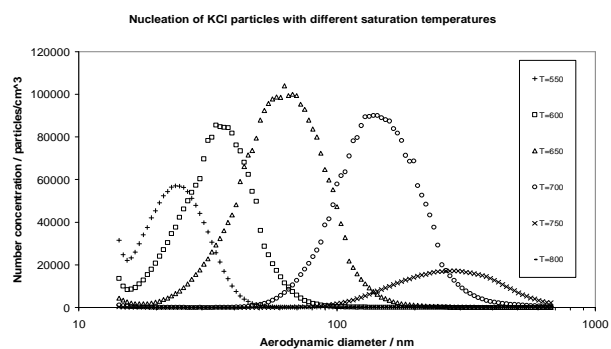


Figure 3: Size distribution of pure KCl-particles from experiments with homogeneous nucleation in a tubular furnace. The temperature of the saturation zone with alumina pellets impregnated with the salt is varied to obtain different values. With increasing temperature the concentration of $\text{KCl}_{(g)}$ is increased and the average particle diameter increases. However, while the mass of particles formed will keep increasing with higher temperature the number of particles formed is highest at some given temperature. Above this temperature coagulation of the small particles with the larger ones will dominate.

